6-2009

Development of Field Data for Effective Implementation of Mechanistic Empirical Pavement Design Procedure

Atorod Azizinamini
University of Nebraska - Lincoln, aazizinamini1@unl.edu

Nima Ala
University of Nebraska - Lincoln

Mohammad Ajmal Stanigzai
University of Nebraska - Lincoln

NDOR Research Project Number P300

FINAL REPORT

Development of Field Data for Effective Implementation of Mechanistic Empirical Pavement Design Procedure

Nima Ala

Mohammad Ajmal Stanigzai

Atorod Azizinamini, Ph.D., P.E.

National Bridge Research Organization (NaBRO)

(http://www.NaBRO.unl.edu)

Department of Civil Engineering

College of Engineering and Technology

W150 Nebraska Hall

Lincoln, Nebraska 68588-0528

Telephone (402) 472-5106

Fax (402) 472-6658

Sponsored By

Nebraska Department of Roads

June, 2009

Table of Contents

List of Figures

List of Tables

Acknowledgments

Funding for this investigation was provided by the Nebraska Department of Roads. The authors would like to express their appreciation for this support. The authors would also like to express their thanks to the staff at the NDOR Material Section for their valuable suggestions and comments.

This report was funded in part through grant[s] from the Federal Highway Administration [and Federal Transit Administration], U.S. Department of Transportation. The views and opinions of the authors [or agency] expressed herein do not necessarily state or reflect those of the U. S. Department of Transportation.

Executive Summary

This report provides summary of the work that was carried out to assess the merits of the Mechanistic Empirical Pavement Design approach and attempts to calibrate the procedure for application in Nebraska.

Mechanistic Empirical (M-E) design of pavements is a new approach to pavement design. The method consists of two components; Mechanistic and Empirical. The Mechanistic part of the procedure tries to predict the response of the pavement to various loading during a very short time period. The empirical part tries to sum up the damages inflected to the pavement during the short time steps that the pavement is subjected to and attempts to predict the accumulated damage as function of time.

This project consisted of two parts. First a parametric study was carried out to identify the parameters that are important and level of sophistication that is needed at the input level. Appendix A provides summary of this effort in detail. It was concluded that there is a need for collecting field data, before making a final conclusion on effectiveness of the new methodology for application in Nebraska.

The next step was to develop filed instrumentation plan and start collecting data and then continue with calibration process.

The computer program that is used in conjunction with MEPDG program and the theoretical background to it published in several reports, were carefully reviewed and a approach for field instrumentation was developed. It was concluded that there is one parameter in the program, referred to as “permanent curl/wrap effective temperature difference” that needs calibration. The default value used in the program is -10 degree F and the output is extremely sensitive to this parameter. A strategy to extract this parameter from field data was developed and presented to NDOR. The approach developed is very unique and it is not mentioned in any other published literatures related to calibration of MEPDG.

After consultation with NDOR, it was concluded that the complexity of the problem, does not warrant, at this point, proceeding with field instrumentation and final calibration of the MEPDG. The information presented in this report provides comprehensive guidelines for proceeding with final calibration of the MEPDG for Nebraska application. The final calibration demands collecting field data for at least three to four years and the step by step procedure for accomplishing this task is outlined in this report.

Chapter 1

Background

Mechanistic Empirical (M-E) Pavement Design is the new approach to analyze and design pavements. Unlike the old designs which are only empirical M-E design is composed of both mechanistic and empirical parts. Where stresses and strains in the pavements are calculated through mechanistic part and then related to pavement distresses through empirical part. To do all this work automatically and in a short span of time, a computer program, Mechanistic Empirical Pavement Design Guide (MEPDG), may be used.

When using the program the designer selects a pavement type, develops a trial design, and provides traffic, climate, material, and structural inputs. The software then estimates the damage for this trail design using mechanistic analysis tools and predicts key distresses over the design life using field-calibrated performance models.

The trial design is then evaluated for adequacy through the prediction of key distresses and smoothness. If the design does not meet desired performance criteria, it is revised and the evaluation process repeated as necessary to meet performance and reliability requirement. Thus, the designer is fully involved in the design process and has the flexibility to consider different design features and materials for the prevailing site conditions. This approach makes it possible to optimize the design and to more fully insure that specific distress types will not develop.

The pavement design approach developed in this design procedure is based on existing techniques as well as some new ones developed to address visco-plasticity and elasto-plasticity. All materials are initially considered linearly elastic, but as time progresses, the visco-elasticity, and then visco-plasticity are introduced into the system using various mechanical principles and laboratory results. Base course and subgrade materials are considered as linear elastic.

The overall objective of the Guide for the Mechanistic-Empirical Design of New and Rehabilitated Pavement Structures is to provide the highway community with a state-of-the-practice tool for the design of new and rehabilitated pavement structures, based on mechanistic-empirical principles.

The mechanistic-empirical (M-E) format of the Design Guide provides a framework for future continuous improvement to keep up with changes in trucking, materials, construction, design concepts, computers, and so on. In addition, guidelines for implementation and staff training have been prepared to facilitate use of the new design procedure, as well as strategies to maximize acceptance by the transportation community.

This approach to design provides the designer with a lot of flexibility in obtaining the design inputs for a design project based on the criticality of the project and the available resources. The hierarchical approach is employed with regard to traffic, materials, and environmental inputs.

In general, the design guide has two types of inputs: General Inputs and Categorical Inputs.

General Inputs: These Inputs require only one value and unlike categorical inputs doesn't have three levels of inputs.

Categorical Inputs: These inputs have three levels of inputs with the Level one being the most ideal and Level 3 the default. Following is the detailed information about these three levels.

Level 1 inputs provide for the highest level of accuracy and thus, would have the lowest level of uncertainty or error. These inputs would typically be used for designing heavily trafficked pavements or wherever there is dire safety or economic consequences of early failure. Level 1 material input require laboratory or field testing, such as the dynamic modulus testing of hot-mix asphalt concrete, site-specific axle load spectra data collections, or nondestructive deflection testing. Obtaining Level 1 inputs requires more resources and time than the other levels.

Level 2 inputs provide an intermediate level of design input and would be closest to the typical procedures used for many years with earlier editions of the AASHTO Guide. This level could be used when resources or testing equipment are not available for tests required for Level 1. Level 2 inputs typically would be user selected possibly from an agency database, could be derived from a limited testing program, or could be estimated through correlations. Examples would be dynamic modulus estimated from binder, aggregate, and mix properties, or PCC elastic moduli estimated from compressive strength tests, or site-specific traffic volume and traffic classification data used in conjunction with agency specific axle load spectra.

Level 3 inputs provide the lowest level of accuracy. This level might be used for design where there are minimal consequences of early failure (lower volume roads). Inputs typically would be user selected default values or typical averages for the region. Examples include default AC dynamic modulus values or default PCC elastic moduli for a given mix classes used by an agency.

Note that the levels used can vary from input parameter to input parameter, which makes the procedure even more open and flexible. For example, on a given project, a designer could use a Level 1 subgrade resilient modulus input value combined with a Level 3 traffic distribution data.

Table 1-1 provides a summary of all the inputs used for designing New JPCP Pavements:

Table 1-1. Summary of all the inputs used for designing New JPCP Pavements (Stanigzai 2007)

		General Inputs	Level I	Level II	Level III
Performance Criteria		Reliability	No Categorical Inputs		
Traffic		- Initial two-way AADTT - Number of lanes in design direction - Percent of trucks in design direction - Percent of trucks in design lane - Operational speed (mph) - Traffic Growth Factor - Hourly Truck Distribution - Mean wheel location (inches from the lane marking) - Traffic wander standard deviation (in) - Design lane width (ft) - Number of Axles per Truck - Average axle width (edge-to-edge) outside dimensions (ft) - Dual tire spacing (in) - Tandem axle Spacing - Tridem axle Spacing - Quad axle Spacing - Wheelbase Distribution Information (% of trucks & their axle spacing in ft)	- Monthly Adjustment Factors (Actual) - AADTT Distribution by Vehicle Class (Actual) - Axle Load Distribution Factors (Actual)	No Level II Inputs	- Monthly Adjustment Factors (Default) - AADTT Distribution by Vehicle Class (Default) - Axle Load Distribution Factors (Default)
Climate		- Depth of Water Table - Regional Climate Difference	No Categorical Inputs		
Material	**JPCP Design Features**	- Surface Short-Wave absorptivity - Permanent Curl/Wrap effective temperature difference (°F) - Joint Spacing (ft) - Sealant Type - Dowel diameter (in) - Dowel Bar Spacing (in) - Tied PCC Shoulder, Long-term LTE (%) - Widened Slab, Slab Width (ft) - PCC-Base Interface - Erodibility Index	No Categorical Inputs		
	PCC Material Properties	- PCC Layer Thickness (in) - PCC Unit Weight (pcf) - PCC Poisson's Ratio - PCC Coefficient of thermal expansion (per F° x 10- 6): - Thermal conductivity (BTU/hr-ft-F°) : - Heat capacity (BTU/lb-F°) - Cement Type - Cementitious Material content (lb/yd^3) - Water/Cement Ratio - Aggregate Type - Reversible Shrinkage (% of Ultimate Shrinkage) - Time to develop 50% of ultimate shrinkage (days) - Curing Method	- 7 day Modulus of Elasticity (psi) - 7 day Rupture Modulus (psi) - 14 day Modulus of Elasticity (psi) - 14 day Rupture Modulus (psi) - 28 day Modulus of Elasticity (psi) - 28 day Rupture Modulus (psi) - 90 day Modulus of Elasticity (psi) - 90 day Rupture Modulus (psi) - Ratio of 20-year to 28-day for Modulus of Elasticity - Ratio of 20-year to 28-day for Rupture Modulus	- 7 day Compressive Strength (psi) - 14 day Compressive Strength (psi) - 28 day Compressive Strength (psi) - 90 day Compressive Strength (psi) - Ratio of 20-year to 28-day of Compressive Strength	- 28-day PCC Modulus of Rupture (psi) - 28-day PCC Compressive Strength (psi) - 28-day PCC Elastic Modulus (psi)
	Granular Material	- Material Type - Material Thickness (in) - Poisson's ratio - Coefficient of lateral pressure (Ko)	No Level One Inputs	- Resilient Modulus	- Resilient Modulus
	Stabilized Base	- Material Type - Layer thickness (in) - Unit Weight (pcf) - Poisson's ratio - Elastic/Resilient Modulus (psi) - Thermal Conductivity (BTU/hr-ft-F°) - Heat Capacity (BTU/lb-F°)	No Categorical Inputs		
	Bedrock	- Material Type - Layer Thickness (in) - Unit Weight (pcf) - Poisson's ratio - Resilient Modulus (psi)	No Categorical Inputs		

1.2 Organization of the report

This report consists of six chapters plus an appendix.

Chapter One introduces the reader a background to the Mechanistic Empirical Pavement Design procedure.

Chapter Two provides a general understanding of how MEPDG works. This chapter provides the analysis procedure used in MEPDG software at first. Subsequently the JPCP distress models used in MEPDG are explained.

Chapter Three addresses the parametric study performed on the MEPDG inputs in order to investigate the sensitivity of the MEPDG results to any of the input parameters.

Chapter Four provides the proposed method in order to determine a very sensitive MEPDG entry through field instrumentation.

Chapter Five is devoted to the conclusions of the performed study.

Chapter Six is the references used in various chapters of the report.

Appendix A demonstrates the graphs associated with the sensitivity analyses done in chapter three.

Chapter 2

General Overview of MEPDG Procedure

In this chapter the analysis method used in the Mechanistic-Empirical Pavement Design Guide (MEPDG) is explained. Once the stresses of the Jointed Plain Concrete Pavement (JPCP) are determined via this analysis, they are entered into the distress models in order to determine the distresses in the pavements. These models are explained in the following sections of this chapter.

2.1 Analysis of the pavement structure

In order to model a concrete pavement section in finite element method (ex. using ILLI-Slab or ABAQUS, etc.), the most widely adopted mechanistic idealization is a plate on a dense liquid (DL) foundation.

2.1.1 Computation of Effective Dynamic k-Value

The real structure with all of the actual layers is modeled and the deflection profile of the surface is developed. Since typically the deviator stresses under a concrete slab and base course is lower than what is used in laboratory modulus of resilient testing, the subgrade resilient modulus of the pavement structure in the modeling is adjusted such a way that reflects the lower deviator stresses. Now, the computed deflection profile is used to back-calculate the effective dynamic k-value.

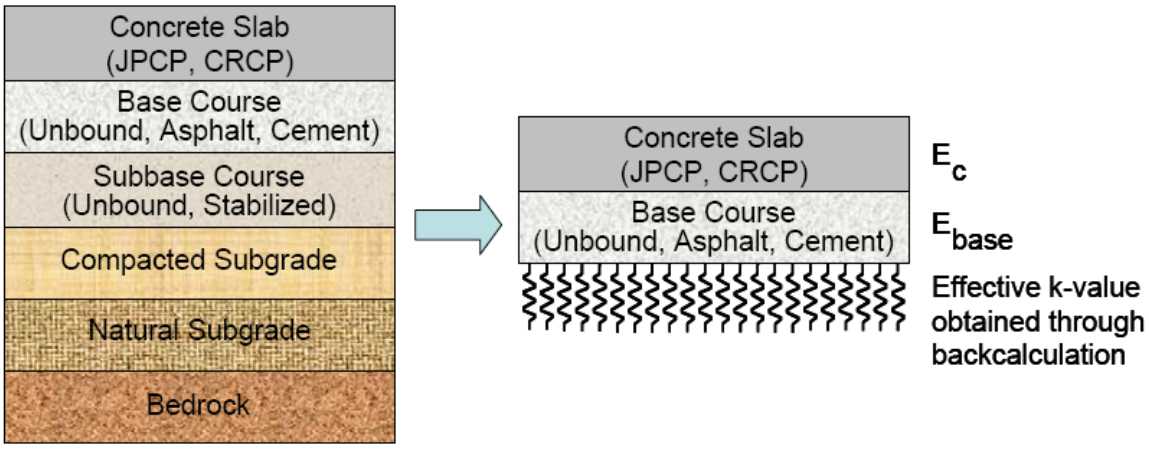

Figure 2-1. Structural model for rigid pavement structural response computations (NCHRP 2003; Appendix QQ).

2.1.2 Determination of critical bending stresses at the bottom surface of JPCP (Jointed Plane Concrete Pavement)

The maximum bending stress from edge loading at the mid-slab location of a JPCP is the critical response that leads to bottom-up fatigue cracking. In fact, the maximum stress due to the combination of edge stress from traffic loading and curling from temperature, shrinkage, and initial condition that leads to fatigue damage needs to be determined.

2.1.3 Equivalency Concept

2.1.3.1 Equivalent Single Layer Slab Concept

The multilayered PCC pavement section is substituted with the equivalent single layer slab which results in the same deflection profiles (NCHRP 2003; Appendix QQ). Now, the stresses in the two-layered slab can be found from the corresponding stresses in the equivalent homogeneous modeled plate.

If no friction exists between the PCC and the base layers, and if the equivalent slab has the same modulus of elasticity and Poisson's ratio as the PCC layer, then the thickness of the equivalent slab can be determined as follows:

$$h_{eff} = \sqrt[3]{h_{pcc}^3 + \frac{E_{base}}{E_{PCC}} h_{base}^3} \qquad 2\text{–}1$$

where

h_{eff} = equivalent slab thickness
E_{PCC} = PCC modulus of elasticity
E_{base} = base modulus of elasticity
h_{PCC} = PCC thickness
h_{base} = base thickness

If full bond exists between the PCC and the base layers then the thickness of the equivalent slab is defined as follows:

$$h_{eff} = \sqrt[3]{h_{PCC}^3 + \frac{E_{base}}{E_{PCC}} h_{base}^3 + 12\left(h_{pcc}\left(x - \frac{h_{PCC}}{2} \right)^2 + \frac{E_{base}}{E_{PCC}}\left(h_{PCC} + \frac{h_{base}}{2} - x \right)^2 h_{base} \right)} \qquad 2\text{–}2$$

where

h_{eff} = equivalent slab thickness
E_{PCC} = PCC modulus of elasticity
E_{base} = base modulus of elasticity
h_{PCC} = PCC thickness
h_{base} = base thickness
x = distance between the neutral plane and the top surface of the PCC layer which can be determined from the following equation:

$$x = \frac{\frac{h_{PCC}^2}{2} + \frac{E_{base}}{E_{PCC}} h_{base}\left(h_{PCC} + \frac{h_{base}}{2}\right)}{h_{PCC} + \frac{E_{base}}{E_{PCC}} h_{base}} \quad 2–3$$

If a JPCP is subjected to an axle loading only (no curling), and if the stresses in the equivalent slab are known, then the corresponding PCC stresses at the bottom of the PCC slab can be found using the following relationship:

Unbonded interface

$$\sigma_{PCC} = \frac{h_{PCC}}{h_e}\sigma_{eff} \quad 2–4$$

Bonded interface

$$\sigma_{PCC} = \frac{2(h_{PCC} - x)}{h_e}\sigma_{eff} \quad 2–5$$

where

σ_{eff} = bottom surface stresses in the equivalent slab
σ_{PCC} = bottom surface PCC stresses
h_{PCC} = PCC thickness
h_{eff} = equivalent slab thickness
x = distance between the neutral plane and the top surface of the PCC layer.

2.1.4 Step-By-Step Procedure for Determination of Critical Bottom Surface Stress in JPCP

Using the trained NN (Neural Networks), JPCP stresses can be determined for a wide range of site conditions, design parameters, and axle loading (NCHRP 2003; Appendix QQ). The detailed procedure is described below.

Step 1. Calculate the Equivalent Slab Thickness

If a PCC slab is not bonded with the base layer then the equivalent slab thickness is determined using equation 2–1; otherwise it is determined using equation 2–2.

Step 2. Calculate Unit Weight of the Equivalent Slab

$$\gamma_{eff} = \frac{\gamma_{PCC} h_{PCC}}{h_{eff}} \quad 2–6$$

where

γ_{eff} = effective unit weight
h_{pcc} = PCC slab thickness
γ_{PCC} = PCC unit weight
h_{eff} = effective unit thickness

Step 3. Calculate Radius of Relative Stiffness

$$l = \sqrt[4]{\frac{E_{PCC} h_{eff}^3}{12 \times (1 - \mu_{eff}^2) \times k}} \qquad 2\text{–}7$$

where

l = radius of relative stiffness
h_{eff} = effective thickness
E_{PCC} = PCC elastic modulus
μ_{PCC} = PCC Poisson's ratio
k = coefficient of subgrade reaction

Step 4. Calculate Effective Temperature Differential

Equivalent temperature difference is determined from equation 2–8 if the interface between the PCC slab and the base is unbonded and from equation 2–9 if the interface between the PCC slab and the base is bonded.

$$\Delta T_{eff} = \frac{12}{h_{eff}^2} \times \int_{-\frac{h_{pcc}}{2}}^{\frac{h_{pcc}}{2}} \left(T(z) - T(\frac{h_{pcc}}{2}) \right) z dz \qquad 2\text{–}8$$

$$\Delta T_{eff} = \frac{12}{h_{eff}^2} \times \int_{-x}^{h_{pcc}-x} \left(T(z) - T(h_{pcc} - x) \right) z dz \qquad 2\text{–}9$$

Where

ΔT_{eff} = difference between temperatures at the top and bottom surfaces of the effective slab.
h_{pcc} = PCC slab thickness.
h_{eff} = Effective slab thickness computed.
$T(z)$ = temperature distribution through the PCC and base layers.
Z = vertical coordinate measured downward from the neutral axis of the PCC slab (unbonded interface) or the composite slab (bonded interface)

Step 5. Compute Korenev's Nondimensional Temperature Gradient

$$\phi = \frac{2\alpha_{PCC}(1 + \mu_{PCC}) l^2}{h_{eff}^2} \frac{k}{\gamma_{eff}} \Delta T_{eff} \qquad 2\text{–}10$$

where

ϕ = Nondimensional Temperature Gradient
h_{PCC} = PCC thickness
α_{PCC} = PCC coefficient of thermal expansion
μ_{PCC} = PCC Poisson's ratio for PCC
γ_{eff} = effective unit weight

k = coefficient of subgrade reaction
l = radius of relative stiffness
ΔT_{eff} = effective temperature gradient

Step 6. Compute Adjusted Load/Pavement Weigh Ratio (Normalized Load)

$$q^* = \frac{P}{LW\gamma_{eff}h_{eff}} \qquad 2\text{–}11$$

where
q^* = adjusted load/pavement weight ratio
P = axle weight
h_{PCC} = PCC thickness
γ_{PCC} = PCC unit weight
L = slab length
W = Slab width

Step 7. Calculate Effective Slab Thickness

The effective slab thickness is a thickness of the slab with the modulus of elasticity and Possion's ratio equal to 4,000,000 psi and 0.15, respectively, resting on the Winkler foundation with the coefficient of subgrade reaction equal to 100 psi/in, and having the same radius of relative stiffness as the equivalent slab. The effective slab is determined using the following equation:

$$h_{eq} = \sqrt[3]{\frac{l^4}{3410}} \qquad 2\text{–}12$$

h_{eq} = equivalent slab thickness, in.
l = radius of relative stiffness, in.

Step 8. Compute Curling-Related Stresses in the Effective Slab

Using NNs (Neural Networks), compute stresses in the effective plate which has the same ratio of radius of relative stiffness to joint spacing, traffic offset and appropriate Korenev's nondimensional temperature gradient, φ, and normalized load ratio q*. If the pavement is loaded by a single axle load, then use the neural network NNA1. For tandem or tridem loads use NNA2. The following cases should be considered:

Case I - resulting stress $\sigma_{eff}^{A}(P,\Delta T)$: Korenev's nondimensional temperature gradient, φ, is equal to the nondimensional temperature gradient determined in Step 5; normalized load ratio q* is equal to normalized load ratio determined in Step 6.

Case II - resulting stress $\sigma_{eff}^{A}(0,\Delta T)$: Korenev's nondimensional temperature gradient, φ, is equal to the nondimensional temperature gradient determined in Step 5; normalized load ratio q* is equal to 0.

Case III - resulting stress $\sigma_{eff}^{A}(P,0)$: Korenev's nondimensional temperature gradient, φ, is equal to 0; normalized load ratio q* is equal to normalized load ratio determined in Step 6.

Step 9. Compute Curling-Related Stresses in the Equivalent Structure

The stresses obtained in step 8 represent stresses in the slab with the modulus of elasticity and Possion's ratio equal to 4,000,000 psi and 0.15, respectively, resting on the Winkler foundation with the coefficient of subgrade reaction equal to 100 psi/in, and having the same radius of relative stiffness as the equivalent slab. Now having that, the stresses in the equivalent slab are determined using the following equation:

$$\sigma^{A}(P,\Delta T)=\frac{h_{eff}\gamma_{eq}}{h_{eq}\gamma_{eff}}\sigma_{eff}^{A}(P,\Delta T) \qquad 2\text{–}13$$

$$\sigma^{A}(0,\Delta T)=\frac{h_{eff}\gamma_{eq}}{h_{eq}\gamma_{eff}}\sigma_{eff}^{A}(0,\Delta T) \qquad 2\text{–}14$$

$$\sigma^{A}(P,0)=\frac{h_{eff}\gamma_{eq}}{h_{eq}\gamma_{eff}}\sigma_{eff}^{A}(P,0) \qquad 2\text{–}15$$

where

σ^{A} = stress in the equivalent structure
σ_{eff}^{A} = stress in the effective structure (Obtained using NNs0)
h_{eff} = effective slab thickness
h_{eq} = equivalent slab thickness
γ_{eff} = effective slab unit weight
γ_{eq} = equivalent slab unit weight
= 0.087 lb/in^2

Step 10. Using NB1, Compute Load-only Caused Stresses in the Effective Structure from the Wheels Located at the Mid-slab

In the case of a single axle loading, compute stresses from all wheels in the axle. In the case of tandem or tridem axle loading, ignore wheels located away from the slab mid-slab, as shown in Figure 2-2.

Step 10.1 Compute stresses in the effective structure assuming that there is no load transfer between the slabs in the system B (LTE=0). If the axle consists from dual tires, subdivide it into two sub-axles as shown in Figure 2-3. Calculate stresses separately from these sub-axles and superimpose the resulting stresses to obtain $\sigma_{eff}^{B1}(0)$.

Step 10.2 Compute stresses in the effective structure assuming that the load transfer efficiency between two slabs in the system B is equal to shoulder LTE. If the axle consists from dual tires, subdivide it into two sub-axles. Calculate stresses

separately from these sub-axles and superimpose the resulting stresses to obtain $\sigma_{eff}^{B1}(LTE_{sh})$.

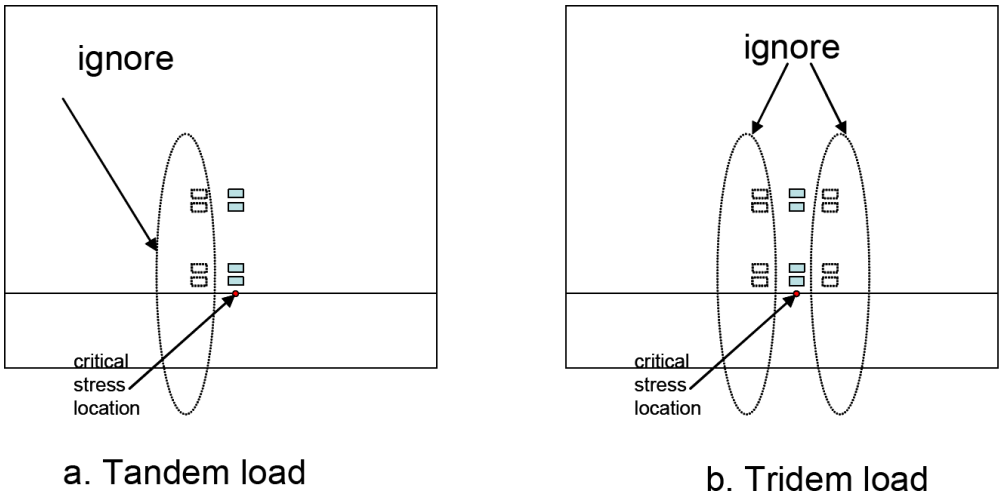

Figure 2-2. Analysis of tandem and tridem axle loading using NNB1 (NCHRP 2003; Appendix QQ).

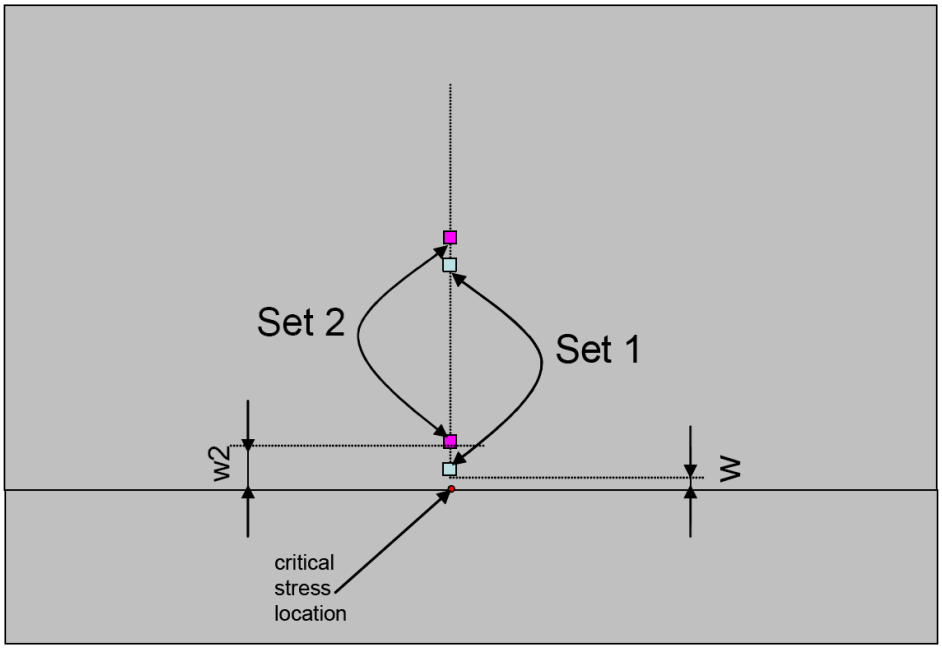

Figure 2-3. Analysis of a single axle load with dual tires using NNB1 (NCHRP 2003; Appendix QQ).

Step 11. (only if tandem or tridem). Compute Stresses from the Remaining Wheels in the Axle using NNB2

Step 11.1 Compute stresses in the effective structure assuming that there is no load transfer between the slabs in the system B (LTE=0). The stresses should be computed from the individual wheels (four for a tandem axle and eight for a tridem). Superimpose these stresses to obtain $\sigma_{eff}^{B2}(0)$.

Step 11.2 Compute stresses in the effective structure assuming that the load transfer efficiency between two slabs in the system B is equal to shoulder LTE. The stresses should be computed from the individual wheels (four for a tandem axle and eight for a tridem). Superimpose these stresses to obtain $\sigma_{eff}^{B2}(LTE_{sh})$.

Step 12. Determine Load-only Caused Stresses in the Effective Structure from the Entire Axle

- Single axle loading

$$\sigma_{eff}^{B}(0) = \sigma_{eff}^{B1}(0) \quad 2\text{–}16$$

$$\sigma_{eff}^{B}(LTE_{sh}) = \sigma_{eff}^{B1}(LTE_{sh}) \quad 2\text{–}17$$

- Tandem or tridem laoding

$$\sigma_{eff}^{B}(0) = \sigma_{eff}^{B1}(0) + \sigma_{eff}^{B2}(0) \quad 2\text{–}18$$

$$\sigma_{eff}^{B}(LTE_{sh}) = \sigma_{eff}^{B1}(LTE_{sh}) + \sigma_{eff}^{B2}(LTE_{sh}) \quad 2\text{–}19$$

Step 13. Determine Load-only Caused Stresses in the Equivalent Structure

The load-only causing stresses in the equivalent structure can be determined using the following expression:

$$\sigma^{B}(0) = \frac{p}{p_{eff}} \frac{h_{eff}^2}{h_{eq}^2} \sigma_{eff}^{B}(0) \quad 2\text{–}20$$

$$\sigma^{B}(LTE_{sh}) = \frac{p}{p_{eff}} \frac{h_{eff}^2}{h_{eq}^2} \sigma_{eff}^{B}(LTE_{sh}) \quad 2\text{–}21$$

where

$\sigma_{eff}^{B}(0)$ = stresses in the effective structure if there is no load transfer between the slabs in the system B (LTE=0)

$\sigma_{eff}^{B}(LTE_{sh})$ = stresses in effective structure if the load transfer efficiency between two slabs in the system B is equal to shoulder LTE.

$\sigma^{B}(0)$ = stresses in the equivalent structure if there is no load transfer between the slabs in the system B (LTE=0)

$\sigma^{B}(LTE_{sh})$ = stresses in equivalent structure if the load transfer efficiency between two slabs in the system B is equal to shoulder LTE.

h_{eff} = effective slab thickness

h_{eq} = equivalent slab thickness

p_{eff} = wheel pressure in the effective system
= 100 psi

p = actual wheel pressure

Step 14. Find Stress Load Transfer Efficiency for the Given Axle Load Configuration and the Axle Load Position

$$LTE_{stress} = \frac{\sigma^{B}(LTE_{sh})}{\sigma^{B}(0)} \quad 2\text{–}22$$

Step 15. Find Axle Loading Induced Component of Bending Stresses (stress in the slab caused by the action of axle loading on top of the temperature curling) in the Equivalent Structure if the Shoulder Provides no Edge Support to the Traffic Lane Slab

$$\sigma_{load,no\ shoulder} = \sigma^{A}(P,\Delta T) - \sigma^{A}(0,\Delta T) - \sigma^{A}(P,0) - \sigma^{B} \quad 2\text{–}23$$

Step 16. Find Axle Loading Induced Component of Bending Stresses (stress in the slab caused by the action of axle loading on top of the temperature curling) Accounting for the Shoulder Edge Support to the Traffic Lane Slab

$$\sigma_{load,shoulder} = \sigma_{load,no\ shoulder} \times LTE_{stress} \quad 2\text{–}24$$

Step 17. Find Combined Stress in the Equivalent System

$$\sigma_{comb} = \sigma_{load,shoulder} + \sigma_{curl} \quad 2\text{–}25$$

Step 18. Find Bending PCC Stresses

Bending stresses (i.e., stresses caused by an axle load and a linear component of the temperature distribution) at the bottom of the PCC slab can be found using the following relationship:

- Unbonded interface

$$\sigma_{PCC,bend} = \frac{h_{pcc}}{h_e}\sigma_{comb} \quad 2\text{–}26$$

- Bonded interface

$$\sigma_{PCC,bend} = \frac{2(h_{pcc} - x)}{h_e}\sigma_{comb} \quad 2\text{–}27$$

where

σcurl = curling stresses in the equivalent slab
σPCC,bend = bottom surface PCC bending stresses
hPCC = PCC thickness
heff = equivalent slab thickness
x = distance between the neural plane and the top surface of the PCC layer

Step 19. Find Total PCC Stresses

$$\sigma_{PCC} = \sigma_{pcc,bend} + \sigma_{NLT} \quad 2\text{–}28$$

where

σ_{pcc} = total stress at the bottom of the PCC slab

$\sigma_{PCC} = \sigma_{pcc,bend} + \sigma_{NLT}$ = bending stress at the bottom of the PCC slab

$\sigma_{PCC} = \sigma_{pcc,bend} + \sigma_{pcc,NLT}$ = stress at the bottom of the PCC layer caused by the nonlinear strain component of the temperature distribution.

2.1.5 NN (Neural Network) Development

Equivalency concepts and the models presented above allow the reduction of number of independent parameters and reduction of the number of cases needed to be considered for successful training of the neural networks for rapid prediction of critical PCC stresses at the bottom of the PCC slab (NCHRP 2003; Appendix QQ). In order to perform the calculations, the following neural networks have been developed:

- NNA1 - for prediction of the maximum edge stresses at the bottom of a single slab subjected to a temperature curling and a single axle loading (Figure 2-4).
- NNA2 - for prediction of the maximum edge stresses at the bottom of a single slab subjected to a temperature curling and a tandem axle loading-NNA1 (Figure 2-5).
- NNB1 - for prediction of the maximum stresses at the bottom of a two-slab system (system B) subjected to a single axle single wheel loading (Figure 2-6).
- NNB2 - for prediction of the maximum stresses at the bottom of a two-slab system (system B) subjected to a single wheel loading (Figure 2-7).

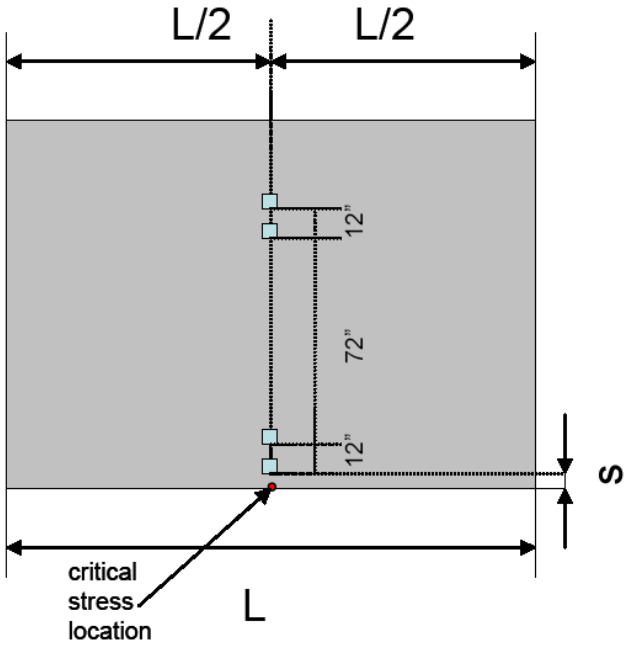

Figure 2-4. Structural model for the NNA1 (NCHRP 2003; Appendix QQ).

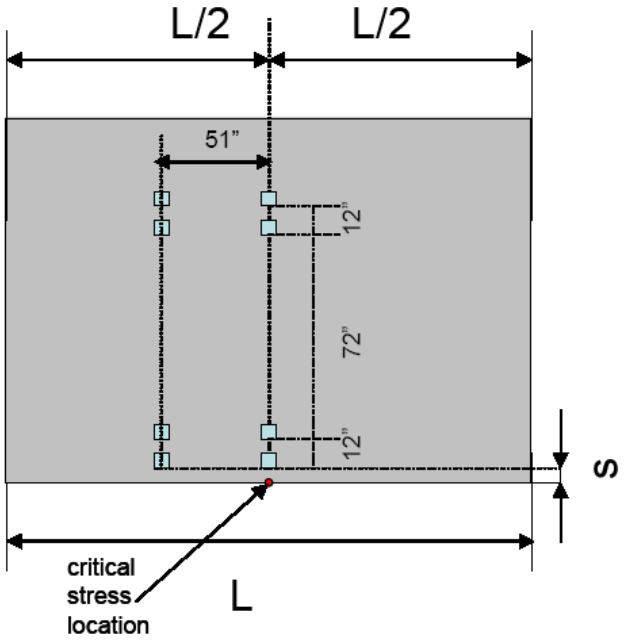

Figure 2-5. Structural model for the NNA2 (NCHRP 2003; Appendix QQ).

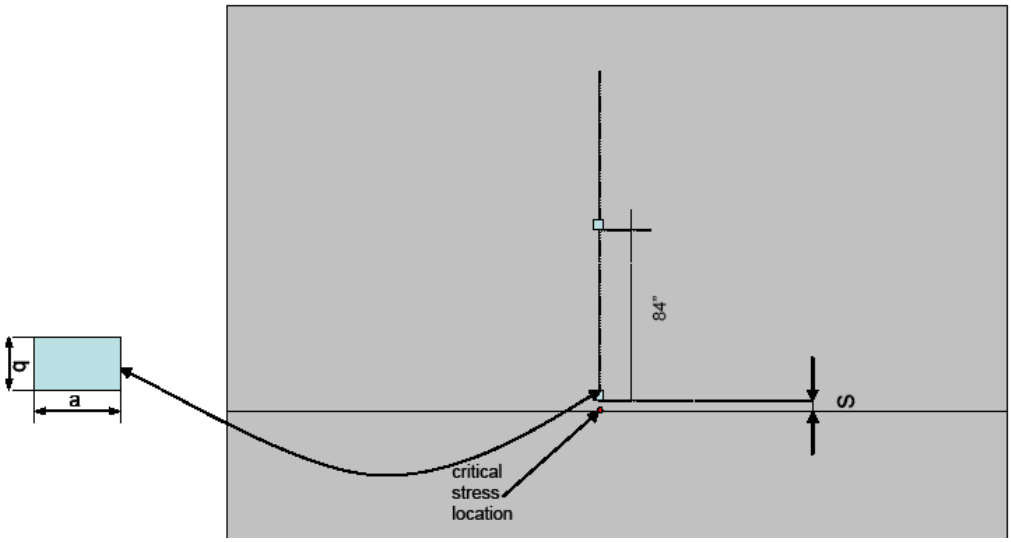

Figure 2-6. Structural model for the NNB1 (NCHRP 2003; Appendix QQ).

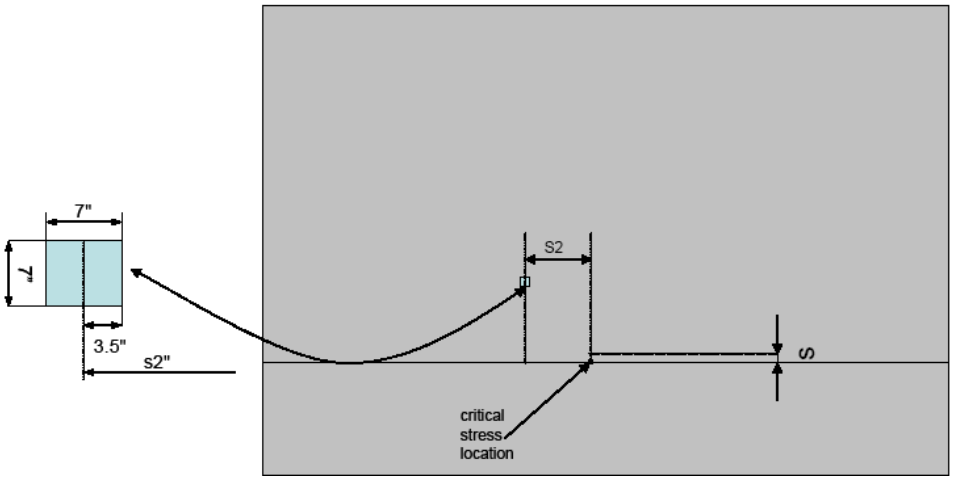

Figure 2-7. Structural model for the NNB2 (NCHRP 2003; Appendix QQ).

In order to train the databases NN1 and NN2 two factorials of 14175 ISLAB2000 runs each were performed. A single-layer slab was analyzed in all cases. The slab width, modulus of elasticity, Poisson's ratio, unit weight, and coefficient of thermal expansion were set equal to 12 ft, 4,000,000 psi, 0.15, 0.087 lb/in^3, and 5.5*10^{-6} 1/^{o}F, respectively. Each tire footprint was modeled using a square with a 7-in side. The coefficient of subgrade reaction was set equal to 100 psi/in. The following parameters were varied:

- Slab length. Slab lengths of 9, 15, 21, 27, and 33 ft were analyzed.
- L/l ratios. L/l ratios of 1.5, 3.5, 4.5, 5.5, 6.5, 7.5, 9.5, 12, and 14.5 were analyzed. To achieve it, the PCC slab thickness was varied 1 in to 112 in.
- Wheel offset was varied from 0 to 36 in (0, 2, 4, 6, 12, 24, and 36 in).
- Korenev's non-dimensional temperature gradient was varied from 0 to 200 (0, 5, 10, 15, 20, 25, 50, 100, and 200).

- Axle weight was varied to set the axle weight to slab weight ratio equal to 0, 1, 2, 3 or 4.

Since some of the ranges above are presented in terms of normalized or dimensionless parameters, it makes it somewhat difficult to understand the ranges of applicability of the database. To illustrate it in terms of real inputs, a baseline case was selected and one parameter at time was allowed to vary. Table 2-1 presents the baseline parameters and calculated ranges for those parameters.

Table 2-1. Ranges of NNA1 and NNA2 parameters if others are equal to the baseline values (NCHRP 2003; Appendix QQ).

Variable	Baseline value	Min value	Max value
PCC thickness, in	9	5.1	27.7
PCC modulus of elasticity, psi	4,500,000	154,000	24,6170,950
Base , in	6	0	>30
Base modulus of elasticity, psi	40,000	0	>10,000,000
PCC coefficient of thermal expansion	5.50E-06	0	5.50E-05
PCC unit weight, lb/in^3	0.087	0	0.87
k-value, psi/in	200	7	1094
Temperature differential, °F	10	0	>100
Axle weight, lb	18,000-NNA1	0	>60,000
	34,000 – NNA2	0	>120,000

2.2 Response Models Used in MEPDG

The model types considered in JPCP are:

- Faulting.
- Transverse cracking.
- IRI.

2.2.1 Transverse Joint Faulting Model

Transverse joint faulting is the differential elevation across the joint measured approximately 1 ft from the slab edge (longitudinal lane to shoulder joint for a conventional 12-ft lane width), or from the lane paint stripe for a widened slab (NCHRP 2003; Appendix JJ). Since joint faulting varies significantly from joint to joint, the mean faulting of all transverse joints in a given section is the parameter predicted by the model used in this Guide for performance evaluation. Faulting is an important deterioration mechanism of JPCP because of its impact on ride quality. Joint faulting also has a major impact on the life cycle costs of rehabilitated pavements, both in terms of increased costs due to early failure of the rehabilitation strategy and on vehicle operating costs as faulting becomes severe.

Transverse joint faulting is the result of a combination of moving heavy axle loads, poor joint load transfer, free moisture beneath the PCC slab and/or base, and base/subbase erosion.

Equations 2–29 through 2–32 are used to predict transverse joint faulting for restored JPCP and JPCP overlays (NCHRP 2003; Appendix JJ):

$$Fault_m = \sum_{i=1}^{m} \Delta Fault_i \qquad 2–29$$

$$\Delta Fault_i = C_{34} \times (FAULTMAX_{i-1} - Fault_{i-1})^2 \times DE_i \qquad 2–30$$

$$FAULTMAX_i = FAULTMAX_0 + C_7 \times \sum_{j=1}^{m} DE_j \times Log(1 + C_5 \times 5.0^{EROD})^{C_6} \qquad 2–31$$

$$FAULTMAX_0 = C_{12} \times \delta_{curling} \times \left[Log(1 + C_5 \times 5.0^{EROD}) \times Log\left(\frac{P_{200} \times WetDays}{p_s} \right) \right]^{C_6} \qquad 2–32$$

where

$Fault_m$ = mean joint faulting at the end of month m, in (at 50 percent reliability)
$\Delta Fault_i$ = incremental change (monthly) in mean transverse joint faulting during month i, in
$FAULTMAX_i$ = maximum mean transverse joint faulting for month i, in
$FAULTMAX_0$ = initial maximum mean transverse joint faulting, in
EROD = base (layer beneath the PCC slab) erodibility factor
DE_i = differential deformation energy accumulated during month i
$\delta curling$ = maximum mean monthly slab corner upward deflection of PCC due to temperature curling and moisture warping
p_s = overburden on subgrade, psi
p_{200} = percent subgrade material passing #200 sieve
WetDays = average annual number of wet days
$C_{12} = C_1 + C_2 \times FR^{0.25}$
$C_{34} = C_3 + C_4 \times FR^{0.25}$
FR = base freeze index defined as percentage of time the top base temperature is below freezing (32 ^{o}F) temperature
C_1 through C_7 = calibration constants

The functional form of the model reflects the hypothesis that faulting potential depends of amount of the PCC slab curling, base erodibility, and the presence of fines and free water in the subgrade. Faulting potential decreases with an increase of overburden pressure on the subgrade.

The rate of faulting development depends on the faulting level and decreases when faulting increases until it stabilizes to a certain level.

Prediction of transverse joint faulting in the 2002 Design Procedure involves the following steps (NCHRP 2003; Appendix JJ):

1. Tabulate input data – summarize all inputs needed for predicting JPCP transverse joint faulting.

2. Process input data and initialize parameters
3. Determine initial maximum faulting
4. Determine PCC free shrinkage strains
5. Calculate joint LTE
6. Calculate effective slab parameters
7. Calculate effective temperature gradient
8. Compute adjusted load/pavement weight ratios (normalized loads)
9. Compute critical deflections
10. Compute differential energy increment deflections
11. Find faulting increment
12. Find current faulting
13. Find current maximum faulting index
14. Evaluate loss of aggregate shear capacity
15. Calculate damage of doweled joins

Although some of the equations for faulting predictions have been presented above, they will be repeated as necessary, for the reader's convenience.

The incremental design procedure requires thousands of deflection calculations to compute damage monthly (for the different loads, joint stiffnesses, and equivalent temperature differences) over a design period of many years. These computations would take hours (if not days) using existing finite element programs. Thus, it is not practical to include a finite element program with the design guide software at this time. To reduce computer time to a practical level, neural networks (NNs) have been developed to accurately compute critical corner deflections virtually instantaneously. This makes it possible to conduct detailed incremental analysis (month by month) to sum damage over time in a realistic way. The neural networks reproduce the same deflections very accurately given the set of required inputs. Neural networks were developed separately for single, tandem, and tridem axles.

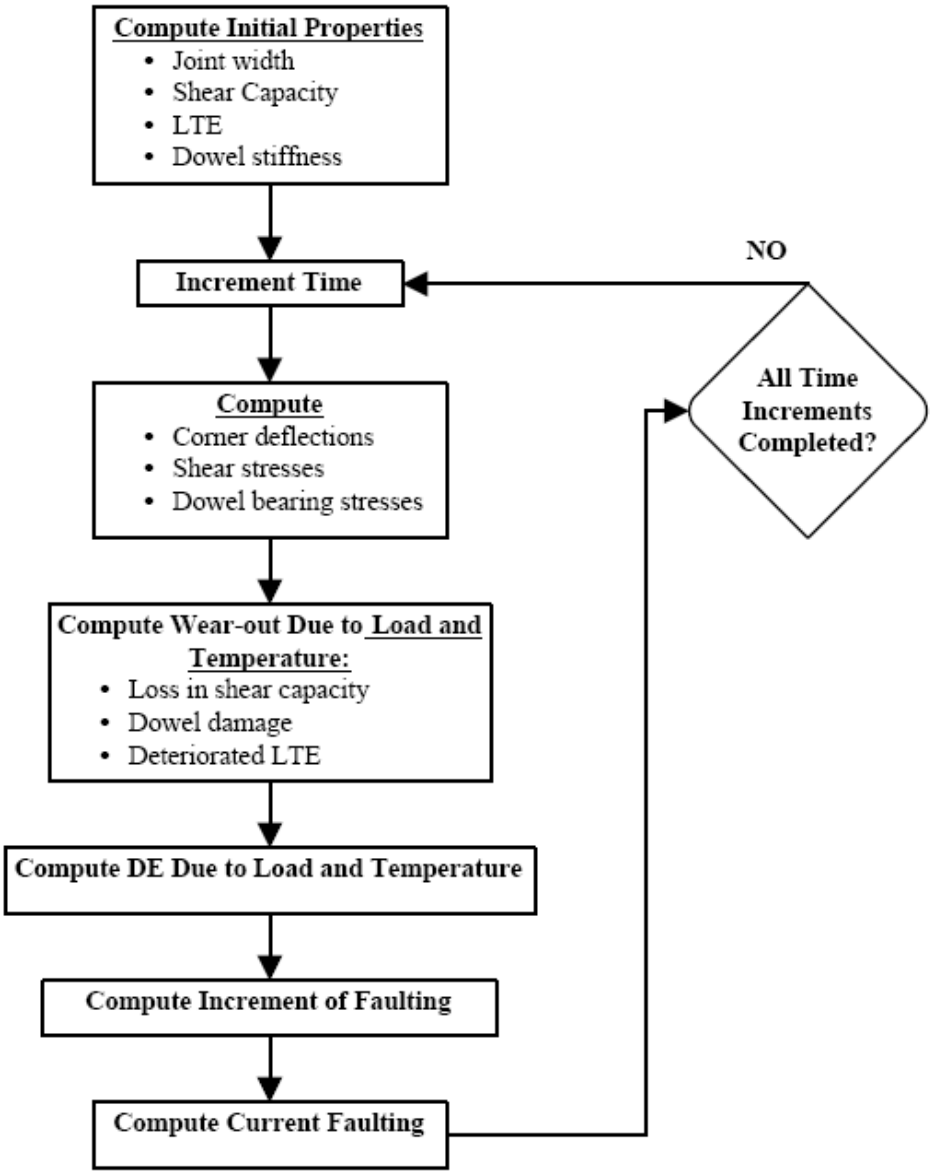

Figure 2-8. Flowchart showing the transverse joint faulting prediction process (computations will be performed by a neural network program) (NCHRP 2003; Appendix JJ).

Step 1: Tabulate input data

The 2002 Design Guide software conducts faulting analysis after execution of the traffic module, EICM module, and determination of the equivalent coefficient of subgrade reaction for each month. The required parameters for faulting predictions are prepared and tabulated by the software. These parameters are summarized in Table 2-2.

Step 2. Process input data and initiate parameters

Step 2.1 Process PCC temperature data

The EICM analysis performed prior to the faulting program generates PCC temperatures at 11 points throughout PCC thickness for each hour of the pavement

life after construction. For the faulting analysis, these data are reduced to the following parameters:

- Mean PCC mid-depth night temperature for each month of a year calculated as mean temperature for at the PCC slab mid-depth which occur in a certain month from 8 p.m. to 8 a.m. over the pavement design life
- Mean nighttime temperature difference between PCC slab top and bottom surfaces for each month of a year calculated as mean difference of temperature between PCC top and bottom surfaces which occur in a certain month from 8 p.m. to 8 a.m. over the pavement design life.
- Base freezing index - percentage of time the bottom of the PCC slab temperature was below 32 ^{o}F.

Table 2-2. Summary of input parameters for JPCP transverse joint faulting prediction (NCHRP 2003; Appendix JJ).

Input	Variation*	Source
Design life (months)	Fixed	Direct design input
Month of project opening	Fixed	Direct design input
PCC age at opening (mo)	Fixed	Direct design input
PCC strength for each month (psi)	Design mo	Result of PCC strength input processing (section 3.4.3.6 *Pavement Structure Input*)
PCC modulus for each month (psi)	Design mo	
Joint spacing (ft)	Fixed	Direct design input
Dowel diameter (in)	Fixed	Direct design input
Lane-shoulder deflection LTE (%)	Fixed	Direct design input
Widened slab (yes/no)	Fixed	Direct design input
Poisson's ratio	Fixed	Direct design input
PCC unit weight (pcf)	Fixed	Direct design input
Coefficient of thermal expansion (/°F)	Fixed	Direct design input
Ultimate shrinkage strain (10^{-6})	Fixed	Direct design input
Reversible shrinkage strain (10^{-6})	Fixed	Direct design input
Time to 50% ult. shrinkage (days)	Fixed	Direct design input
Base thickness (in)	Fixed	Direct design input
Base unit weight (pcf)	Fixed	Direct design input
Monthly base modulus (psi)	Calendar mo	Result of Seasonal Analysis (section 3.4.3.6 *Pavement Structure Input*)
Base erodibility	Fixed	Direct design input
Monthly effective subgrade k-value (psi/in)	Calendar mo	Results of "E-to-k" conversion (section 3.4.3.6 *Pavement Structure Input*)
Permanent curl/warp (°F)	Fixed	Direct design input
PCC zero-stress temperature	Fixed	Direct design input or estimated from construction month and cement content
Lane width (ft)	Fixed	Direct design input
Mean wheel path (in)	Fixed	Direct design input
Traffic wander standard deviation (in)	Fixed	Direct design input
Axle load spectrum for each month of pavement life	monthly	Results of traffic analysis
Slab width (ft)	Fixed	Direct design input

* Design mo: parameters that vary with pavement age; Calendar mo: parameters that vary seasonally.

Step 2.2 Determine maximum and average mean monthly relative humidity

The EICM analysis provides mean ambient relative humidity for each month of a year. From these values, the maximum value should be determined.

$$RH_{Max} = \max(RH_m) \qquad \text{m} = 1,12 \qquad \text{2–33}$$

$$RH_{average} = \frac{1}{12}\sum_{m=1}^{12} RH_m \qquad \text{2–34}$$

where

RH_{max} = max RH maximum ambient relative humidity
$RH_{average}$ = average RH average yearly ambient relative humidity
RH_m = m RH average monthly ambient relative humidity for month m.

Step 2.3 Determine base LTE for each month

The base LTE for each month depends on base type and the mean PCC temperature at the PCC mid-depth. If for a certain month the PCC mid-depth temperature is less than 32 ^{o}F, then the base LTE is assigned to be 90 percent; otherwise it is determined based on the base type from Table 2-3.

Table 2-3. Assumed effective base LTE for different base types

Base Type	LTE_{Base}
Aggregate base	20%
ATB or CTB base	30%
LCB base	40%

Step 2.4 Determine shoulder-lane LTE for each month

The shoulder-lane base LTE for faulting analysis is determined from the user-provided shoulder– lane LTE input. Considering that the LTE at nighttime near a transverse joint is lower than daytime LTE at mid-slab, shoulder LTE for the faulting analysis is reduced using the following equation:

$$LTE_{sh} = 5 + \frac{LTE_{shoulder,input}}{2} \qquad \text{2–35}$$

where

LTE_{sh} = Shoulder/lane deflection LTE used in faulting analysis.
$LTE_{shoulder,input}$ = User-provided shoulder/lane deflection LTE.

Step 2.5 Set initial parameters

Set initial values for the aggregate joint initial shear capacity, dowel damage, dowel joint stiffness, aggregate interlock damage, and aggregate interlock stiffness using the following equations:

$$\Delta S_{tot} = 0 \qquad \text{2–36}$$

$$J_0 = \frac{38.20 A_d}{h_{PCC}} \qquad 2\text{–}37$$

$$\text{DOWDAM}_0 = 0 \qquad 2\text{–}38$$

$$J_d^* = \begin{cases} 118 & if \ \frac{A_d}{h_{PCC}} > 0.835 \\ 52.52 \frac{A_d}{h_{PCC}} - 19.8 & if \ 0.039 \le \frac{A_d}{h_{PCC}} \le 0.835 \\ 0.4 & if \ \frac{A_d}{h_{PCC}} < 0.039 \end{cases} \qquad 2\text{–}39$$

where

S_0 = Initial cumulative loss of shear capacity of the aggregate joint.
DOWDAM0 = Initial damage of dowel/PCC contact.
J_0 = Initial nondimensional dowel stiffness.
J^*_d = Critical initial nondimensional dowel stiffness.
A_d = Area of dowel cross-section:
$= \pi d^2/4$
d = dowel diameter

Step 3. Determine initial maximum faulting

Step 3.1 Find effective slab thickness

Using representative PCC modulus of elasticity (modulus of elasticity at the end of the first year after opening of the pavement to traffic, find effective slab thickness for every month, m, to account for seasonal variation in the base modulus.

$$H_{eff,m} = \sqrt{h_{PCC}^2 + \frac{E_{BASE,m}}{E_{PCC}} H_{BASE}^2} \qquad \text{m} = 1,12 \qquad 2\text{–}40$$

where

Heff,m = Effective slab thickness.
hPCC = PCC slab thickness.
HBASE = Base thickness.
EPCC = Representative PCC modulus of elasticity
EBASE, m = Base modulus of elasticity for month m

Step 3.2 Calculate unit weight of the equivalent slab

The weight of a unit area of the effective slab should be equal to the weight of a unit area of the original two-layered (PCC slab and base). Since the base layer is assumed to be weightless, the weight of a unit area of the effective slab should be equal to the weight of a unit area of the PCC slab. However, since the effective slab thickness is different for different months then the unit weight of the effective slab should be adjusted as follows:

$$\gamma_{eff,m} = \frac{\gamma_{PCC} h_{PCC}}{H_{eff,m}} \qquad \text{m} = 1,12 \qquad 2\text{–}41$$

where

γ_{eff} = Effective unit weight.
h_{PCC} = PCC slab thickness.
γ_{PCC} = PCC unit weight.
h_{eff} = Effective thickness.

Step 3.3 Find radius of relative stiffness for this month

$$l_m = \sqrt[4]{\frac{E_{PCC} H_{eff,m}^3}{12 \times (1-\mu^2) \times k_m}} \qquad 2\text{–}42$$

$H_{eff,m}$ = Effective slab thickness for month m.
E_{pcc} = PCC modulus of elasticity for this month.
μ = PCC Poisson's ratio.
$k_{eff,m}$ = Coefficient of subgrade reaction for this month.

Step 3.4 Calculate reversible shrinkage contributions to long-term curling

Seasonal variations in relative humidity cause changes in slab curling. This can be described through an equivalent temperature gradient that would cause the same deflection basin.

Calculation of the effective temperature gradient involves the following steps:

Step 3.4.1 Determine free shrinkage strains if the relative is equal to the average relative

Humidity For each month, free shrinkage strain of an old concrete pavement would be determined using the following equation:

$$\varepsilon_{sh,average}(t) = \begin{cases} \varepsilon_{su}.(1.4 - 0.01 \times RH_{average}) & if \quad RH_{average} < 80 \\ \varepsilon_{su}.(3.0 - 0.03 \times RH_{average}) & if \quad RH_{average} \geq 80 \end{cases} \qquad 2\text{–}43$$

where

$\varepsilon_{sh,average}$ = Shrinkage strain for the average relative humidity, $\times 10^{-6}$.
ε_{sh} = Ultimate shrinkage strain for the relative humidity equal to 40 percent, $\times 10^{-6}$.
$RH_{average}$ = Average mean monthly ambient relative humidity, percent.

Step 3.4.2 Determine free shrinkage stress as if the relative humidity is equal to the relative humidity of the driest month using equations:

$$\varepsilon_{sh,m}(t) = \begin{cases} \varepsilon_{su}.(1.4 - 0.01 \times RH_m) & if \quad RH_m < 80 \\ \varepsilon_{su}.(3.0 - 0.03 \times RH_m) & if \quad RH_m \geq 80 \end{cases} \quad \Rightarrow \quad \text{m} = 1,12 \qquad 2\text{–}44$$

where

$\varepsilon_{sh,m}$ = Free shrinkage strain for the mean relative humidity of month m, $\times 10^{-6}$.
ε_{sh} = Ultimate shrinkage strain for the relative humidity equal to 40 percent,$\times 10^{-6}$.
RH_m = Ambient relative humidity for month m, percent.

Step 3.4.3 Calculate shrinkage contribution to curling

Moisture warping is adjusted seasonally based on atmospheric relative humidity as follows:

$$\Delta T_{SH,m} = \frac{3.0\varphi.(\varepsilon_{h,m} - \varepsilon_{h,average}).h_s.\left(\frac{h_{PCC}}{2} - \frac{h_s}{3}\right)}{\alpha.h^2.100} \quad 2\text{–}45$$

where
$\Delta T_{SH,m}$ = Temperature gradient equivalent of moisture warping for month i, °F.
φ = Reversible shrinkage factor, fraction of total shrinkage. Use 0.5 unless more accurate information is available.
ε_{su} = Ultimate shrinkage, $\times 10^{-6}$.
RH_{hi} = Average relative humidity for month i, percent.
$S_{h,ave}$ = Annual average relative humidity, percent.
h_s = Depth of the shrinkage zone (typically 2 in).
h_{PCC} = PCC slab thickness, in.
α = PCC coefficient of thermal expansion, in/in/°F.

Step 3.5 Calculate effective temperature differential

Equivalent temperature differential is determined from equation:

$$\Delta T_{eff,m} = \frac{h_{PCC}^2}{H_{eff}^2} \times \left[\left(T_{top,m} - T_{bot,m}\right) + \Delta T_{BI} + \Delta T_{sh,m}\right] \quad 2\text{–}46$$

where
$\Delta_{Teff,m}$ = Difference between temperatures at the top and bottom surfaces of the effective slab for month m.
$T_{top,m}$ = Mean night temperature of the top PCC surface for month m.
$T_{bot,m}$ = Mean night temperature of the bottom PCC surface for month m.
ΔT_{BI} = Built-in curling and temperature shrinkage temperature differential.
$\Delta T_{sh,m}$ = Equivalent temperature differential due to reversible portion of shrinkage.
h_{PCC} = PCC thickness.
H_{eff} = Effective thickness computed.

Step 3.6. Compute Korenev's nondimensional temperature gradient

$$\phi_m = \frac{2\alpha_{PCC}(1+\mu_{PCC})l_m^2}{H_{eff,m}^2} \frac{k_m}{\gamma_{eff,m}} \Delta T_{eff,m} \quad 2\text{–}47$$

where

φ_m = Nondimensional temperature gradient for month m.
h_{PCC} = PCC slab thickness.
α_{PCC} = PCC coefficient of thermal expansion.
μ_{PCC} = Poisson's ratio for PCC.
γ_{eff} = Effective unit weight for month m.
k = Modulus of subgrade reaction (k-value) for month m.
l_m = Radius of relative stiffness for month m.
$\Delta T_{eff,\,m}$ = Effective temperature gradient for month m.

Step 3.7 Compute corner deflections due to temperature curling

Using neural networks, compute deflections in the equivalent slab system due to temperature curling only. This deflection is defined as a difference between the deflection due to temperature curling and self weight and deflection due to self weight only.

$$\delta_{curl,m} = \frac{34100596.7 h_{eff,m}}{l_m^4 k_m}\left[NN_c(JTSpace, l_m, \phi_m) - NN_c(JTSpace, l_m, 0)\right] \qquad 2\text{–}48$$

where

$\delta_{m,curl}$ = Corner deflection due to curling only.
JTSpace = Mean transverse joint spacing.
l_m = Radius of relative stiffness for month m.
φ_m = Nondimensional temperature gradient for month m.
$NN_c(JTSpace, l_m, \varphi_m)$ = Neural network trained to determine corner deflections due to slab curling only (no axle loading)

Step 3.8. Determine maximum corner deflection

Determine maximum deflections from the twelve deflections computed in step 3.7:

$$\delta_{curl,\max} = \max_{m=1,12} \delta_{curl,m}$$

$\delta_{curl,max}$ = Corner deflection due to curling only for month m.
$\delta_{curl,m}$ = Maximum corner deflection due to curling.

Step 3.9. Determine overburden pressure

$$p_s = h_{PCC}\,\gamma_{PCC} + h_{base}\,\gamma_{base} \qquad 2\text{–}49$$

where

p_s = Overburden pressure.
h_{PCC} = PCC slab thickness.
γ_{PCC} = PCC unit weight.
h_{base} = PCC slab thickness.
γ_{base} = PCC unit weight.

Step 3.10. Determine maximum initial faulting

$$FMAX_0 = C_{12} \times \delta_{eff,\max} \times \left[Log \frac{P200 \times WetDays}{p_s} Log\left(1 + C_5 \times 5^{EROD}\right) \right]^{C_6} \quad 2\text{–}50$$

where

$FMAX_0$ = Initial maximum faulting.
P200 = Percent subgrade material passing 0.075-mm (#200) sieve.
EROD = Erodibility of the base layer.
WetDays = Number of wet days per year.
$\delta_{eff,max}$ = Maximum corner deflection due to curling.
$C_{12} = C_1 + C_2 \times FR^{0.25}$
FR = base freezing index

C_1, C_2, C_5, and C_6 are calibration parameters:

$C_1 = 1.29$
$C_2 = 1.1$
$C_5 = 250$
$C_6 = 0.4$

Steps 4 through 15 should be repeated for each month of the pavement design life.

Step 4. Determine PCC free shrinkage strains

Step 4.1 Determine PCC age

Determine PCC age in days using the following equation:

$$t = 30.4 \times (MONTH + MOPEN) \quad 2\text{–}51$$

where

t = Average PCC age for this month, days.
MONTH = Pavement age from the traffic opening, month.
MOPEN = Pavement age at the opening to traffic.

Step 4.2 Determine free shrinkage stress as if the relative is equal to the relative humidity of the driest month using equations:

$$\varepsilon_{sh,\max}(t) = \begin{cases} \varepsilon_{su} \cdot \dfrac{t}{n+t}(1.4 - 0.01 \times RH_{\max}) & if \quad RH_{\max} < 80\% \\ \varepsilon_{su} \cdot \dfrac{t}{n+t}(3.0 - 0.03 \times RH_{\max}) & if \quad RH_{\max} \geq 80\% \end{cases} \quad 2\text{–}52$$

where

$\varepsilon_{sh,max}$ = Shrinkage strain at time t days from placement, $\times 10^{-6}$.
ε_{su} = Ultimate shrinkage strain (discussed in section 2.6.1), $\times 10^{-6}$.
t = Time since placement, days.
n = Time to achieve 50 percent of ultimate shrinkage strain, days.
= 35, unless more accurate information is available.
RH_{max} = Ambient relative humidity, percent.

Step 4.3 Determine free shrinkage stress as if the relative humidity is equal to the relative humidity of the driest month using equations:

$$\varepsilon_{sh,MONTH}(t) = \begin{cases} \varepsilon_{su} \cdot \dfrac{t}{n+t}(1.4 - 0.01 \times RH_{MONTH}) & if \quad RH_a < 80\% \\ \varepsilon_{su} \cdot \dfrac{t}{n+t}(3.0 - 0.03 \times RH_{MONTH}) & if \quad RH_a \geq 80\% \end{cases} \qquad 2\text{–}53$$

where

$\varepsilon_{sh,MONTH}$ = Shrinkage strain at time t days from placement, $\times 10^{-6}$.
ε_{su} = Ultimate shrinkage strain (discussed in section 2.6.1), $\times 10^{-6}$.
t = Time since placement, days.
n = Time to achieve 50 percent of ultimate shrinkage strain, days.
= 3,unless more accurate information is available.
RHMONTH = Ambient relative humidity for this month, percent.

Step 4.4 Determine total free shrinkage strain at the top surface of the PCC slab

$$\varepsilon'_{sh,MONTH} = \varepsilon_{sh,\max} - (\varepsilon_{sh,\max} - \varepsilon_{s,MONTH}).\varphi \qquad 2\text{–}54$$

where

$\varepsilon'_{sh,MONTH}$ = Shrinkage strain for month i at any time t days from placement,$\times 10^{-6}$.
$\varepsilon_{sh,max}$ = Shrinkage strain for the driest month determined using, $\times 10^{-6}$.
$\varepsilon_{sh,MONTH}$ = Nominal shrinkage strain for month i determined using, $\times 10^{-6}$.
φ = Reversible shrinkage factor, fraction of total shrinkage. Use 0.5 unless more accurate information is available.

Step 4.5 Determine free shrinkage stress as if the relative humidity is equal to the relative humidity at the bottom of the PCC slab

$$\varepsilon_{sh,bot}(t) = \begin{cases} \varepsilon_{su} \cdot \dfrac{t}{n+t}(1.4 - 0.01 \times RH_{bot}) & if \quad RH_{bot} < 80\% \\ \varepsilon_{su} \cdot \dfrac{t}{n+t}(3.0 - 0.03 \times RH_{bot}) & if \quad RH_{bot} \geq 80\% \end{cases} \qquad 2\text{–}55$$

where

$\varepsilon_{sh,bot}$ = Shrinkage strain at the bottom of the PCC slab for the current month,$\times 10^{-6}$.
ε_{su} = Ultimate shrinkage strain, $\times 10^{-6}$.
t = Time since placement, days.
n = Time to achieve 50 percent of ultimate shrinkage strain, days.
= 35, unless more accurate information is available.
RH_{bot} = PCC relative humidity at the bottom slab surface.

Step 5. Calculate joint LTE

Step 5.1 Calculate PCC aggregate LTE

Step 5.1.1 Determine mean shrinkage strain (thought PCC slab)

The average shrinkage strain, $\varepsilon_{sh,mean}$, is defined as follows:

$$\varepsilon_{sh,mean} = \varepsilon_{sh,bot} + \left(\varepsilon_{sh,MONTH} - \varepsilon_{sh,bot}\right) \times \frac{h_d}{h_{PCC}} \quad 2\text{–}56$$

where

$\varepsilon_{sh,bot}$ = Free shrinkage strain at the bottom surface of the PCC slab.
$\varepsilon_{sh,MONTH}$ = Fee shrinkage strain at the top surface of the PCC slab.
h_d = Depth of a drier portion of the PCC slab, in.

Step 5.1.2 Determine overall joint opening

$$jw = \text{Max}(12000 \times STSpace \times \beta \times (\alpha_{PCC} \times (T_{constr} - T_{mean}) + \varepsilon_{sh,mean}), 0) \quad 2\text{–}57$$

where

jw = Joint opening, mils (0.001 in).
$\varepsilon_{sh,mean}$ = PCC slab mean shrinkage strain.
α_{PCC} = PCC coefficient of thermal expansion, in/in/0F.
JTSpace = Joint spacing, ft.
β = Joint open/close coefficient assumed equal to 0.85 for a stabilized base
= 0.65 for a unbound granular base.
Tmean = Mean monthly nighttime mid depth temperature, 0F.
Tconstr = PCC temperature at set, 0F.

Step 5.1.3 Determine joint shear capacity

$$S = 0.05 \times h_{PCC} \times e^{-0.032jw} - \Delta S_{tot} \quad 2\text{–}58$$

where

S = Dimensionless aggregate joint shear capacity.
jw = Joint opening, mils (0.001 in).
h = PCC slab thickness, in.
ΔS_{tot} = Cumulative loss of sheer capacity at the beginning of the current month.

Step 5.1.4 Calculate aggregate joint stiffness

The aggregate joint stiffness is determined as a function of load shear capacity, S.

$$Log(J_{AGG}) = -28.4 \times e^{-e^{-\left(\frac{S-e}{f}\right)}} \quad 2\text{–}59$$

where

J_{AGG} = $(Agg/kl)_c$
= Joint stiffness on the transverse joint for current increment.
e = 0.35.
f = 0.38.
S = Joint shear capacity (equal to s_0 at the first time increment).

Step 5.1.5 Calculate aggregate interlock LTE

Load transfer efficiency due to aggregate interlock is determined using the following equation:

$$LTE_{AGG} = \frac{100}{1 + 1.2 \times J_{AGG}^{-0.849}} \quad 2\text{–}60$$

where

LTE_{AGG} = Load transfer efficiency on the transverse joint due to aggregate interlock.
AGG = Transverse joint stiffness.

Step 5.1.6 Calculate dowel contribution to joint stiffness (if dowels are present).

A nondimensional stiffness of a joint due to dowel is determined as follows:

$$J_d = J_d^* + (J_0 - J_d^*)\exp(-DAM_{dowels}) \quad 2\text{–}61$$

where

J_d = Nondimensional dowel stiffness.
J_0 = Initial nondimensional dowel stiffness.
J^*_d = Critical nondimensional dowel stiffness.
DAM_{dowels} = Damage accumulated by a doweled joints due to past traffic.

Step 5.1.7 Calculate dowel component of LTE

Dowel component of LTE is determined as follows:

$$LTE_{dowel} = \frac{100}{1 + 1.2 \times J_d^{-0.849}} \quad 2\text{–}62$$

Step 5.1.8 Calculate total joint LTE for the current month

$$LTE_{joint} = 100\left(1 - \left(1 - \frac{LTE_{dowel}}{100}\right)\left(1 - \frac{LTE_{agg}}{100}\right)\left(1 - \left(\frac{LTE_{base}}{100}\right)\right)\right) \quad 2\text{–}63$$

Step 6. Calculate effective slab parameters

Step 6.1 Find effective slab thickness

$$H_{eff,MONTH} = \sqrt{h_{PCC}^2 + \frac{E_{BASE,MONTH}}{E_{PCC,MONTH}} H_{BASE}^2} \quad 2\text{–}64$$

where

$H_{eff,MONTH}$ = Effective slab thickness.
h_{PCC} = PCC slab thickness.
HBASE = Base thickness.
$E_{PCC,MONTH}$ = Representative PCC modulus of elasticity for month MONTH.
$H_{BASE,\ MONTH}$ = Base modulus of elasticity for month MONTH.

Step 6.2 Calculate unit weight of the equivalent slab

$$\gamma_{eff,MONTH} = \frac{\gamma_{PCC} h_{PCC}}{H_{eff,MONTH}} \quad 2\text{–}65$$

where

$\gamma_{eff,MONTH}$ = Effective unit weight.
h_{PCC} = PCC slab thickness.
γ_{PCC} = PCC unit weight.
h_{eff} = Effective thickness.

Step 6.3 Find radius of relative stiffness for this month

$$l = \sqrt[4]{\frac{E_{PCC,MONTH} H_{eff,MONTH}^3}{12(1-\mu_{PCC}^2) k_{MONTH}}} \quad 2\text{–}66$$

where

$_{eff,MONTH}$ = Effective slab thickness.
$_{PCC,MONTH}$ = Representative PCC modulus of elasticity for month MONTH.
$_{PCC}$ = Poisson's ratio for PCC.
$_{MONTH}$ = Coefficient of subgrade reaction for this month.

Step 7. Calculate effective temperature difference

Step 7.1 Calculate shrinkage contribution to curling

Moisture warping is adjusted seasonally based on atmospheric relative humidity as follows:

$$\Delta T_{SH,MONTH} = \frac{t}{t+n} \Delta T_{SH,m} \quad 2\text{–}67$$

where

$\Delta T_{SH,MOMTH}$ = Temperature gradient equivalent of moisture warping for month, MONTH, °F.
$\Delta T_{SH,mHi}$ = Equivalent temperature gradient of long term moisture warping for month m (the same month of the year as MONTH) determined in Step2, °F.
t = Time since placement, days.
n = Time to achieve 50 percent of ultimate shrinkage strain, days.
Use n = 35, unless more accurate information is available.

Step 7.2 Calculate effective temperature differential

Equivalent temperature differential is determined from the following equation:

$$\Delta T_{eff,MONTH} = \frac{h_{PCC}^2}{H_{eff,MONTH}^2} \times \left[\left(T_{top,MONTH} - T_{bot,MONTH} \right) + \Delta T_{BI} + \Delta T_{SH,MONTH} \right] \quad \text{MONTH} = 1, \quad 2\text{–}68$$

where

ΔT_{eff} = Difference between temperatures at the top and bottom surfaces of the effective slab.
$T_{top,MONTH}$ = Mean night temperature of the top PCC surface for month m.
$T_{bot,MONTH}$ = Mean night temperature of the bottom PCC surface for month m.
ΔT_{BI} = Built-in curling and temperature shrinkage temperature differential.
$\Delta T_{sh,MONTH}$ = Equivalent temperature differential due to reversible portion of shrinkage.
h_{PCC} = PCC thickness.
$H_{eff,MONTH}$ = Effective thickness computed.

Step 7.3 Compute Korenev's nondimensional temperature gradient

$$\phi_{MONTH} = \frac{2\alpha_{PCC}(1+\mu_{PCC})l^2_{MONTH}}{H^2_{eff,MONTH}} \frac{k_{MONTH}}{\gamma_{eff,MONTH}} \Delta T_{eff,MONTH} \qquad 2\text{–}69$$

where
φ_{MONTH} = Nondimensional temperature gradient for month m.
h_{PCC} = PCC slab thickness.
α_{PCC} = PCC coefficient of thermal expansion.
μ_{PCC} = Poisson's ratio for PCC.
$\gamma_{eff,MONTH}$ = Effective unit weight for month m.
k_{MONTH} = Modulus of subgrade reaction (k-value) for month m.
l_{MONTH} = Radius of relative stiffness for month m.
$\Delta T_{eff,MONTH}$ = Effective temperature gradient for month m.

Step 8. Compute adjusted load/pavement weigh ratios (normalized loads)

For each category of axle types and weights, compute normalized load:

$$q_i^* = \frac{P_i}{A\gamma_{eff,MONTH}H_{eff,MONTH}} \qquad 2\text{–}70$$

where
q_i^* = Adjusted load/pavement weigh ratio.
P_i = Axle load.
h_{PCC} = PCC slab thickness.
γ_{PCC} = PCC unit weight.
A = Parameter depending on axle type.
= 1 for single axles.
= 2 for tandem axles.
= 3 for tridem axles.

Step 9. Compute critical deflections

Step 9.1 Compute NN (Neural Networks) deflections in the loaded slab

Using NN (Neural Networks), compute axle loading induced deflections in the equivalent structure that has the same radius of relative stiffness, joint spacing, Korenev's nondimensional temperature gradient, traffic offset, normalized load ratio, transverse joint Load Transfer Efficiency (LTE), and shoulder LTE.

$$\delta_{L,i,A} = \frac{34100596.7 H_{eff,MONTH}}{l_{MONTH}^4 k_{MONTH}} \left[NN_{L,A}\left(JTSpace, l, LTE_{sk}, LTE_{jt}, \phi, q_i *_{L,i}, S\right) - NN_{L,A}\left(JTSpace, l, LTE_{sk}, LTE_{jt}, \phi, 0, S\right) \right] \quad 2\text{–}71$$

where

$\delta_{L,i,A}$ = Corner deflections of the loaded slab caused by axle loading of type A and weigh category i.
$NN_{L,A}$ = Neural networks for computing deflections at the loaded slab corners due to temperature curling and axle type A.
A = Axle type index.
= 1 for single axles.
= 2 for tandem axles.
= 3 for tridem axles.
i = Parameter defining axle weight.
JTSpace = Mean transverse joint spacing.
q_i* = Adjusted load/pavement weigh ratio.
φ = Nondimensional temperature gradient for the current month.
l = Radius of relative stiffness for the current month.
LTE_{sh} = Shoulder load transfer efficiency for flat slab conditions.
LTE_{jt} = Transverse joint load transfer efficiency for flat slab conditions.
S = Traffic wander.

Step 9.2 Compute Neural Networks (NN) deflections in the unloaded slab

Using Neural Networks (NN), compute axle loading induced deflections in the equivalent structure that has the same radius of relative stiffness, joint spacing, Korenev's nondimensional temperature gradient, traffic offset, normalized load ratio, transverse joint Load Transfer Efficiency (LTE), and shoulder LTE.

$$\delta_{L,i,A} = \frac{34100596.7 H_{eff,MONTH}}{l_{MONTH}^4 k_{MONTH}} \left[NN_{U,A}\left(JTSpace, l, LTE_{sk}, LTE_{jt}, \phi, q_i *_{A,i}, S\right) - NN_{U,A}\left(JTSpace, l, LTE_{sk}, LTE_{jt}, \phi, 0, S\right) \right] \quad 2\text{–}72$$

where

$\delta_{U,i,A}$ = Corner deflections of the loaded slab caused by axle loading of type A and weigh category i.
$NN_{U,A}$ = Neural networks for computing deflections at the loaded slab corners due to temperature curling and axle type A.
A = Axle type index.
=1 for single axles.
=2 for tandem axles.
=3 for tridem axles.
i = Parameter defining axle weight.
JTSpace = Mean transverse joint spacing.
q_i* = Adjusted load/pavement weight ratio.
φ = Nondimensional temperature gradient for the current month.

l = Radius of relative stiffness for the current month.
LTE_{sh} = Shoulder load transfer efficiency for flat slab conditions.
LTE_{jt} = Transverse joint load transfer efficiency for flat slab conditions.
S = Traffic wander.

Step 10. Compute differential energy increment deflections

$$DE_{MONTH} = \sum_{A=1}^{3}\sum_{i=1}^{N_A} n_{i,A}\left(k_{MONTH}\frac{\delta_{L,i,A}^2}{2} - k_{MONTH}\frac{\delta_{U,i,A}^2}{2}\right) \quad 2\text{–}73$$

where
DE_{MONTH} = Differential energy density of subgrade deformation accumulated for month MONTH.
$\delta_{L,i,A}$ = Corner deflections of the loaded slab caused by axle loading.
$\delta_{U,i,A}$ = Corner deflections of the unloaded slab caused by axle loading.
$n_{i,A}$ = Number of axle load applications for current increment and load group j.
N_A = Number of load categories for the axle type A.

Step 11. Find faulting increment

Determine increment of faulting accumulated for month MONTH.

$$\Delta Fault = C_{34}*(FMAX_{MONTH-1}-FAULT_{MONTH-1})^2 \times DE_{MONTH} \quad 2\text{–}74$$

where
$\Delta Fault$ = Increment of faulting accumulated for month MONTH.
$FAULT_{MONTH-1}$ = Magnitude of faulting at the beginning of month MONTH.
= 0 if MONTH =1.
$FMAX_{MONTH-1}$ = Maximum faulting parameter at the beginning of month MONTH.
= $FMAX_0$ if MONTH =1.
DE_{MONTH} = Differential energy density of subgrade deformation accumulated for month MONTH.
$C_{34} = C_3 + C_4 \times FR^{0.25}$
FR = Base freezing index.
C_3 and C_4 are calibration parameters:
C_3 = 0.001725
C_4 = 0.0008

Step 12. Find current faulting

$$FAULT_{MONTH} = FAULT_{MONTH-1} + \Delta Fault \quad 2\text{–}75$$

where
$FAULT_{MONTH}$ = Magnitude of faulting at the end of month MONTH.
$FAULT_{MONTH-1}$ = Magnitude of faulting at the beginning of month MONTH.
= 0 if MONTH =1.

ΔFault = Increment of faulting accumulated for month MONTH.

NOTE: steps 13 through 15 are not necessary for the last month of the design period.

Step 13. Find current maximum faulting index

Find current maximum faulting index

$$FMAX_{MONTH} = FMAX_{MONTH-1} + C_7 \times DE_{MONTH}[Log(1+C_5 \times 5^{EROD})]^{C6} \quad 2–76$$

where

$FMAX_{MONTH}$ = Maximum faulting parameter at the end of month MONTH.
$FMAX_{MONTH-1}$ = Maximum faulting parameter at the beginning of month MONTH
= $FMAX_0$ if MONTH =1.
DE_{MONTH} = Differential energy density of subgrade deformation accumulated for month MONTH.
EROD = Erodibility of the base layer.
C_5 = 250
C_6 = 0.4
C_7 = 1.2.

Step 14 Evaluate loss of aggregate shear capacity

Step 14.1 Calculate reference shear stress

$$\tau_{ref} = 111.1 \times \exp(-\exp(0.9988 \times \exp(-0.1089 \log JAGG))) \quad 2–77$$

where

τ_{ref} = Reference shear stress derived from the PCA test results.
J_{AGG} = Aggregate joint stiffness computed for the time increment.

Step 14.2 Calculate shear stress induced by each axle

$$\tau_{iA} = J_{AGG} \times (\delta_{L,i,A} - \delta_{U,i,A}) \quad 2–78$$

where

τ_{iA} = Maximum shear stress at the PCC slab joint surface caused by axle loading of type A and weigh category i.
J_{AGG} = Aggregate joint stiffness computed for the time increment.
$\delta_{L,i,A}$ = Corner deflections of the loaded slab caused by axle loading.
$\delta_{U,i,A}$ = Corner deflections of the unloaded slab caused by axle loading.
A = Axle type index.
= 1 for single axles.
= 2 for tandem axles.
= 3 for tridem axles.
i = Parameter defining axle weight.

Step 14.3 Calculate loss of aggregate shear capacity accumulated during the month

$$\Delta s_{i,A} = \begin{cases} 0 & \text{if} \quad jw < 0.001 h_{PCC} \\ \dfrac{0.005 \times 10^{-6}}{1.0 + 6.0 \times \left(jw / h_{PCC} - 3\right)^{-5.7}} \left(\dfrac{\tau_{i,A}}{\tau_{ref}} \right) & \text{if} \quad 0.001 h_{PCC} < jw < 3.8 h_{PCC} \\ \dfrac{0.068 \times 10^{-6}}{1.0 + 6.0 \times \left(jw / h_{PCC} - 3\right)^{-1.98}} \left(\dfrac{\tau_{i,A}}{\tau_{ref}} \right) & \text{if} \quad jw > 3.8 h_{PCC} \end{cases} \qquad 2\text{–}79$$

where

$\Delta s_{i,A}$ = Loss of shear from a single repetition of an axle load of group i and axle type A.
h_{PCC} = PCC slab thickness, in.
jw = Joint opening, mils (0.001 in).
$\tau_{i,A}$ = Shear stress on the transverse joint surface from the response model for the load group i and axle type A.
τ_{ref} = Reference shear stress derived from the PCA test results.

Step 14.4 Calculate shear stress accumulated during the month

$$\Delta s_{tot} = \sum_{A=1}^{3} \sum_{i=1}^{N_A} \Delta s_{i,A} n_{i,A} \qquad 2\text{–}80$$

where

Δs_{tot} = cumulative loss of shear for the current month.
$\sum_{i=1}^{N_A} \Delta s_{i,A} n_{i,A}$ = Loss of shear from a single repetition of an axle load of group i and axle type A.
$n_{i,A}$ = Number of axle load applications for current increment and load group j.
N_A = Number of load categories for the axle type A.

Step 14.5 Calculate loss of shear capacity

$$S_{MONTH} = S_{MONTH-1} + \Delta s_{tot} \qquad 2\text{–}81$$

Step 15. Calculate damage of doweled LTE

Step 15.1 Calculate dowel shear force

$$F_{i,A} = J_d \times \left(\delta_{L,i,A} - \delta_{U,i,A}\right) \times DowelSpace \qquad 2\text{–}82$$

where

$F_{i,A}$ = Dowel shear force induced by axle loading of type A and load category i.
J_d = Joint stiffness on the doweled joint computed for the time increment.

$\delta_{L,i,A}$ = Corner deflections of the loaded slab caused by axle loading of type A and load category i.
$\delta_{U,i,A}$ = Corner deflections of the unloaded slab caused by axle loading of type A and load category i.
A = Axle type index.
= 1 for single axles.
= 2 for tandem axles.
= 3 for tridem axles.
i = Parameter defining axle weight.
DowelSpace = Space between adjacent dowels in the wheel path, in.

Step 15.2 Calculate increment of dowel joint damage

Dowel joint damage accumulated for the current month is determined from the following equation:

$$\Delta DOWDAM_{tot} = \sum_{A=1}^{3}\sum_{i=1}^{N_A} C_8 \times F_{i,A}\frac{n_{i,A}}{df_c^*} \quad 2\text{–}83$$

where
$\Delta DOWDAM_{tot}$ = Cumulative dowel damage for the current month.
$F_{i,A}$ = Dowel shear force induced by axle loading of type A and load category i.
$n_{i,A}$ = Number of axle load applications for current increment and load group i.
N_A = Number of load categories for the axle type A.
f_c* = PCC compressive stress estimated from the PCC modulus of rupture, Mr, using the following equation:

$$f_c^* = \left(\frac{Mr}{9.5}\right)^2 \quad 2\text{–}84$$

C_8 = Calibration constant.
C_8 = 400.

Step 15.3 Find total dowel damage

$$DOWDAM_{MONTH} = DOWDAM_{MONTH-1} + \Delta DOWDAM_{tot} \quad 2\text{–}85$$

where
DOWDAMMONTH = Dowel damage at the end of month MONTH.
DOWDAMMONTH-1 = Dowel damage at the beginning of month MONTH.
= 0 if MONTH=1
ΔDOWDAMtot = Cumulative dowel damage for the current month.

2.2.2 Transverse Cracking

For JPCP transverse cracking, two modes of failure are considered:

- Bottom-up cracking.

- Top-down cracking.

Any given slab may crack either from the bottom-up or the top-down, but not both. Therefore, the predicted bottom-up and top-down cracking are not particularly meaningful by themselves, and combined cracking must be determined, excluding the possibility of both modes of cracking occurring on the same slab. JPCP transverse cracking is predicted using equation 2–86 below (NCHRP 2003; Appendix NN):

$$TCRACK = \left(CRK_{Bottom-up} + CRK_{Top-down} - CRK_{Bottom-up}.CRK_{Top-down}\right) \times 100 - CRK_{\mathrm{Re}\,pai} \qquad 2\text{–}86$$

where,

TCRACK = total cracking (percent).
$CRK_{Bottop-up}$ = predicted amount of bottom-up cracking (fraction).
$CRK_{Top-down}$ = predicted amount of top-down cracking (fraction).
$CRK_{Repaired}$ = percent of existing transverse cracks repaired (for restored JPCP only; otherwise, it is assumed to be zero).

The model combines bottom-up and top-down cracking to obtain total cracking. The expected amount of cracking from each mode is calculated separately.

The general expression for fatigue damage accumulations (for both bottom-up and top-down mechanisms) is as follows (NCHRP 2003; Appendix NN):

$$FD = IDAM + \sum \frac{n_{i,j,k,l,m,p}}{N_{i,j,k,l,m,p}} \qquad 2\text{–}87$$

where

FD = total fatigue damage (top-down or bottom-up).
$n_{i,j,k,\ldots}$ = applied number of load applications at condition i, j, k, l, m, n.
$N_{i,j,k,\ldots}$ = allowable number of load applications at condition i, j, k, l, m, n.
IDAM = estimate of past bottom-up or top-down fatigue damage
i = age (accounts for change in PCC modulus of rupture, layer bond condition, deterioration of shoulder LTE).
j = month (accounts for change in base and effective dynamic modulus of subgrade reaction).
k = axle type (single, tandem, and tridem for bottom-up cracking; short, medium, and long wheelbase for top-down cracking).
l = load level (incremental load for each axle type).
m = temperature difference (probability distribution [2 ^{o}F increments ranging from 10 ^{o}F to 40 ^{o}F] applied to total traffic within the time interval); the "effective temperature difference" due to construction curling and moisture warping is subtracted from the temperature gradient for stress computation.
p = traffic path (mean position and standard deviation used to obtain probability function of load position).

For restored JPCP, the initial bottom-up and top-down fatigue damage is required when computing future bottom-up and top-down fatigue damage (NCHRP 2003;

Appendix NN). For bonded PCC over JPCP, only the initial bottom-up fatigue damage is required since initial top-down fatigue damage in the overlay PCC is assumed to be zero. Initial bottom-up and top-down fatigue damage is assumed to be zero for all other overlay types. A description of the procedure for estimating initial fatigue damage is presented later in this appendix.

The applied number of load applications ($n_{i,j,k,l,m,n}$) is the actual number of axle combination k of load Level l that passed through traffic path n under each condition (age, season, and temperature difference). The allowable number of load applications is the number of load cycles at which fatigue failure is expected (corresponding to 50 percent slab cracking) and is a function of the applied stress and PCC strength. The allowable number of load applications is determined using the following fatigue model (NCHRP 2003; Appendix NN):

$$\log(N_{i,j,k,l,m,p}) = C_1 . \left(\frac{M_R}{\sigma} \right)^{C_2}_{i,j,k,l,m,p} \qquad 2\text{–}88$$

where

$N_{i,j,k,\ldots}$ = allowable number of load applications at condition i, j, k, l, m, n
MR_i = PCC modulus of rupture at age i, psi
$\sigma_{i,j,k,\ldots}$ = applied stress at condition i, j, k, l, m, n
C_1 = calibration constant = 2.0
C_2 = calibration constant = 1.22

Note that the location of the critical stresses for bottom-up and top-down cracking is different. The differences in the joint spacing calls for use of different neural networks for computing topdown stresses.

Also, unlike bottom-up cracking, the location of critical damage is not predefined for topdown cracking. The critical damage location depends on axle load distribution, temperature gradients, permanent curl/warp, joint spacing, and axle spacing, and it could be any point along the lane-shoulder joint between about 36 in and 0 in from the middle of the slab (mid-point between two transverse joints along the lane-shoulder joint.

The fatigue damages calculated for bottom-up and top-down cracking are mechanistic parameters that represent the occurrence and coalescing of micro-cracks to form larger cracks at the bottom and top of the PCC slabs. This mechanistic parameter is related to the physical distress of transverse cracking that is visible at the pavement surface through calibrated curves that relate damage to distress. The model used to compute bottom-up and top- down cracking is based on computed fatigue damage and is presented as equation below (NCHRP 2003; Appendix NN).

$$CRK_{TDorBU} = \frac{1}{1 + 1.0 . FD^{C_3}_{TDorBU}} \qquad 2\text{–}89$$

where

$CRK_{TD\ or\ BU}$ = predicted amount of bottom-up or top-down cracking (fraction)
$FD_{TD\ or\ BU}$ = calculated fatigue damage (top-down or bottom-up)
C_3 = calibration factor

2.2.3 IRI Model

In the current version of MEPDG software, the IRI model was calibrated and validated using LTPP and other field conditions. The following is the final calibration model (NCHRP 2004; Part 3-Chapter 4-Rigid Design):

$$IRI = IRI_1 + C_1*CRK + C_2*SPALL + C_3*TFAULT + C_4*SF \quad 2–90$$

where

IRI = predicted IRI, in/mi.
IRI_1 = initil smoothness measured as IRI, in/mi.
CRK = Percent slabs with transverse cracks (all severities).
SPALL = percentage of joints with spalling (medium and high severities).
TFAULT = total joint faulting cumulated per mi, in.
C_1 = 0.8203
C_2 = 0.4417
C_3 = 1.4929
C_4 = 25.24
SF = site factor
= $AGE(1+0.5556*FI)(1+P_{200})\times 10^{-6}$

where

AGE = pavement age, yr.
FI = freezing index, °F-days.
P_{200} = percent subgrade material passing No. 200 sieve.

The transverse cracking and faulting are determined from the previous sections. The transverse joint spalling is determined using the following model calibration using LTPP and other data (NCHRP 2004; Part 3-Chapter 4-Rigid Design):

$$SPALL = \left[\frac{AGE}{AGE + 0.01}\right]\left[\frac{100}{1+1.005^{(-12*AGE+SCF)}}\right] \quad 2–91$$

where

SPALL = percentage joints spalled (medium and high severities).
AGE = pavement age since construction, years.
SCF = scaling factor based on site-, design-, and climate-related variables:

$$SCF = -1400 + 350.AIR\%.(0.5 + PREFORM) + 3.4f_c'.0.4 - 0.2(FTCYC.AGE) + 43h_{PCC} - 536WC\_Ratio \quad 2–92$$

where

SCF = spalling prediction scaling factor used in equation 2–91
AIR% = PCC air content, percent.
AGE = time since construction, years
PREFORM = 1 if preformed sealant is present; 0 if not.
f'_c = PCC compressive strength, psi.
FTCYC = average annual number of freeze-thaw cycles.
h_{PCC} = PCC slab thickness, in.

WC_Ration = PCC water/cement ratio.

2.2.3.1 IRI Prediction Procedure

The IRI prediction is simple once the cracking and faulting predictions have been completed (NCHRP 2004; Part 3-Chapter 4-Rigid Design). The steps for predicting IRI are as follows:

Step 1. Predict transverse cracking and faulting

- Follow the procedure for JPCP transverse cracking prediction to obtain predicted cracking.
- Follow the procedure for JPCP joint faulting prediction to obtain predicted faulting.

Step 2. Predicted joint spalling

Use the empirical model given

Step 3. Select initial IRI and predict IRI

The initial IRI depends on the project smoothness specifications. Typical values of initial IRI range from 50 to 100 in/mi. Select the initial IRI and use the IRI model given to predict IRI over the project life.

Chapter 3

Parametric Study of MEPDG

MEPDG software utilizes various entries obtained from the user in order to analyze the pavement structure and determine the distresses. Changing these entries however, have different degrees of impact on the pavement distresses. Therefore, a sensitivity analysis was carried out on the MEPDG inputs in order to investigate the effect of change of its inputs.

In the parametric study of MEPDG the Traffic, climate and material input values were analyzed through sensitivity analysis and their effects on the output were checked and categorized (Stanigzai 2007.)

A design example of an actual pavement (Leshara West & Leshara Spur located in Nebraska near Omaha) with some defaults and assumed values have been selected as design sample for the sensitivity analyses.

3.1 Sensitivity Analysis

During the sensitivity analyses a single input is changed each time while the initial criteria and the other inputs are kept the same through out the process in order to know its sensitivity level based on 50 years life span.

The MEPDG gives an upper and lower limit for each input. Using this range the input was chosen each time with smaller and larger increments and the effects were noted.

In Stanigzai's (2007) study the results of the sensitivity analysis are categorized into the following four categories.

1. Very Sensitive Inputs: If a minor or major change in these inputs bring about large changes in one or more outputs in other words if the output life is increased or decreased by a minimum of 20 years, they are Very Sensitive Inputs.

2. Sensitive Inputs: If a minor or major change in these inputs bring about noticeable changes in one or more outputs in other words if the output life is increased or decreased by 5-20 years, they are Sensitive inputs.

3. Some What Sensitive Inputs: If a major change in this value bring about noticeable changes in one or more outputs in other words if the output life is increased or decreased by up to 5 years, they are Some What Sensitive Inputs.

4. Insensitive Inputs: If a minor or major change in this value doesn't bring about any changes in one or more outputs in other words if the output life is not affected by the change in this value, they are Insensitive Inputs. Although these inputs are insensitive

based on the output charts of the sensitivity analyses, they do have effects over other input values which can be more sensitive.

For example the curing of concrete is an insensitive input according to the charts from the sensitivity analyses but they do affect the strength of concrete which is another input.

The sensitivity analysis' detailed results for all the inputs required for designing new JPCP pavements can be found in the thesis done by Stanigzai (2007). The graphs showing the sensitivity of all inputs can be found in Appendix A.

The Project used, is a part of highway number 64, begins at its intersection with highway 77, proceeds East for 3.7+ miles, curves north for 0.5+ miles.

3.2 Performance Criteria

Reliability: Practically everything associated with the design of new and rehabilitated pavements is variable or uncertain in nature. Following is a summary of the sources of uncertainties in a pavement project.

- Errors in estimating traffic loadings.
- Fluctuations in climate over many years.
- Variations in layer thicknesses, materials properties, and subgrade characteristics along the project.
- Differences between as-designed and as-built materials and other layer properties.
- Errors in the measurement of the distress and IRI quantities.
- Prediction model limitations and errors.

Reliability has been incorporated in the Guide in a consistent and uniform fashion for all pavement types. An analytical solution that allows the designer to design for a desired level of reliability for each distress and smoothness is available.

Design reliability is defined as the probability that each of the key distress types and smoothness will be less than a selected critical level over the design period.

$$R = P\,[\text{Distress over Design Period} < \text{Critical Distress Level}]$$

Design reliability is defined for smoothness (IRI) as following:

$$R = P\,[\text{IRI over Design Period} < \text{Critical IRI Level}]$$

For example, the reliability say for fatigue cracking is defined as following:

$$R = P\,[\text{Fatigue Cracking over Design Period} < 20 \text{ percent lane area}]$$

The designer begins the design process by configuring a trial design. The software accompanying the Design Guide procedure then provides a prediction of key distress types and smoothness over the design life of the pavement. This prediction is based on mean or average values for all inputs. The distresses and smoothness predicted therefore represent mean values that can be thought of as being at a 50 percent reliability estimate (i.e., there is a 50 percent chance that the predicted distress or IRI will be greater than or less than the mean prediction).

For nearly all projects, the designer will require a higher probability that the design will meet the performance criteria over the design life. In fact, the more important the project in terms of consequences of failure, the higher the desired design reliability. The consequence of failure of an urban freeway is far more than the failure of a farm-to-market roadway. Often, agencies have used the level of traffic volume or truck traffic as the parameter for selecting design reliability.

3.3 Results of Sensitivity Analyses

The following conclusions are based on the sensitivity analyses of the design guide 2002 (Version 1. April 2007) and are applicable to the state of Nebraska (Stanigzai's 2007).

3.3.1 Discussion of the results

3.3.1.1 Initial Criteria

Very Sensitive Inputs: Reliability is a very sensitive input based on the sensitivity analyses since a small change in reliability can bring about large changes in the output design life. A small change in reliability can increase or decrease the amount of material, time and cost therefore it must be chosen with extreme care and based on the necessity and the importance of the pavements and their failure consequences. Normally the DOTs are in charge of specifying the reliability.

3.3.1.2 Traffic

Very sensitive Inputs: AADTT and Traffic Growth Factor are the very sensitive values amongst traffic inputs.

Sensitive Inputs: Mean Wheel location is a sensitive input according to sensitivity analyses.

Somewhat Sensitive Inputs: Hourly Truck Distribution, Traffic Wander Standard Deviation, Number of Axles per Truck, Monthly Adjustment Factors (Level 1 & 3), and AADTT Distribution by Vehicle Class (Level 1 & 3 inputs) are all values with little effects on pavements according to the sensitivity analyses. These values don't seem to be very sensitive since they don't increase or decrease pavement loading or load repetitions.

Insensitive Inputs: Design Lane Width, Percent Trucks in Design Lane, Operational Speed, Average Axle Width (edge to edge outside Dimensions), Dual Tire Spacing, Tandem Axle Spacing, Tridem Axle Spacing and Quad Axle Spacing are all insensitive values according to the sensitivity analyses. However a deeper understanding of the concept of "Percent of Trucks in Design Lane", shows that this input seems to be amongst the mores sensitivity inputs since it is related to traffic load repetitions and a change in it can make a difference in the output. Such outputs risk the validity of the design guide software (Stanigzai's 2007).

3.3.1.3 Climate

Sensitive Input: Regional Climate Difference is a sensitive input even inside Nebraska according to the sensitivity analyses. It is thus vital to use the actual site climate for each pavement section.

Insensitive Inputs: Depth of Water Table is an insensitive input according to the sensitivity analysis. This result needs deeper consideration because if the water table is closer to the surface it possibly will have more effects on subbase and the subgrade and influence the distresses.

3.3.1.4 Material

Typically the inputs in material sections related to material type, thickness, thermal properties and strength tend to be more sensitive than those related to other properties.

3.3.1.5 JPCP Design Features

Very sensitive Inputs: Permanent Curl/Wrap Effective Temperature Difference, Joint Spacing and Tied PCC shoulder are very sensitive inputs according to sensitivity analyses which is predictable. This parameter will be discussed in more detail later in the current report.

Simply considering the concrete panels between the joints as members lying on a flexible foundation, the longer the joint spacing the longer the member between these joints thus resulting in more moments and cracks in the member, and therefore it should be a very sensitive input.

Also in order to have less or no edge stresses we have to connect the shoulders to the pavement. Pavements with no shoulders have deteriorated edges due to high edge stresses.

All the above three inputs are very sensitive and the analyses results also confirms it.

Sensitive Inputs: PCC base interface is a sensitive input according to the sensitivity analyses. If the PCC layer is bonded to the base it will resist more stress because section modulus increases significantly due to composite action of layers and thus less cracking and faulting will develop compared to unbonded layers. It makes this input sensitive which is also confirmed by the program.

Somewhat Sensitive: Surface Short-Wave Absorptivity, Dowel Diameter, Dowel Bar Spacing, and Erodibility Index are somewhat sensitive entries based on the results from the sensitivity analyses.

Insensitive Inputs: Sealant Type and Widened slab are insensitive inputs according to the sensitivity analyses. Sealant type can have some effects on joint durability which needs further investigation.

3.3.1.6 PCC Material Properties

Very sensitive Inputs: PCC Layer Thickness, PCC Poisson's Ratio, Coefficient of Thermal Expansion, Thermal Conductivity, Heat Capacity, Ratio of 20-year to 28-day of Modulus of Elasticity (Level 1), Ratio of 20-year to 28-day of Rupture Modulus (Level

1), Ratio of 20-year to 28-day of Compressive Strength (Level 2), 28-day PCC Compressive Strength (Level 3) and 28-day Modulus of Rupture (Level 3) are very sensitive inputs based on the sensitivity analyses results. Since all these values are related to PCC layer thickness, PCC thermal conductivity and PCC strength, this categorization seems to be predictable.

Sensitive Inputs: PCC Unit Weight, 7-day Modulus of Elasticity (Level 1) and 7-day Rupture Modulus (Level 1) are sensitive inputs according to the sensitivity analyses. This seems logical since 7-day modulus of elasticity and 7-day modulus of rupture are PCC strength properties and they affect the output.

Somewhat Sensitive Inputs: Cementitious Material Content, Water Cement Ratio, 14-day Modulus of Elasticity (Level 1), 28-day Modulus of Elasticity (Level 1), 7-day Compressive Strength (Level 2), 14-day Compressive Strength (Level 2) and 28-day Compressive Strength (Level 2) are somewhat sensitive based on the sensitivity analyses.

Insensitive Inputs: Cement Type, Aggregate Type, Reversible Shrinkage (% of Ultimate Shrinkage), Time to develop 50% of Ultimate Shrinkage (days) and Curing Method are insensitive values according to the sensitivity analyses.

3.3.1.7 Granular Base/Subbase/Subgrade

Very sensitive Inputs: Material thickness of the granular layer is a very sensitive input based on the sensitivity analyses.

Sensitive Inputs: Material type of the granular layer is a sensitive input according to the sensitivity analyses.

Insensitive Values: Poisson's Ratio, Coefficient of Lateral Pressure, Resilient Modulus (Level 2) and Resilient Modulus (Level 3) are insensitive inputs based on the sensitivity analyses.

3.3.1.8 Stabilized Material

Insensitive Inputs: Material Type, Layer thickness, Unit Weight, Poisson's ratio, Elastic Modulus, Thermal Conductivity and Heat Capacity are insensitive inputs according to the sensitivity analyses. Stabilized material type would not have a great effect on the distress results by its own, yet its specifications like resilient modulus etc reflects the effects of material type and has influence on the results. The design guide software categorizes them as insensitive inputs resulting in questioning the validity of the software.

3.3.1.9 Bedrock

Sensitive Inputs: Bedrock Material Unit Weight is considered as a sensitive input according to the sensitivity analyses.

Insensitive Inputs: Material Type, Layer Thickness, Poisson's Ratio and Resilient Modulus are considered insensitive inputs based on the sensitivity analyses.

Tables Table 3-1 to Table 3-4 show the summary results for the sensitivity analysis performed on the MEPDG inputs.

Table 3-1. Summary results for the sensitivity analysis performed on the MEPDG inputs (Based on Faulting) (Stanigzai's 2007)

Sensitivity based on Faulting					
		Very Sensitive	**Sensitive**	**Somewhat Sensitive**	**Insensitive**
Performance Criteria		Reliability			
Traffic		AADTT Traffic Growth Factor	Mean wheel location (inches from the lane marking)	Hourly Truck Distribution	Design Lane Width Percent Trucks in Design Lane Operational Speed Design Lane Width Average Axle Width (edge to edge outside Dimensions) Dual Tire Spacing Tandem Axle Spacing Tridem Axle Spacing Quad Axle Spacing Number of Axles per Truck Traffic Wander Standard Deviation Monthly Adjustment Factors AADTT Distribution by Vehicle Class
Climate					Depth of Water Table Regional Climate Difference
Material	**JPCP Design Features**		Permanent Curl/Wrap effective temperature difference		Sealant Type Widened slab[2] Surface Short-Wave absorptivity Joint Spacing Dowel Diameter Dowel Bar Spacing Tied PCC Shoulder, Long-term LTE (Load Transfer Efficiency) PCC-Base Interface Erodibility Index
	PCC Material Properties	Coefficient of thermal expansion	PCC Layer Thickness PCC Unit Weight PCC Poisson's Ratio Thermal conductivity	28-day PCC Compressive Strength	Cement Type Aggregate Type Reversible Shrinkage (% of Ultimate Shrinkage) Time to develop 50% of Ultimate Shrinkage (days) Curing Method Heat capacity Cementitious Material Content Water/Cement Ratio 7 day Modulus of Elasticity 28 day Modulus of Elasticity Ratio of 20-year to 28-day for Modulus of Elasticity 7 day Rupture Modulus Ratio of 20-year to 28-day for Rupture Modulus 7 day Compressive Strength 28 day Compressive Strength Ratio of 20-year to 28-day for Compressive Strength 28-day PCC Modulus of Rupture
	Granular Base/Subbase/Subgrade				Poisson's Ratio Coefficient of Lateral Pressure Resilient Modulus (Level 2) Resilient Modulus (Level 3) Material Type Material Thickness
	Stabilized Base Inputs				Material Type Layer thickness Unit Weight Poisson's ratio Elastic Modulus Thermal Conductivity Heat Capacity
	Bedrock				Material Type Layer Thickness Poisson's Ratio Resilient Modulus Unit weight

Table 3-2. Summary results for the sensitivity analysis performed on the MEPDG inputs (Based on Cracking) (Stanigzai's 2007)

Sensitivity based on Cracking					
		Very Sensitive	Sensitive	Somewhat Sensitive	Insensitive
Performance Criteria		Reliability			
Traffic		AADTT Traffic Growth Factor	Mean wheel location (inches from the lane marking)	Hourly Truck Distribution	Design Lane Width Percent Trucks in Design Lane Operational Speed Design Lane Width Average Axle Width (edge to edge outside Dimensions) Dual Tire Spacing Tandem Axle Spacing Tridem Axle Spacing Quad Axle Spacing Number of Axles per Truck Traffic Wander Standard Deviation Monthly Adjustment Factors AADTT Distribution by Vehicle Class
Climate			Regional Climate Difference		Depth of Water Table
Material	JPCP Design Features	Permanent Curl/Wrap effective temperature difference (°F) Joint Spacing Tied PCC Shoulder, Long-term LTE (Load Transfer Efficiency, %)	PCC-Base Interface		Sealant Type Widened slab[2] Surface Short-Wave absorptivity Dowel Diameter Dowel Bar Spacing Erodibility Index
	PCC Material Properties	PCC Layer Thickness PCC Poisson's Ratio Coefficient of thermal expansion Thermal conductivity Heat capacity Ratio of 20-year to 28-day for Modulus of Elasticity Ratio of 20-year to 28-day for Rupture Modulus Ratio of 20-year to 28-day for Compressive Strength 28-day PCC Compressive Strength 28-day PCC Modulus of Rupture	7 day Modulus of Elasticity 7 day Rupture Modulus	PCC Unit Weight 28 day Modulus of Elasticity 7 day Compressive Strength 28 day Compressive Strength	Cement Type Aggregate Type Reversible Shrinkage (% of Ultimate Shrinkage) Time to develop 50% of Ultimate Shrinkage (days) Curing Method Cementitious Material Content Water/Cement Ratio
	Granular Base/Subbase/Subgrade	Material Thickness	Material Type		Poisson's Ratio Coefficient of Lateral Pressure Resilient Modulus (Level 2) Resilient Modulus (Level 3)
	Stabilized Base Inputs				Material Type Layer thickness Unit Weight Poisson's ratio Elastic Modulus Thermal Conductivity Heat Capacity
	Bedrock				Material Type Layer Thickness Poisson's Ratio Resilient Modulus Unit weight

Table 3-3. Summary results for the sensitivity analysis performed on the MEPDG inputs (Based on IRI) (Stanigzai's 2007)

Sensitivity based on IRI					
		Very Sensitive	**Sensitive**	**Somewhat Sensitive**	**Insensitive**
Performance Criteria		Reliability			
Traffic		AADTT Traffic Growth Factor	Mean wheel location (inches from the lane marking)	Traffic Wander Standard Deviation Number of Axles per Truck Monthly Adjustment Factors AADTT Distribution by Vehicle Class	Design Lane Width Percent Trucks in Design Lane Operational Speed Design Lane Width Average Axle Width (edge to edge outside Dimensions) Dual Tire Spacing Tandem Axle Spacing Tridem Axle Spacing Quad Axle Spacing Hourly Truck Distribution
Climate			Regional Climate Difference		Depth of Water Table
Material	**JPCP Design Features**	Permanent Curl/Wrap effective temperature difference (°F)	Joint Spacing Tied PCC Shoulder, Long-term LTE (Load Transfer Efficiency, %)	Surface Short-Wave absorptivity Dowel Bar Spacing PCC-Base Interface Erodibility Index	Sealant Type Widened slab[2] Dowel Diameter
	PCC Material Properties	PCC Layer Thickness Coefficient of thermal expansion Thermal conductivity Ratio of 20-year to 28-day for Modulus of Elasticity Ratio of 20-year to 28-day for Rupture Modulus Ratio of 20-year to 28-day for Compressive Strength 28-day PCC Compressive Strength 28-day PCC Modulus of Rupture	PCC Unit Weight PCC Poisson's Ratio Heat capacity 7 day Modulus of Elasticity 7 day Rupture Modulus	Cementitious Material Content Water/Cement Ratio 28 day Modulus of Elasticity 7 day Compressive Strength 28 day Compressive Strength	Cement Type Aggregate Type Reversible Shrinkage (% of Ultimate Shrinkage) Time to develop 50% of Ultimate Shrinkage (days) Curing Method
	Granular Base/Subbase/Subgrade		Material Type Material Thickness		Poisson's Ratio Coefficient of Lateral Pressure Resilient Modulus (Level 2) Resilient Modulus (Level 3)
	Stabilized Base Inputs				Material Type Layer thickness Unit Weight Poisson's ratio Elastic Modulus Thermal Conductivity Heat Capacity
	Bedrock			Unit weight	Material Type Layer Thickness Poisson's Ratio Resilient Modulus

Table 3-4. Summary results for the sensitivity analysis performed on the MEPDG inputs (Stanigzai's 2007)

Summary of the Sensitivity Analysis					
		Very Sensitive Inputs	**Sensitive Inputs**	**Somewhat Sensitive Inputs**	**Insensitive Inputs**
Performance Criteria		Reliability			
Traffic		ADTT (Average Annual Daily Truck Traffic) Traffic Growth Factor	Mean Wheel Location	Hourly Truck Distribution Traffic Wander Standard Deviation No. Axles per Truck Monthly Adjustment Factors (Level 1 & 3) ADTT Distribution by Vehicle Class (Level 1 & 3)	Design Lane Width Percent Trucks in Design Lane Operational Speed Design Lane Width Average Axle Width (edge to edge outside Dimensions) Dual Tire Spacing Tandem Axle Spacing Tridem Axle Spacing Quad Axle Spacing
Climatic			Regional Climate Difference		Depth of Water Table
JPCP Design Features		Permanent Curl/Wrap Effective Temperature Difference Joint Spacing Tied PCC shoulder	PCC Base Interface	Surface Short-Wave Absorptivity Dowel Diameter[1] Dowel Bar Spacing Erodibility Index	Sealant Type Widened slab[2]
Material Properties	**PCC Material Properties**	PCC Layer Thickness PCC Poisson's Ratio Coefficient of Thermal Expansion Thermal Conductivity Heat Capacity Ratio of 20-year to 28-day of Modulus of Elasticity (Level 1) Ratio of 20-year to 28-day of Rupture Modulus (Level 1) Ratio of 20-year to 28-day of Compressive Strength (Level 2) 28-day PCC Compressive Strength (Level 3) 28-day Modulus of Rupture (Level 3)	PCC Unit Weight 7-day Modulus of Elasticity (Level 1) 7-day Rupture Modulus (Level 1)	Cementitious Material Content Water Cement Ratio 14-day Modulus of Elasticity (Level 1) 28-day Modulus of Elasticity (Level 1) 7-day Compressive Strength (Level 2) 14-day Compressive Strength (Level 2) 28-day Compressive Strength (Level 2)	Cement Type Aggregate Type Reversible Shrinkage (% of Ultimate Shrinkage) Time to develop 50% of Ultimate Shrinkage (days) Curing Method

Continued on following page;

Continue…

Summary of the Sensitivity Analysis

		Very Sensitive Inputs	Sensitive Inputs	Somewhat Sensitive Inputs	Insensitive Inputs
Material Properties	Granular Base/Subbase/Subgrade	Material Thickness	Material Type		Poisson's Ratio Coefficient of Lateral Pressure Resilient Modulus (Level 2) Resilient Modulus (Level 3)
	Stabilized Base Inputs				Material Type Layer thickness Unit Weight Poisson's ratio Elastic Modulus Thermal Conductivity Heat Capacity
	Bedrock		Unit Weight		Material Type Layer Thickness Poisson's Ratio Resilient Modulus

1. Using & not using Dowel bars, is very sensitive but once used the diameter difference is somewhat sensitive.
2. The difference between Widened and Un-Widened slabs is very sensitive but once widened by a width then the difference in that width is insensitive

3.3.1.10 Recommendations

Very Sensitive Inputs: The following inputs are very sensitive and therefore using more accurate values is extremely important in order to calculate the actual life, performance and cost of pavements. Most of these values can be obtained using laboratory tests (Stanigzai's 2007).

Table 3-5 shows a summary of the sensitivity of these inputs as well as how to calculate them.

Table 3-5. Sensitivity analysis results; Very Sensitive Inputs and their method of determination (Stanigzai's 2007)

Input	Source of Determination
Reliability	Federal/State given/Designer Choice
AADTT	WIM/Manual Traffic Count
Traffic Growth Factor	Site Traffic History
Effective Temp. Difference	Program Default/Electronic Equipment
Joint Spacing	Federal/State/Designer Choice (Usually less than 16ft)
Tied PCC Shoulders	Federal/State/Designer Choice/Project Requirement
PCC Layer Thickness	Project Requirement/Designer Choice
PCC Poisson's Ratio	ASTM C 469
PCC Coefficient of Thermal Expansion	AASHTO TP60, Standard Test Method for the Coefficient of Thermal Expansion of Hydraulic Cement Concrete
PCC Thermal Conductivity	ASTM E 1952
PCC Heat Capacity	ASTM D 2766
PCC Ratio of 20-year to 28-day of Modulus of Elasticity (Level 1)	ASTM C 469
PCC Ratio of 20-year to 28-day of Rupture Modulus (Level 1)	ASTM C 78 or AASHTO T 97
PCC Ratio of 20-year to 28-day of Compressive Strength (Level 2)	ASTM C 39 or AASHTO T 22 *(Compressive Strength of Cylindrical Concrete Specimens)*
PCC 28-day PCC Compressive Strength (Level 3)	ASTM C 39 or AASHTO T 22 *(Compressive Strength of Cylindrical Concrete Specimens)*
PCC 28-day Modulus of Rupture (Level 3)	ASTM C 78 or AASHTO T 97
Granular Material Thickness	Project Requirement/Designer Choice

Sensitive Inputs: These inputs affect the life (about 5-20 years), performance and cost of the pavements therefore it is important to determine more accurate values for them. Most of these values can be obtained through laboratory tests (Stanigzai's 2007).

Table 3-6 shows a summary of these inputs as well as how to calculate them.

Table 3-6. Sensitivity analysis results; Sensitive Inputs and their method of determination (Stanigzai's 2007)

Input	Source of Determination
Mean Wheel Location	Electronic/Manual Observation
Site Climate Input	Closest to Site Weather Station
PCC Base Interface	Laboratory Tests
PCC Unit Weight	Laboratory Tests
PCC 7-day Modulus of Elasticity (Level 1)	ASTM C 469
PCC 7-day Rupture Modulus (Level 1)	ASTM C 78 or AASHTO T 97
Granular Material Type	Site Material Tests
Bedrock Unit Weight	Laboratory Tests

Somewhat Sensitive Inputs: These inputs don't have much effect on pavement life and performance but might affect the cost of the pavement. It is recommended to use more accurate values for them if available or if they are easy to determine. The default

values for these inputs can be also used resulting in an output life difference of 1-5 years (Stanigzai's 2007).

Table 3-7 shows a summary of these inputs as well as how to calculate them.

Table 3-7. Sensitivity analysis results; Somewhat Sensitive Inputs and their method of determination (Stanigzai's 2007)

Input	Source of Determination
Hourly Truck Distribution	WIM/Manual Traffic Count/Program Default Value
Traffic Wander Standard Deviation	Manual Traffic Observation/ProgramDefault Value
No. Axles per Truck	WIM/Manual Traffic Observation/Program Default Value
Monthly Adjustment Factors (Level 1 & 3)	WIM/Manual Traffic Observation/Program Default Value
ADTT Distribution by Vehicle Class (Level 1 & 3)	WIM/Manual Traffic Observation/Program Default Value
Surface Short-Wave Absorptivity	Laboratory Tests/Program Default Values
Dowel Diameter	Project Requirement (Thicker Pavement, Bigger Dowels)/Program Default Values
Dowel Bar Spacing	Project Requirement/Program Default Values (12in)
Erodibility Index	Project Requirement (Material Type Beneath PCC)/Program Default Values
Cementitious Material Content	Project Requirement/Program Default Values
Water Cement Ratio	Project Requirement/Program Default Values
PCC 28-day Modulus of Elasticity (Level 1)	ASTM C 469
PCC 7-day Compressive Strength (Level 2)	ASTM C 39 or AASHTO T 22 *(Compressive Strength of Cylindrical Concrete Specimens)*
PCC 28-day Compressive Strength (Level 2)	ASTM C 39 or AASHTO T 22 *(Compressive Strength of Cylindrical Concrete Specimens)*

Insensitive Inputs: The pavement life and performance would not be sensitive to the change in these inputs (until 50 years). Still actual values are recommended but the default values can be also used which should result in similar outputs as the actual values (Stanigzai's 2007).

Table 3-8 shows a summary of these inputs as well as how to calculate them.

Table 3-8. Sensitivity analysis results; Insensitive Inputs and their method of determination (Stanigzai's 2007)

Input	Source of Determination
Design Lane Width	Project Requirement/Designer Choice/Default Value
Percent Trucks in Design Lane	WIM/Manual Traffic Count/Program Default Value
Operational Speed	WIM/Program Default Value
Average Axle Width (edge to edge outside Dimensions)	WIM/Manual Check/Program Default Value
Dual Tire Spacing	WIM/Manual Check/Program Default Value
Tandem Axle Spacing	WIM/Manual Check/Program Default Value
Tridem Axle Spacing	WIM/Manual Check/Program Default Value
Quad Axle Spacing	WIM/Manual Check/Program Default Value
Depth of Water Table	Manual Test/Program Default Value
Sealant Type	Best Suitable/Designer Choice/Default Value
Widened slab	Project Requirement/Designer Choice/Default Value
PCC Cement Type	Designer Choice/Material Availability
PCC Aggregate Type	Designer Choice/Material Availability
PCC Reversible Shrinkage (% of Ultimate Shrinkage)	Laboratory Tests/Default Values
PCC Time to develop 50% of Ultimate	Laboratory Tests/Default Values
PCC Shrinkage (days)	Laboratory Tests/Default Values
PCC Curing Method	Project Requirement/Designer Choice/Default Value
Granular Material Poisson's Ratio	Laboratory Tests/Default Values
Granular Material Coefficient of Lateral Pressure	Laboratory Tests/Default Values
Granular Material Resilient Modulus (Level 2)	AASHTO T 307, *Determining the Resilient Modulus of Soil and Aggregate Materials*
Granular Material Resilient Modulus (Level 3)	AASHTO T 307, *Determining the Resilient Modulus of Soil and Aggregate Materials*
Stabilized Base Material Type	Designer Choice/Material Availability
Stabilized Base Layer thickness	Designer Choice/Material Availability
Stabilized Base Unit Weight	Laboratory Tests/Program Default Values
Stabilized Base Poisson's ratio	Laboratory Tests/Program Default Values
Stabilized Base Elastic Modulus	For new JPCP using structural analysis & for in-service
	pavements and rehabilitation design, through non-destructive using the Falling Weight Deflectometer (FWD) data back calculation or the Dynamic Cone Penetrometer (DCP).
Stabilized Base Thermal Conductivity	ASTM E 1952/Program Default Values
Stabilized Base Heat Capacity	ASTM D 2766/Program Default Values
Bedrock Material Type	Site Tests/Program Default Values
Bedrock Layer Thickness	Site Tests/Program Default Values
Bedrock Poisson's Ratio	Laboratory Tests/Program Default Values
Bedrock Resilient Modulus	Laboratory Tests/Program Default Values

Chapter 4

Field Instrumentation Proposal

This section explains a method that can be used in order to determine a more accurate value for a very sensitive MEPDG input using field instrumentation. This very sensitive input is called Permanent Curl/Warp Effective Temperature Difference and currently a default value of -10 is being used in the MEPDG.

4.1 Permanent Curl/Warp Effective Temperature Difference

The equivalent temperature differential between the top and bottom layers of the concrete slab that can is quantitatively described with "Permanent Curl/Warp Effective Temperature Difference" and basically this parameter is the locked in stresses in the slab due to the following effects:

1. Construction temperatures,
2. Shrinkage,
3. Creep,
4. Curing conditions.

This temperature difference is typically a negative number, representing the case when the top of the slab is cooler than the bottom of the slab. The magnitude of permanent curl/warp is a sensitive factor that affects JPCP performance. This is a direct input in the MEPDG software which is -10 by default (Figure 4-1).

The Curl/warp effective temperature difference, coefficient of thermal expansion, and thermal conductivity are the most critical design input parameters that affect all of the performance criteria. The second and third parameters can be directly determined from laboratory tests. The third one however, needs to be determined accurately especially since default values cannot be used for this input parameter as they affect the results significantly. The sensitivity of the model to these parameters is extremely high; therefore, pavement performance outputs can vary significantly.

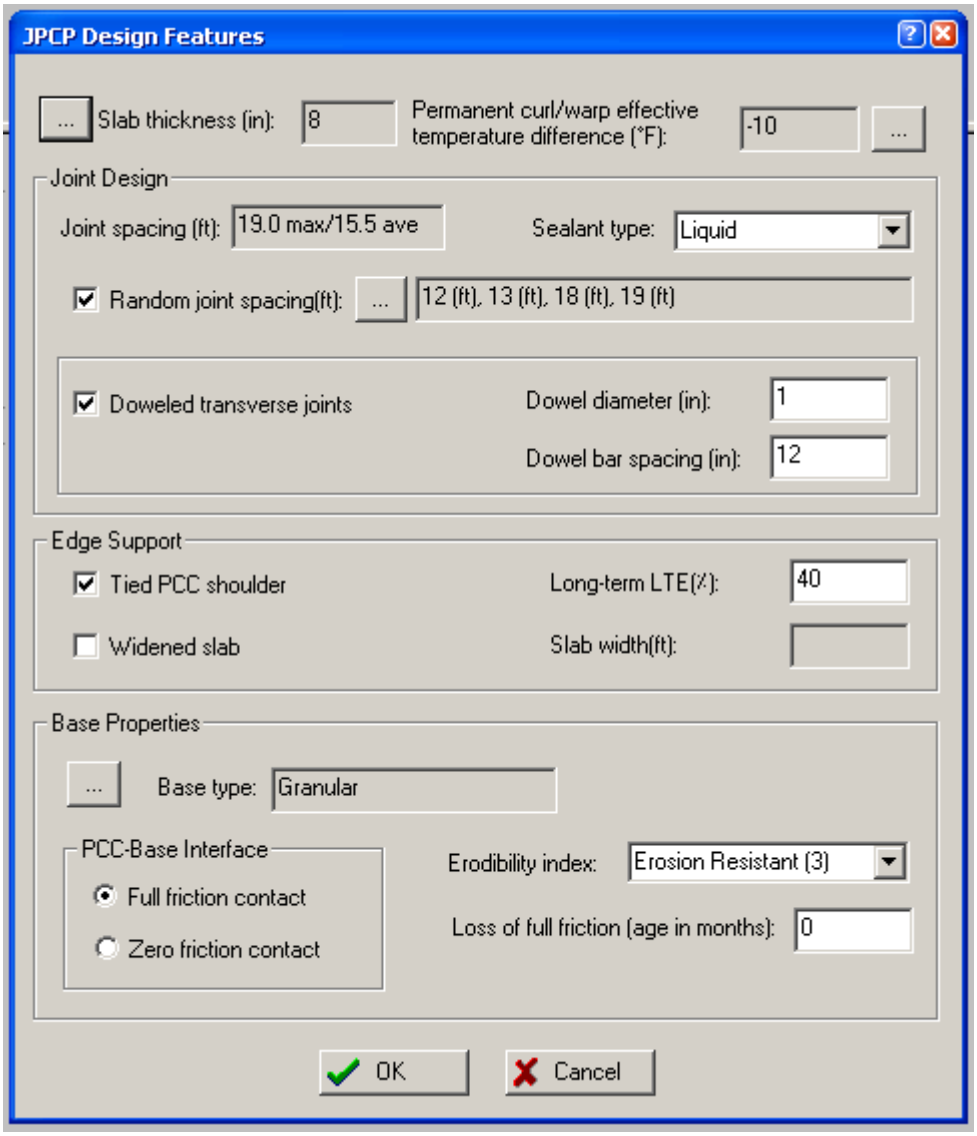

Figure 4-1. MEPDG software window for entering the Permanent curl/warp effective temperature difference (oF)

Some of the factors that affect the permanent curl/warp include the following:

- Climate (air temperature, solar radiation, relative humidity, wind speed) during and after PCC placement.
- Construction time and curing procedure (morning construction with intense solar radiation, nighttime construction, regular curing compound, reflective curing compound, wet curing).
- PCC mix properties including cement type, water-cement ratio, cement quantity, and aggregate type.
- Creep of the PCC slab from self weight and edge constraints such as tied shoulder and doweled joints.

- Base stiffness (or the ability of slab to settle into the base to relieve curl/warp stresses).

4.2 Permanent Curling and Warping

PCC paving is often performed during the mornings of hot sunny days, a condition that tends to expose the newly paved PCC slabs to a high positive temperature difference from intense solar radiation plus the heat of hydration. The PCC slabs are flat when they harden, but depending on the exposure conditions a significant amount of positive temperature gradient (upper portion of the slab is much warmer than bottom) may be present at the time of hardening. This temperature has been termed the "built-in temperature gradient" or in this guide it is called the "zero-stress temperature gradient". Whenever the temperature gradient in the slabs fall below the amount locked into the slab at the time of construction (the zero-stress gradient), the slabs will attempt to curl upward causing tensile stress at the top of the slab which can lead to top down cracking of JPCP. Thus, an effective negative temperature gradient is permanently "built" into the slabs.

The upward curling of pavement slabs is restrained by several factors, including the slab self weight, dowels, and the weight of any base course bonded to the slab. This hypothesis has been supported using data from instrumented field slabs located in different climatic conditions.

These factors affect the amount of actual permanent curl, as well as the amount of creep relaxation that may take place.

If the PCC paving is performed in the morning, the maximum heat of hydration and the maximum solar radiation coincides at about the same time resulting in a large built-in temperature gradient when the slab solidifies. If PCC paving is performed later in the afternoon or at night so that the highest temperature from the heat of hydration does not correspond with the most intense solar radiation, the amount of permanent temperature gradient "built" into the slab will be much lower and could potentially even be negative. Also, moist curing with water spray, wet burlap, or perhaps curing with reflective curing compounds can also produce a lower "zero-stress" or "built-in" permanent temperature gradient than regular curing compound.

As discussed under "Moisture Warping," differential moisture gradient causing a shrinkage gradient through the slab also produces a "permanent warping", which is superimposed on the zero-stress thermal gradient and is basically indistinguishable from permanent built-in curling.

The permanent components of curling and warping are, therefore, considered together. The magnitude of permanent curling and warping is estimated from calibration of JPCP cracking and is expressed in terms of effective temperature difference from the top to bottom of the slab (called "permanent curl/warp"). It is important to note that only a portion of permanent curl/warp actually affects pavement response, because settlements that occur over time negate some of the effects of permanent curvature present in PCC slabs. The magnitude of permanent curl/ warp estimated from calibration reflects the effects of settlement into the base and creep.

4.3 Consideration of Climatic Effects in Cracking Prediction

The temperature and moisture effects are directly considered in the design of the JPCP as follows:

- The permanent built-in curling that occurs during construction (the zero-stress temperature gradient) is combined with the permanent warping due to differential shrinkage and expressed in terms of effective temperature difference between top and bottom (called "permanent curl/warp"). This parameter is a direct and influential input to the prediction of JPCP cracking.
- Transient hourly negative and positive temperature differences (from top to bottom of the slab) caused by solar radiation are computed using the EICM.
- Transient negative moisture shrinkage in the top of the slab caused by changes in relative humidity during each month of the year is converted to an equivalent temperature difference for every month.

All three of the above temperature and moisture differences through the PCC slab are predicted and appropriately combined along with axle loads to compute critical slab stresses, which are used within a monthly increment to accumulate damage at the bottom and at the top of the slab.

The actual slab curvature can be highly variable even along a given project, and a combination of adverse factors (e.g., a high shrinkage PCC mix, excessive temperature gradient at the time of PCC placement, and placement in morning hours and inadequate curing) can lead to extremely high permanent curl/warp, resulting in early top down cracking.

The current value used in the MEPDG software has been determined via calibration of this input value using an optimization technique using the fatigue damage algorithm and the field cracking from over 500 observations. The goal of the calibration technique was to select the permanent curl/warp that resulted in the lowest prediction error between measured and predicted cracking for those 500 observations. The calibration results indicate that the values of long-term effective permanent curl/warp is fairly uniform, with no obvious bias based on climate or design factors, including slab thickness and base type. The recommended value for an effective linear permanent curl/warp is -10 °F from top to bottom of the slab for JPCP for all climatic regions. This is an equivalent linear temperature difference from top to bottom of the slab.

Various design situations may occur where an increase or decrease in this parameter may be warranted. For example, nighttime construction should result in a lower value due to no solar radiation at night. Another example identified during calibration of the JPCP cracking model indicated that when a significant amount of erosion occurs beneath a non-doweled transverse joint and loss of support occurs, an increased top down stress results. This often caused a transverse crack near the transverse joint on the leave side. Use of an increased value for permanent curl/warp (such as -15 °F) helps to account for this critical situation and predicts more accurately the amount of cracking that develops over time.

Note that this situation could be handled in design through use of dowel bars and a more non-erodible base course.

Knowing the importance of the parameter, there is a great need to well establish the "Permanent Curl/Warp Effective Temperature Difference" for the state of Nebraska.

4.4 Proposed procedure to experimentally determine ΔTBI

In order to determine the Permanent Curl/Warp Effective Temperature an iterational back-calculation approach can be performed on the Faulting model.

Difference between temperatures at the top and bottom surfaces of the effective slab for month m, $\Delta T_{eff,m}$, is a function of ΔT_{BI} (Built-in curling and temperature shrinkage temperature differential.) Therefore, having ΔT_{BI} (Built-in curling and temperature shrinkage temperature differential), the value of $\Delta T_{eff,m}$, is calculated directly from the following equation. For the first iteration, a value (say -10 which is the default value in the MEPDG software) can be assumed for ΔT_{BI} and calculate the $\Delta T_{eff,m}$ from the following equation;

$$\Delta T_{eff,m} = \frac{h_{PCC}^2}{H_{eff}^2} \times \left[\left(T_{top,m} - T_{bot,m} \right) + \Delta T_{BI} + \Delta T_{sh,m} \right] \qquad 4\text{–}1$$

where

$\Delta T_{eff,m}$ = Difference between temperatures at the top and bottom surfaces of the effective slab for month m.
$T_{top,m}$ = Mean night temperature of the top PCC surface for month m.
$T_{bot,m}$ = Mean night temperature of the bottom PCC surface for month m.
ΔT_{BI} = Built-in curling and temperature shrinkage temperature differential.
$\Delta T_{sh,m}$ = Equivalent temperature differential due to reversible portion of shrinkage.
h_{PCC} = PCC thickness.
H_{eff} = Effective thickness computed.

In equation 4–1 the parameters $\Delta T_{top,m}$ and $\Delta T_{bot,m}$ are read from the climate model in the software MEPDG. For the specific instrumented site, it can be determined through temperature gages installed in the pavement section. So the value of the "difference between temperatures at the top and bottom surfaces of the effective slab for month m", $\Delta T_{eff,m}$ is determined.

The procedure for calculating the shrinkage contribution ($\Delta T_{sh,m}$) to curling is as the following;

Calculate the reversible shrinkage contribution to long-term curling from

$$\varepsilon_{sh,average}(t) = \begin{cases} \varepsilon_{su}.(1.4 - 0.01 \times RH_{average}) & if \quad RH_{average} < 80 \\ \varepsilon_{su}.(3.0 - 0.03 \times RH_{average}) & if \quad RH_{average} \geq 80 \end{cases} \qquad 4\text{–}2$$

where

$\varepsilon_{sh,average}$ = Shrinkage strain for the average relative humidity, $\times 10^{-6}$.
ε_{sh} = Ultimate shrinkage strain for the relative humidity equal to 40 percent, $\times 10^{-6}$.
$RH_{average}$ = Average mean monthly ambient relative humidity, percent.

The value of the parameter $RH_{average}$ is read from the climate model in the software MEPDG. For the specific instrumented site, it can be determined through humidity gages installed in the pavement section.

The free shrinkage strain as if the relative humidity is equal to the relative humidity of the driest month can be determined using following equation

$$\varepsilon_{sh,m}(t) = \begin{cases} \varepsilon_{su}.(1.4 - 0.01 \times RH_m) & if \quad RH_m < 80 \\ \varepsilon_{su}.(3.0 - 0.03 \times RH_m) & if \quad RH_m \geq 80 \end{cases} \quad \Rightarrow \quad m = 1,12 \qquad 4\text{–}3$$

where

$\varepsilon_{sh,m}$ = Free shrinkage strain for the mean relative humidity of month m,$\times 10^{-6}$.
ε_{sh} = Ultimate shrinkage strain for the relative humidity equal to 40 percent,$\times 10^{-6}$.
RH_m = Ambient relative humidity for month m, percent

And from all above information the shrinkage contribution to curling can be determined:

$$\Delta T_{SH,m} = \frac{3.0\varphi.(\varepsilon_{h,m} - \varepsilon_{h,average}).h_s.\left(\frac{h_{PCC}}{2} - \frac{h_s}{3}\right)}{\alpha.h^2.100} \qquad 4\text{–}4$$

where

$\Delta T_{SH,m}$ = Temperature gradient equivalent of moisture warping for month i, °F.
φ = Reversible shrinkage factor, fraction of total shrinkage. Use 0.5 unless more accurate information is available.
ε_{su} = Ultimate shrinkage, × 10-6.
RH_{hi} = Average relative humidity for month i, percent.
$S_{h,ave}$ = Annual average relative humidity, percent.
h_s = Depth of the shrinkage zone (typically 2 in).
h_{PCC} = PCC slab thickness, in.
α = PCC coefficient of thermal expansion, in/in/°F.

In equations 4–2 to 4–4 all of the parameters are either geometric specifications of the pavement section or can be calculated via laboratory tests, field tests, or previous equations. The "ambient relative humidity" parameters for the specific instrumented site can be determined through temperature gages installed in the pavement section. Therefore, the value of the $\Delta T_{sh,m}$ is determined and can be inserted into equation 4–1 in order to determine the value of $\Delta_{Teff,m}$.

Having all of the above information, the parameter φ_m (Korenev's Nondimensional temperature gradient) can be determined from the following equation.

$$\phi_m = \frac{2\alpha_{PCC}(1+\mu_{PCC})l_m^2}{H_{eff,m}^2}\frac{k_m}{\gamma_{eff,m}}\Delta T_{eff,m} \quad 4–5$$

where

φ_m = Nondimensional temperature gradient for month m.
h_{PCC} = PCC slab thickness.
α_{PCC} = PCC coefficient of thermal expansion.
μ_{PCC} = Poisson's ratio for PCC.
γ_{eff} = Effective unit weight for month m.
k = Modulus of subgrade reaction (k-value) for month m.
l_m = Radius of relative stiffness for month m.
$\Delta T_{eff,\,m}$ = Effective temperature gradient for month m.

Curling deflection, the amount of JPCP faulting due to only the temperature gradients for month m, $\delta_{curl,m}$, is a parameter used in transverse faulting model. This parameter can be calculated from the following equation

$$\delta_{curl,m} = \frac{34100596.7h_{eff,m}}{l_m^4 k_m}\left[NN_c(JTSpace, l_m, \phi_m) - NN_c(JTSpace, l_m, 0)\right] \quad 4–6$$

where

$\delta_{m,curl}$ = Corner deflection due to curling only.
JTSpace = Mean transverse joint spacing.
l_m = Radius of relative stiffness for month m.
φ_m = Nondimensional temperature gradient for month m.
$NN_c(JTSpace, l_m, \varphi_m)$ = Neural network trained to determine corner deflections due to slab curling only (no axle loading)

Curling deflection due to curling only for month m, $\delta_{curl,m}$, on the other hand, is a measurable parameter via field instrumentation using a JDMD (Joint Deflection Measurement Device), a LVDT or a Multi-Depth Deflectometer. This measurement is compared to the calculated deflection. If they are not equal, the assumed value for the ΔT_{BI} is changed and the process will be repeated again until the deflections are equal.

4.5 Instruments needed to determine the Permanent Curl/Warp Effective Temperature

- Deflection due to curling for month m, $\delta_{curl,m}$, can be measured using a JDMD (Joint Deflection Measurement Device), a LVDT or a Multi-Depth Deflectometer.
- The parameter $\Delta T_{eff,m}$, which is the difference between temperatures at the top and bottom surfaces of the effective slab for month m, can be determined through temperature gages installed in the pavement section.
- The value of Relative Humidity, $RH_{average}$, can be determined through humidity gages installed in the pavement section.

Chapter 5

Conclusions and Recommendations

The findings of this research project provide valuable information as NDOR continues to evaluate implementation of the MEPDG. Due to the fact that sensitive and very sensitive inputs can change the pavement responses significantly, NDOR believes it is necessary to not only research "permanent curl/warp effective temperature difference", but also many of the other sensitive variables that need calibration for Nebraska's condition. NDOR will continue to actively evaluate the MEPDG process in preparation for future implementation nationwide.

Followings are some of the conclusions that can be obtained from this report.

MEPDG package can be adequately used for pavement design applications if acceptable design inputs are used. In fact, the level of accuracy of MEPDG is highly dependent on the level of accuracy of input values.

Extreme attention is needed to determine accurate values for very sensitive and sensitive inputs as they can change the pavement responses significantly.

A default value of -10 ^{o}F is used in MEPDG for "permanent curl/warp effective temperature difference" for all design applications although this is a very sensitive entry that can significantly change the final results. In fact, "permanent curl/warp effective temperature difference" is given as a constant with little guidance for variance.

The value of "permanent curl/warp effective temperature difference" can be determined for the State of Nebraska through instrumentation of pavement sections. This can be done with a back-calculation of the MEPDG faulting model.

Chapter 6

References

NCHRP (2003). "Guide for Mechanistic-Empirical Design of New and Rehabilitated Pavement Structures; APPENDIX JJ: Transverse Joint Faulting Model." Final Report for Project 1-37A, APPENDIX JJ. Transportation Research Board, National Research Council, NCHRP. Washington, DC.

NCHRP (2003). "Guide for Mechanistic-Empirical Design of New and Rehabilitated Pavement Structures; APPENDIX KK: Transverse Cracking of JPCP." Final Report for Project 1-37A, APPENDIX KK. Transportation Research Board, National Research Council, NCHRP. Washington, DC.

NCHRP (2003). "Guide for Mechanistic-Empirical Design of New and Rehabilitated Pavement Structures; APPENDIX NN: Calibration of Rehabilitation of Existing Pavements with PCC." Final Report for Project 1-37A, APPENDIX NN. Transportation Research Board, National Research Council, NCHRP. Washington, DC.

NCHRP (2003). "Guide for Mechanistic-Empirical Design of New and Rehabilitated Pavement Structures; APPENDIX QQ: Structural Response Models for Rigid Pavement Structures." Final Report for Project 1-37A, APPENDIX QQ. Transportation Research Board, National Research Council, NCHRP. Washington, DC.

NCHRP (2004). "Guide for Mechanistic-Empirical Design of New and Rehabilitated Pavement Structures." Final Report for Project 1-37A, Part 1 & Part 3, Chapter 4. Transportation Research Board, National Research Council, NCHRP. Washington, DC.

Stanigzai, M.A. (2007). "A Parametric Study of Mechanistic-Empirical Design Guide for Jointed Plain Concrete Pavements." *A Master's THESIS, The Graduate College at the University of Nebraska*, Lincoln, Nebraska.

Appendix A

Detailed Results of Sensitivity Analysis

The graphs resulting from the sensitivity analyses carried out on the MEPDG software inputs for JPCP are presented in this appendix. Every analysis is associated with three major distress types; Faulting, Cracking, and IRI which are each depicted in separate plots. There are three major sets of inputs associated with MEPDG; structural inputs, traffic inputs, and climate inputs. In addition to these major sets there is also a general input of design reliability.

A1 Reliability

The design reliability is one of the general inputs for the MEPDG.

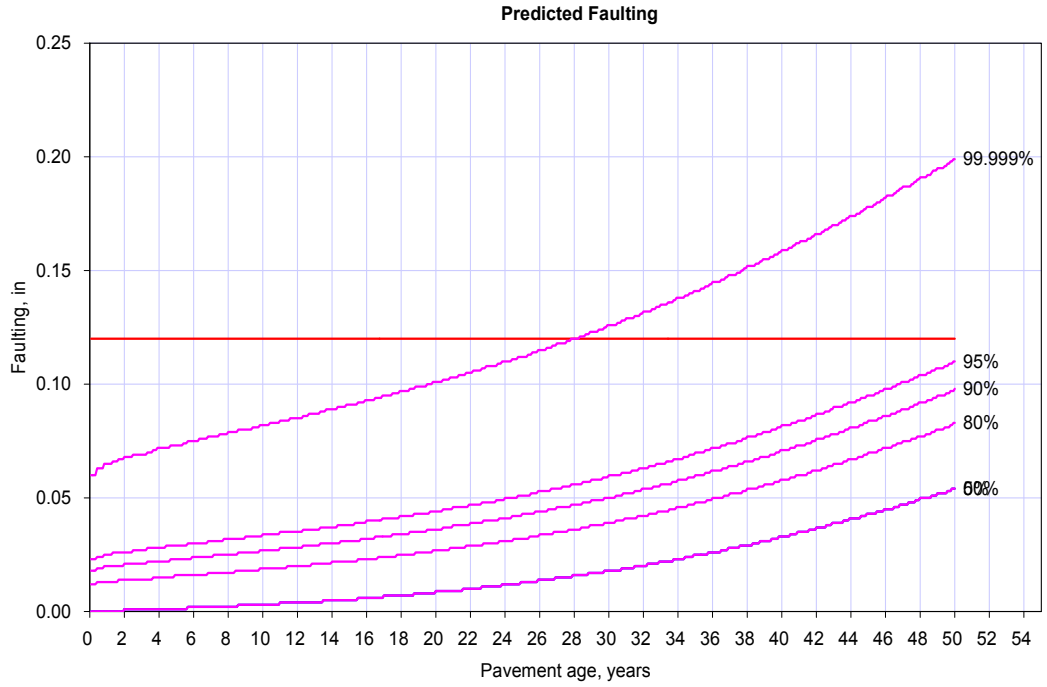

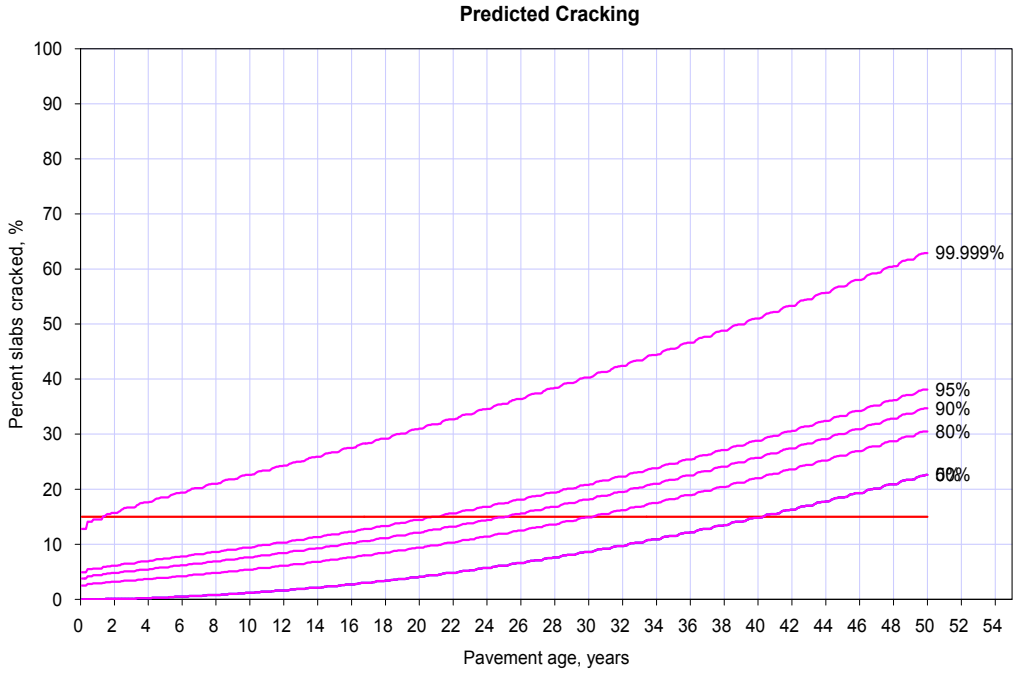
Predicted Cracking
Percent slabs cracked, %
Pavement age, years
99.999%
95%
90%
80%
50%

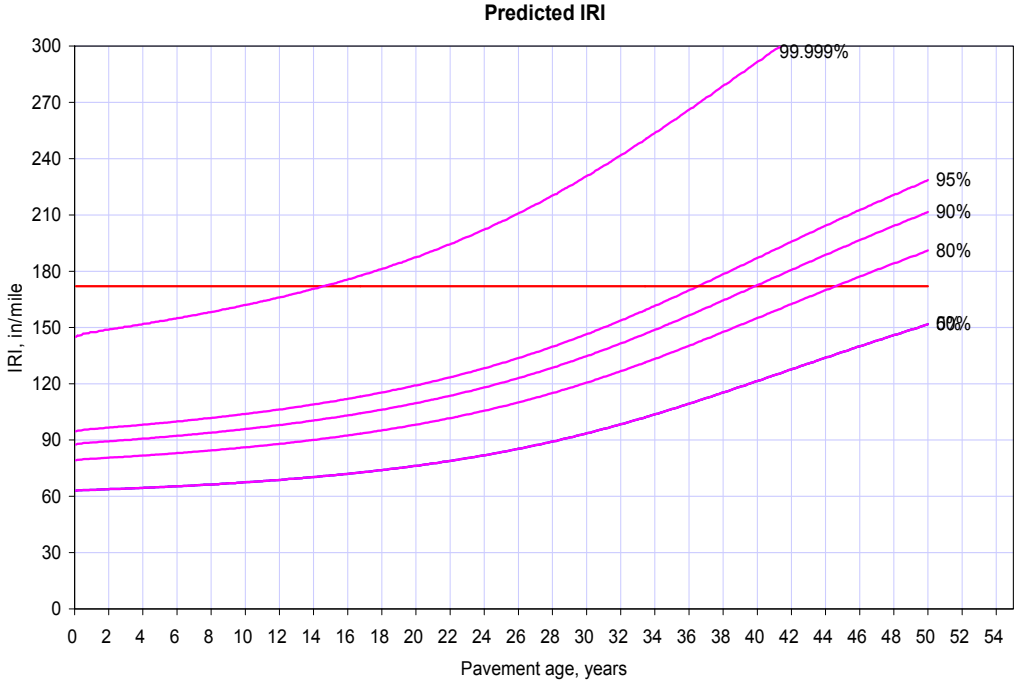
Predicted IRI
IRI, in/mile
Pavement age, years
99.999%
95%
90%
80%
50%

A2 Traffic Inputs

A2.1 AADTT (Average Annual Daily Truck Traffic)

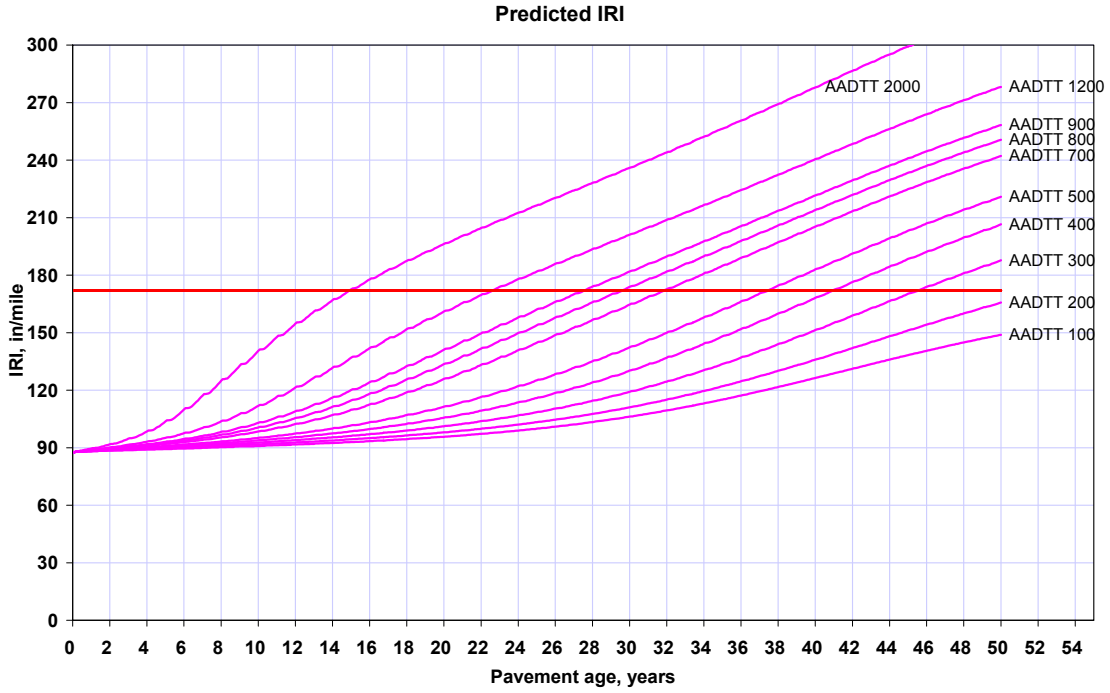

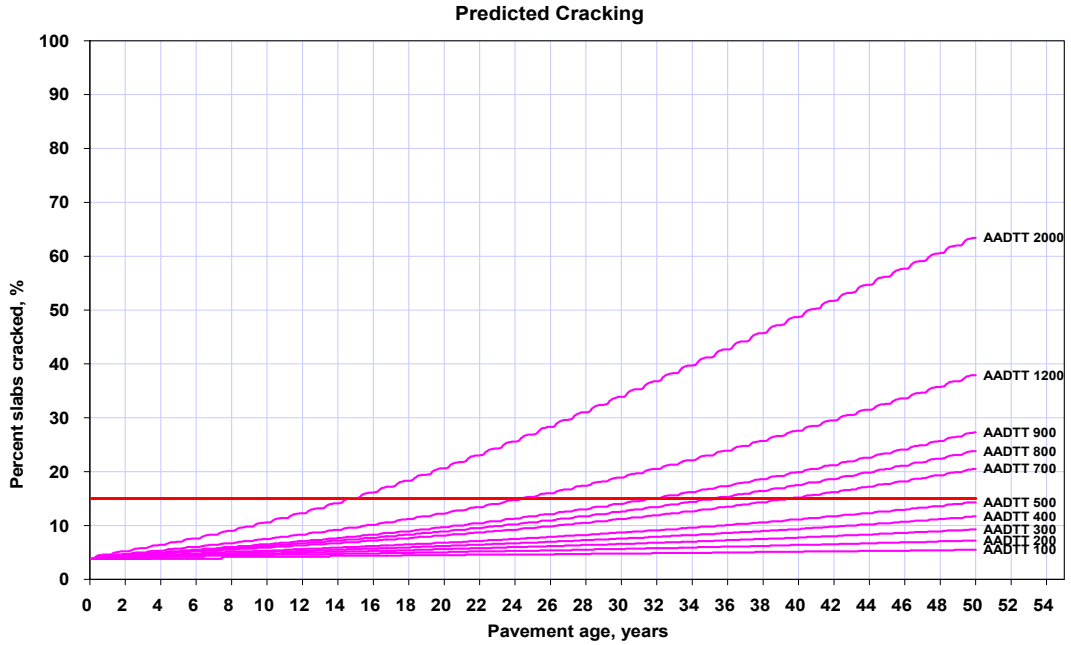

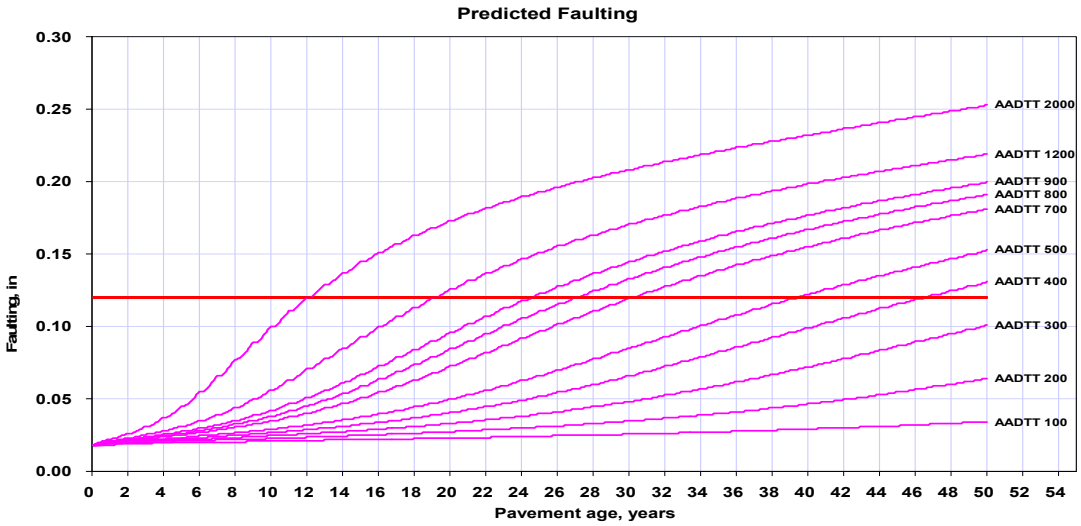

A2.2 Design Lane Width

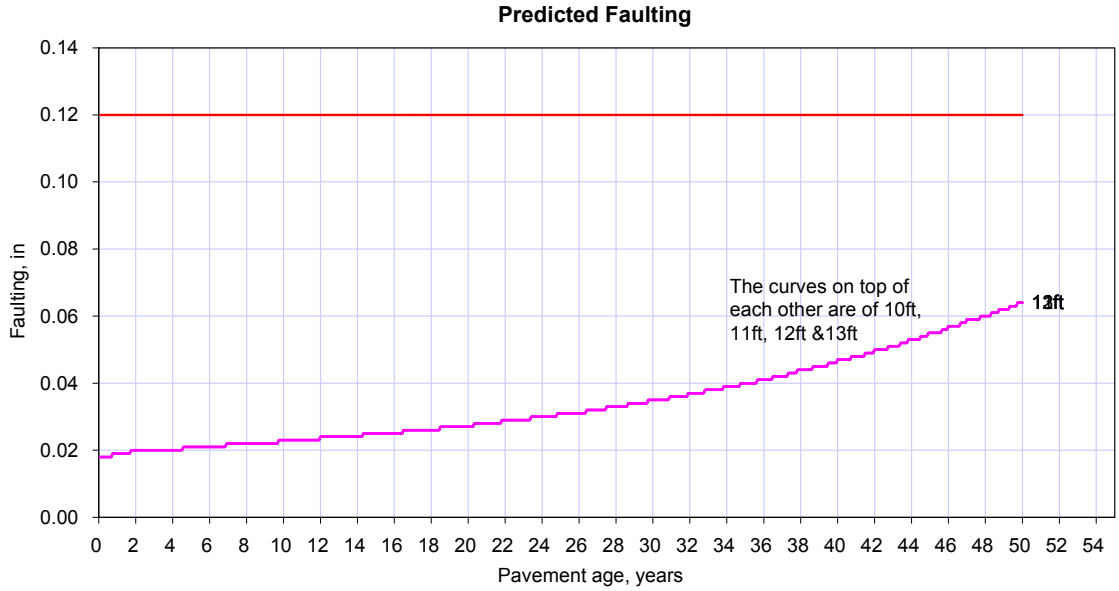

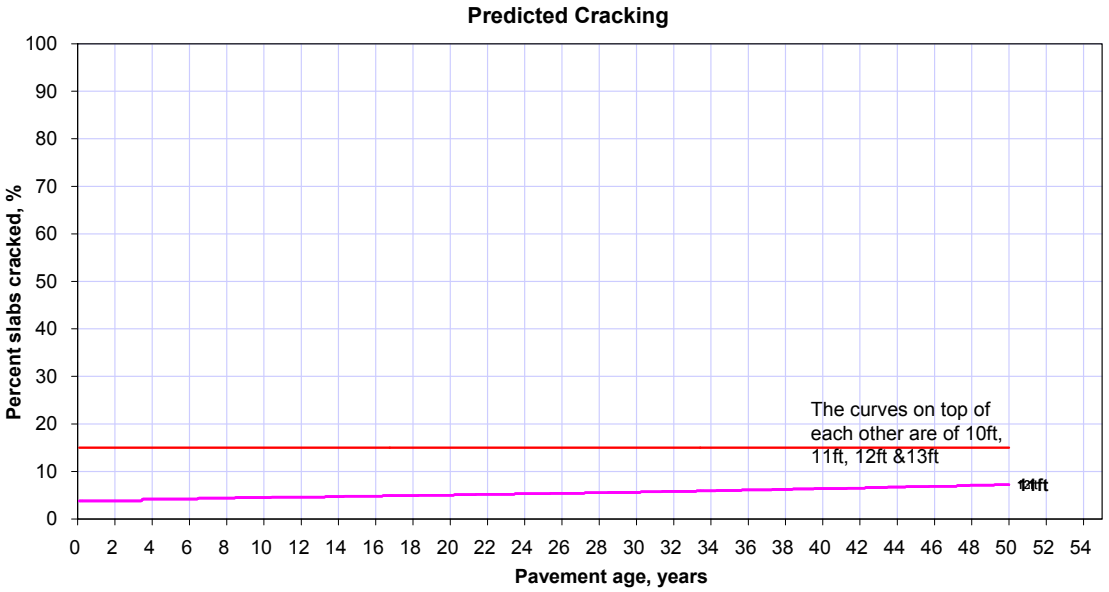
Predicted Cracking
Percent slabs cracked, %
100
90
80
70
60
50
40
30
20
10
0
0 2 4 6 8 10 12 14 16 18 20 22 24 26 28 30 32 34 36 38 40 42 44 46 48 50 52 54
Pavement age, years
The curves on top of each other are of 10ft, 11ft, 12ft &13ft

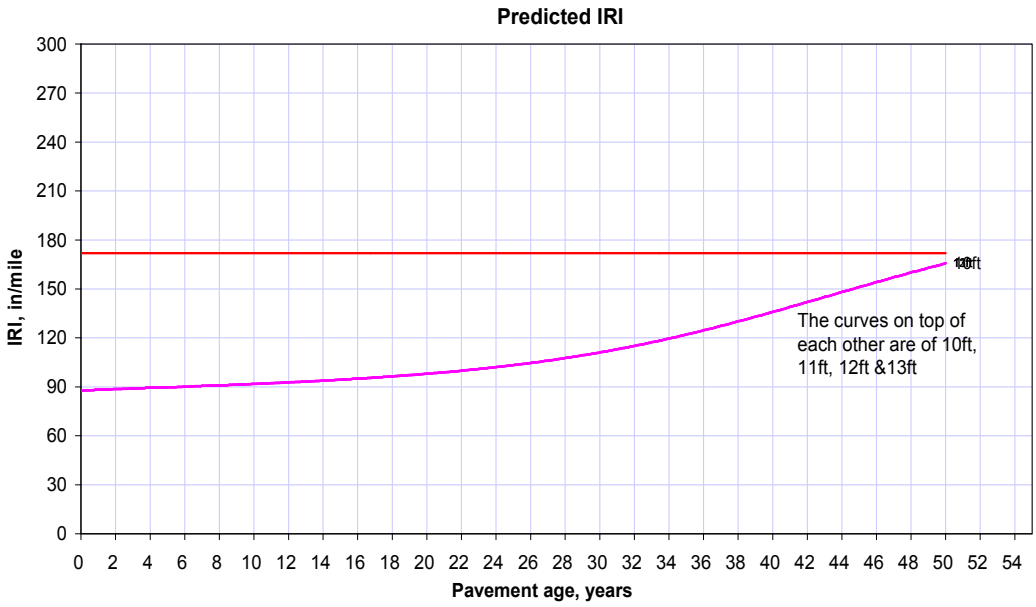
Predicted IRI
IRI, in/mile
300
270
240
210
180
150
120
90
60
30
0
0 2 4 6 8 10 12 14 16 18 20 22 24 26 28 30 32 34 36 38 40 42 44 46 48 50 52 54
Pavement age, years
The curves on top of each other are of 10ft, 11ft, 12ft &13ft

A2.3 Percent Trucks in Design Lane

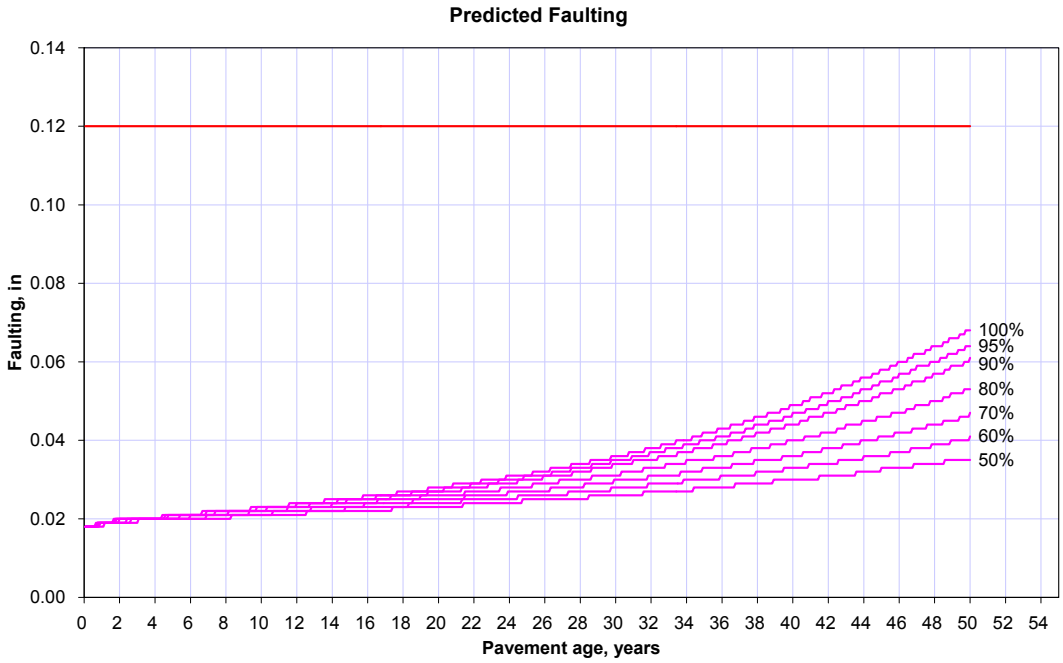

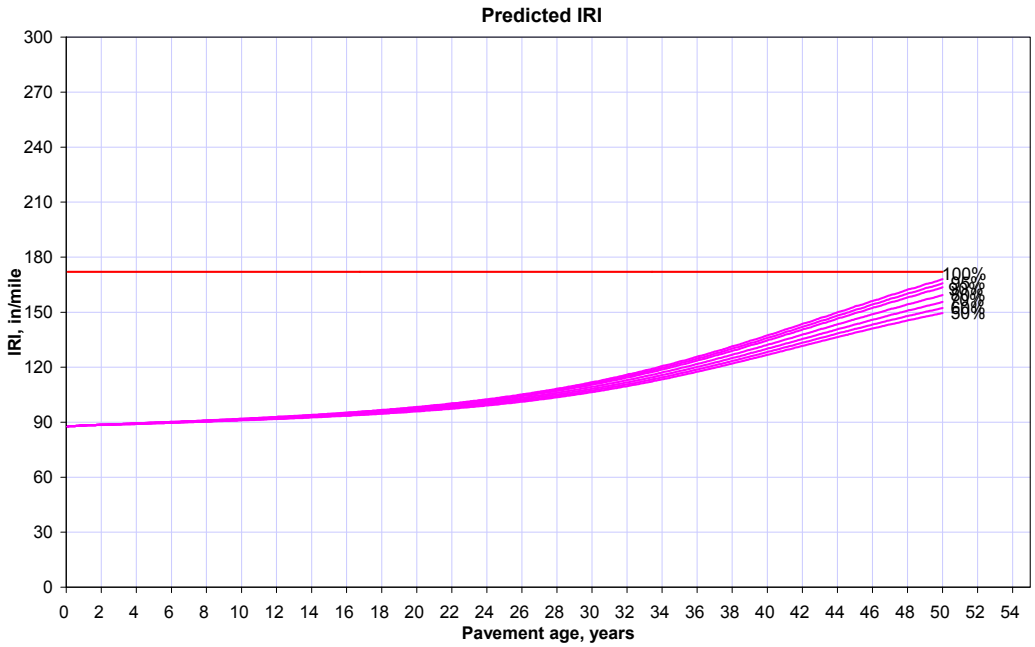

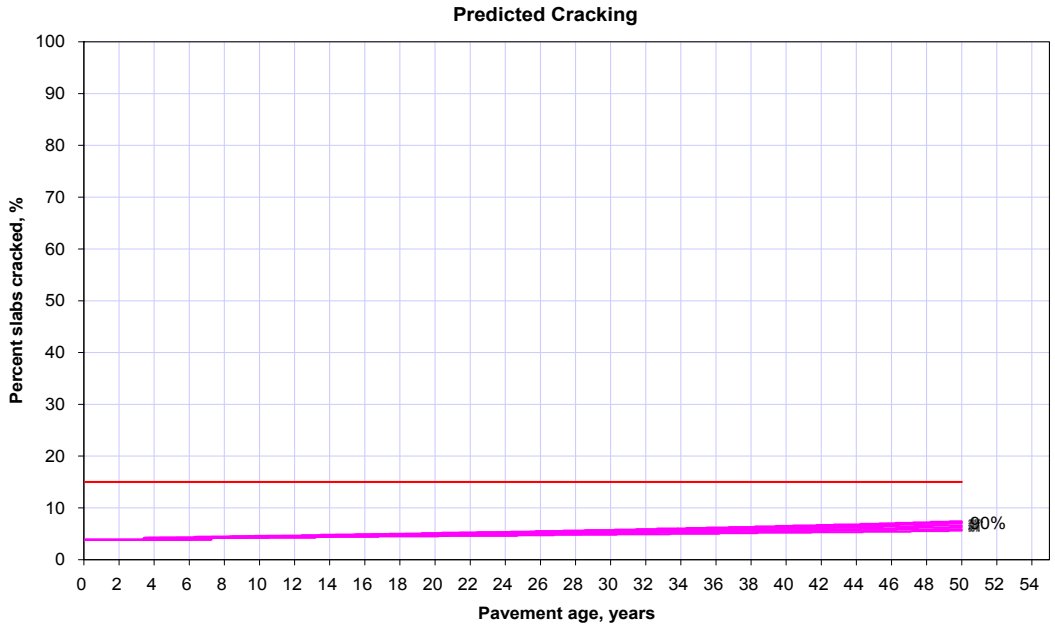

A2.4 Speed of traveling

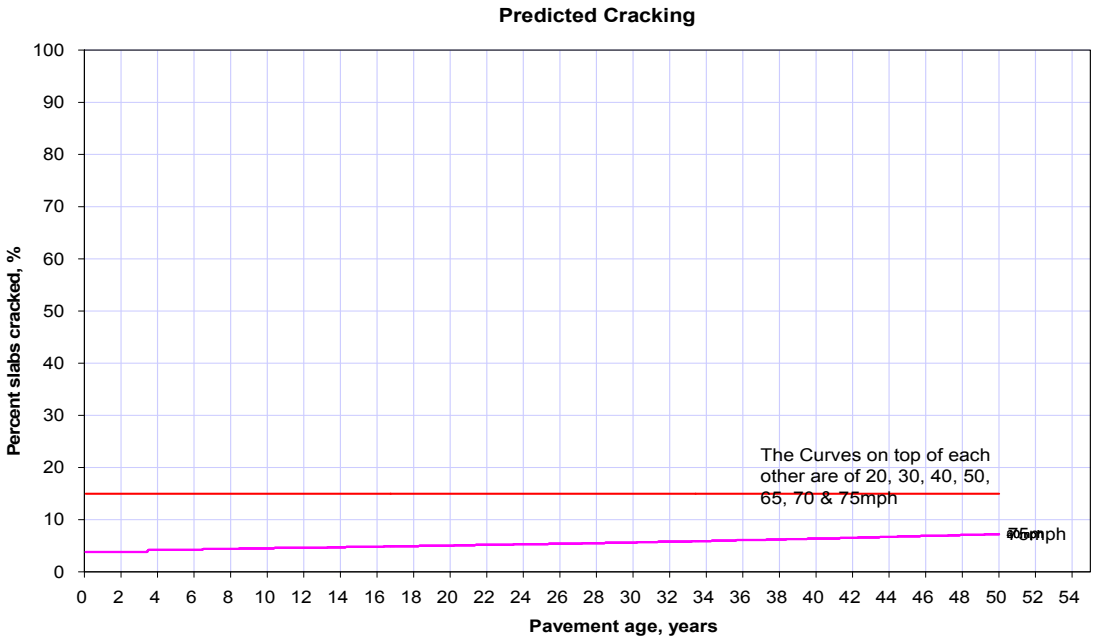

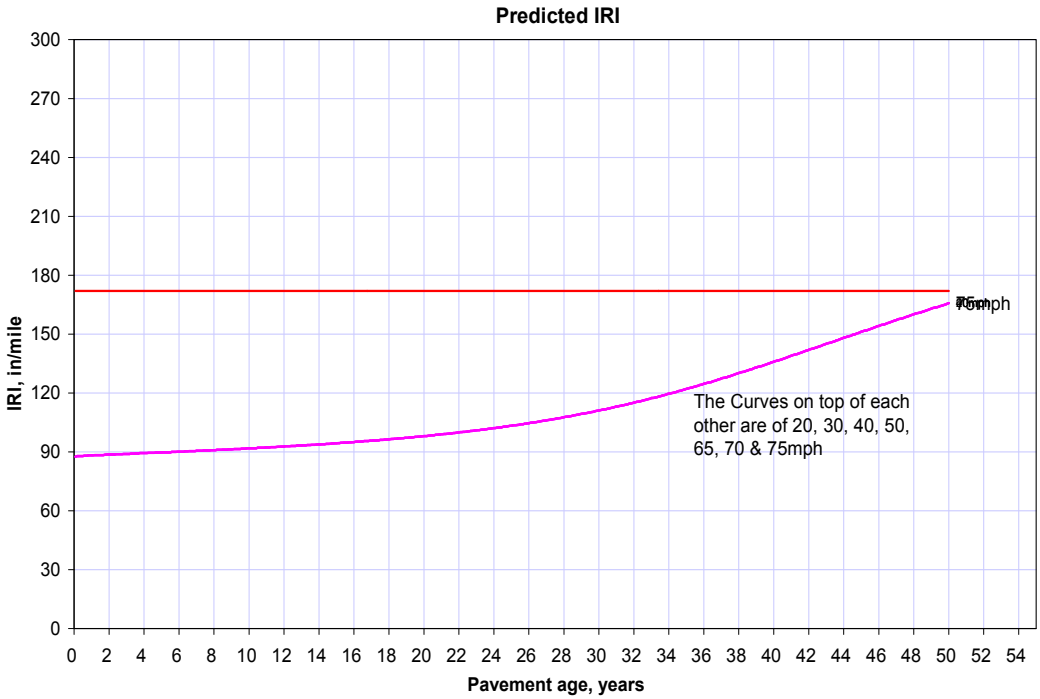
Predicted IRI
IRI, in/mile
Pavement age, years
The Curves on top of each other are of 20, 30, 40, 50, 65, 70 & 75mph

A2.5 Traffic Growth Factor

The Design Guide software considers the growth for each truck class separately. The user has the option of choosing one of three growth functions:

No Growth: Traffic volume remains the same through out the design life.

Linear Growth: The traffic volume increases by constant percentage of the base year traffic across each truck class

Compound growth: The traffic volume increases by constant percentage of the preceding year traffic across each truck class

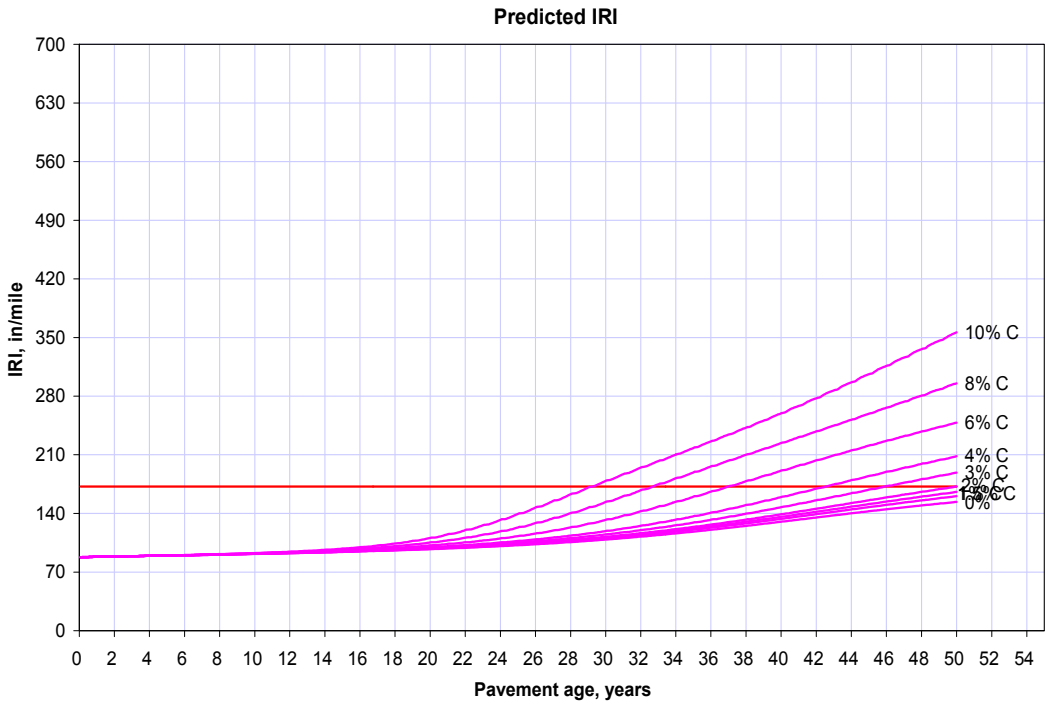

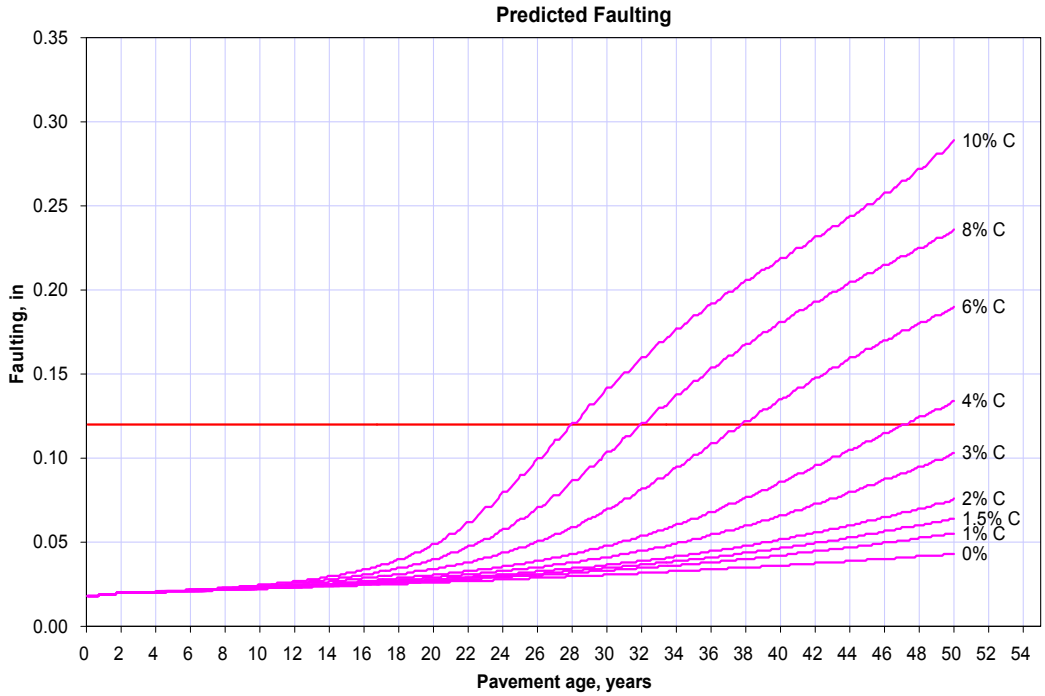
Predicted Faulting
Faulting, in
0.35
0.30
0.25
0.20
0.15
0.10
0.05
0.00
0 2 4 6 8 10 12 14 16 18 20 22 24 26 28 30 32 34 36 38 40 42 44 46 48 50 52 54
Pavement age, years
10% C
8% C
6% C
4% C
3% C
2% C
1.5% C
1% C
0%

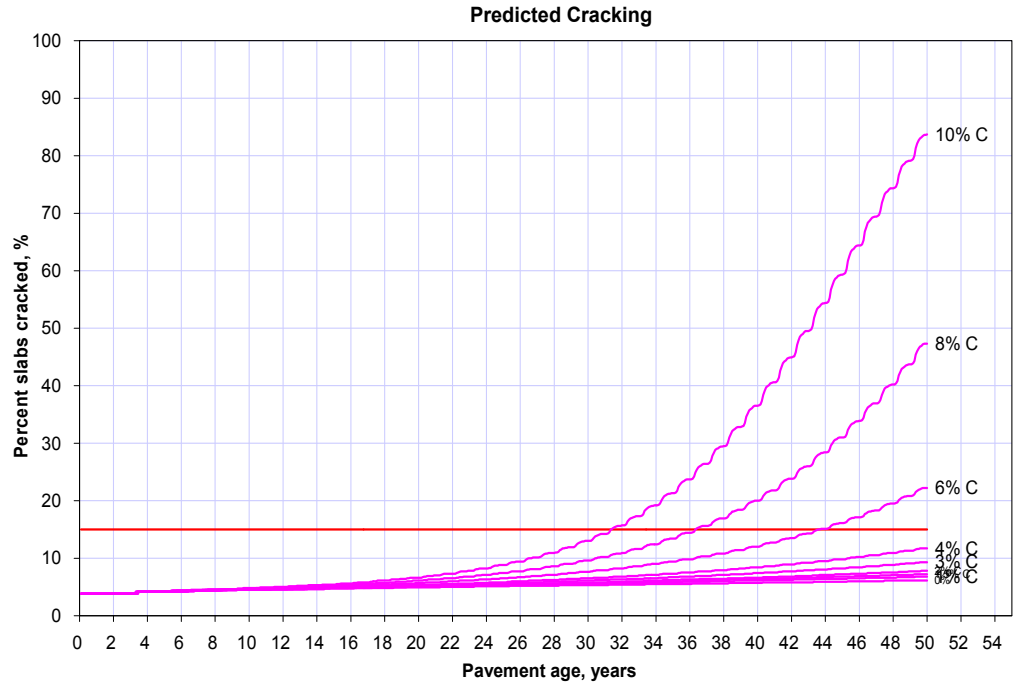

A2.6 Hourly Truck Distribution

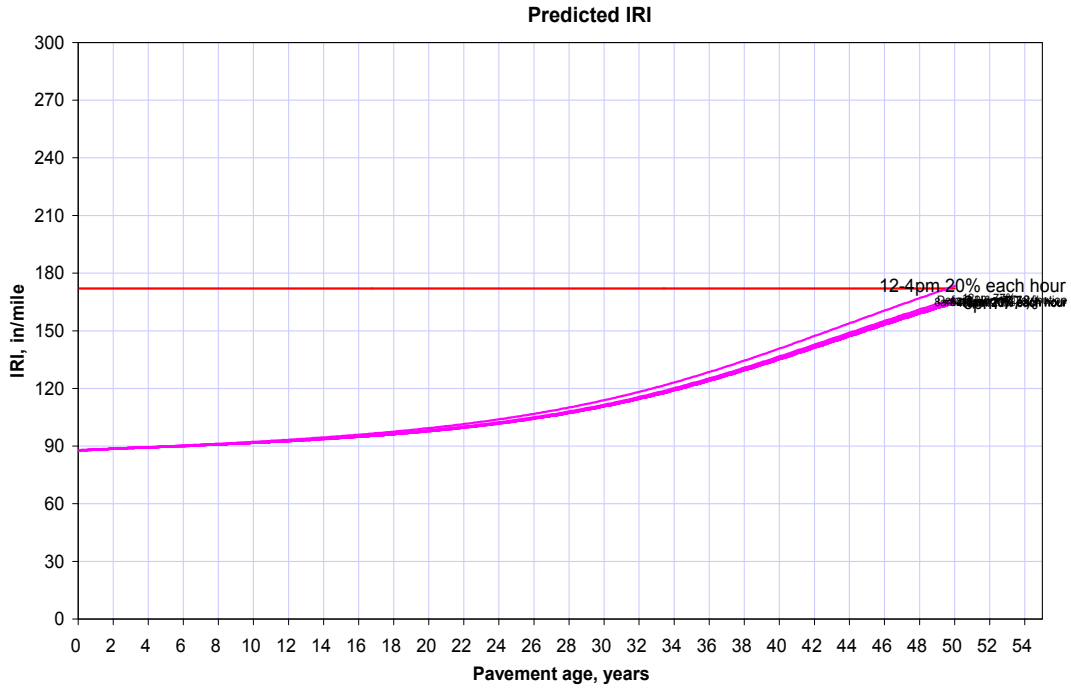

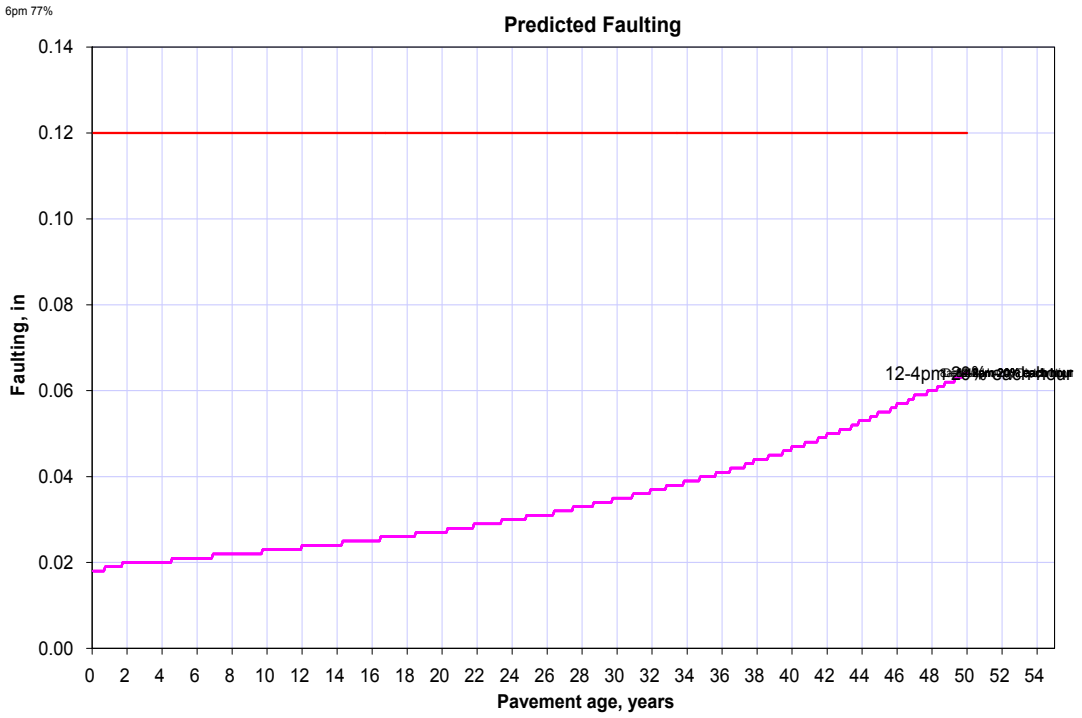
6pm 77%
Predicted Faulting
Faulting, in
0.14
0.12
0.10
0.08
0.06
0.04
0.02
0.00
0 2 4 6 8 10 12 14 16 18 20 22 24 26 28 30 32 34 36 38 40 42 44 46 48 50 52 54
Pavement age, years

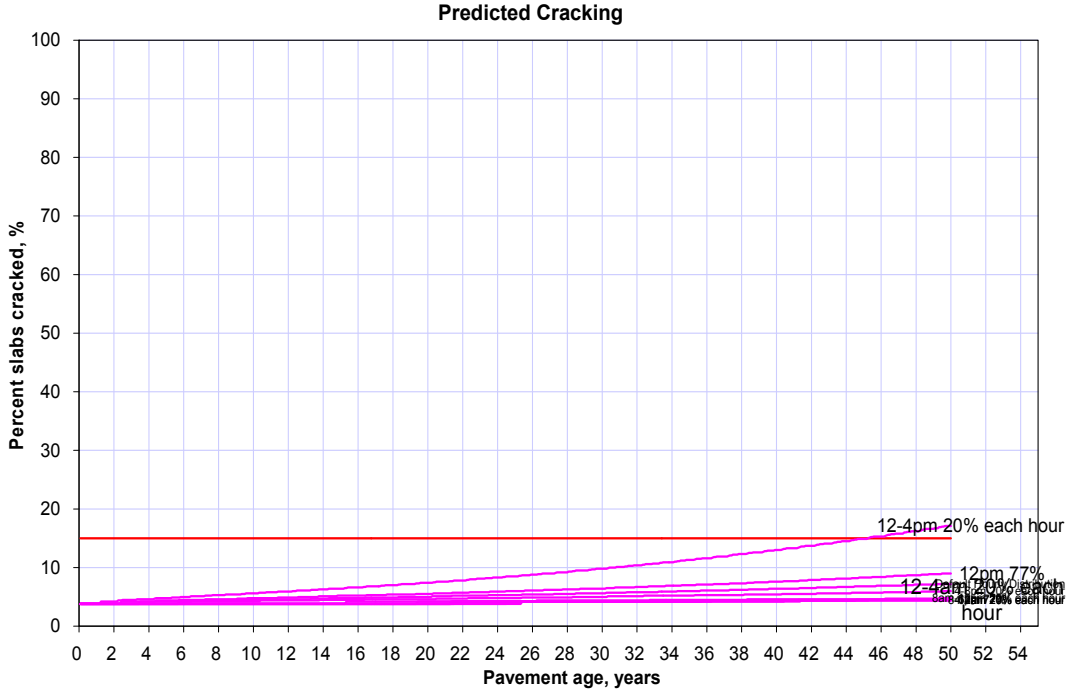
Predicted Cracking
Percent slabs cracked, %
100
90
80
70
60
50
40
30
20
10
0
0 2 4 6 8 10 12 14 16 18 20 22 24 26 28 30 32 34 36 38 40 42 44 46 48 50 52 54
Pavement age, years
12-4pm 20% each hour
12pm 77%

A2.7 Mean wheel location (inches from the lane marking)

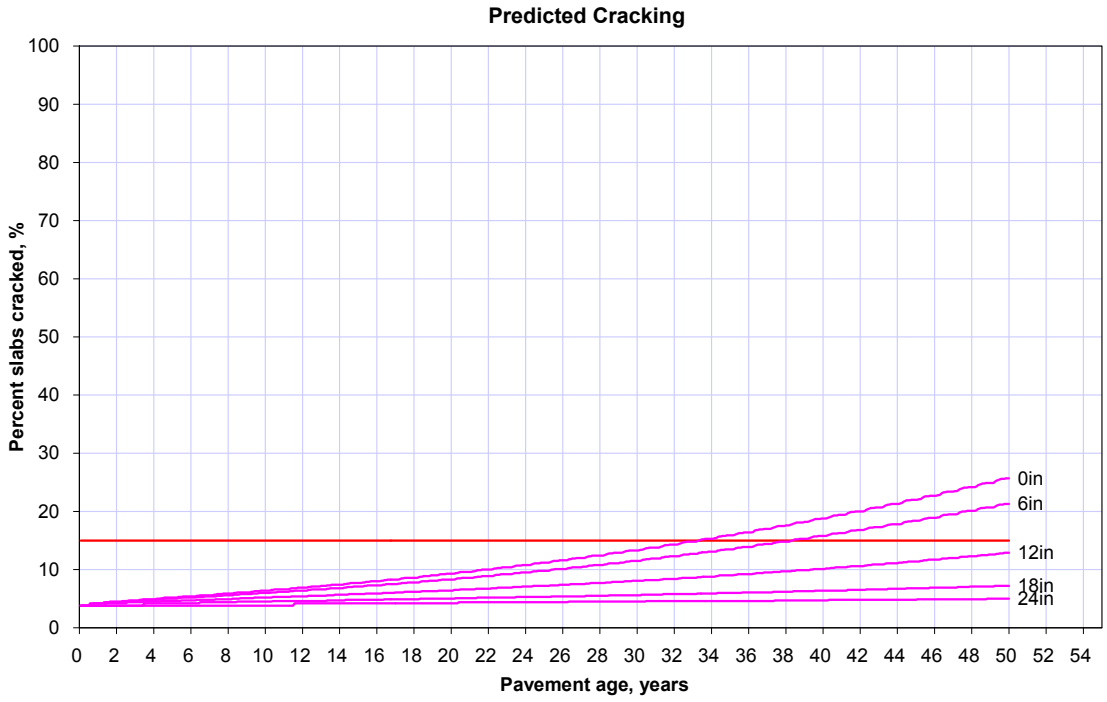

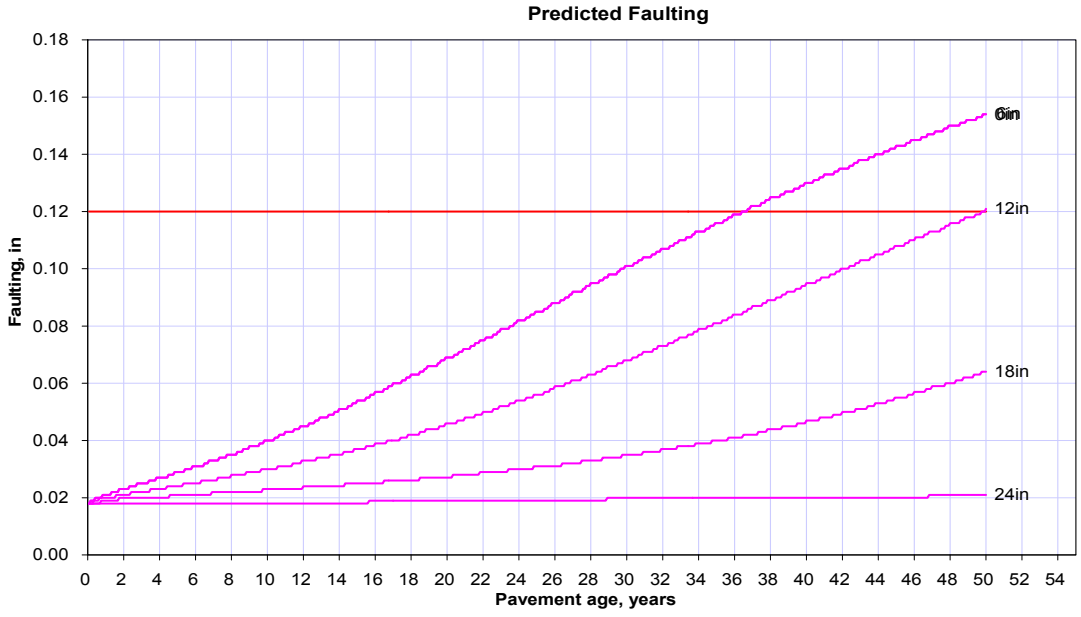

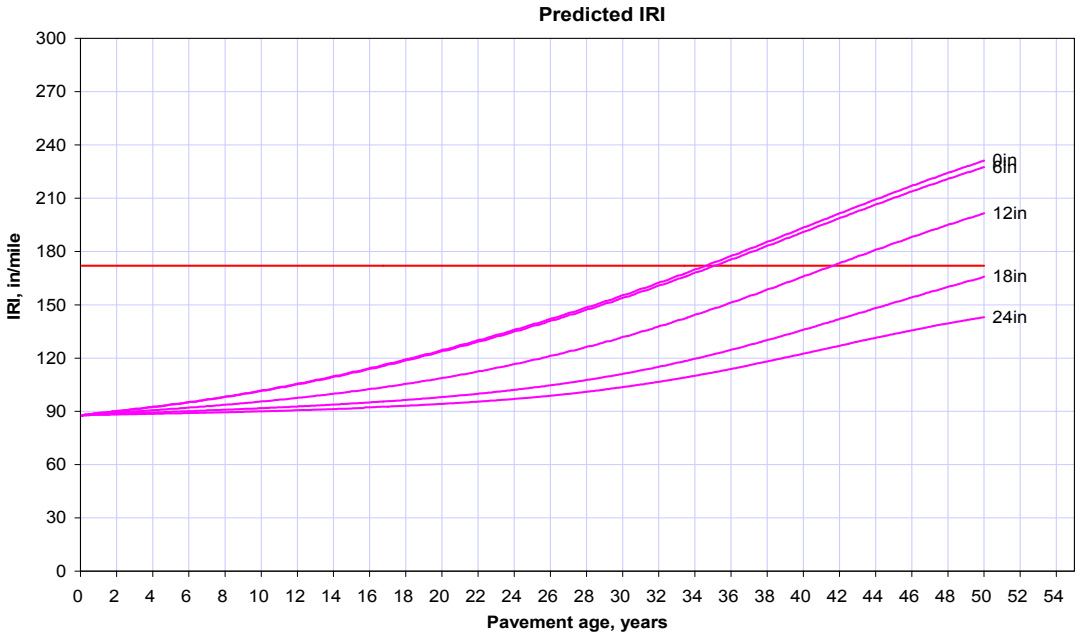

A2.8 Traffic wander standard deviation (in)

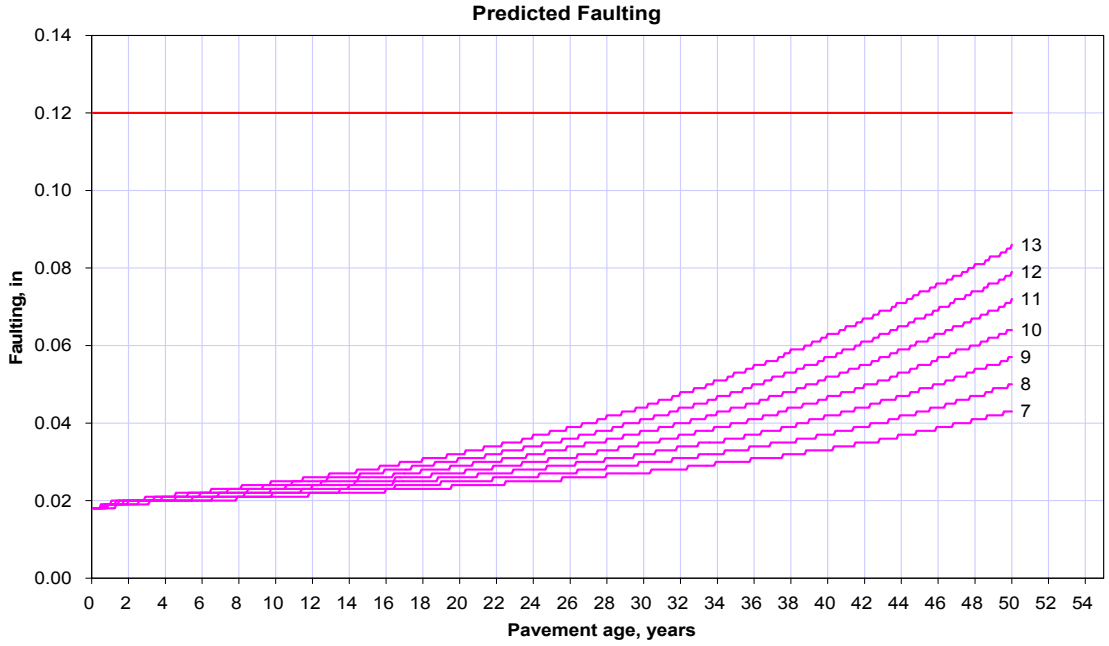

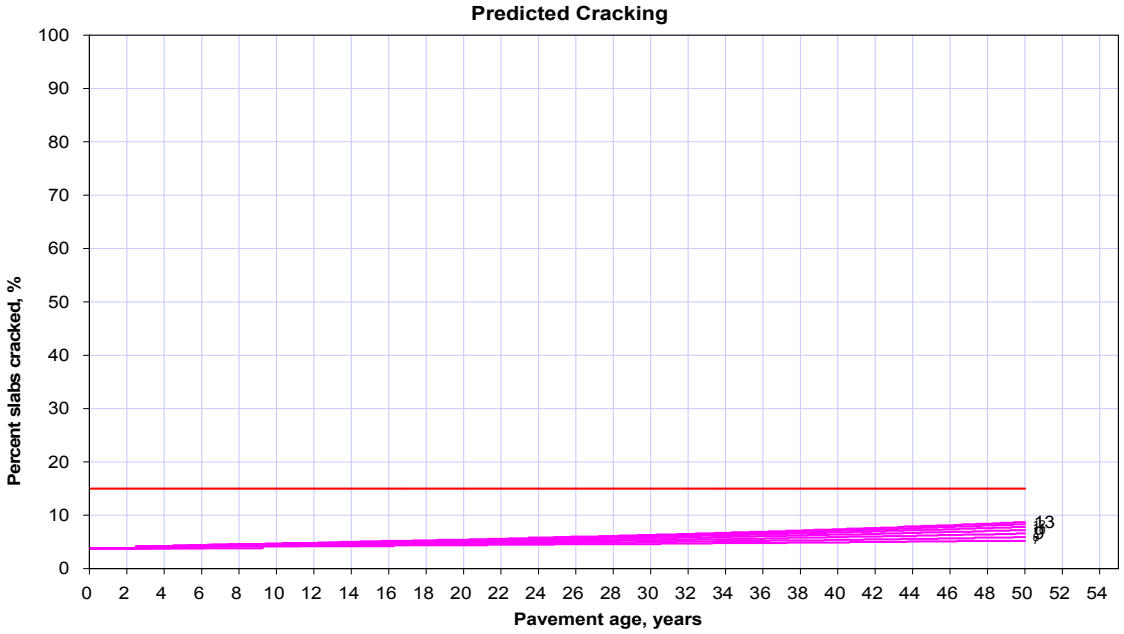
Predicted Cracking
Percent slabs cracked, %
100
90
80
70
60
50
40
30
20
10
0
0 2 4 6 8 10 12 14 16 18 20 22 24 26 28 30 32 34 36 38 40 42 44 46 48 50 52 54
Pavement age, years
13

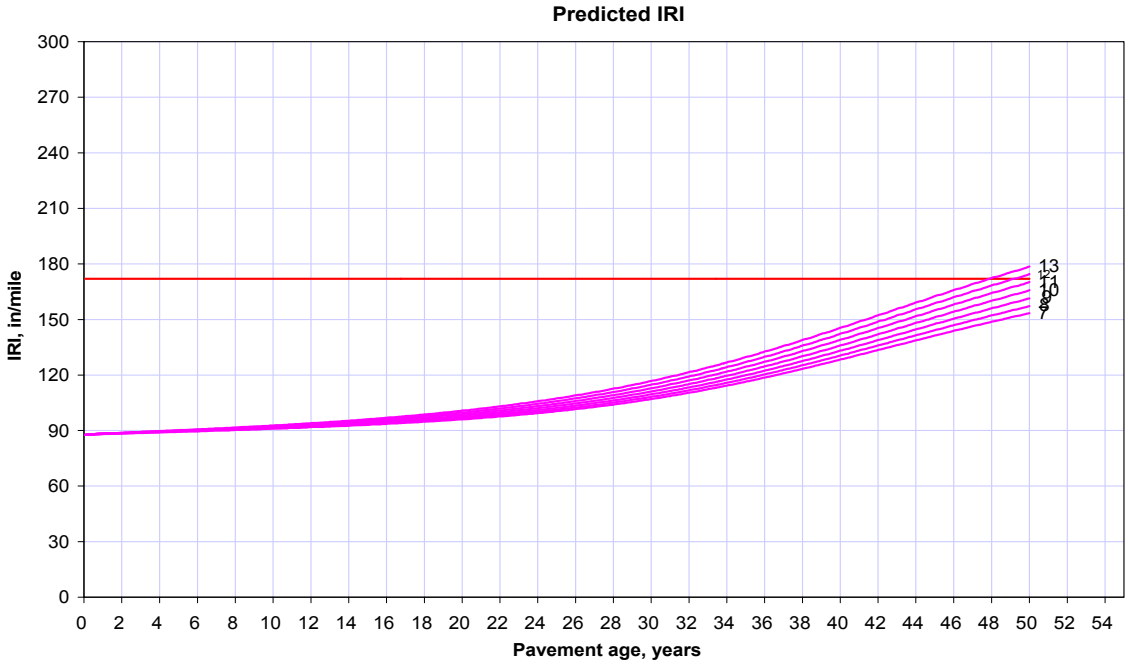
Predicted IRI
IRI, in/mile
300
270
240
210
180
150
120
90
60
30
0
0 2 4 6 8 10 12 14 16 18 20 22 24 26 28 30 32 34 36 38 40 42 44 46 48 50 52 54
Pavement age, years
13
12
11
10
9
8
7

A2.9 Number of Axles per Truck

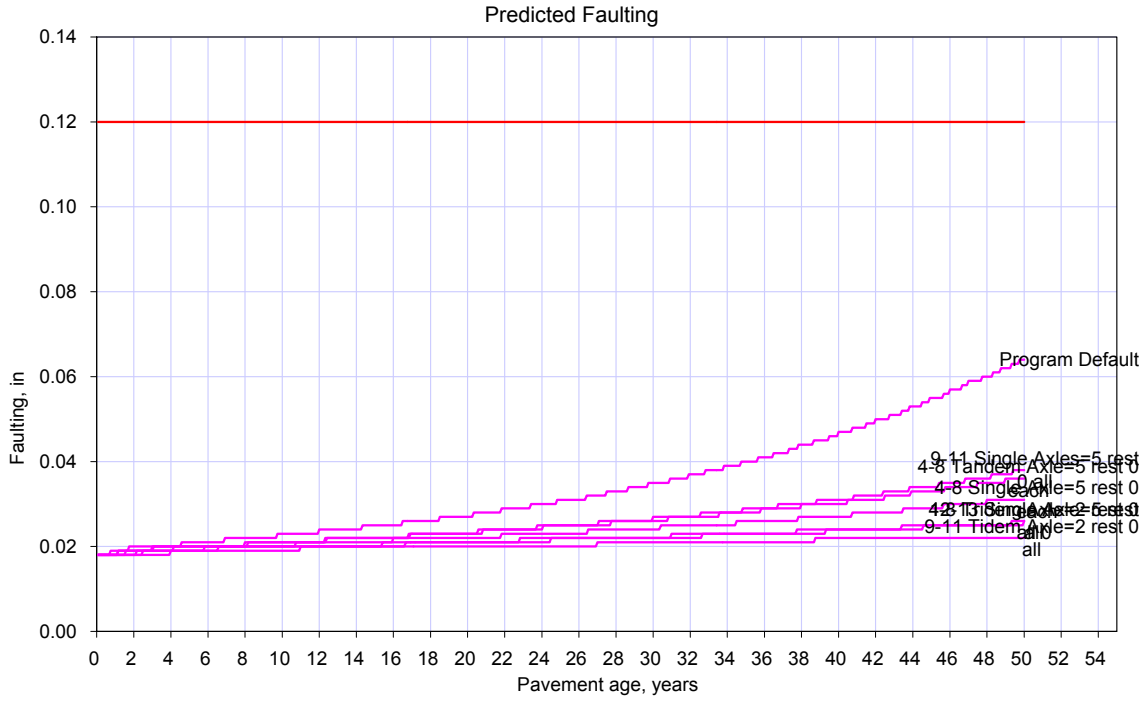

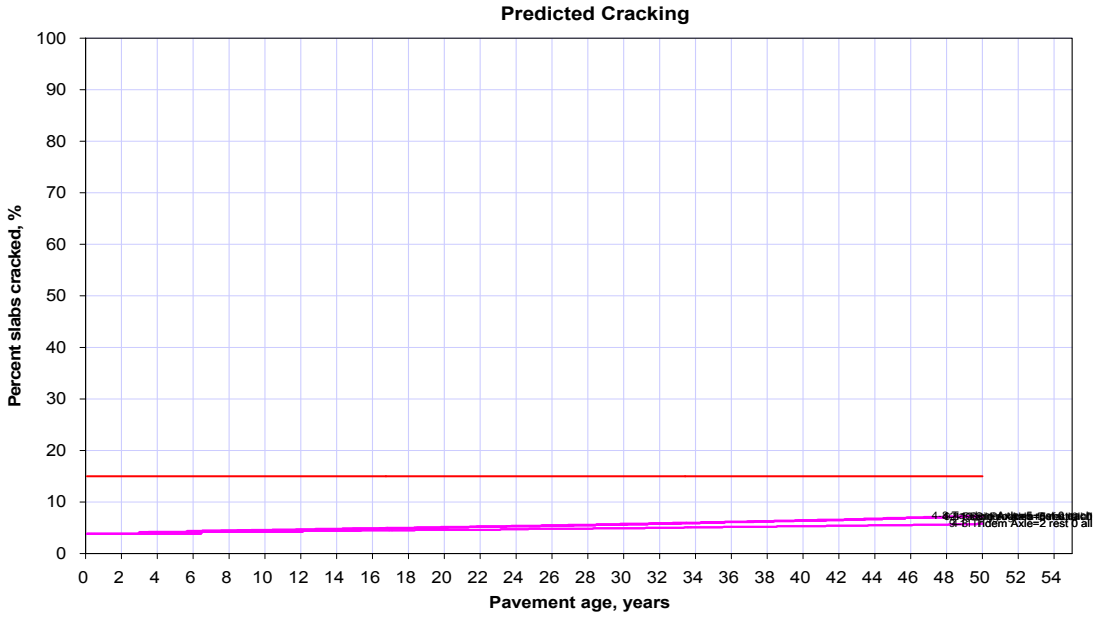

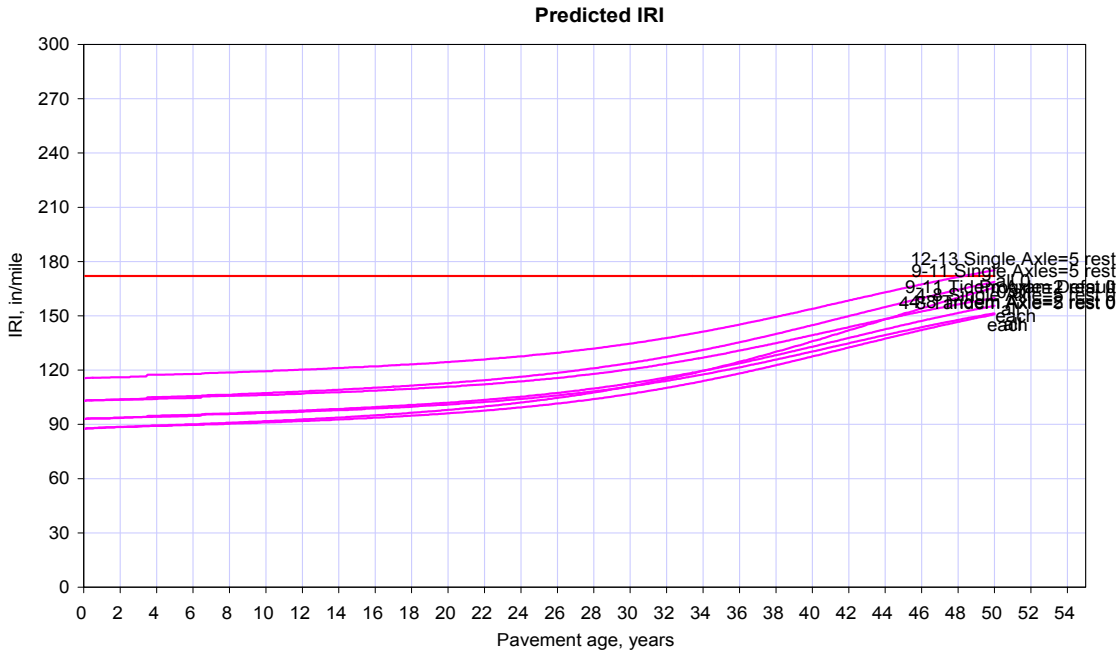

A2.10 Average axle width (edge-to-edge) outside dimensions (ft)

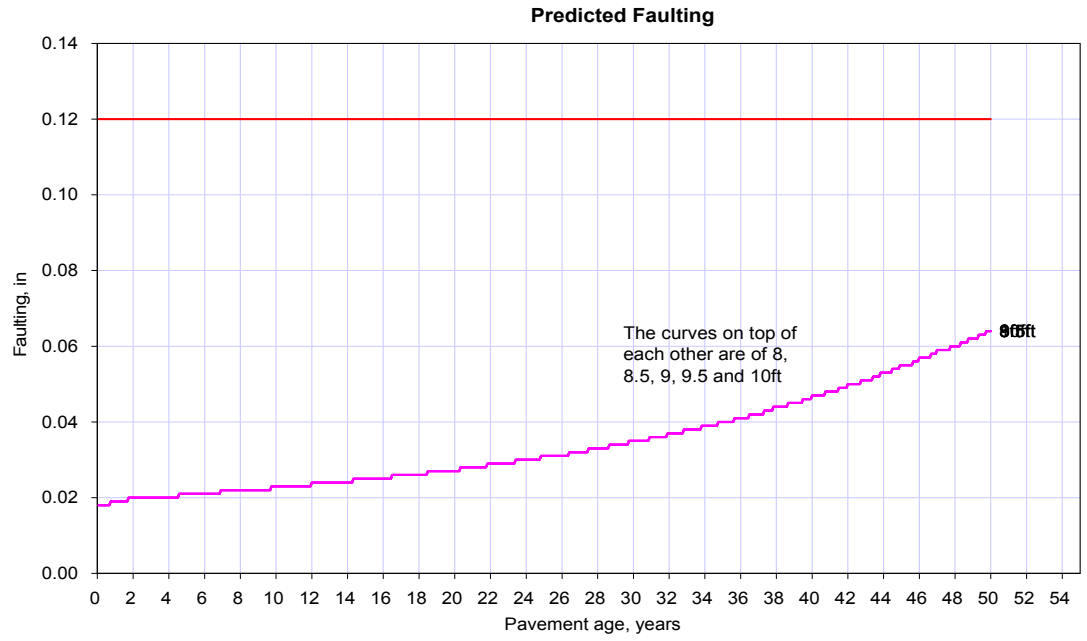

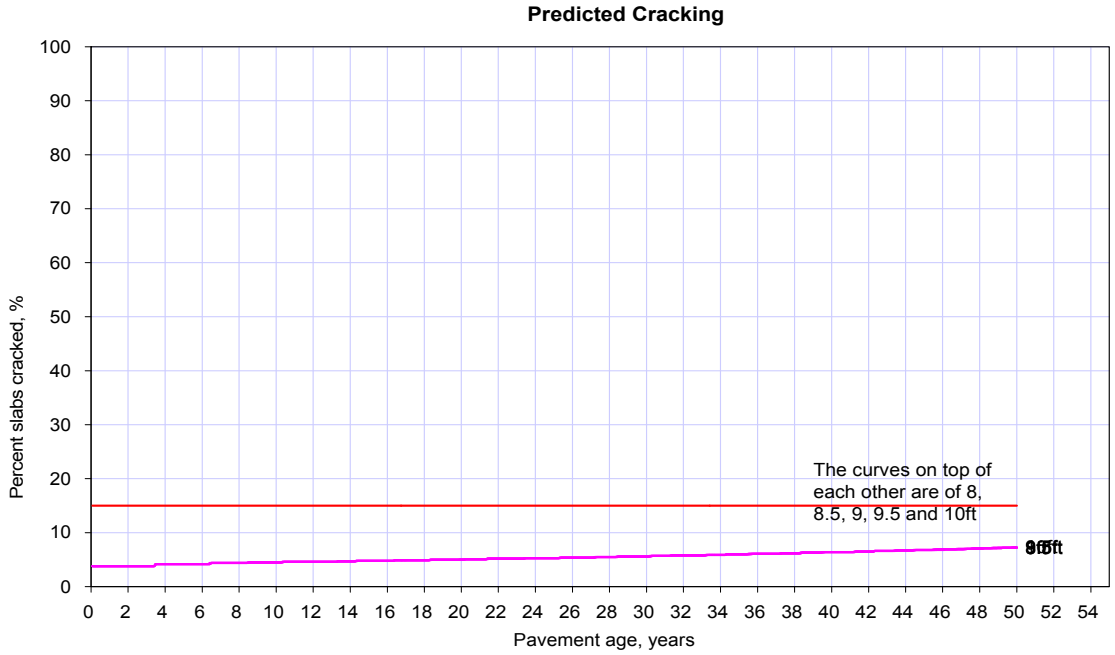
Predicted Cracking
Percent slabs cracked, %
Pavement age, years
The curves on top of each other are of 8, 8.5, 9, 9.5 and 10ft

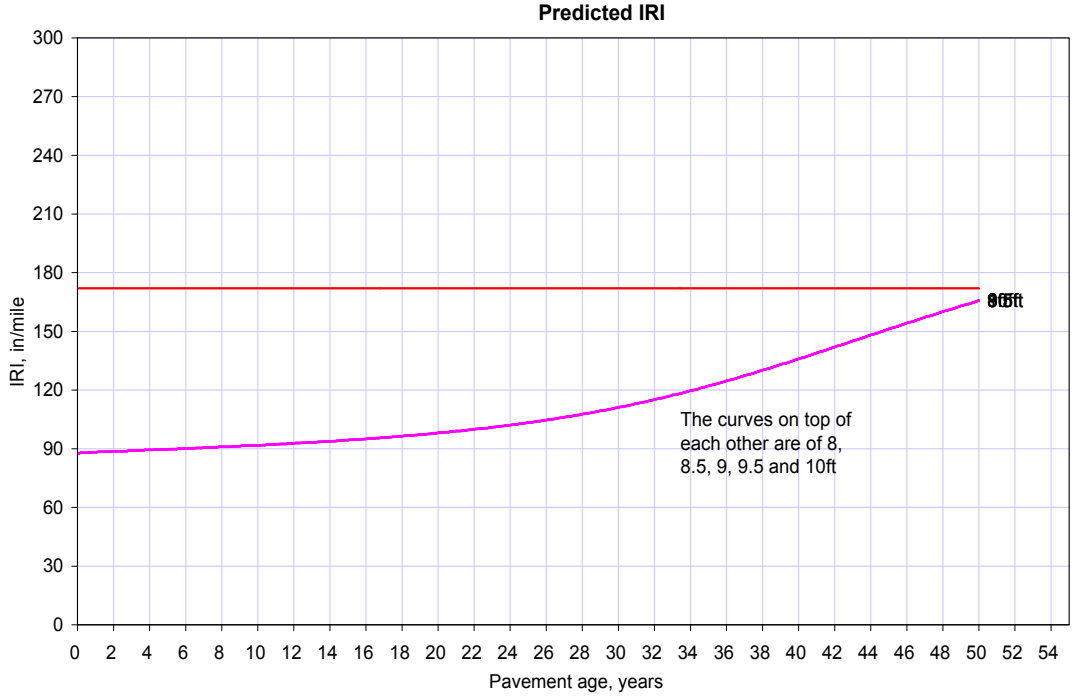
Predicted IRI
IRI, in/mile
Pavement age, years
The curves on top of each other are of 8, 8.5, 9, 9.5 and 10ft

A2.11 Dual tire spacing (in)

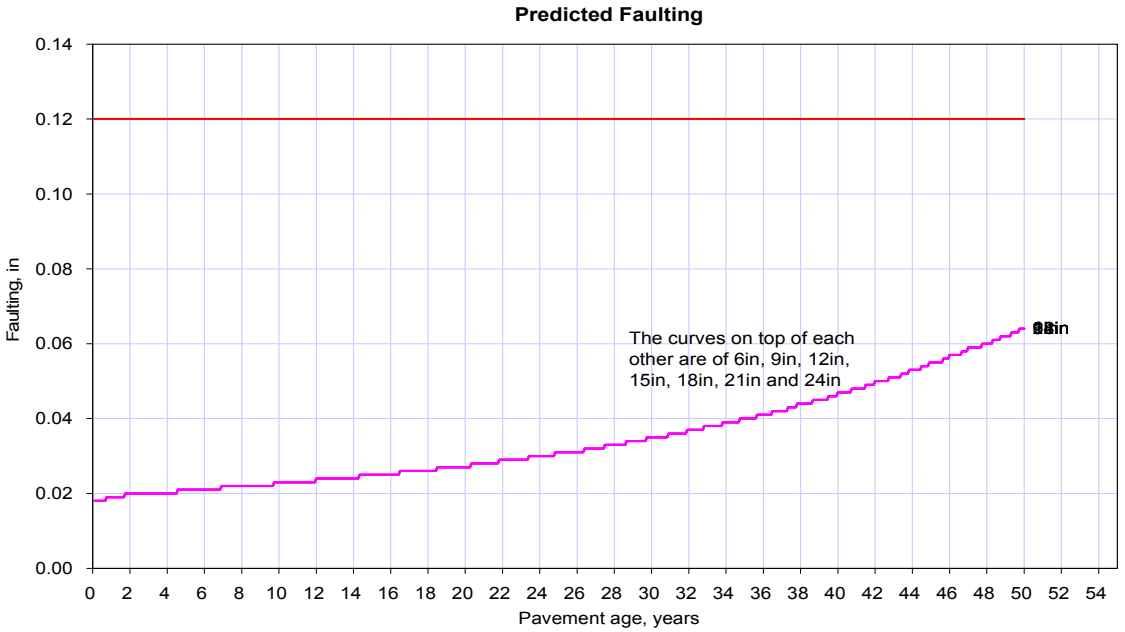

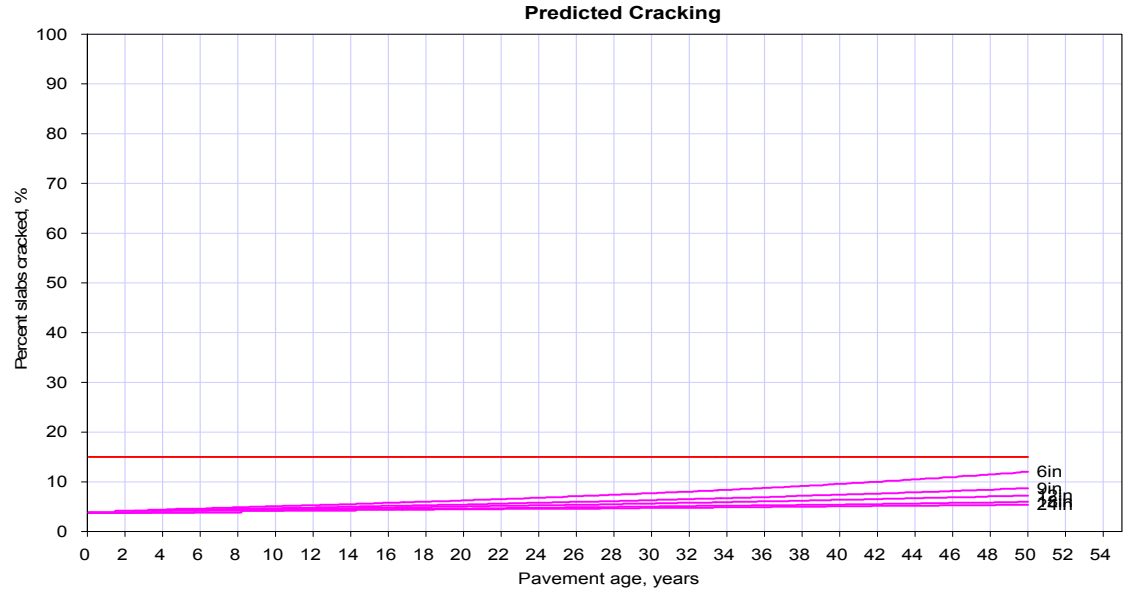

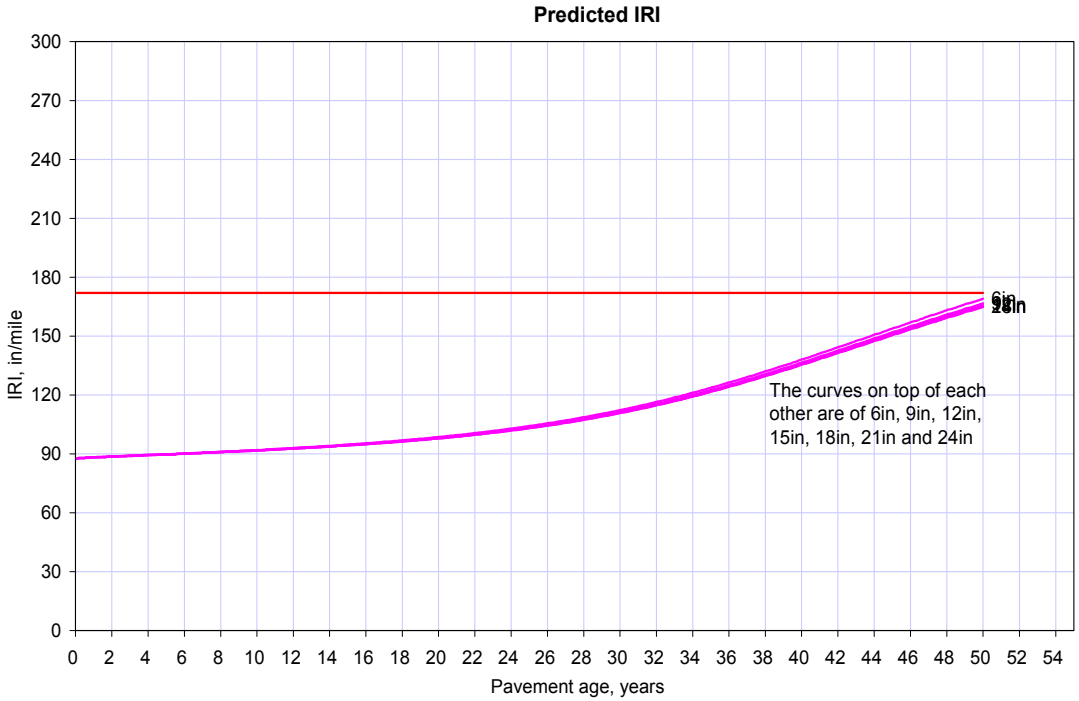

A2.12 Tandem axle Spacing (in)

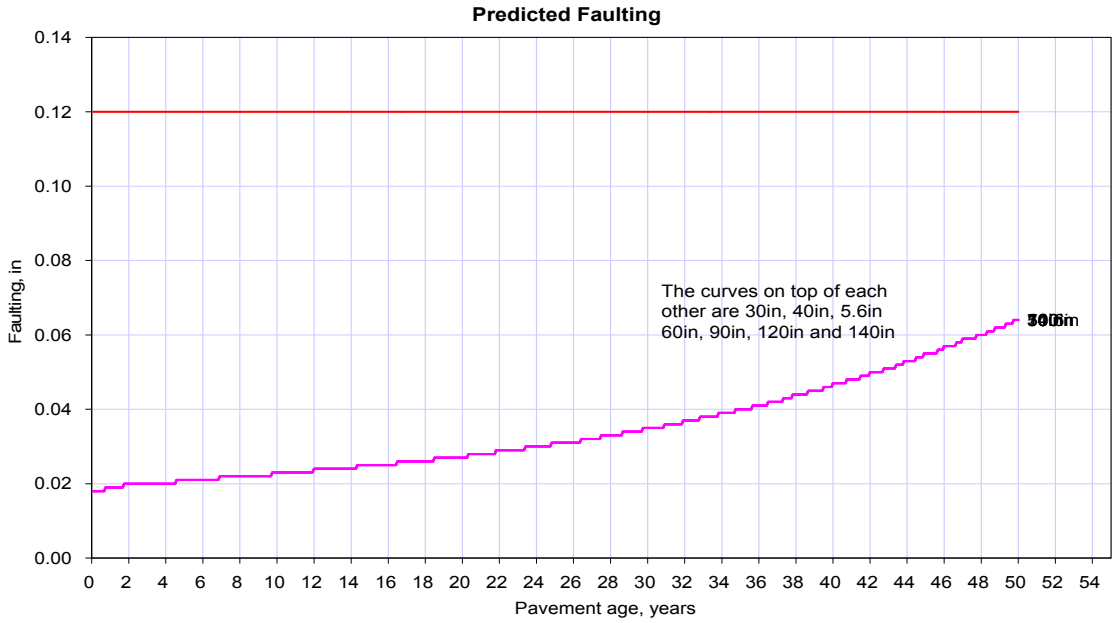

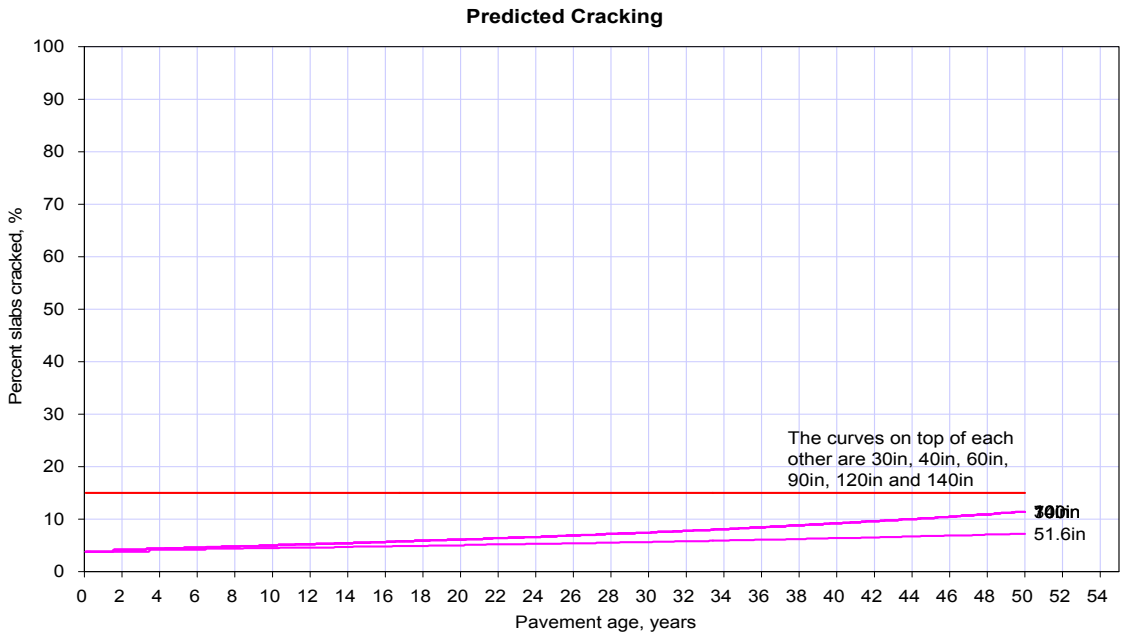
Predicted Cracking
Percent slabs cracked, %
Pavement age, years
The curves on top of each other are 30in, 40in, 60in, 90in, 120in and 140in
51.6in

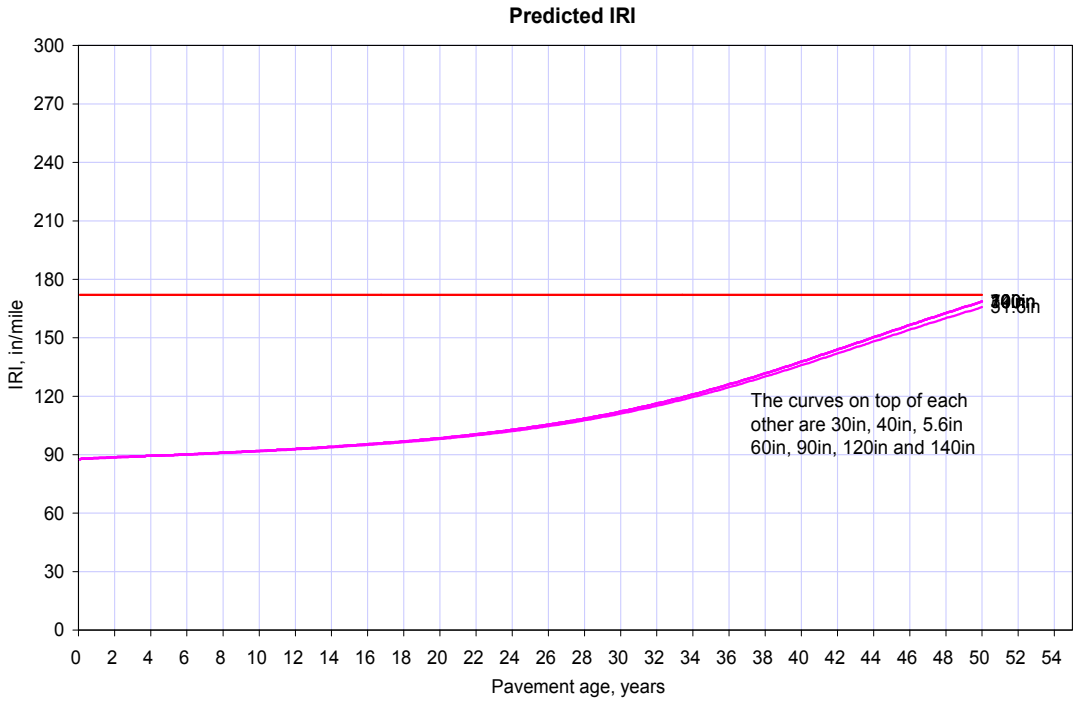
Predicted IRI
IRI, in/mile
Pavement age, years
The curves on top of each other are 30in, 40in, 5.6in 60in, 90in, 120in and 140in

A2.13 Tridem axle Spacing (in)

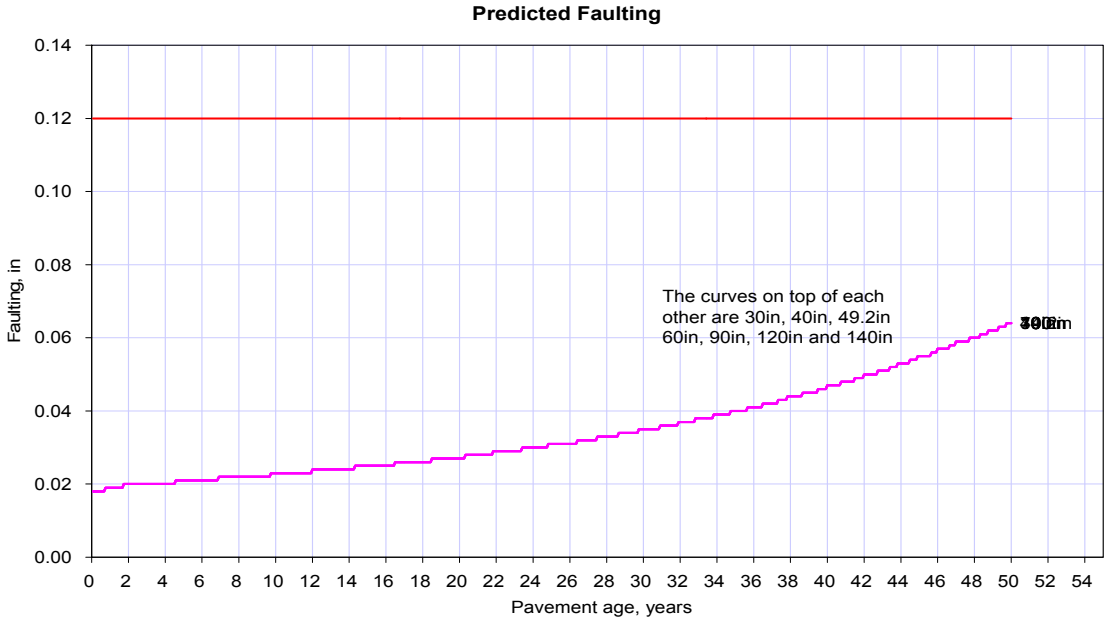

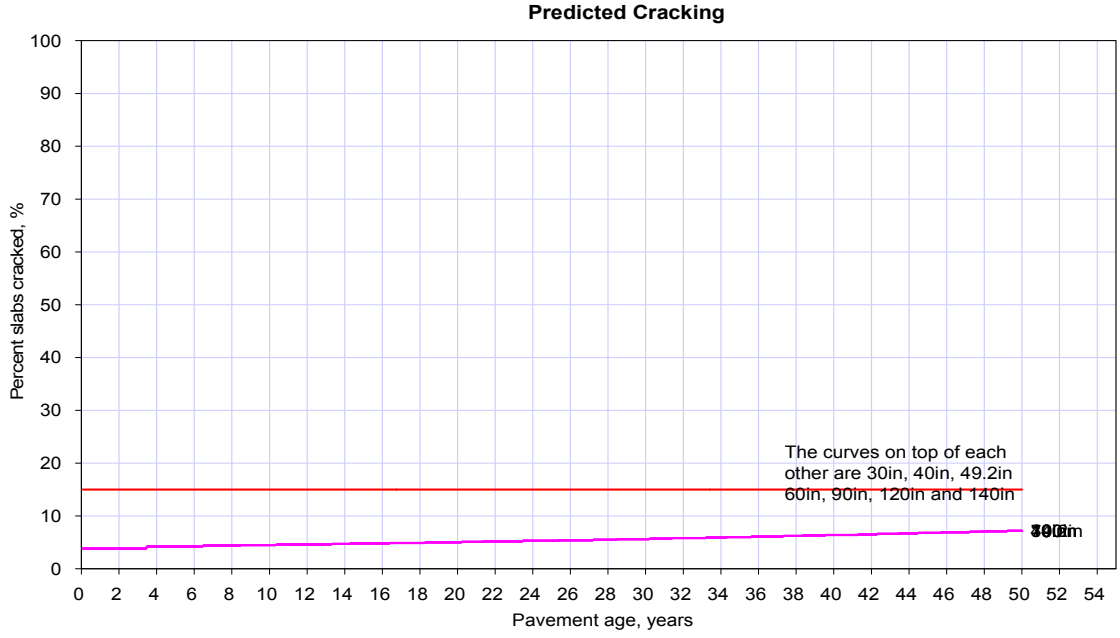

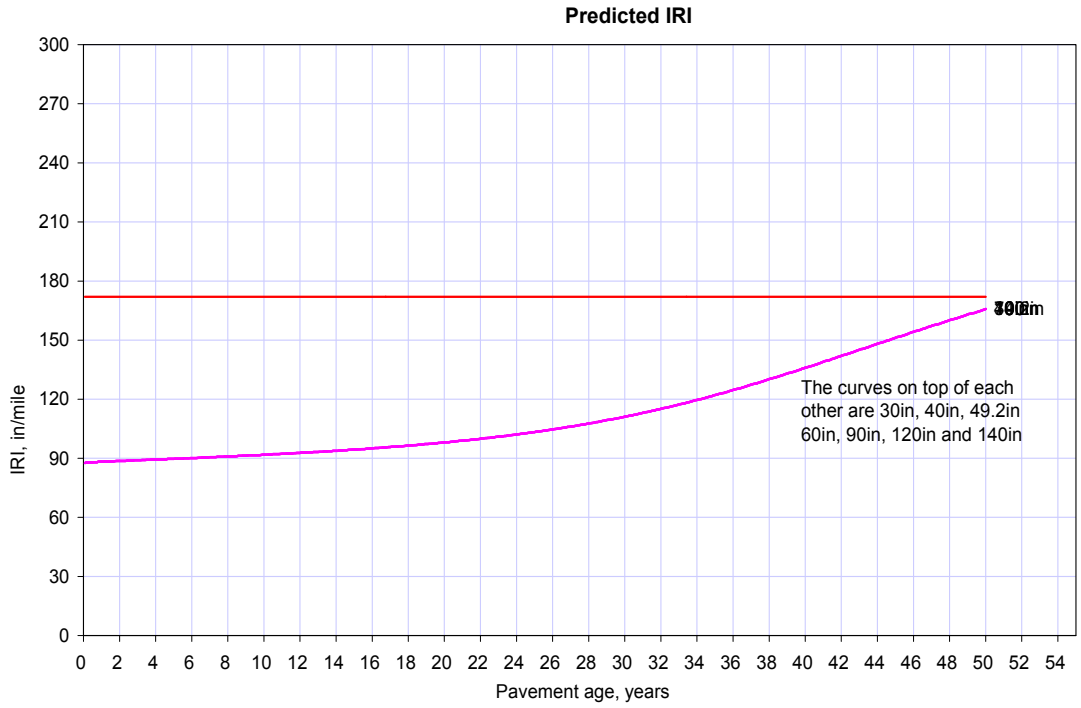

A2.14 Quad axle Spacing (in)

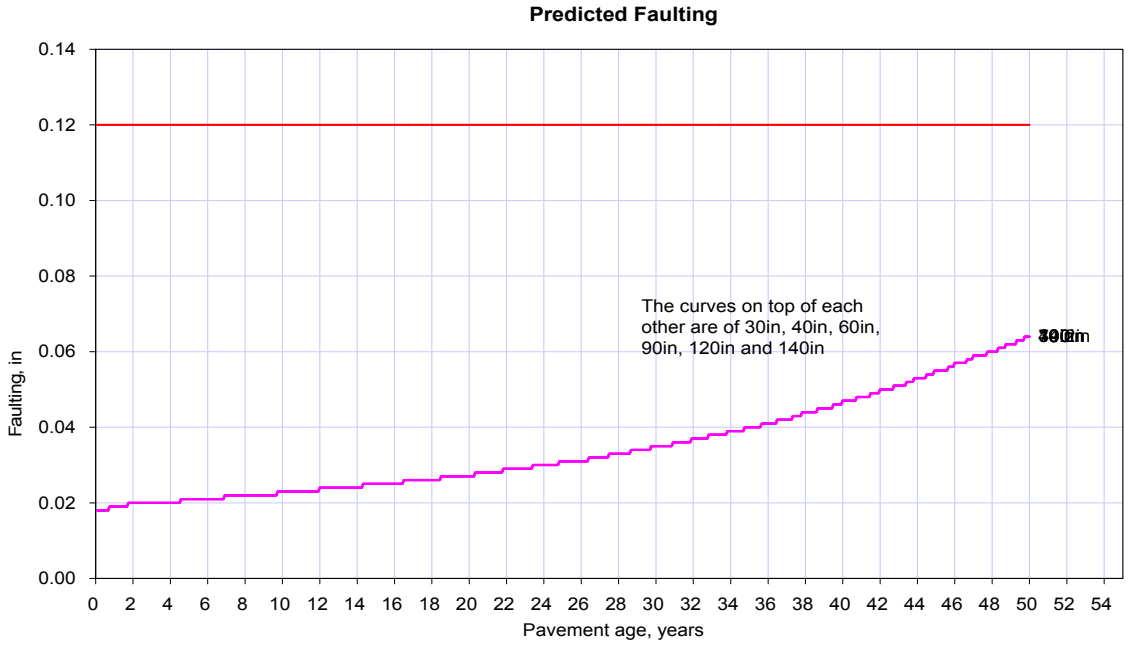

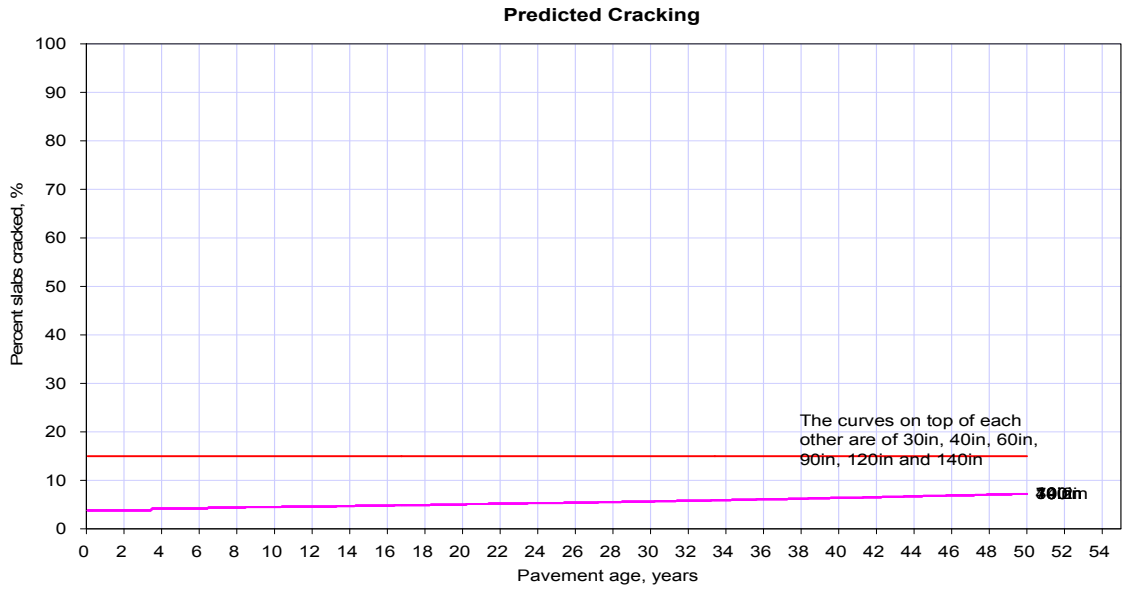
Predicted Cracking
Percent slabs cracked, %
Pavement age, years
The curves on top of each other are of 30in, 40in, 60in, 90in, 120in and 140in

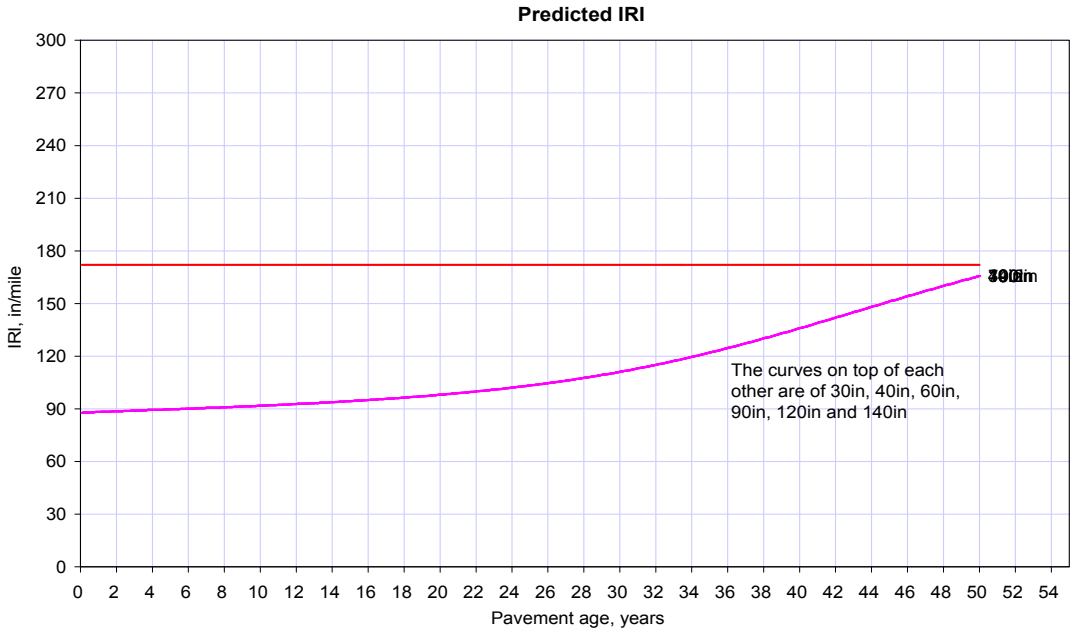
Predicted IRI
IRI, in/mile
Pavement age, years
The curves on top of each other are of 30in, 40in, 60in, 90in, 120in and 140in

A2.15 Monthly Adjustment Factors

The monthly adjustment factor (MAF) is the proportion of the AADTT for a specific truck class that will occur on an average 24-hour day within a given month of the year.

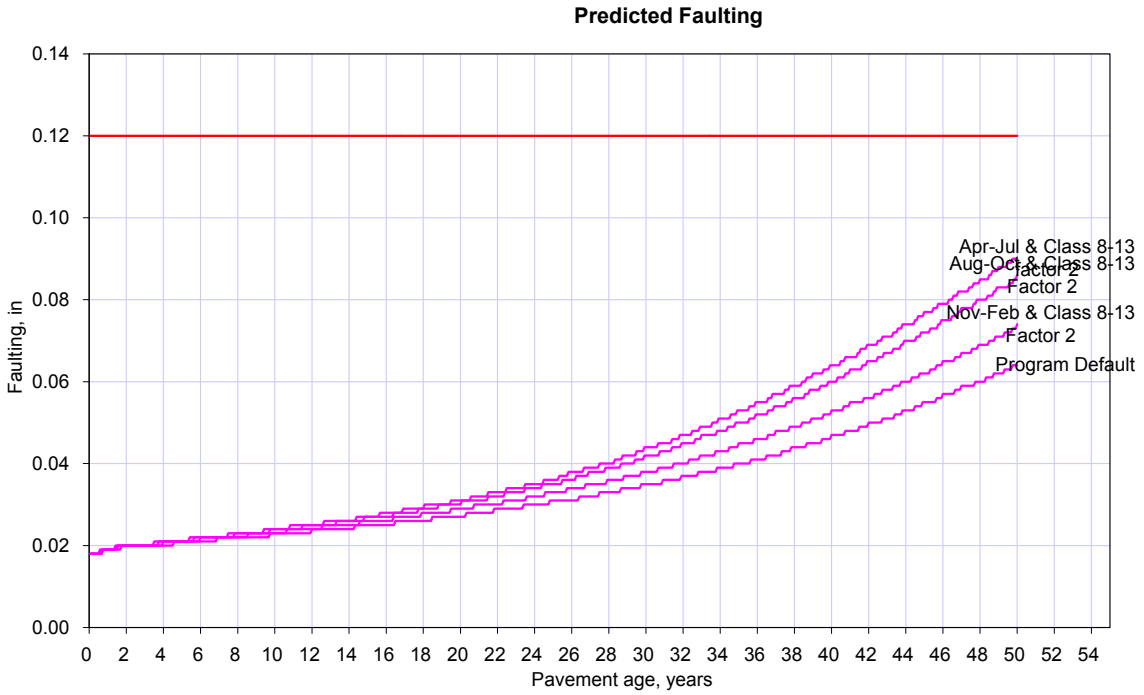

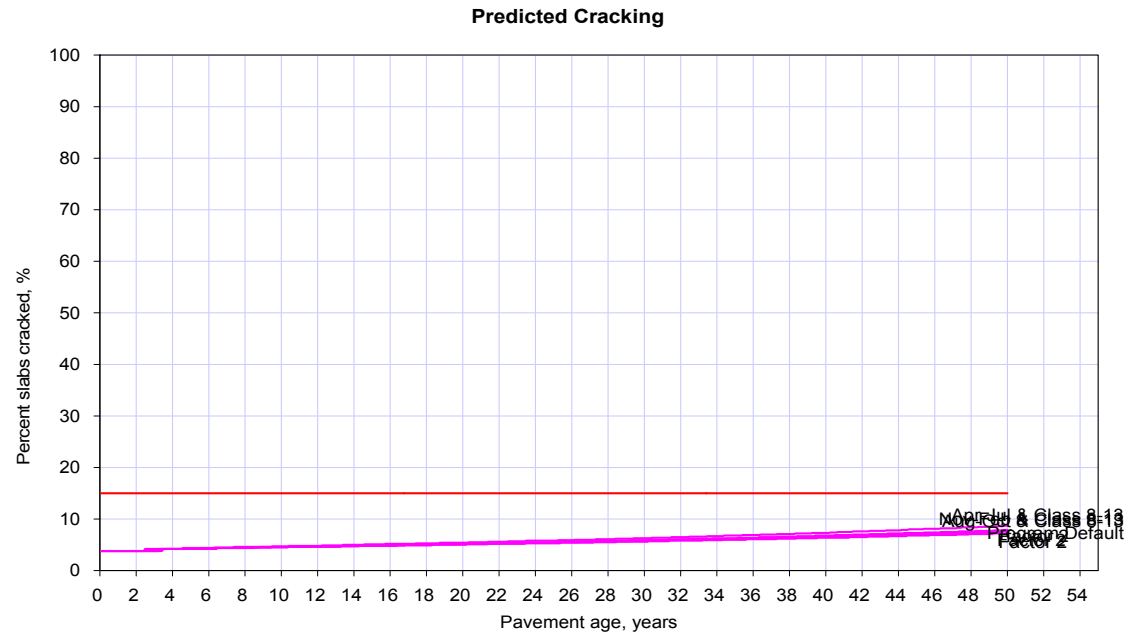

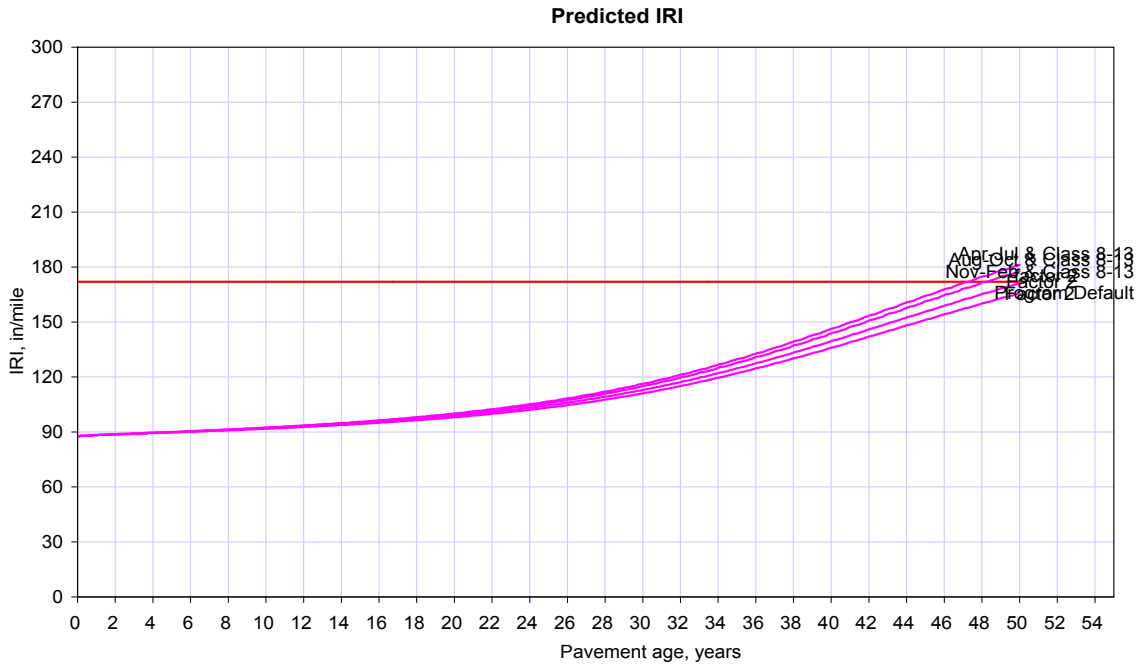
Predicted IRI
IRI, in/mile
Pavement age, years
0
30
60
90
120
150
180
210
240
270
300
0
2
4
6
8
10
12
14
16
18
20
22
24
26
28
30
32
34
36
38
40
42
44
46
48
50
52
54
Apr-Jul & Class 8-13
Default

A2.16 AADTT Distribution by Vehicle Class

This screen requires the user to input information regarding the distribution of truck classes in the design traffic or in the volume entered on the main traffic screen. The Design Guide software offers the user a choice of 13 truck classes to define the distribution of truck traffic based on truck classes. The truck classes include 10 truck classes as defined by FHWA (Vehicle Classes 4-13) and 3 additional classes are included in software to be defined by agency, if needed. The FHWA truck classes 4 through 13 as shown in the figure.

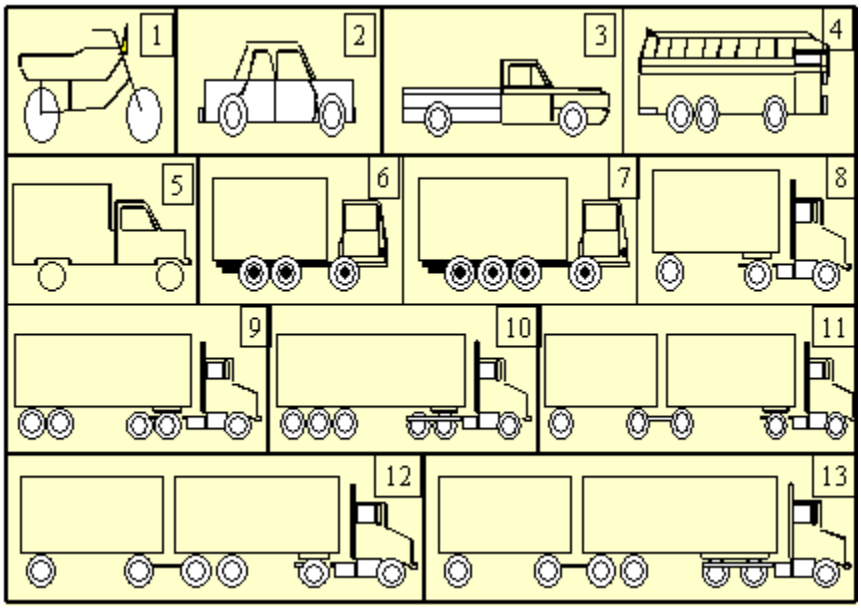

The vehicle class distribution can be entered either as Level 1 or Level 3 inputs. Level 1 inputs are based on site specific class distribution while Level 3 is based on the Truck Traffic Classification (TTC) factors. TTC factors are developed based on default traffic patterns noted from LTPP data for different classes of highway. Default TTC factors can be accessed by clicking on "Load Default Distribution" and selecting the truck classification based on the functional class of highway. A brief guideline for selecting the TTC factors is given in the table on the next page; however, the agency must choose the TTC class that best represents the distribution of the design traffic.

Truck Traffic Classification (TTC) Factors for functional class of highway:

Functional Classification	Applicable TTC Group
Principal arterials, interstate & defense routes	1–5, 8, 11, 13
Principal arterials, intrastate routes including freeways & expressways	1–4, 6–12, 14, 16
Minor arterials	4, 6, 8–12, 15–17
Major collectors	6, 9, 12, 14, 15, 17
Minor collectors	9, 12, 14, 17
Local routes & streets	9, 12, 14, 17

A number of different AADTT distributions and their combinations were analyzed for detailed output.

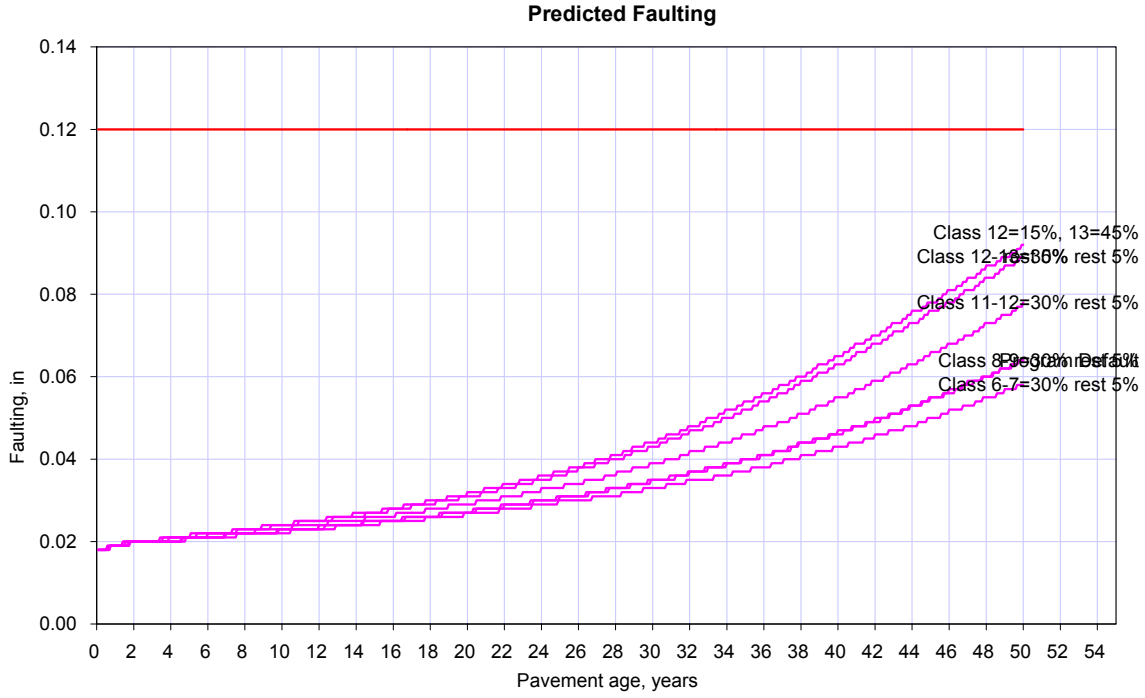

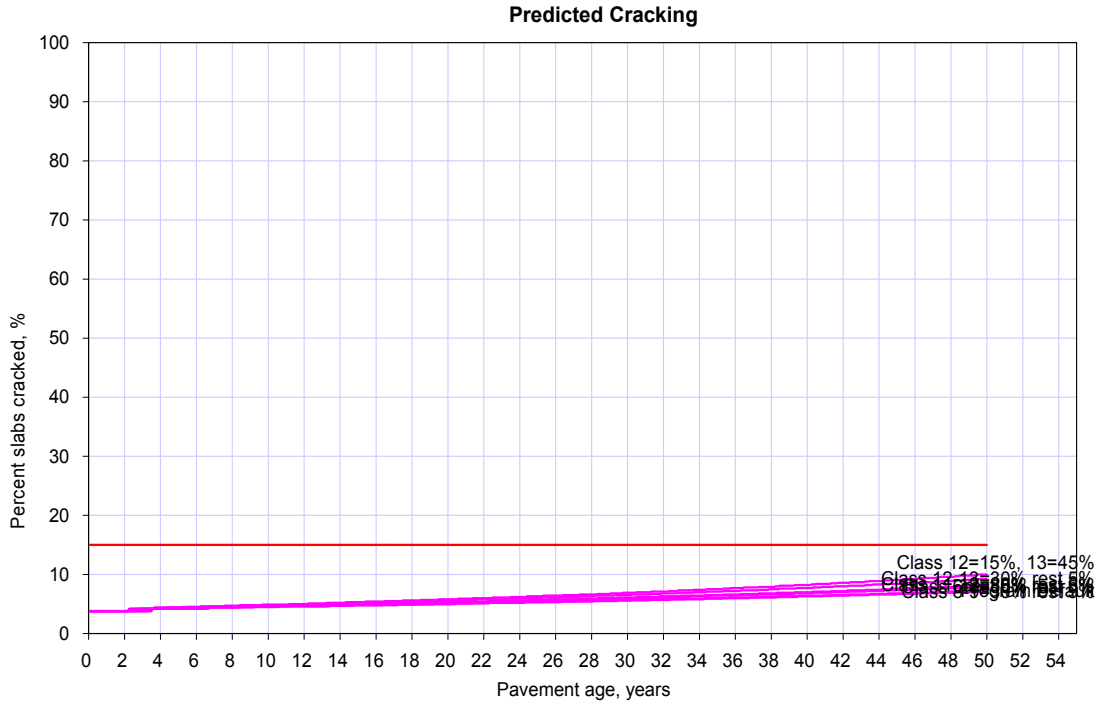
Predicted Cracking
Percent slabs cracked, %
Pavement age, years
Class 12=15%, 13=45%

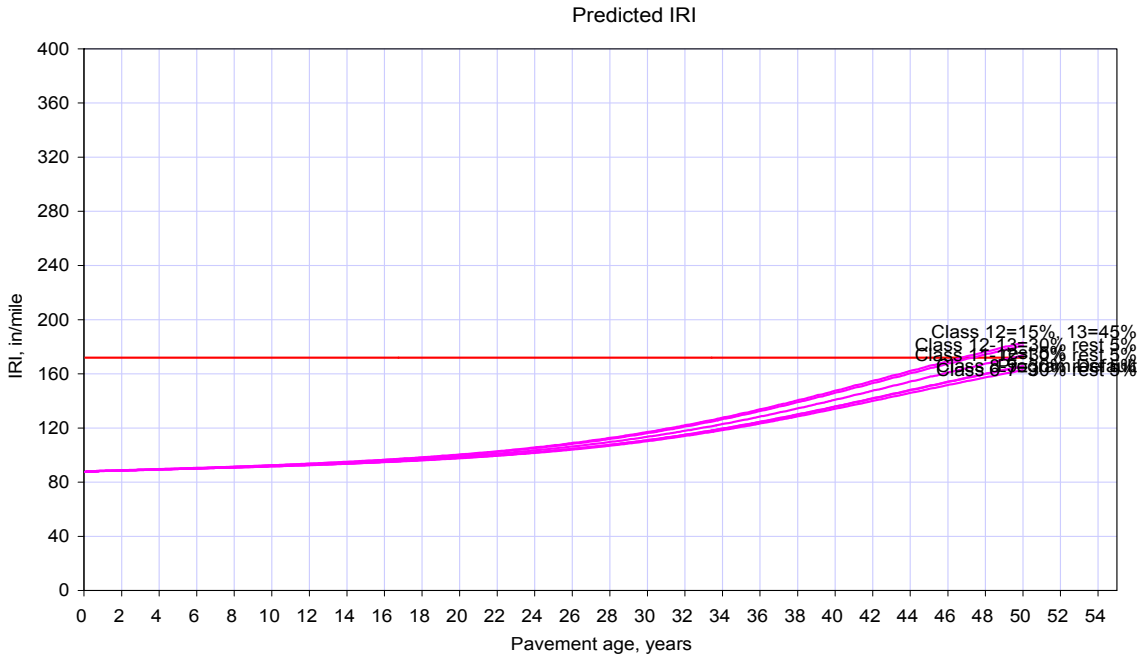
Predicted IRI
IRI, in/mile
Pavement age, years
Class 12=15%, 13=45%

A3 Climatic Input

A3.1 Depth of Water Table

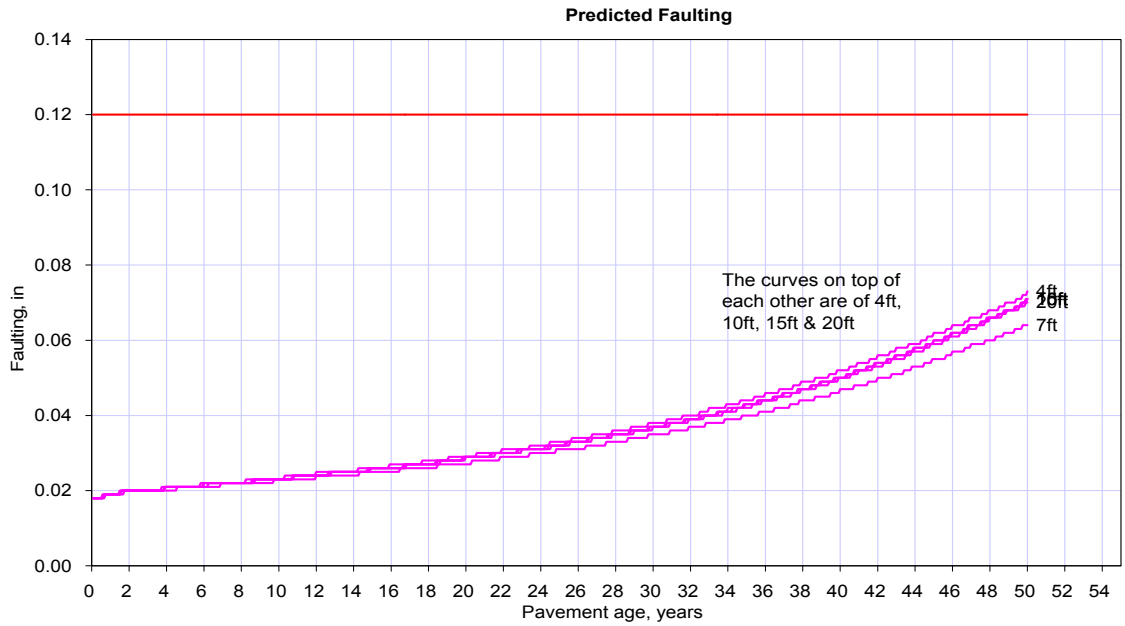

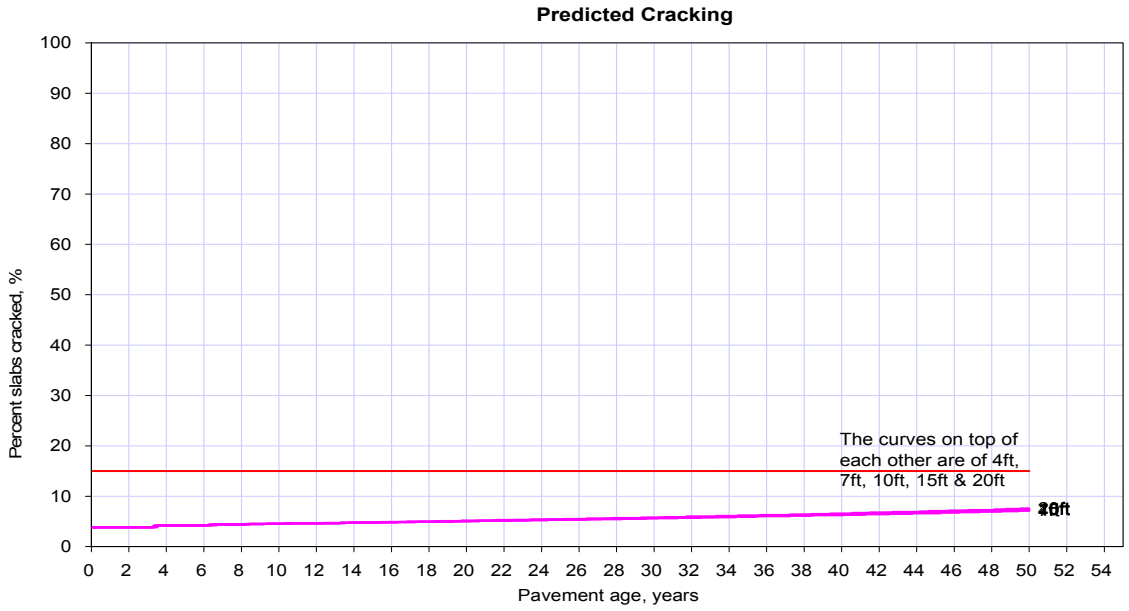

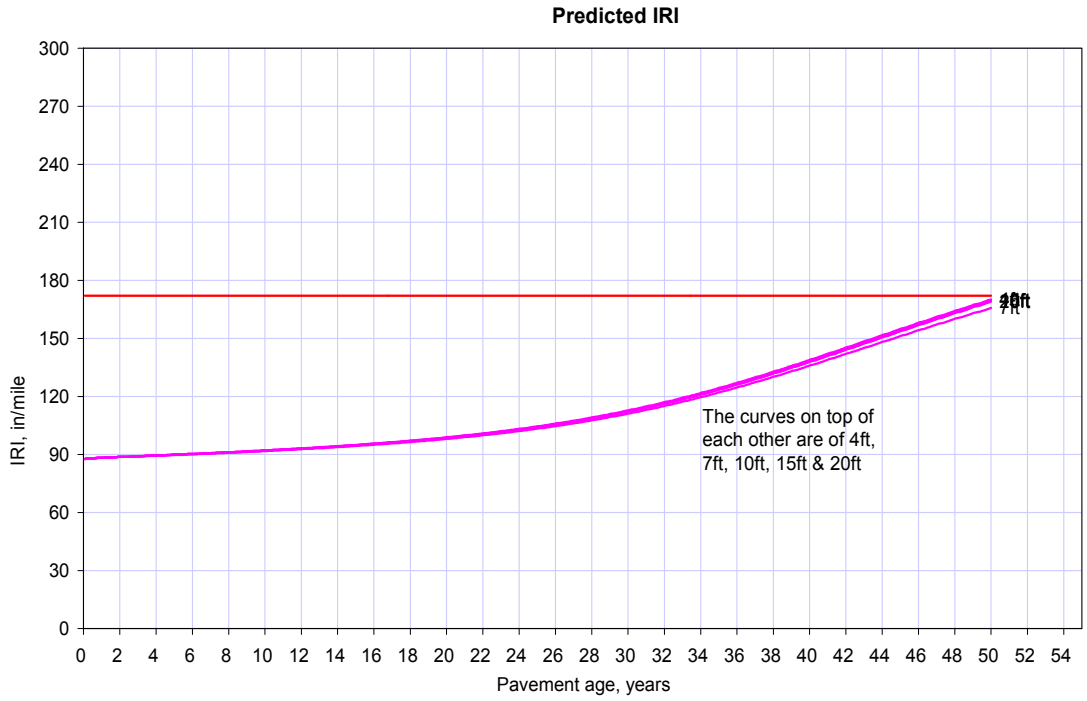

A3.2 Regional Climate Difference

In this analysis almost all the weather stations in Nebraska are compared and the outputs are plotted together.

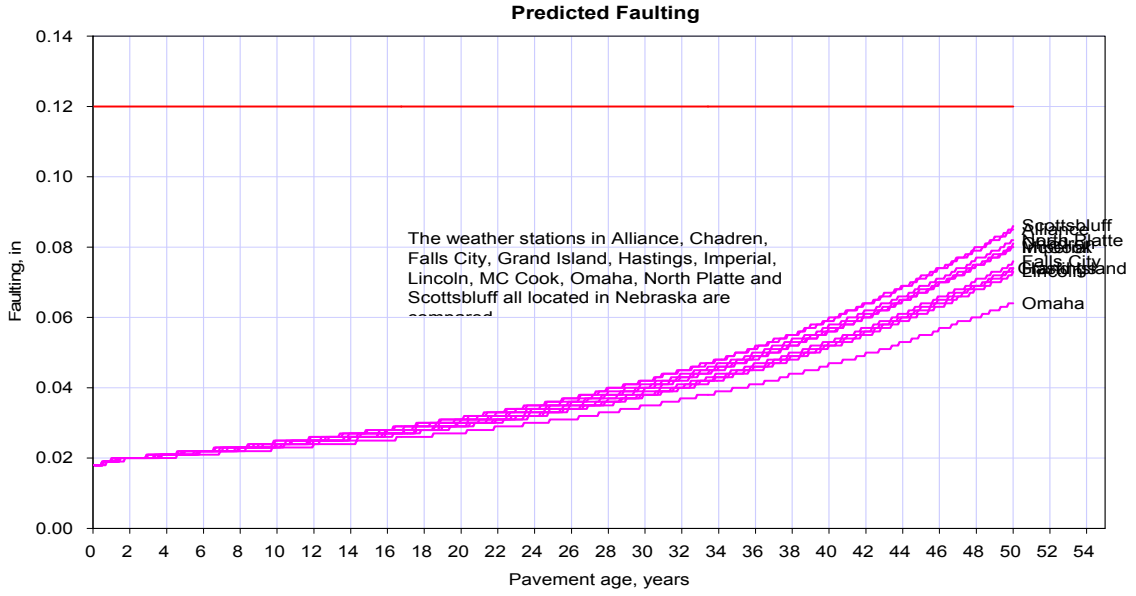

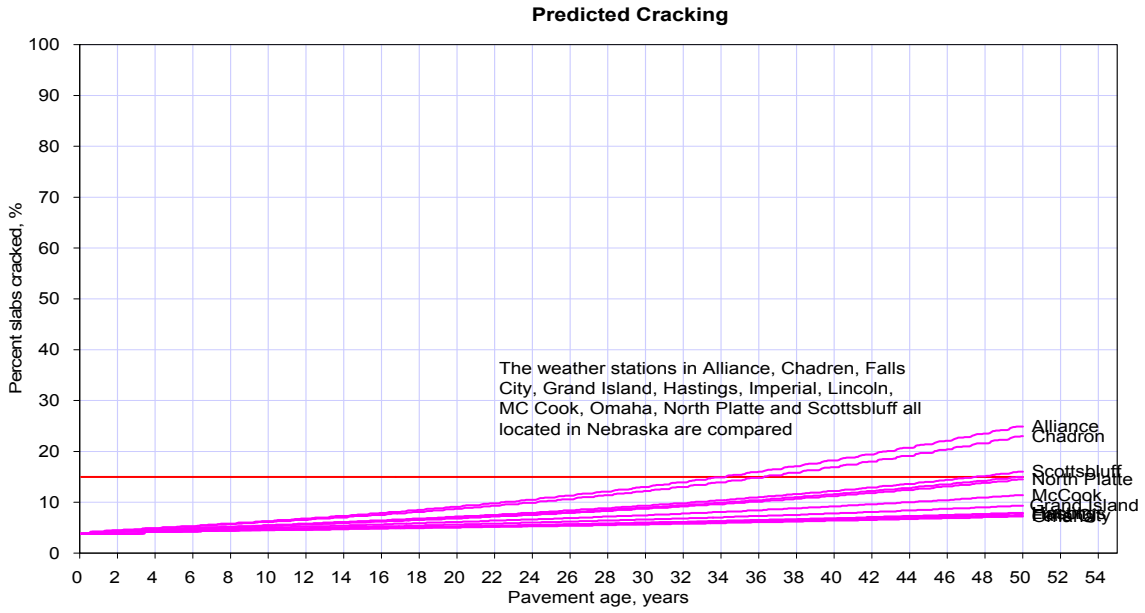
Predicted Cracking
Percent slabs cracked, %
Pavement age, years
The weather stations in Alliance, Chadren, Falls City, Grand Island, Hastings, Imperial, Lincoln, MC Cook, Omaha, North Platte and Scottsbluff all located in Nebraska are compared
Alliance
Chadron
Scottsbluff
North Platte
McCook
Grand Island

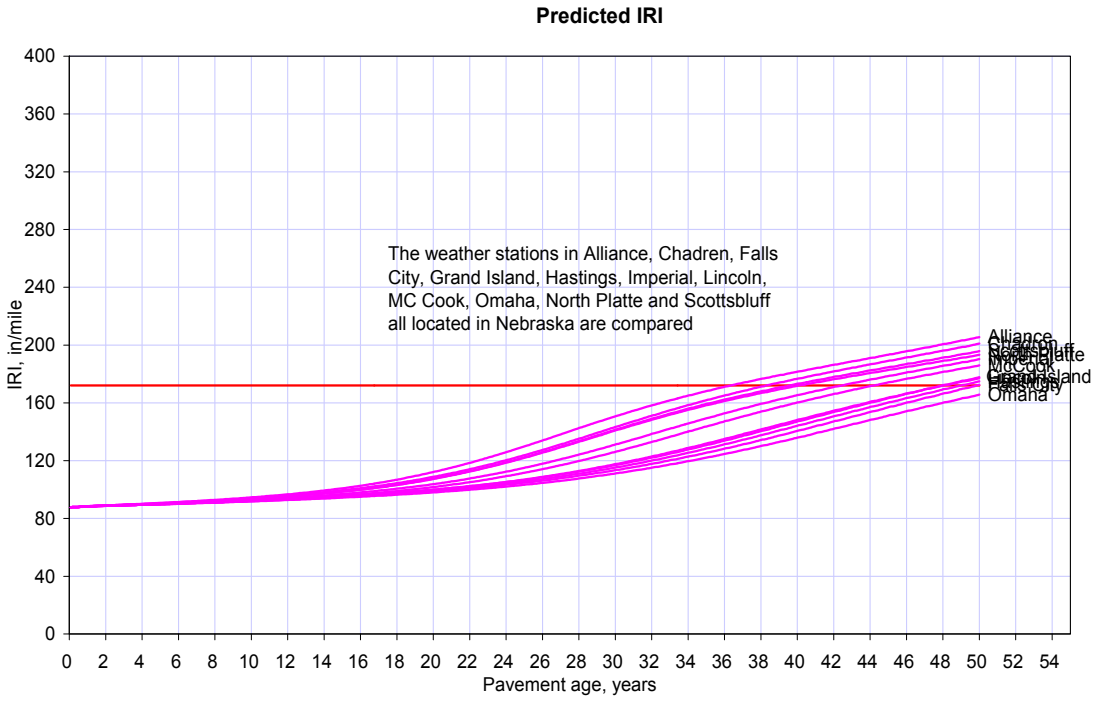
Predicted IRI
IRI, in/mile
Pavement age, years
The weather stations in Alliance, Chadren, Falls City, Grand Island, Hastings, Imperial, Lincoln, MC Cook, Omaha, North Platte and Scottsbluff all located in Nebraska are compared
Alliance
Omaha

A4 Material Inputs

A4.1 Surface Short-Wave absorptivity

This input parameter pertains to AC and PCC surface layers, and is a measure of the amount of available solar energy that is absorbed by the pavement surface. The lighter and more reflective the surface, the lower the surface shortwave absorptivity. The suggested ranges for this value are:

- Aged PCC layer: 0.70-0.90
- Weathered asphalt (gray): 0.80-0.90
- Fresh asphalt (black): 0.90-0.98

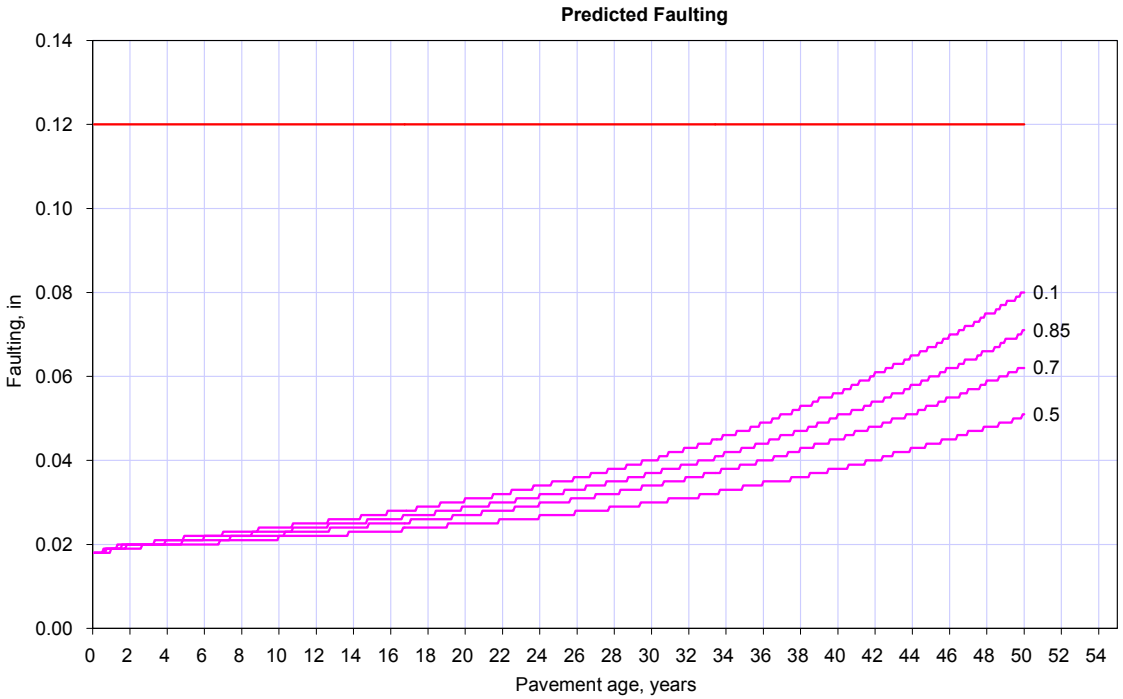

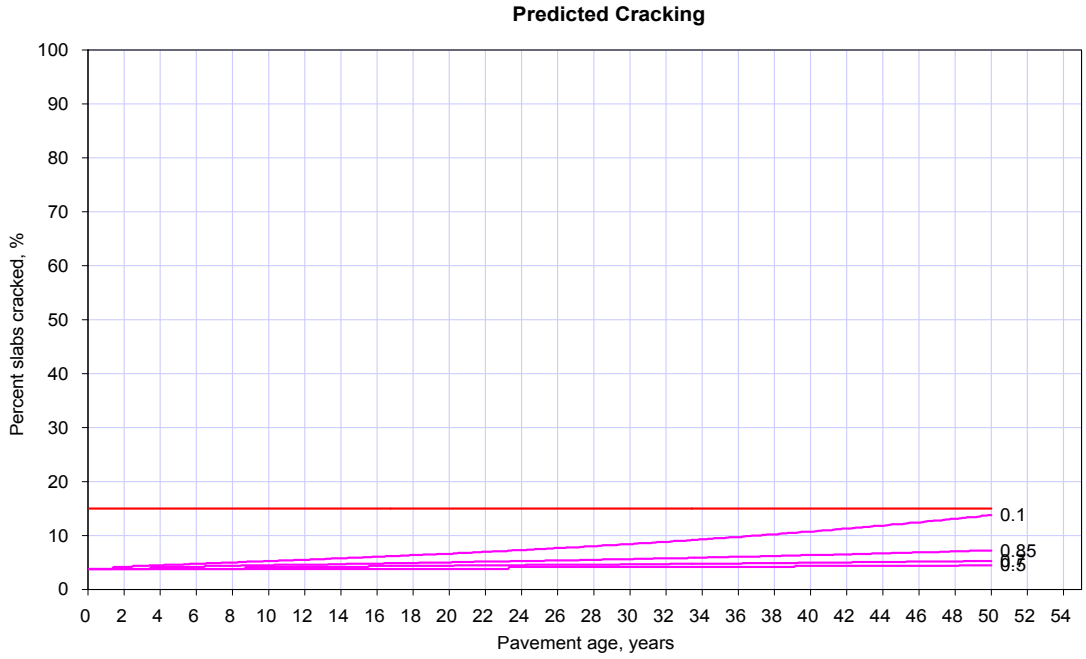
Predicted Cracking
Percent slabs cracked, %
Pavement age, years
0.1
0.85
0.7
0.5

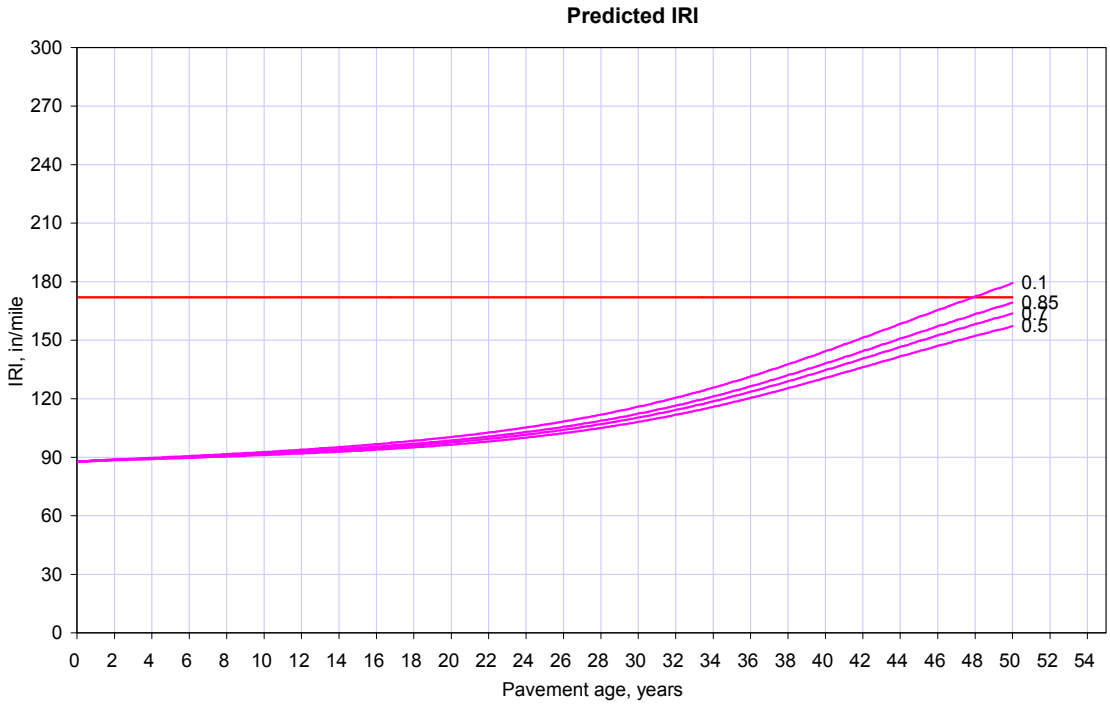
Predicted IRI
IRI, in/mile
Pavement age, years
0.1
0.85
0.7
0.5

A4.2 Permanent Curl/Wrap effective temperature difference (˚F)

This is the Equivalent Temperature Differential (ETD) between the top and bottom layers of the concrete slab that can quantitatively describe the locked stresses in the slab due to construction temperatures, shrinkage, creep and curing conditions. This temperature difference is typically a negative number, i.e. effectively represents a case when the top of the slab is cooler than the bottom of the slab. The magnitude of permanent curl/warp is a sensitive factor that affects JPCP performance.

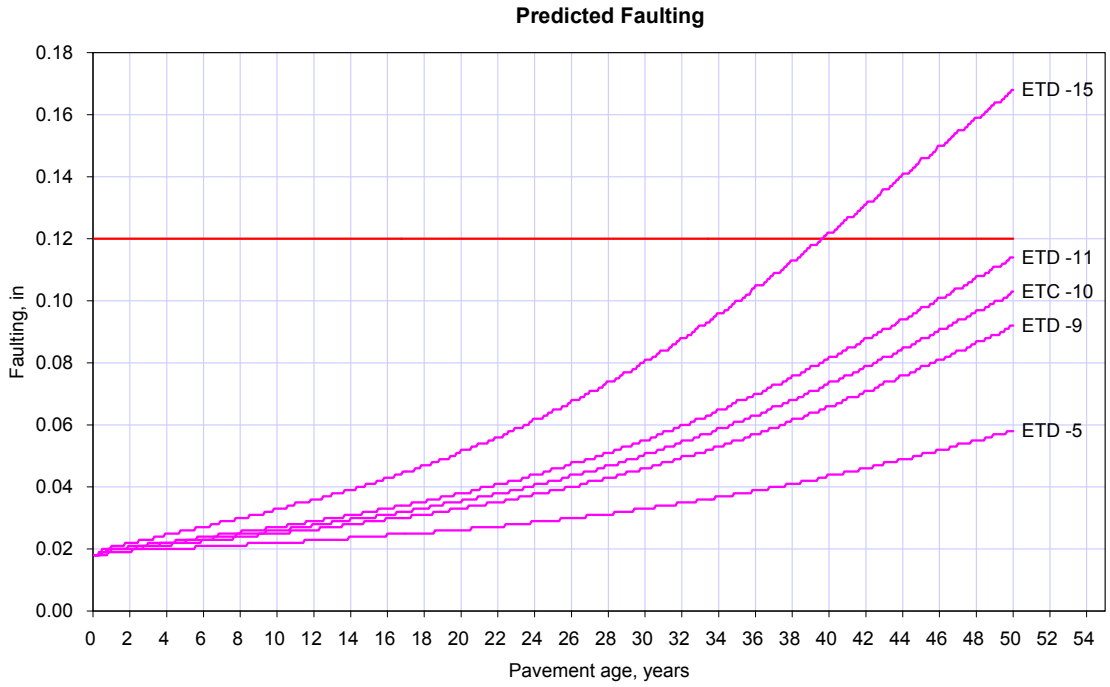

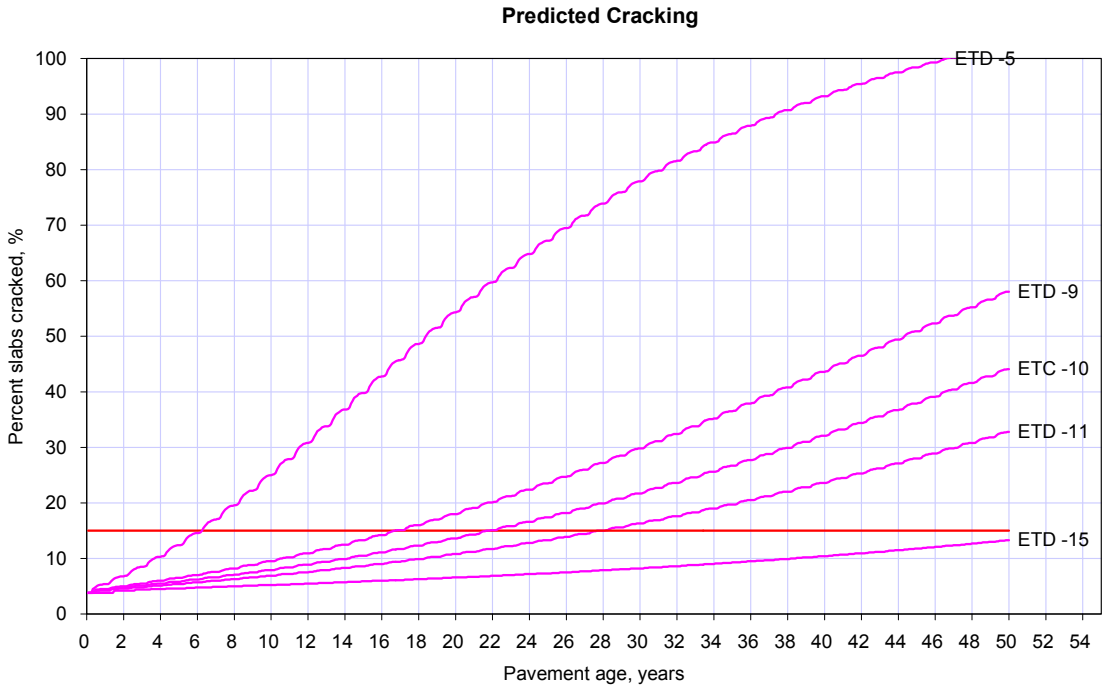

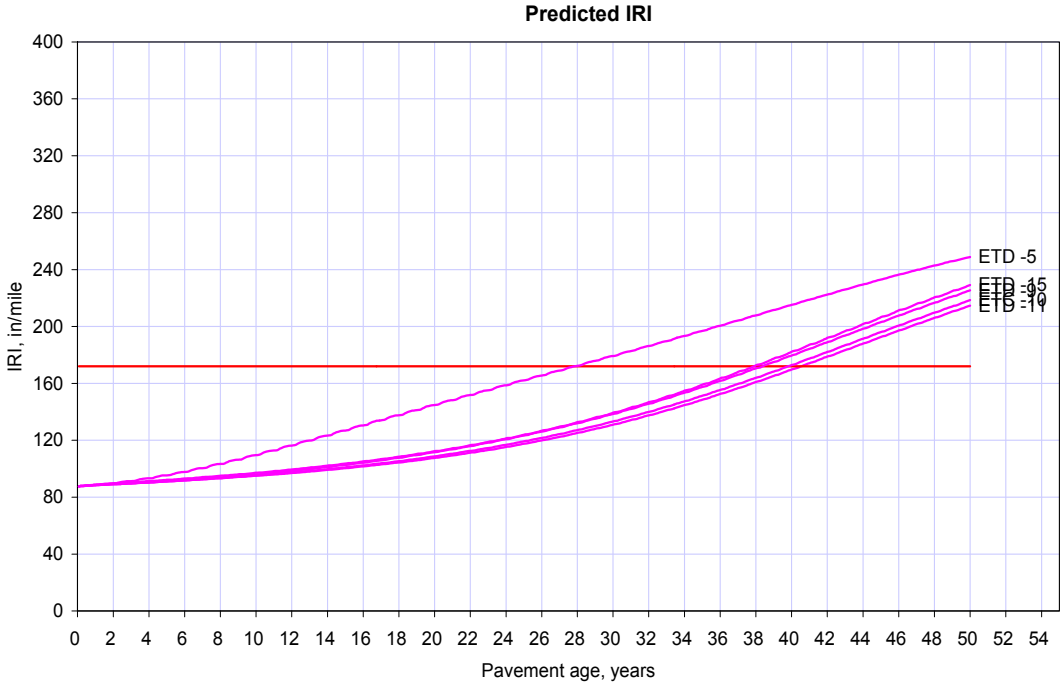

The Top-down Cracking, Bottom-up cracking plus the Faulting added together results in cumulative damage in MEPDG. For the "Permanent Curl/Wrap effective temperature difference (˚F)" this is shown in the following plot.

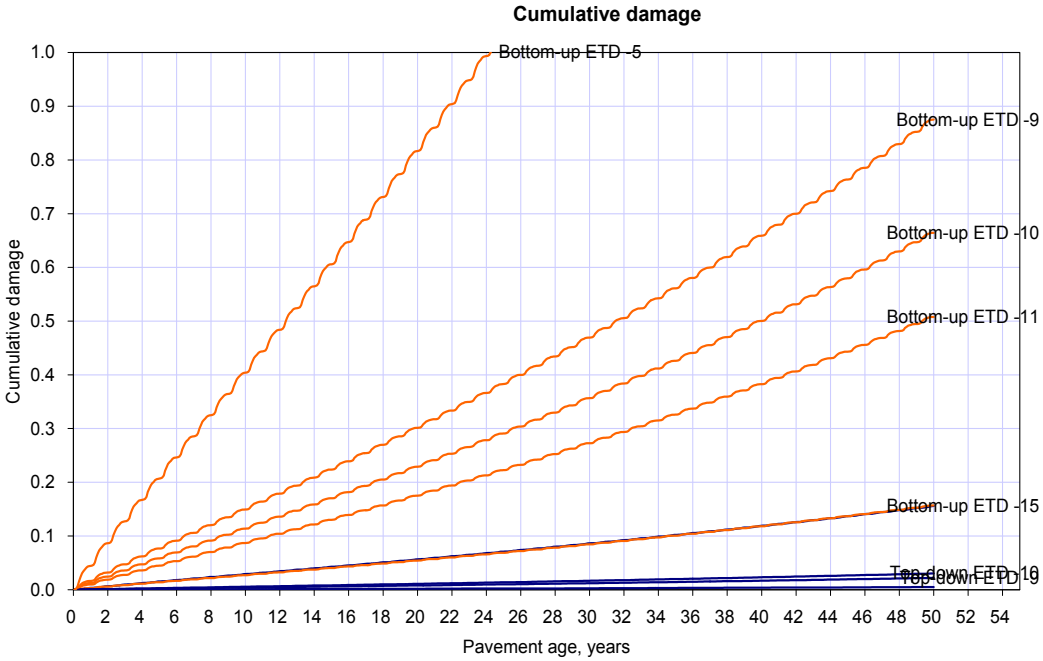

It is therefore recommended that we use the site specific concrete temperature difference which can be calculated through using different electronic equipments. Or otherwise we have to use the program default input.

A4.3 Joint Spacing (ft)

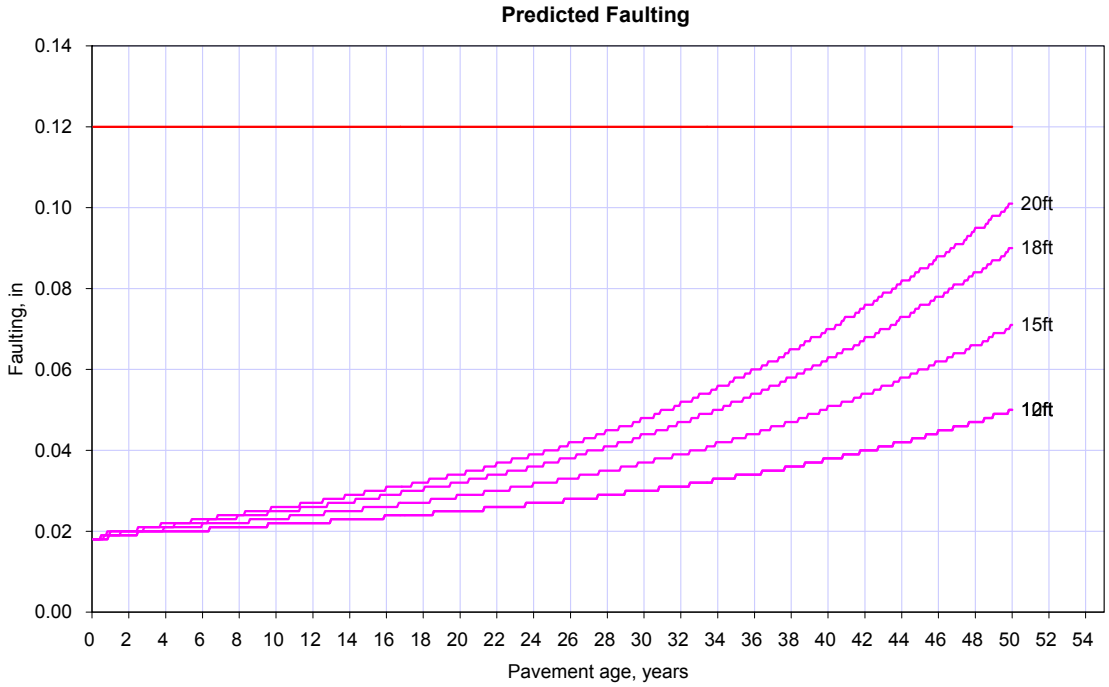

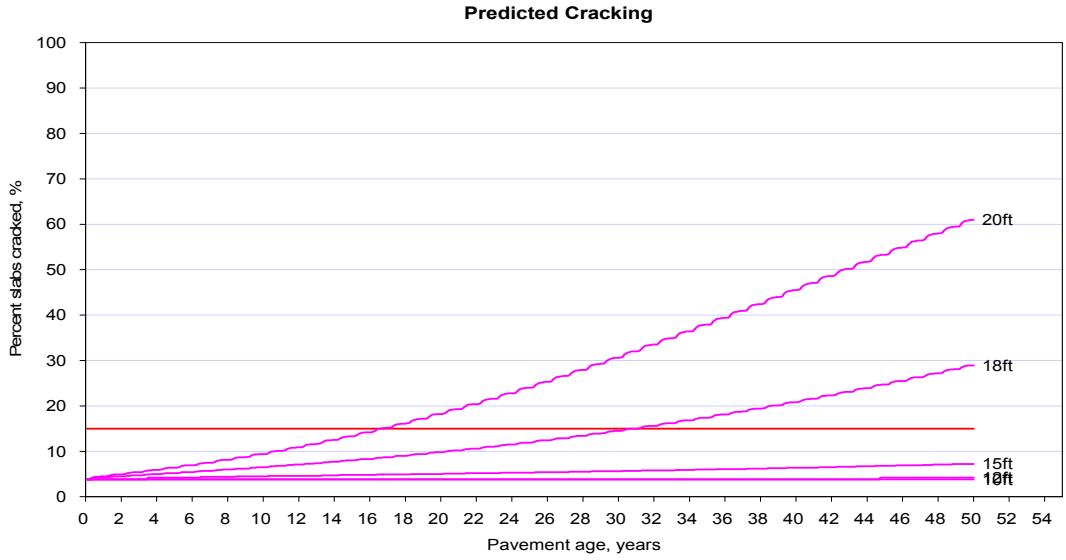

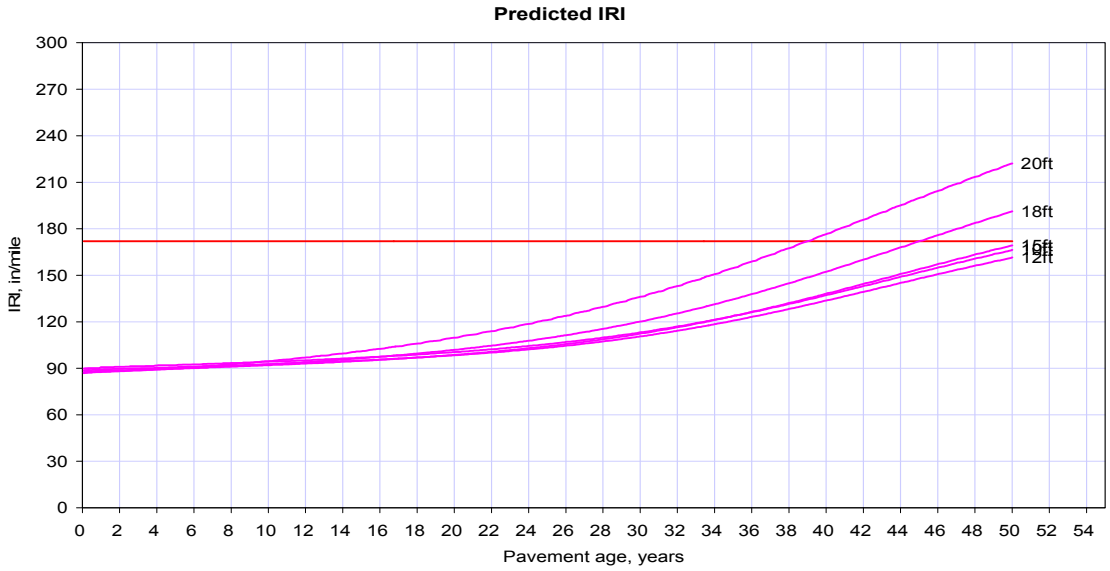

A4.4 Sealant Type

The sealant options are liquid, silicone, and preformed. Sealant type is an input to the empirical model used to predict spalling. Spalling is used in smoothness predictions, but it is not considered directly as a measure of performance in this Guide.

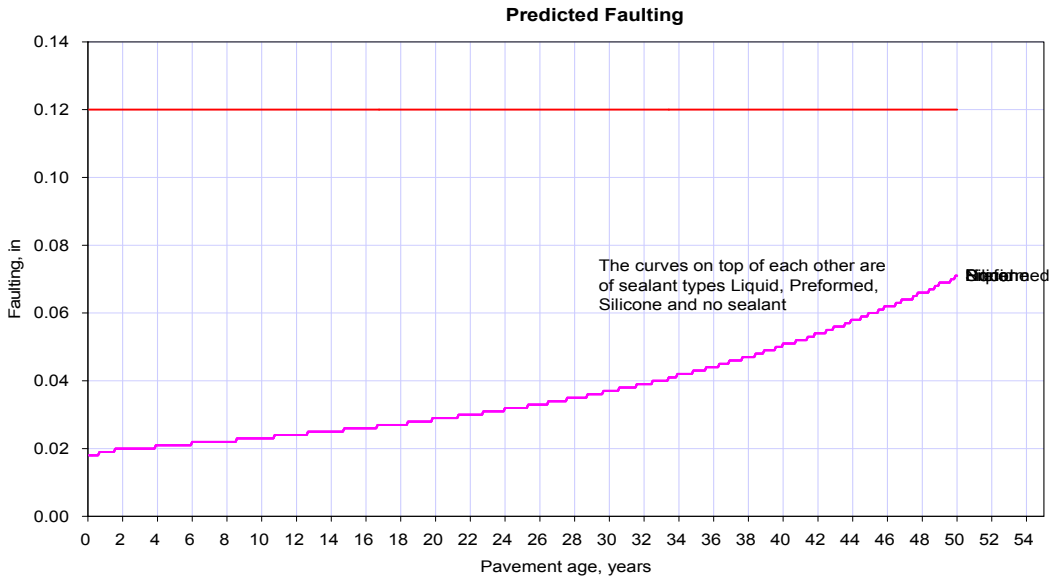

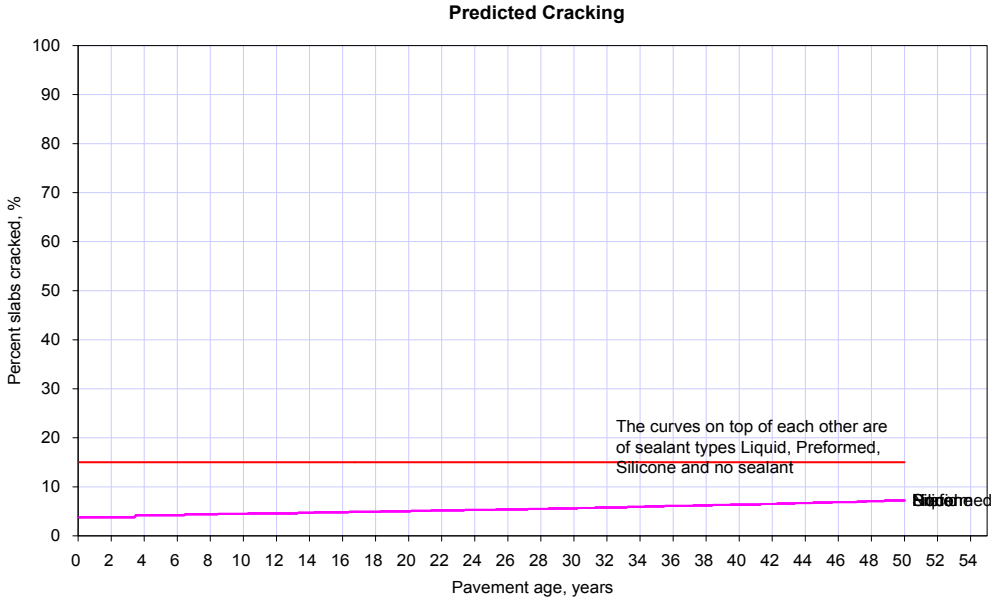
Predicted Cracking
Percent slabs cracked, %
Pavement age, years
The curves on top of each other are of sealant types Liquid, Preformed, Silicone and no sealant

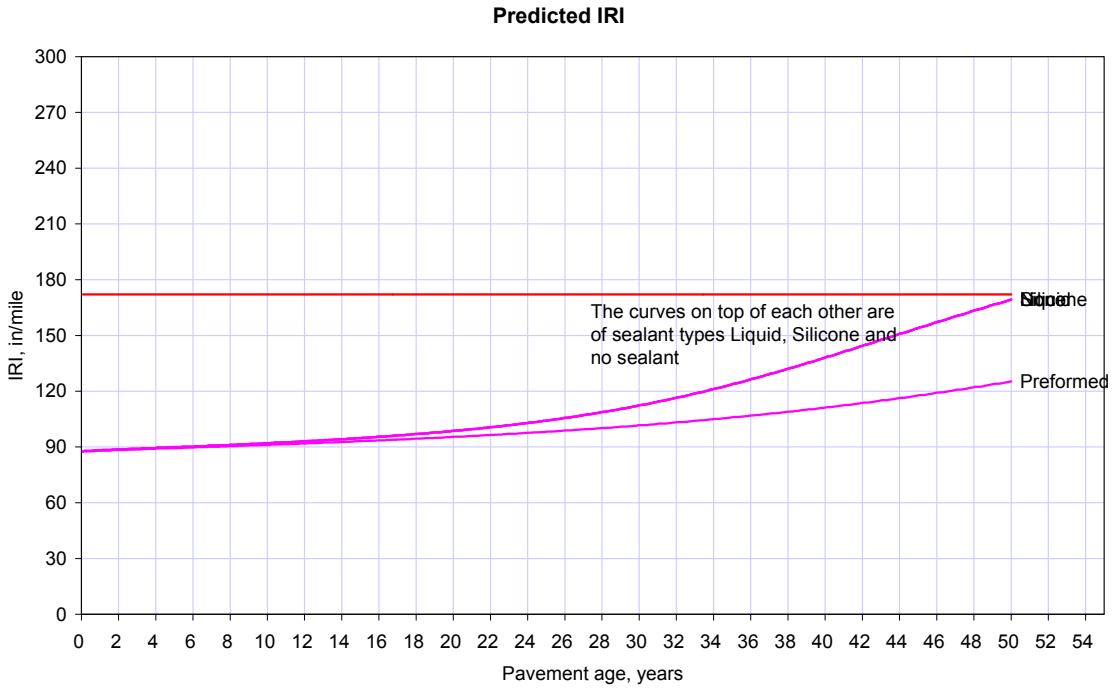
Predicted IRI
IRI, in/mile
Pavement age, years
The curves on top of each other are of sealant types Liquid, Silicone and no sealant
Preformed

A4.5 Dowel diameter (in)

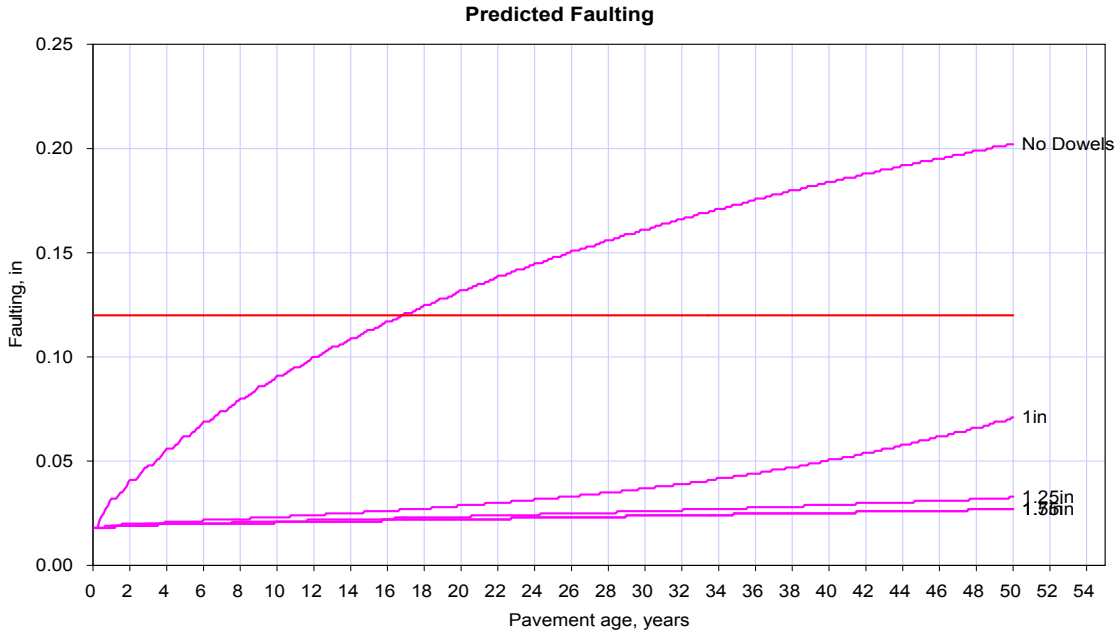

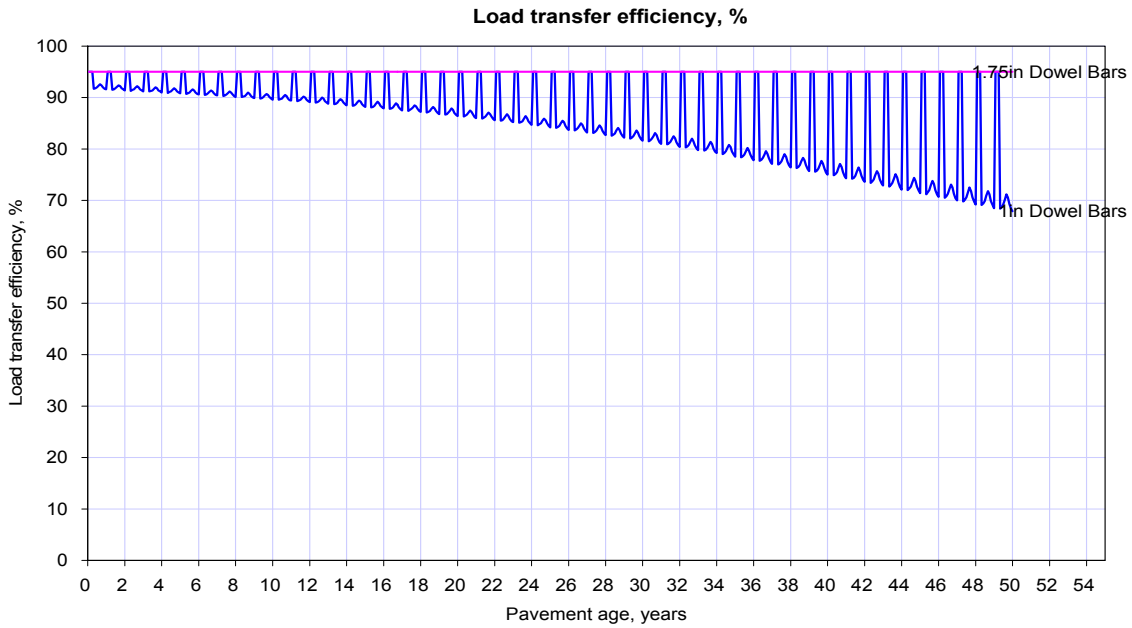

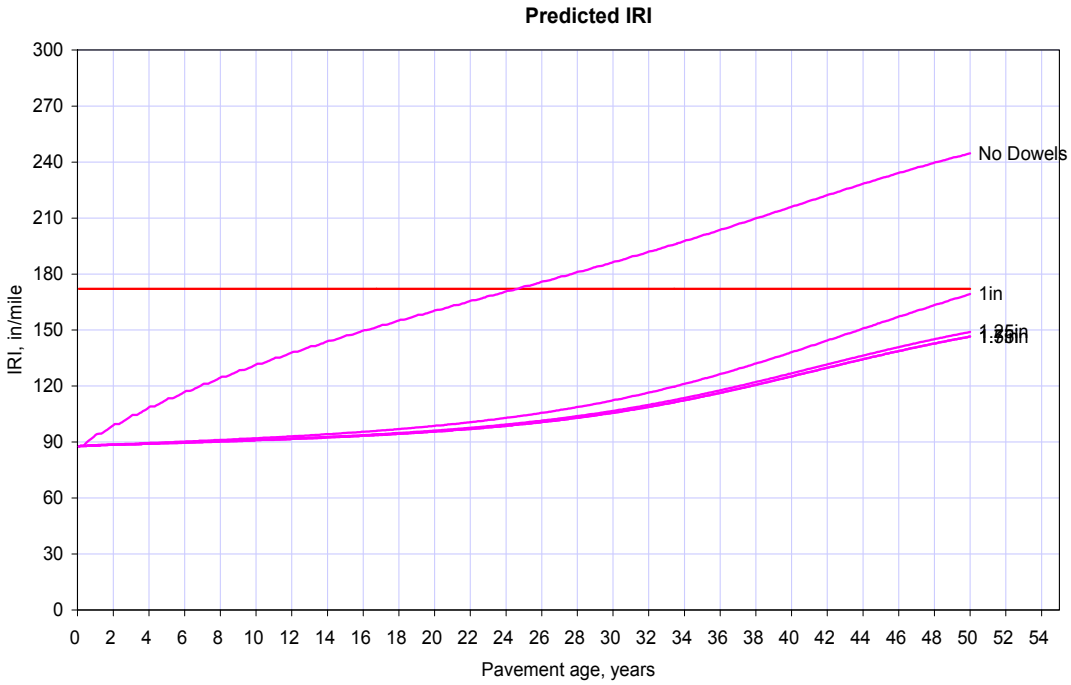

A4.6 Dowel Bar Spacing (in)

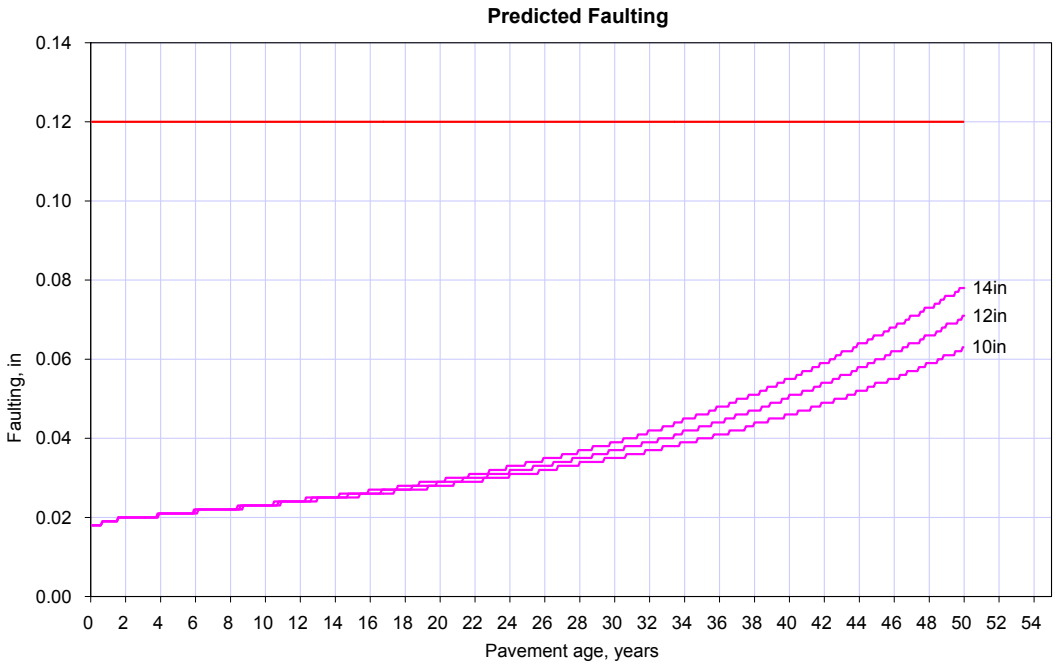

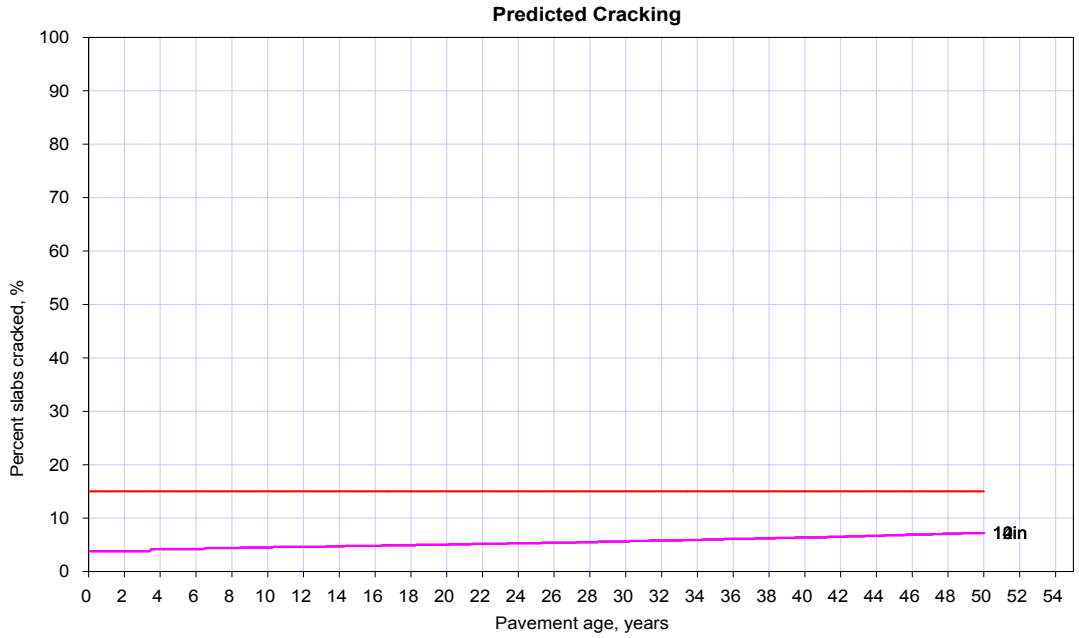
Predicted Cracking
Percent slabs cracked, %
Pavement age, years
12in

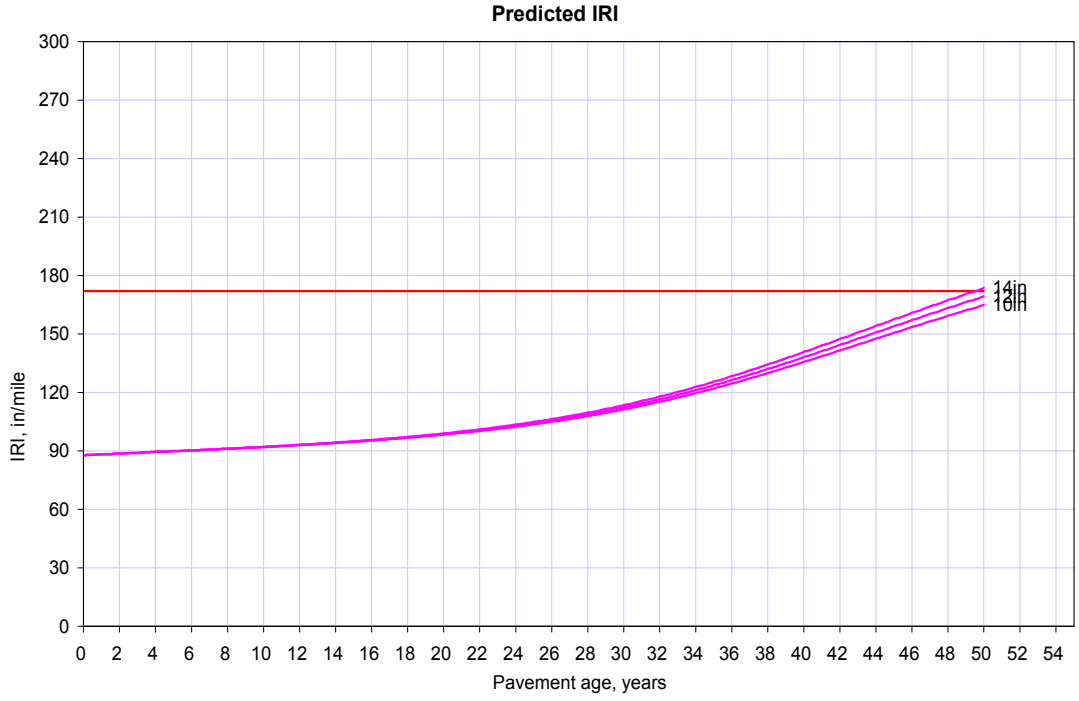
Predicted IRI
IRI, in/mile
Pavement age, years
14in

A4.7 Tied PCC Shoulder, Long-term LTE (Load Transfer Efficiency, %)

Tied PCC shoulders can significantly improve JPCP performance by reducing critical deflections and stresses. The shoulder type also affects the amount of moisture infiltration into the pavement structure. The effects of moisture infiltration are considered in the determination of seasonal moduli values of unbound layers. The structural effects of the edge support features are directly considered in the design process. For tied concrete shoulders the long-term LTE between the lane and shoulder must to be provided.

Long-term LTE

Load Transfer Efficiency (LTE) is defined as the ratio of deflections of the unloaded and loaded slabs. The higher the LTE, the greater the support provided by the shoulder to reduce critical responses of the mainline slabs. Typical long-term deflection LTE are:

- 50 to 70 percent for monolithically constructed tied PCC shoulder.
- 30 to 50 percent for separately constructed tied PCC shoulder.

Analyses were done for untied & tied PCC shoulders with different load transfer efficiencies.

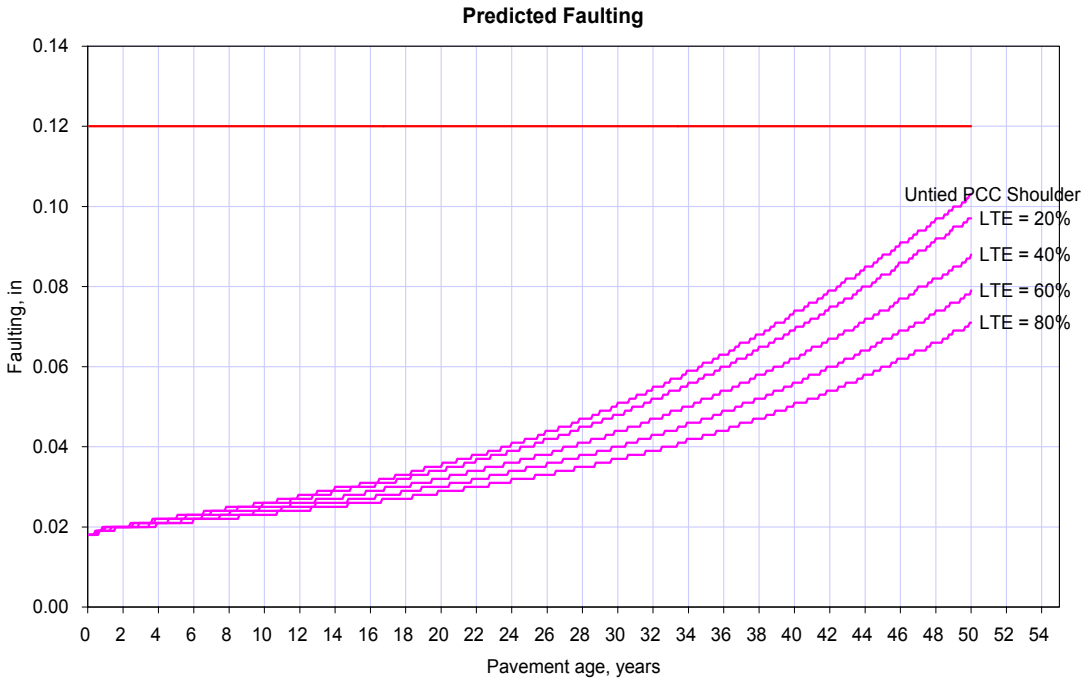

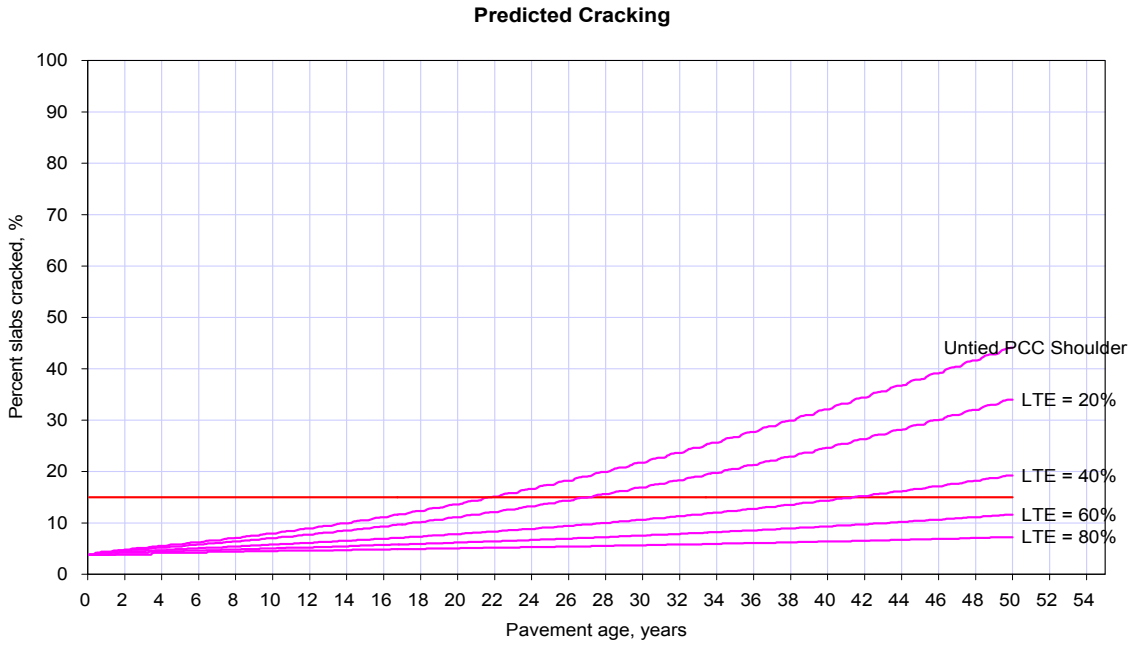
Predicted Cracking
Percent slabs cracked, %
Pavement age, years
Untied PCC Shoulder
LTE = 20%
LTE = 40%
LTE = 60%
LTE = 80%

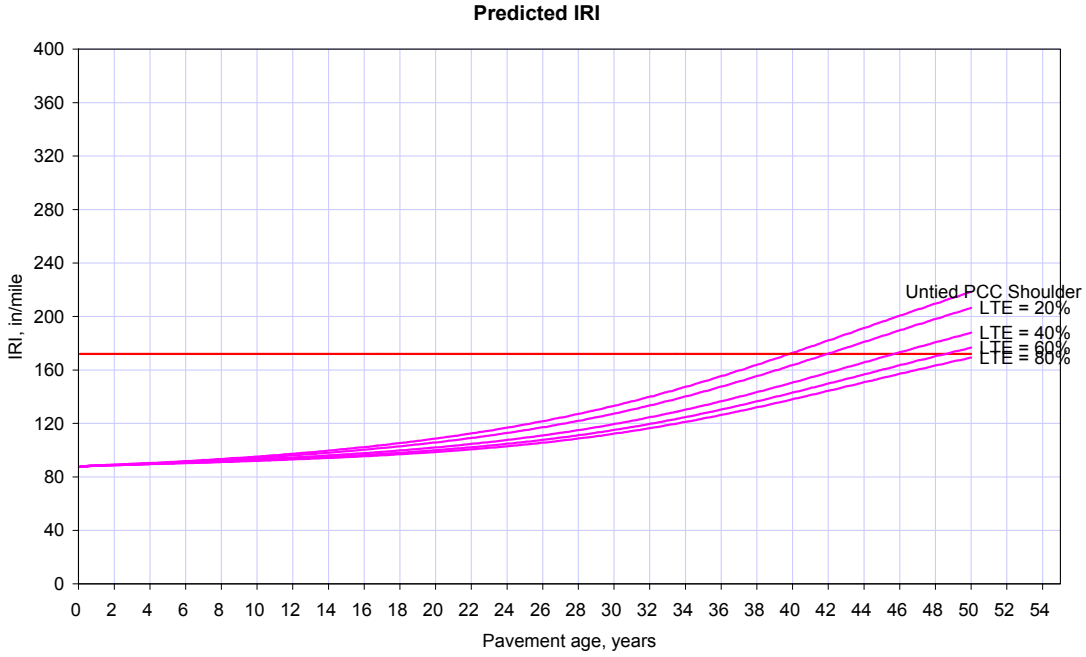
Predicted IRI
IRI, in/mile
Pavement age, years
Untied PCC Shoulder
LTE = 20%
LTE = 40%
LTE = 60%
LTE = 80%

A4.8 Widened Slab (ft)

The JPCP slab can be widened to accommodate the outer wheel path further away from the longitudinal edge. Widened slab can significantly improve JPCP performance as they result in reduced edge stresses and corner deflections.

Slab Width: This input is the selected width of the widened slab. Note that this is not same as the lane width.

Analyses were done for un-widened and widened (12ft, 13ft & 14ft) slabs as shown in the graphs below.

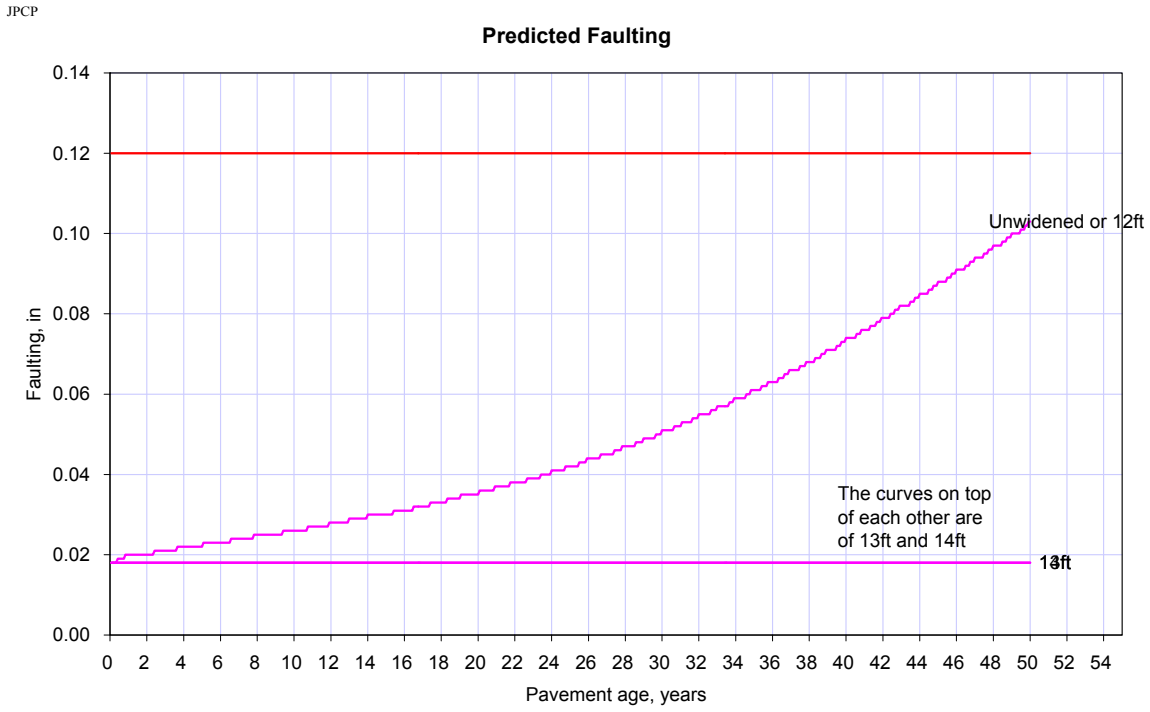

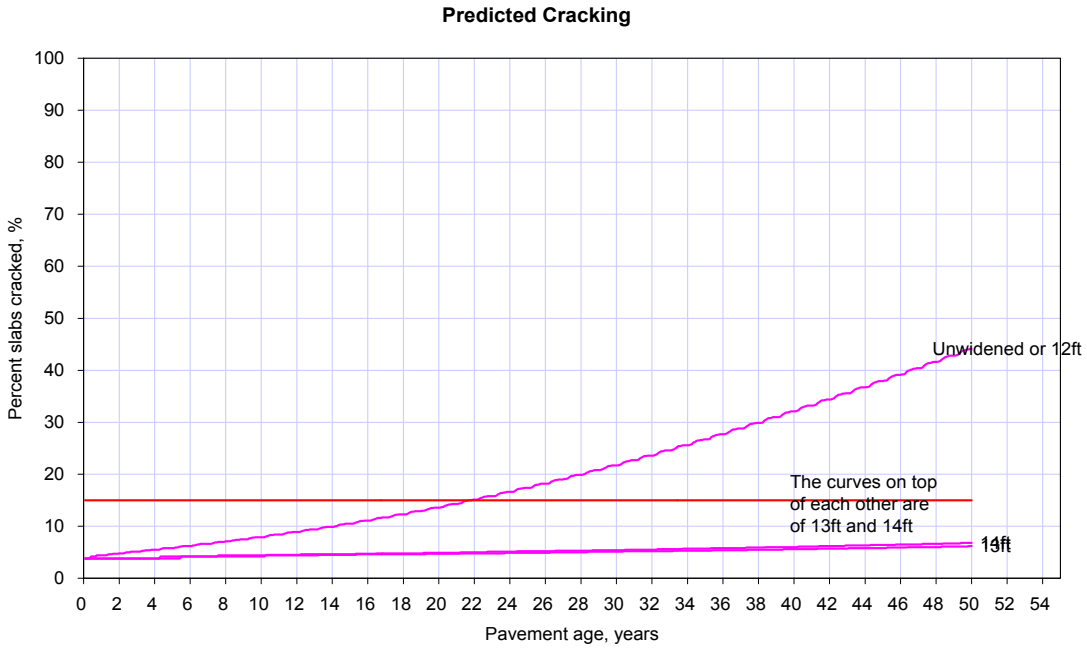
Predicted Cracking
Percent slabs cracked, %
Pavement age, years
Unwidened or 12ft
The curves on top
of each other are
of 13ft and 14ft
14ft
13ft

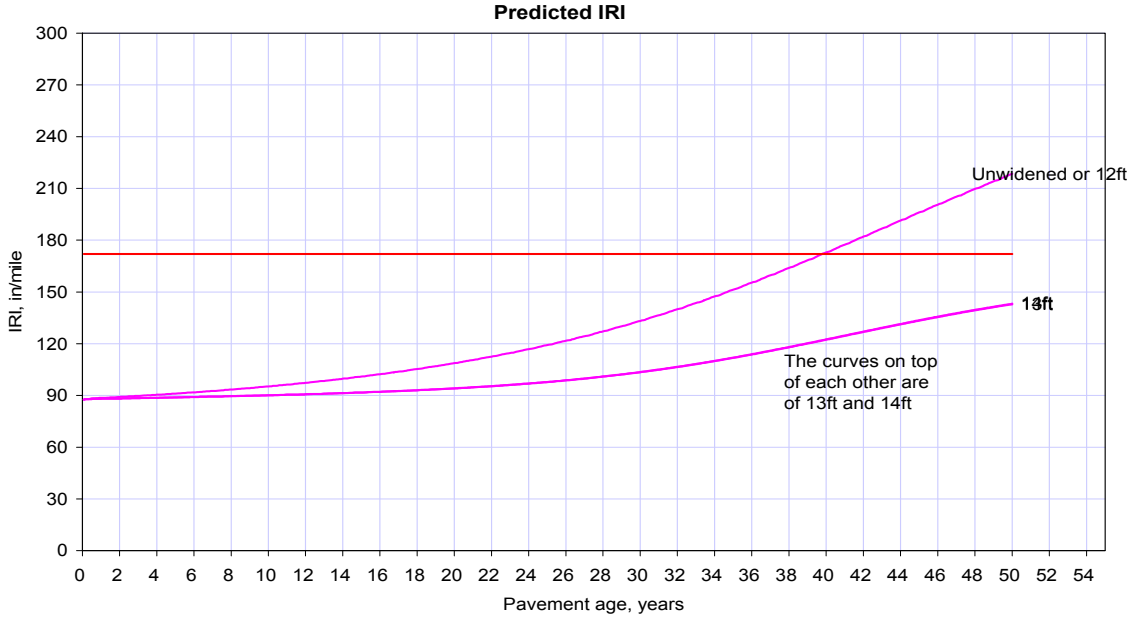
Predicted IRI
IRI, in/mile
Pavement age, years
Unwidened or 12ft
The curves on top
of each other are
of 13ft and 14ft
14ft
13ft

A4.9 PCC-Base Interface

Interface type and the quality of bond between the slab and the base

The Stabilized bases (especially asphalt-stabilized bases) are often bonded to the slab, and the deflection testing conducted at slab interior typically shows a bonded response. However, the effects of environmental and traffic loading tend to weaken this bond over time around the edges, and the bonded-interface assumption over the entire design period may be un-conservative.

Bonded: The structural contribution of a bonded layer is considered by means of a composite section analysis, i.e. its structural contribution is integrated with that of the PCC slab proportional to the stiffness of the base layer. For example, the structural contribution of a stabilized base is significant, if the base is fully bonded to the slab.

Unbonded: The base layer is treated as a separate layer in the analysis and its contribution to the structural capacity of the PCC slab is minimized. For example, the structural contribution of a stabilized unbonded base layer is lesser than that of a stabilized bonded layer.

If the base is bonded to PCC then we have to enter the loss of bond in a specified time in months. The program requires that this time of bond be from 0 to 360 months with zero the same as unbonded.

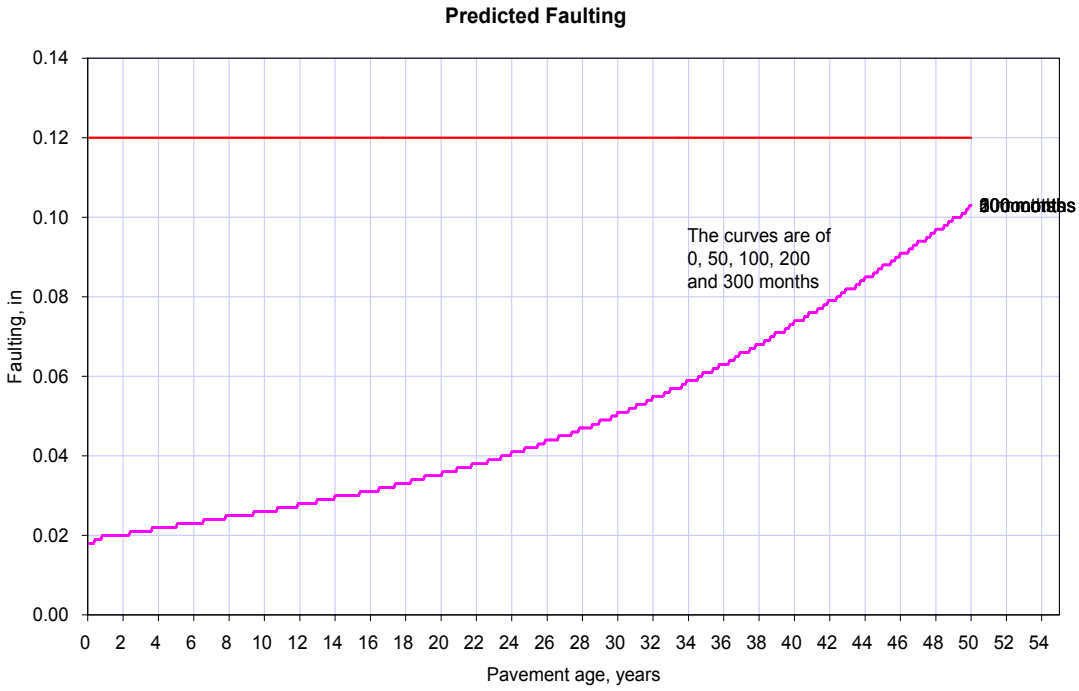

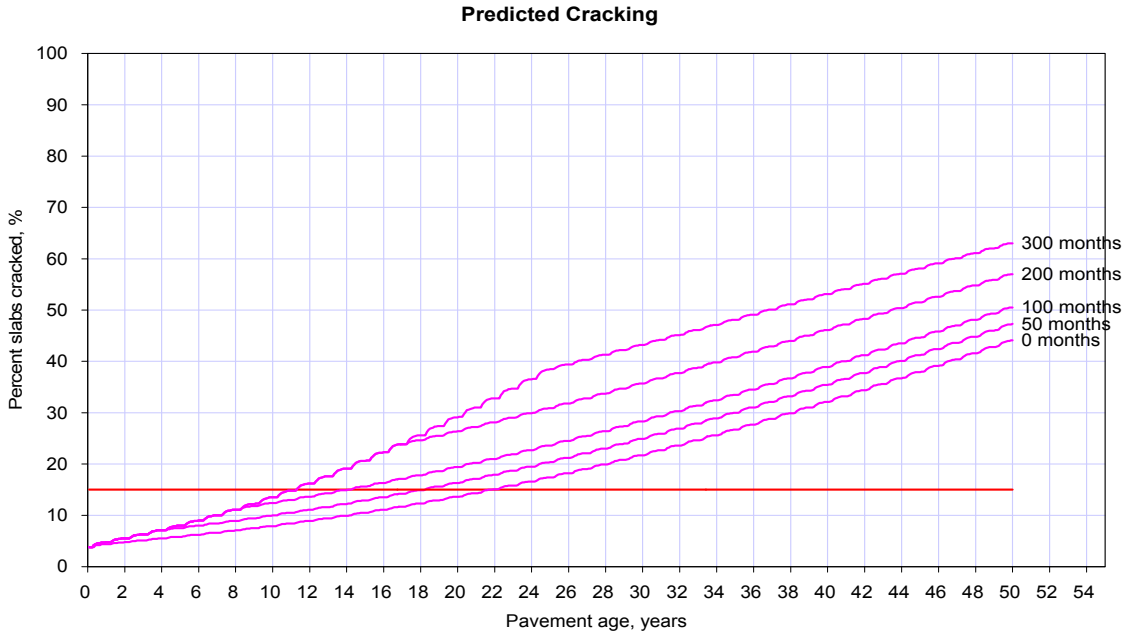
Predicted Cracking
Percent slabs cracked, %
Pavement age, years
300 months
200 months
100 months
50 months
0 months

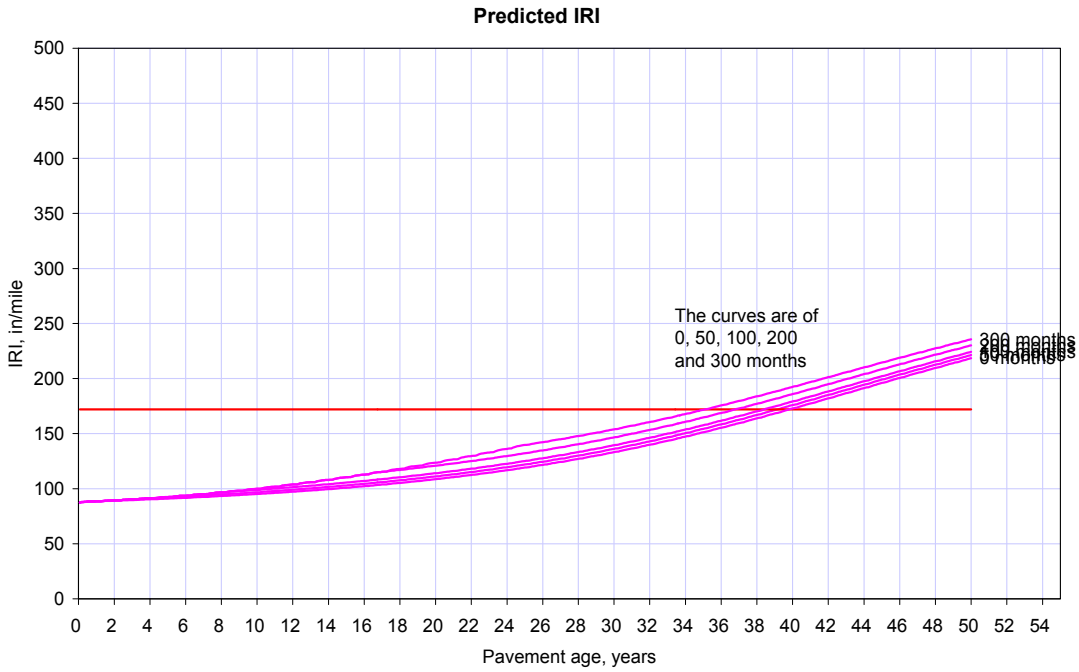
Predicted IRI
IRI, in/mile
Pavement age, years
The curves are of
0, 50, 100, 200
and 300 months

A4.10 Erodibility Index

This is an index on a scale of 1 to 5 to rate the potential for erodibility of the base material. The potential for base or subbase erosion (layer directly beneath the PCC layer) has a significant impact on the initiation and propagation of pavement distress. Different base types are classified based on long-term erodibility behavior as follows:

Class 1 – Extremely erosion resistant materials.

Class 2 – Very erosion resistant materials.

Class 3 – Erosion resistant materials.

Class 4 – Fairly erodible materials.

Class 5 – Very erodible materials.

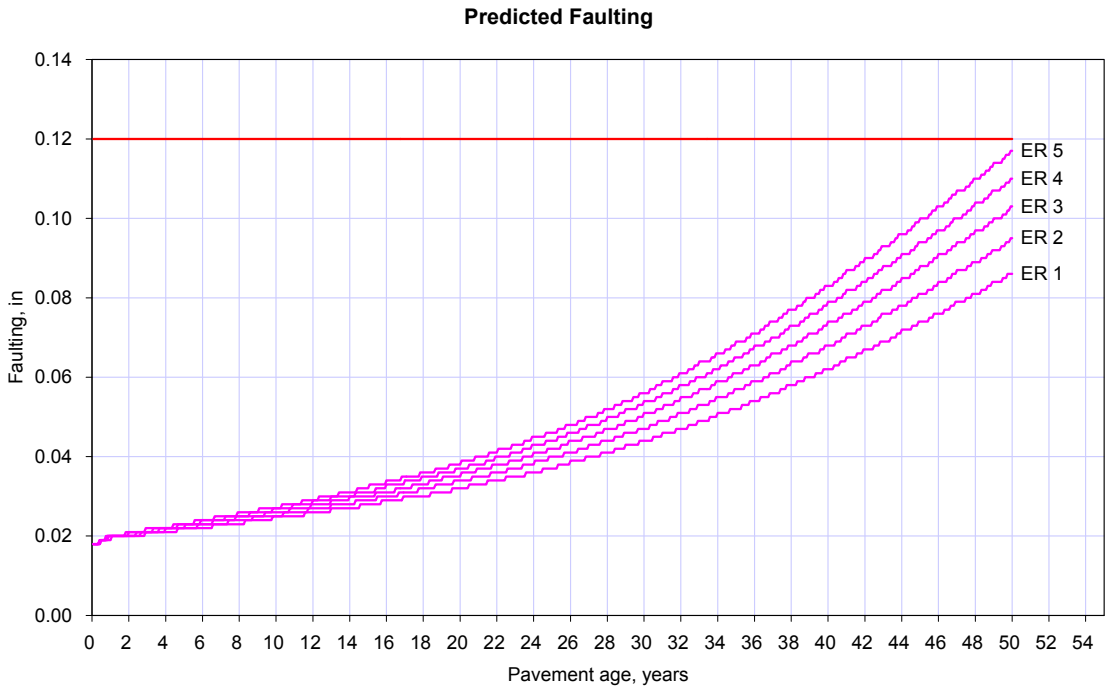

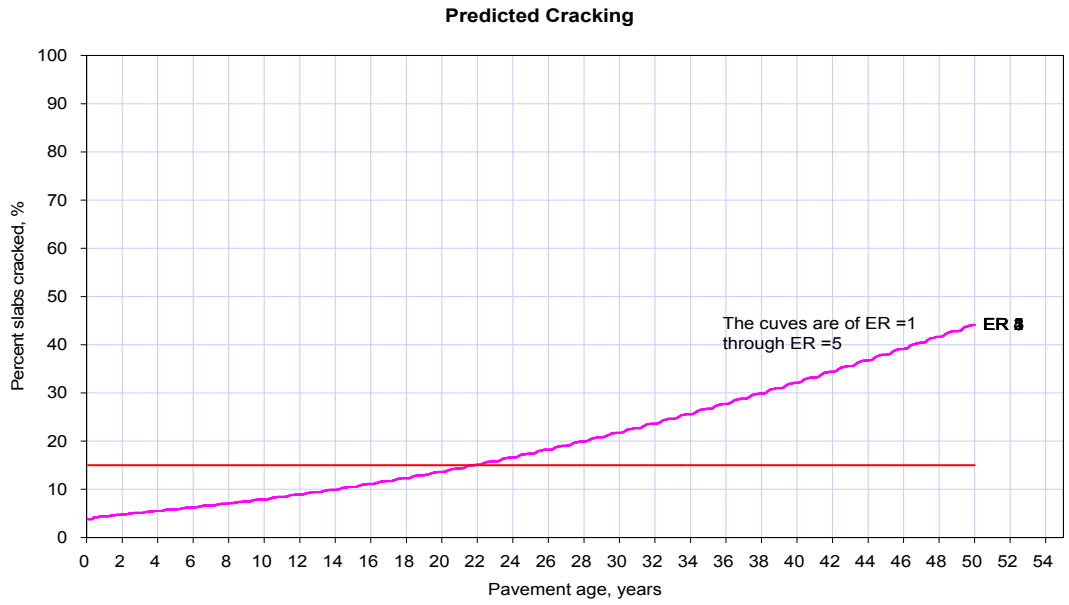
Predicted Cracking
Percent slabs cracked, %
Pavement age, years
The cuves are of ER =1 through ER =5
ER 5

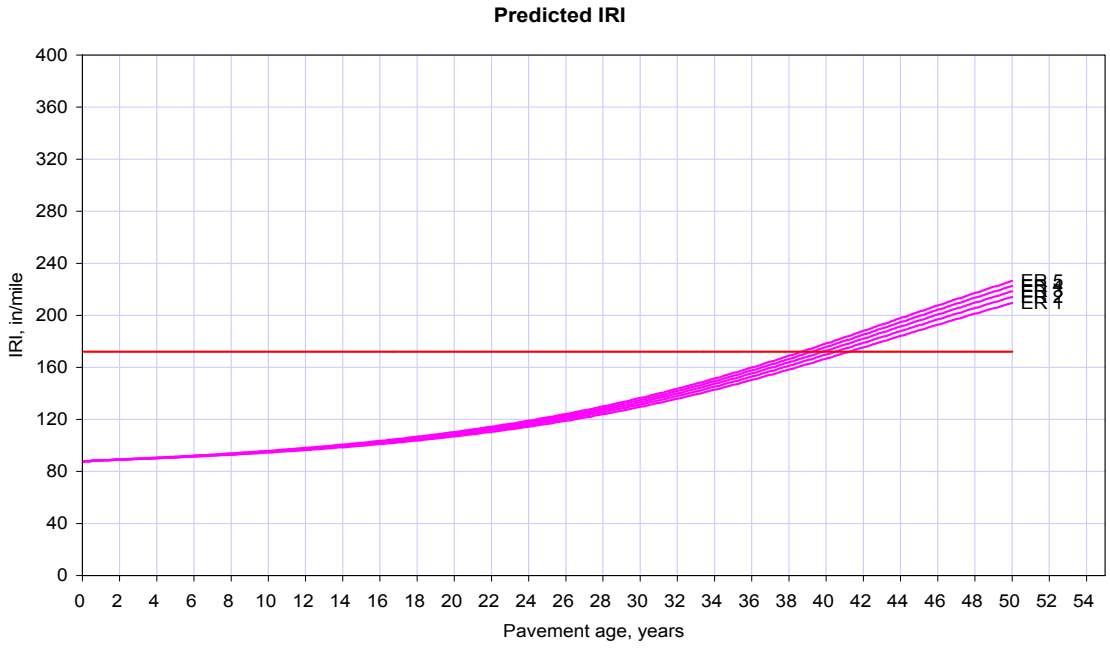
Predicted IRI
IRI, in/mile
Pavement age, years
ER 5
ER 4

A5 PCC Material Properties

These inputs are related to Portland Cement Concrete (PCC) properties such as its layer thickness, strength, material etc.

A5.1 PCC Layer Thickness (in)

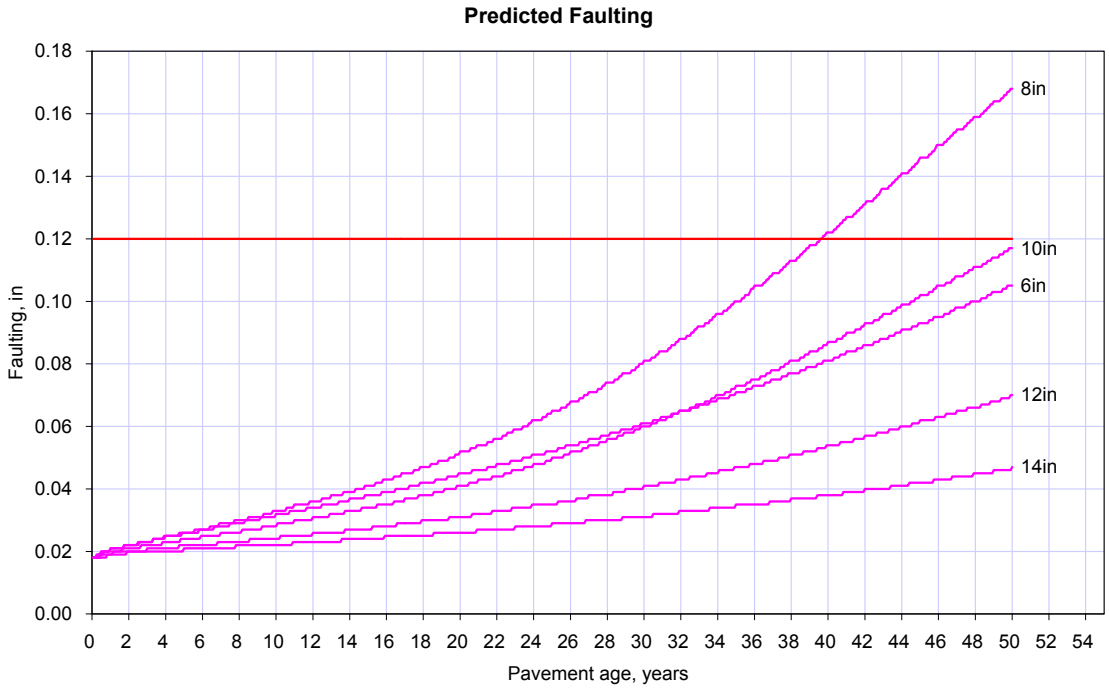

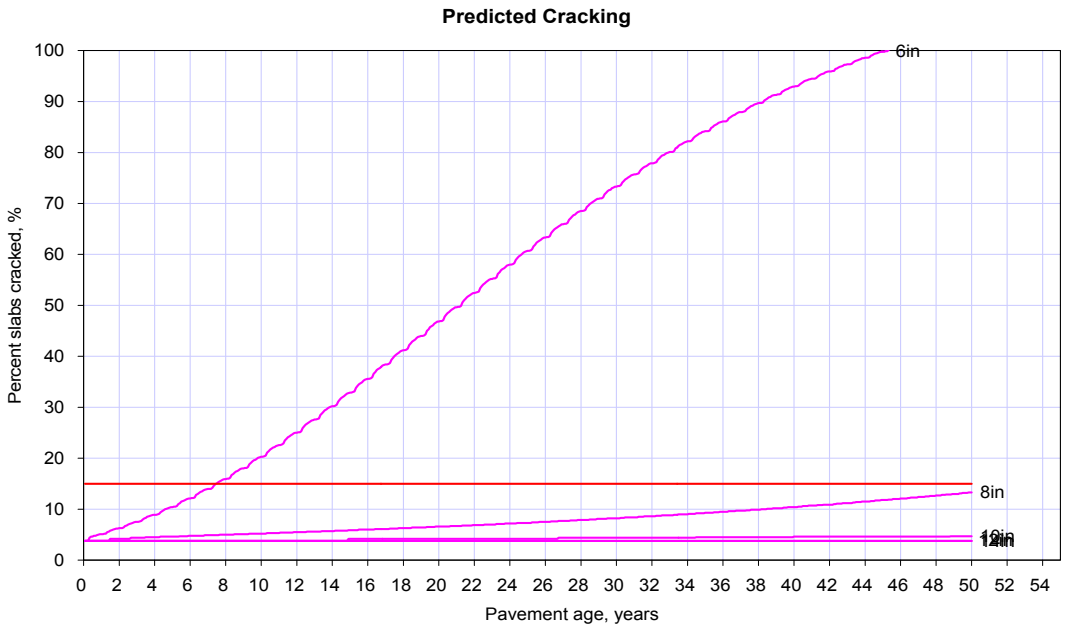
Predicted Cracking
Percent slabs cracked, %
Pavement age, years
6in
8in
10in
12in
14in

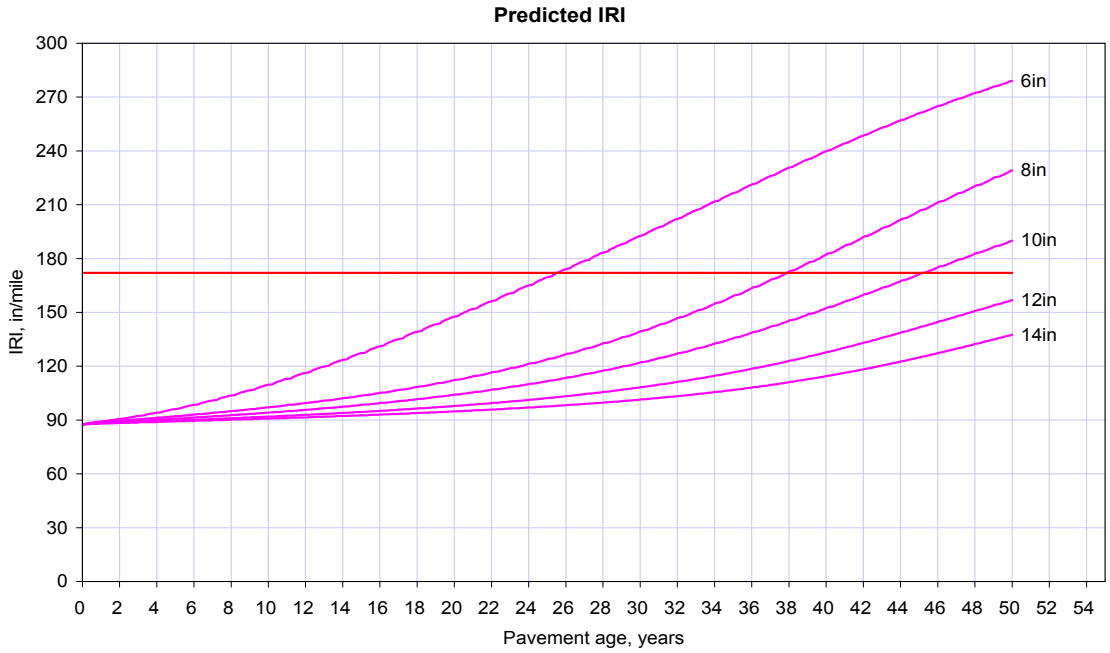
Predicted IRI
IRI, in/mile
Pavement age, years
6in
8in
10in
12in
14in

A5.2 PCC Unit Weight (pcf)

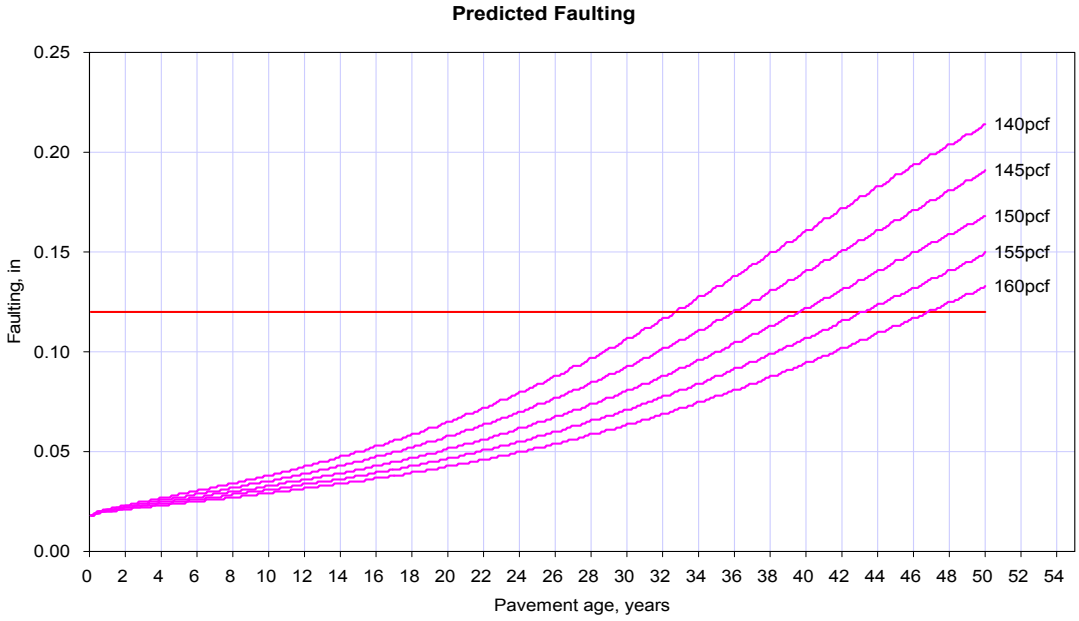

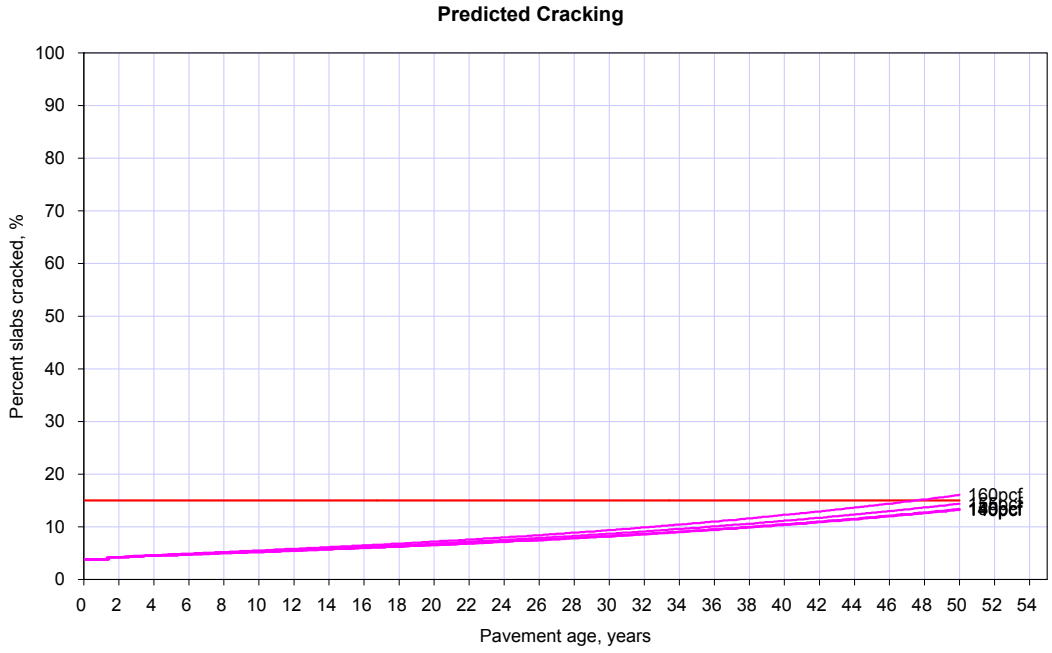

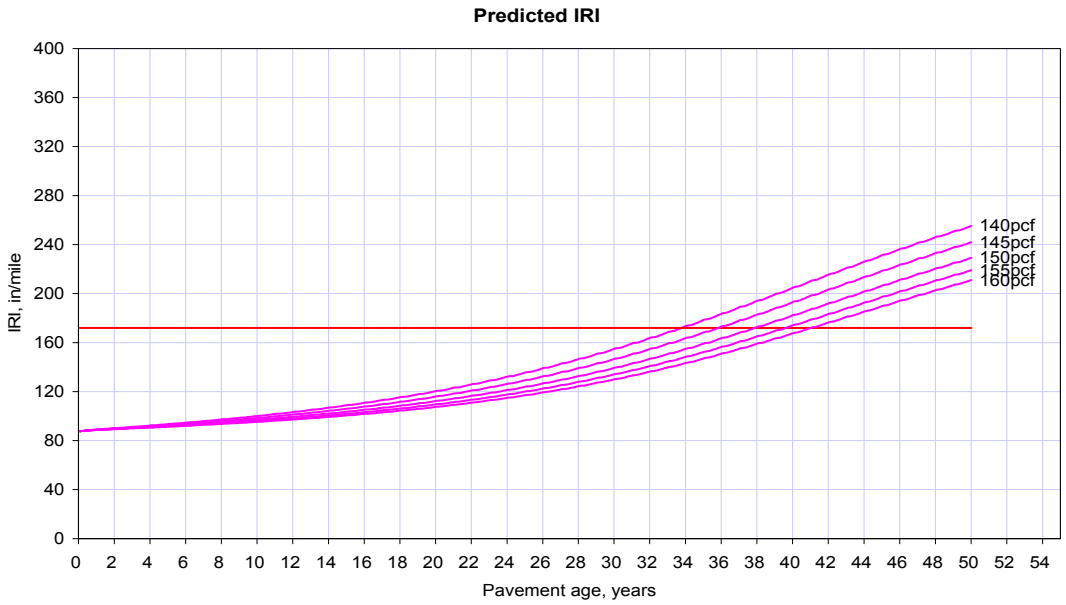

A5.3 PCC Poisson's Ratio

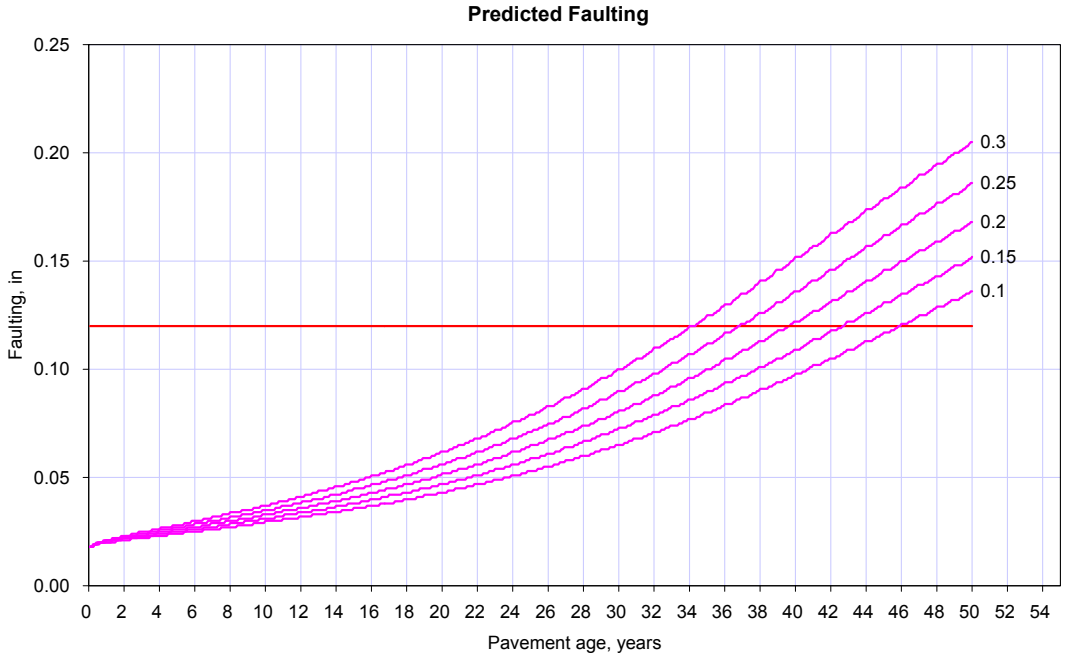

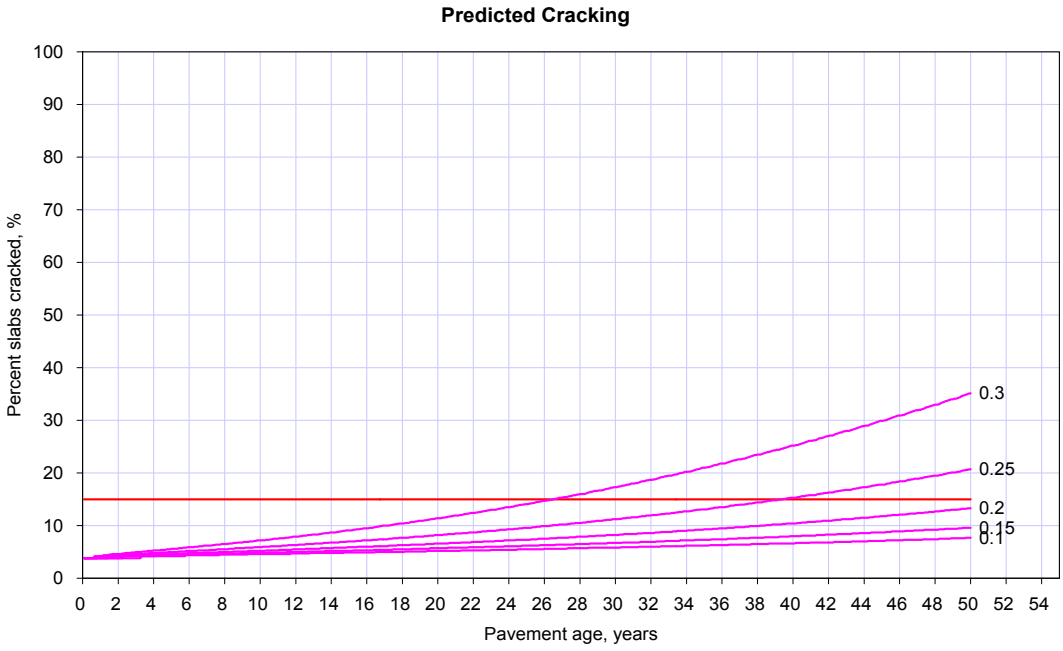
Predicted Cracking
Percent slabs cracked, %
Pavement age, years
0.3
0.25
0.2
0.15
0.1

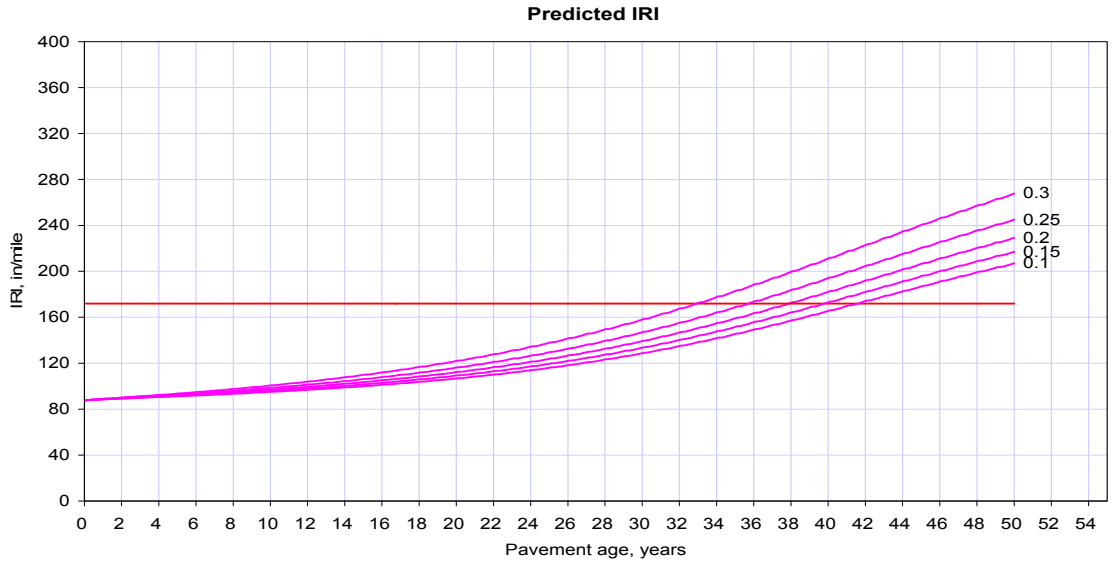
Predicted IRI
IRI, in/mile
Pavement age, years
0.3
0.25
0.2
0.15
0.1

A5.4 Coefficient of thermal expansion (CTE) (per F° × 10-6)

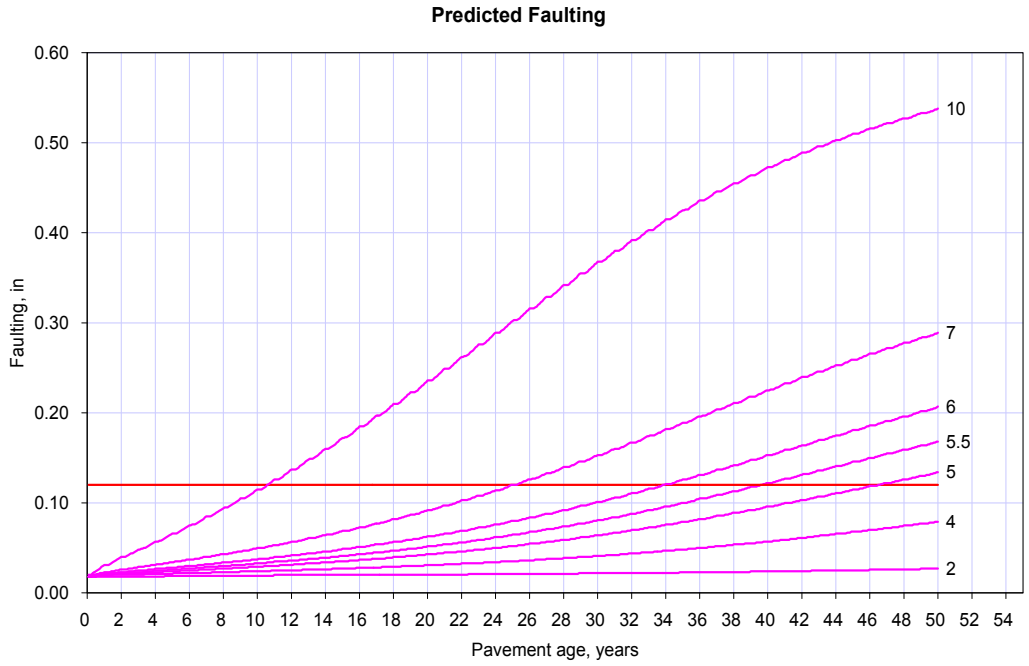

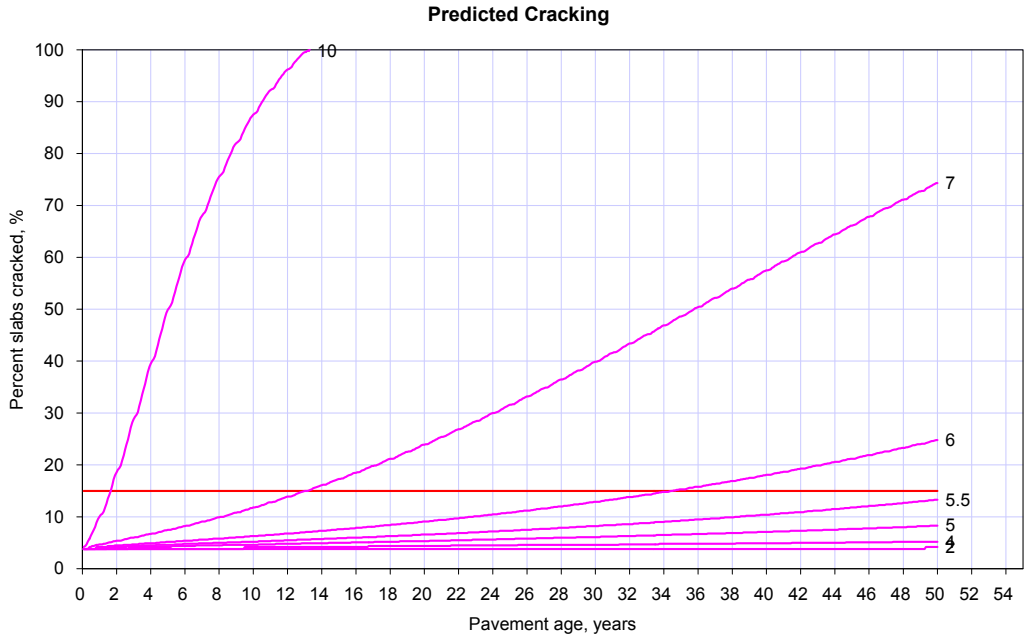

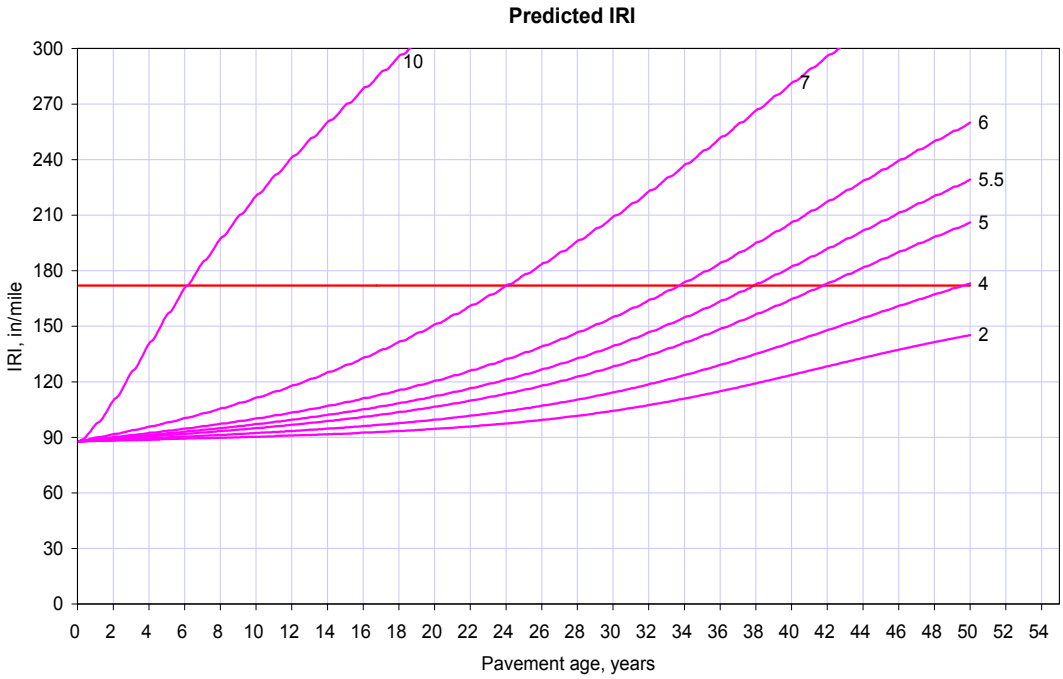

A5.5 Thermal conductivity (BTU/hr-ft-F°)

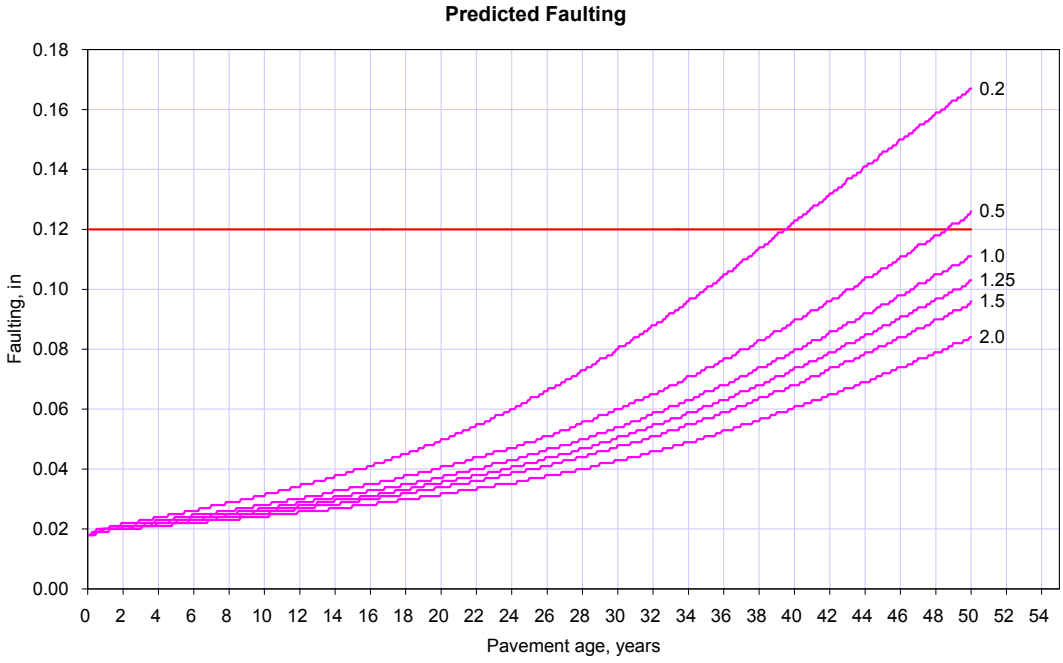

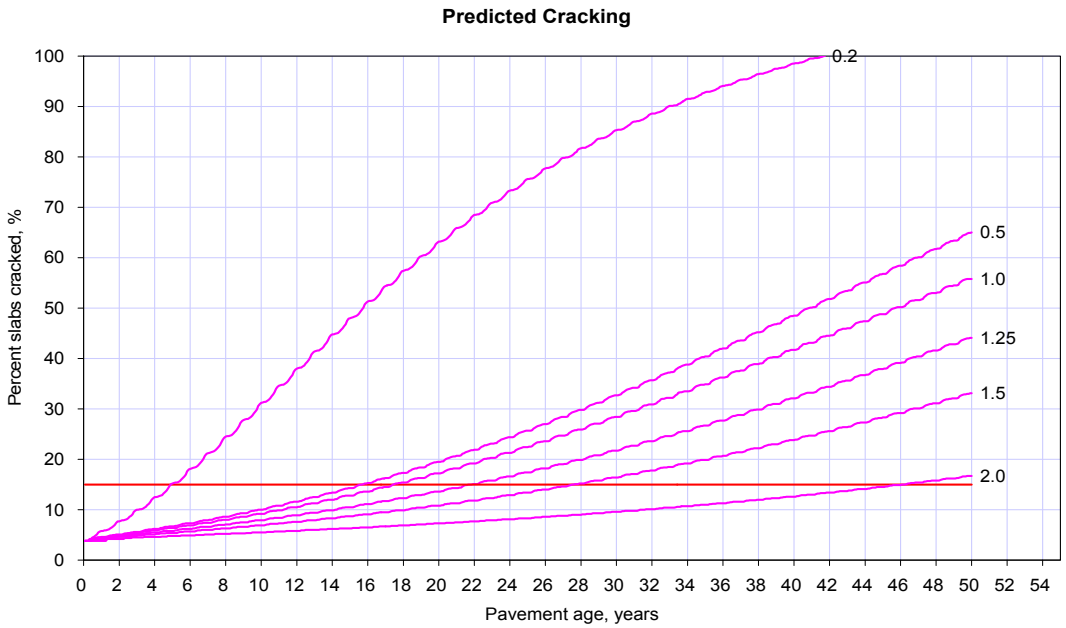
Predicted Cracking
Percent slabs cracked, %
Pavement age, years
0.2
0.5
1.0
1.25
1.5
2.0

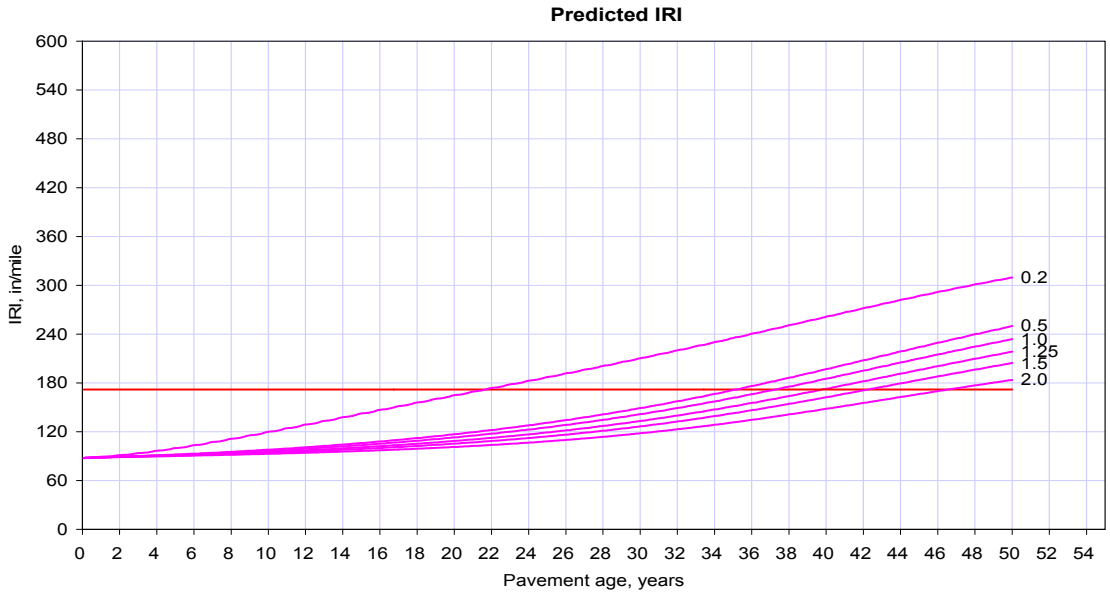
Predicted IRI
IRI, in/mile
Pavement age, years
0.2
0.5
1.0
1.25
1.5
2.0

A5.6 Heat capacity (BTU/lb-F°)

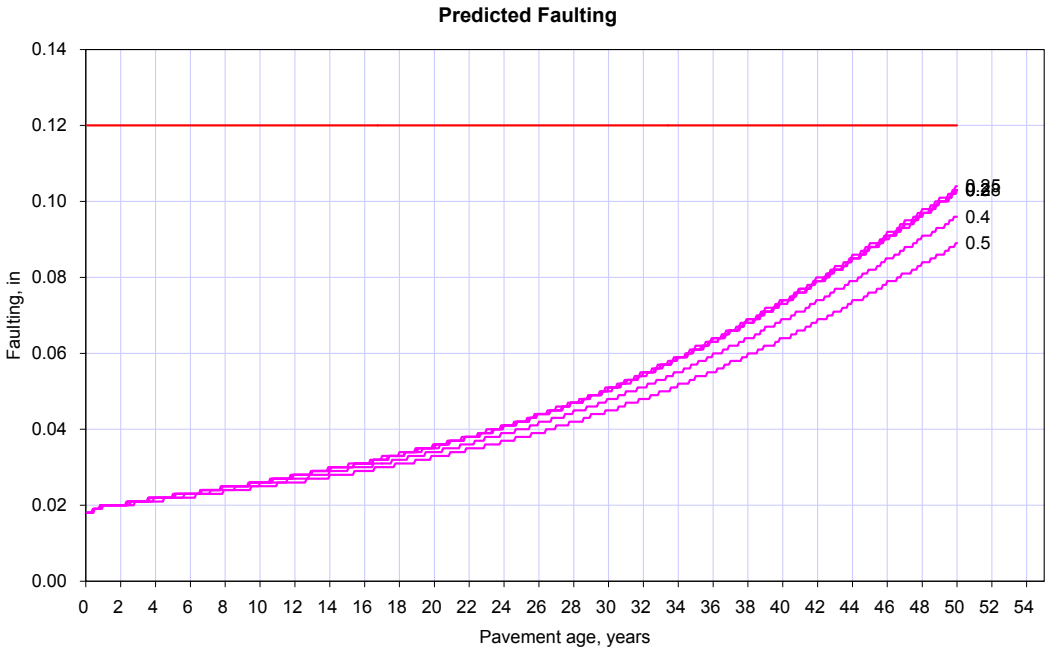

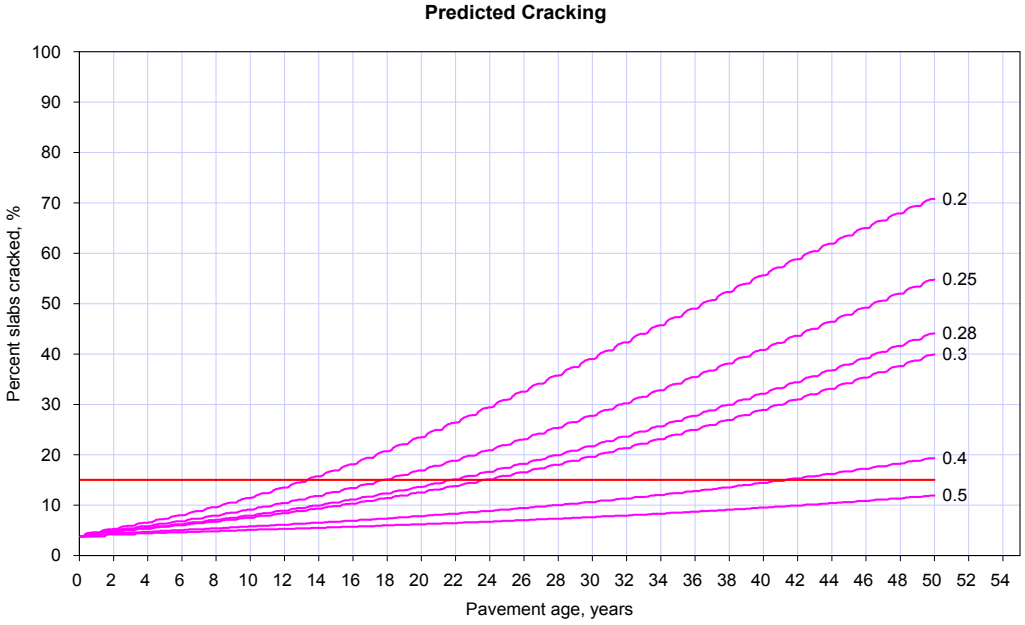

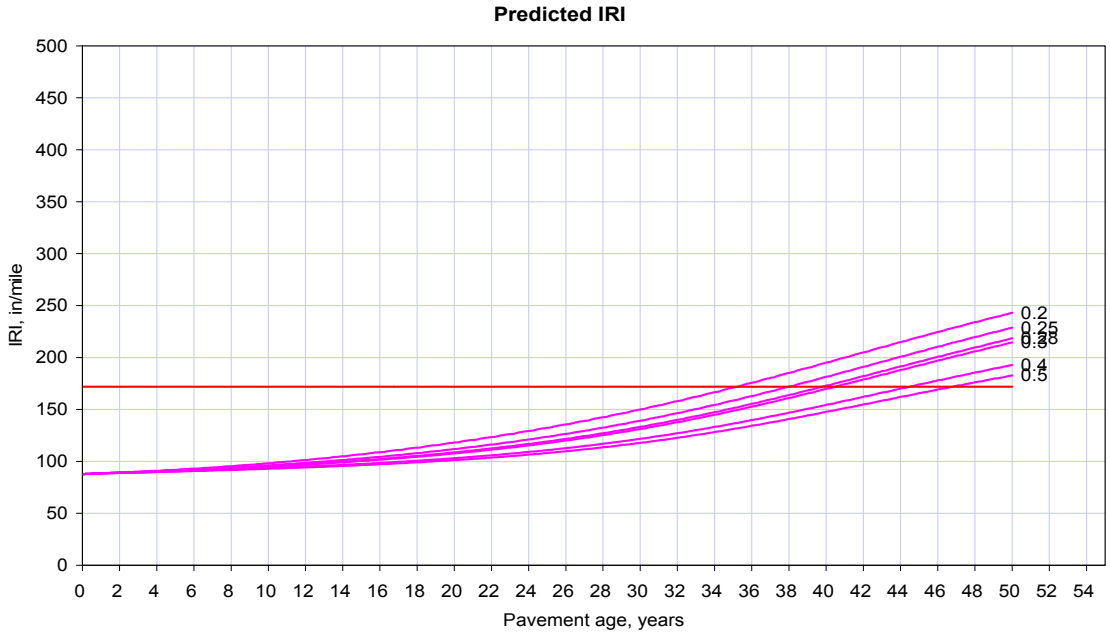

A5.7 Cement Type

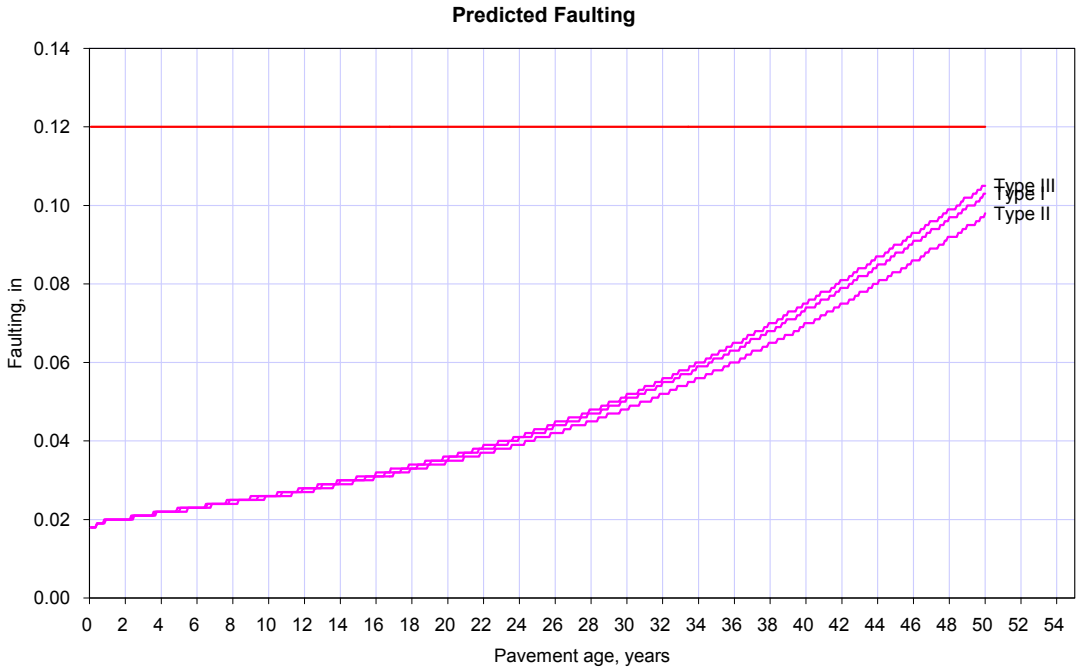

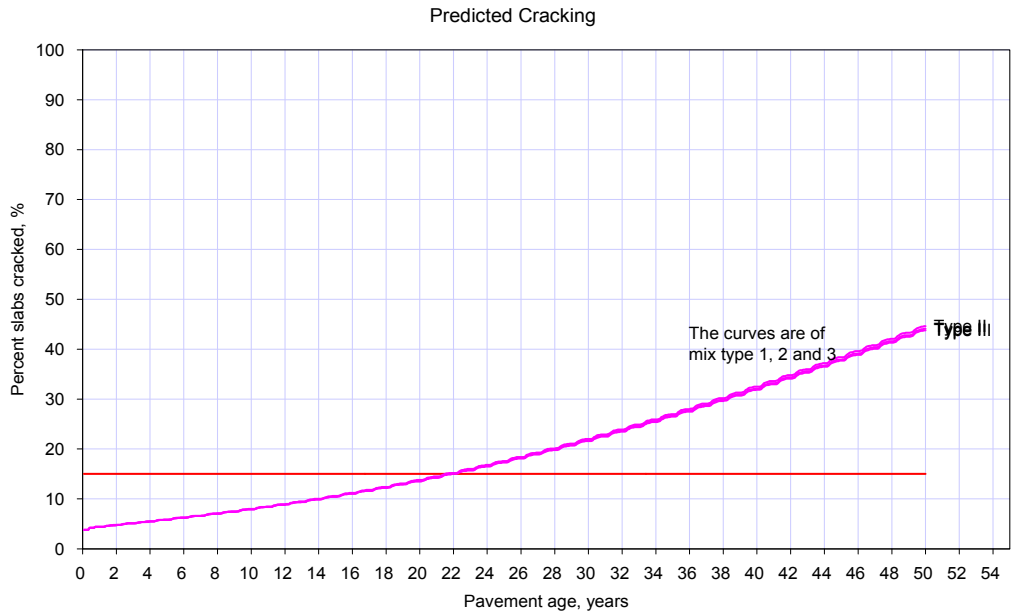
Predicted Cracking
Percent slabs cracked, %
Pavement age, years
The curves are of
mix type 1, 2 and 3
Type III

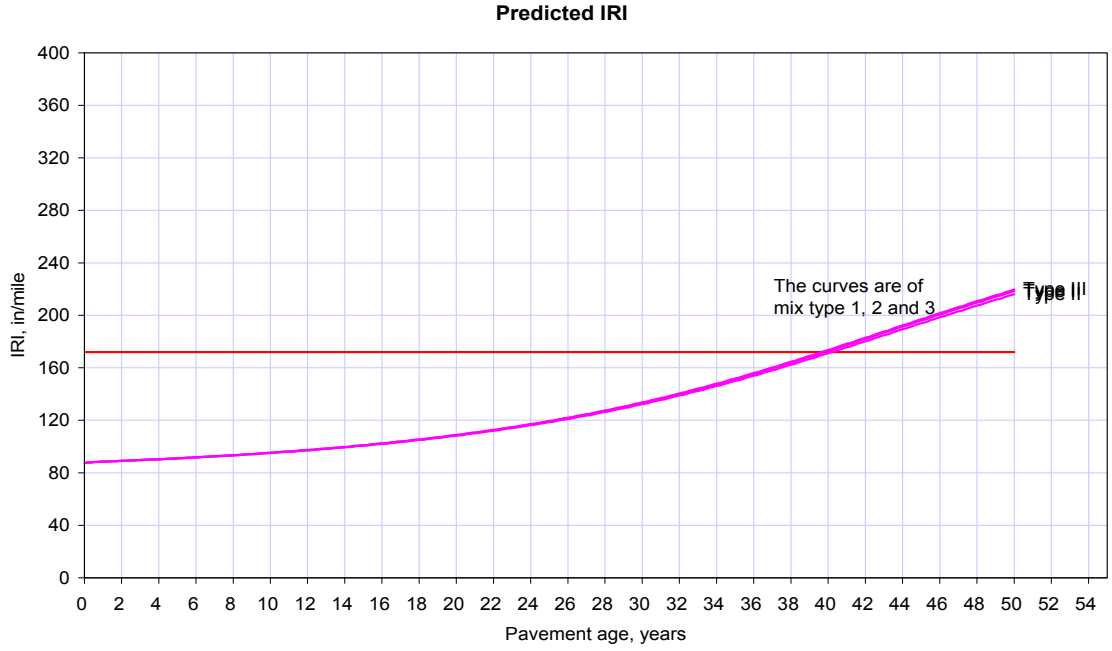
Predicted IRI
IRI, in/mile
Pavement age, years
The curves are of
mix type 1, 2 and 3
Type III

A5.8 Cementitious Material Content (lb/yd^3)

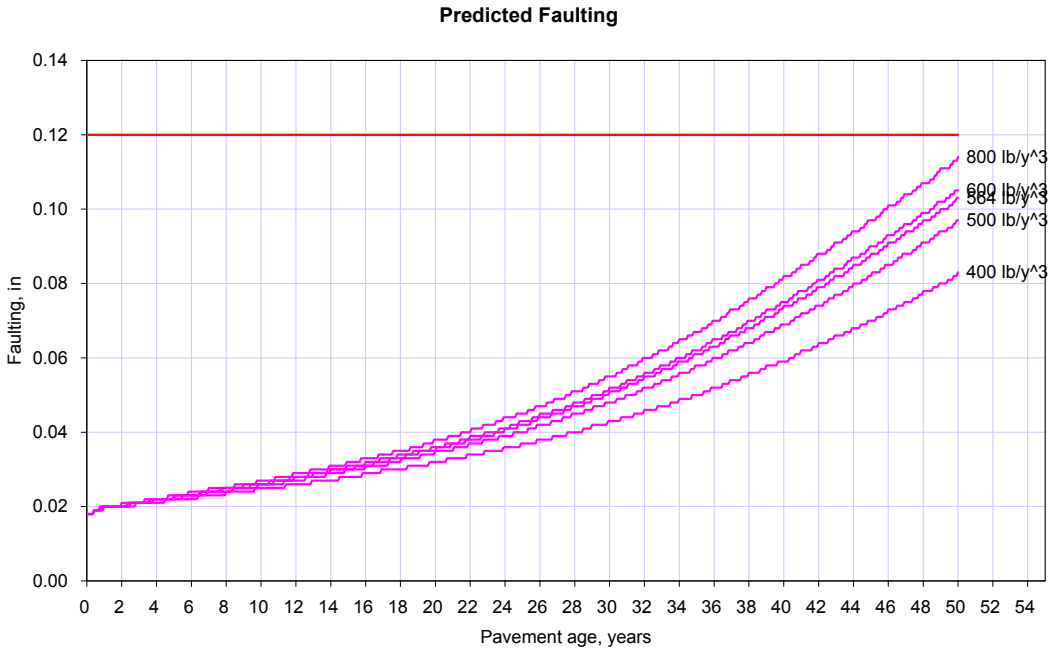

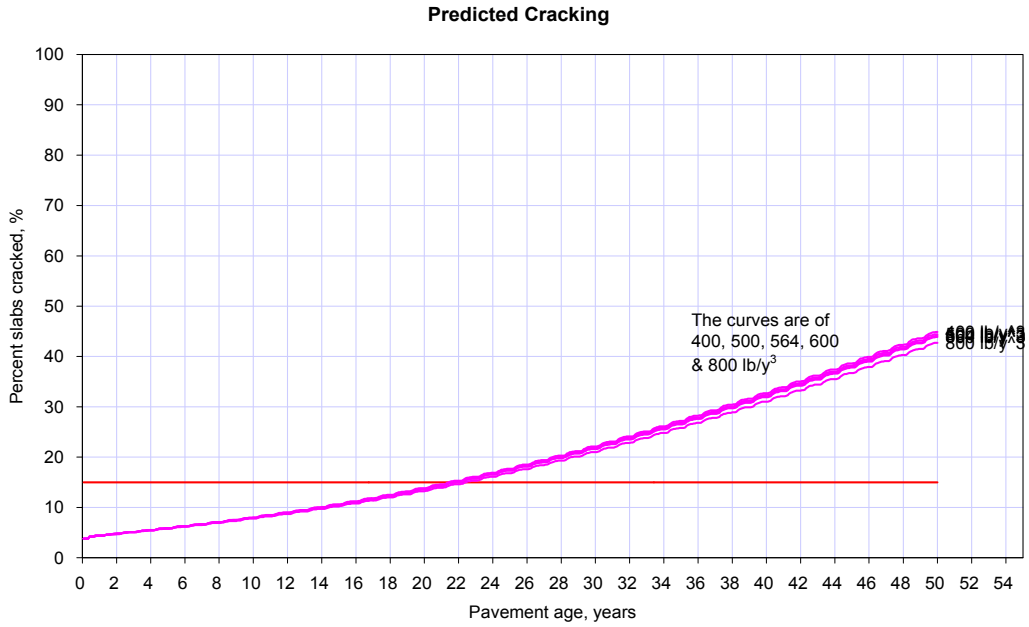

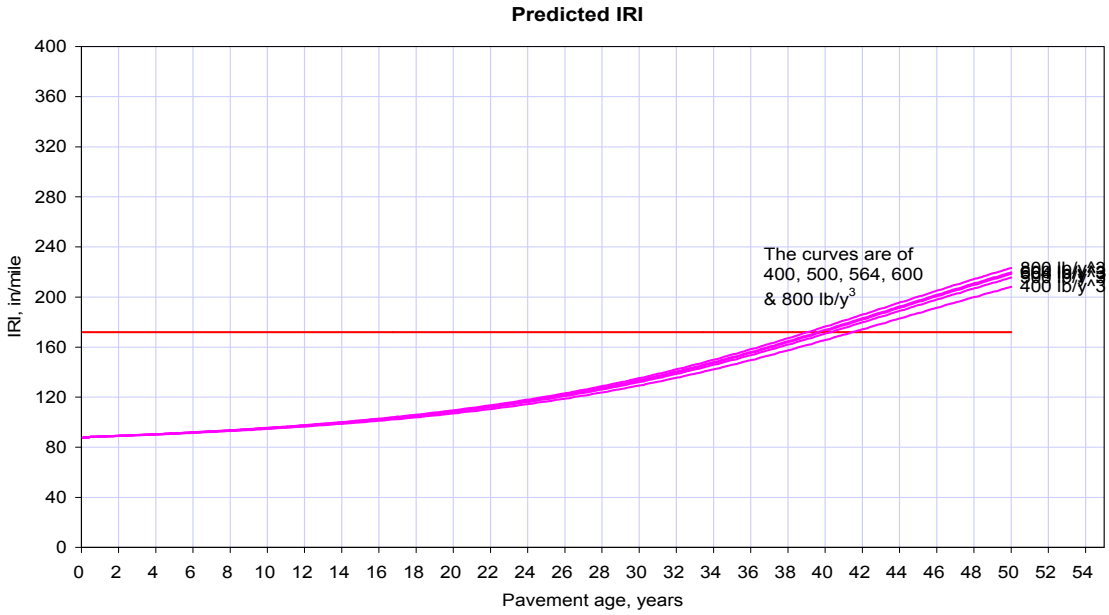

A5.9 Water/Cement Ratio

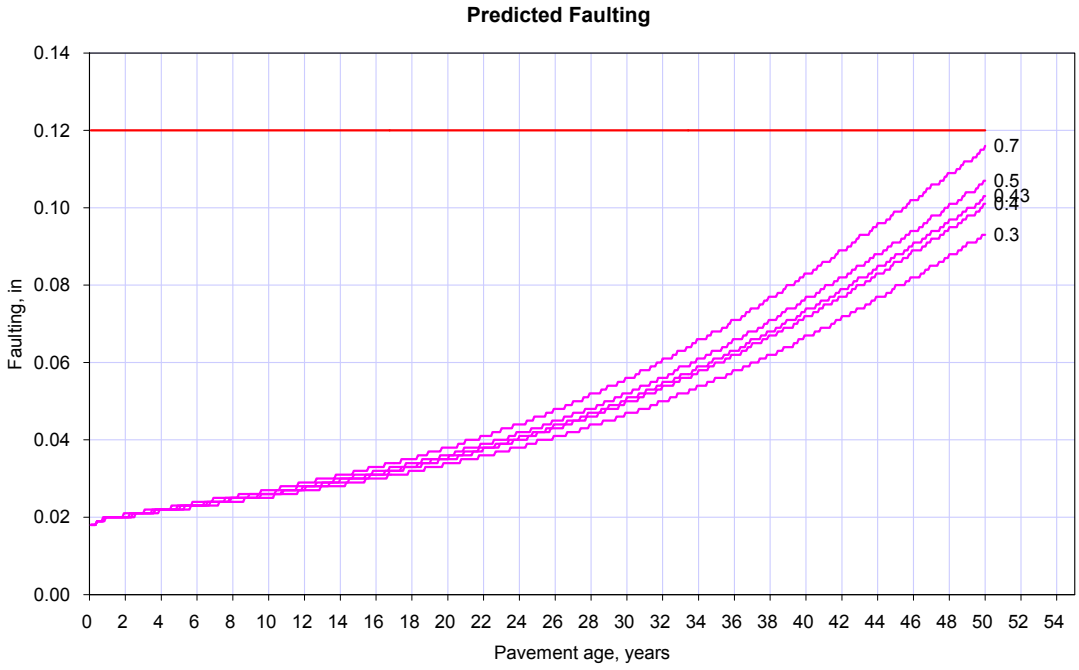

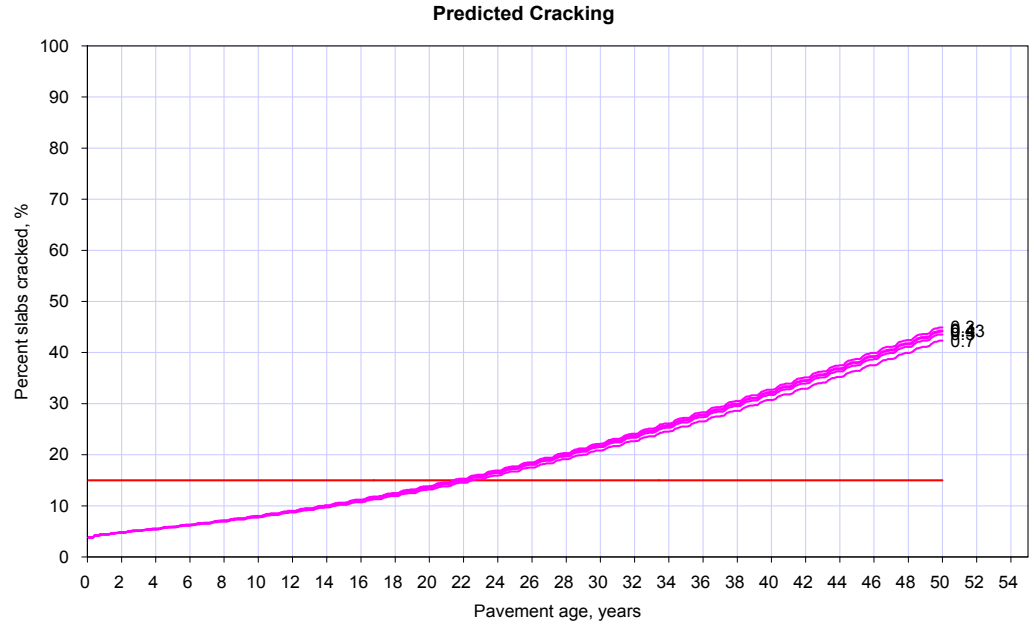
Predicted Cracking
Percent slabs cracked, %
Pavement age, years
0 2 4 6 8 10 12 14 16 18 20 22 24 26 28 30 32 34 36 38 40 42 44 46 48 50 52 54
0 10 20 30 40 50 60 70 80 90 100

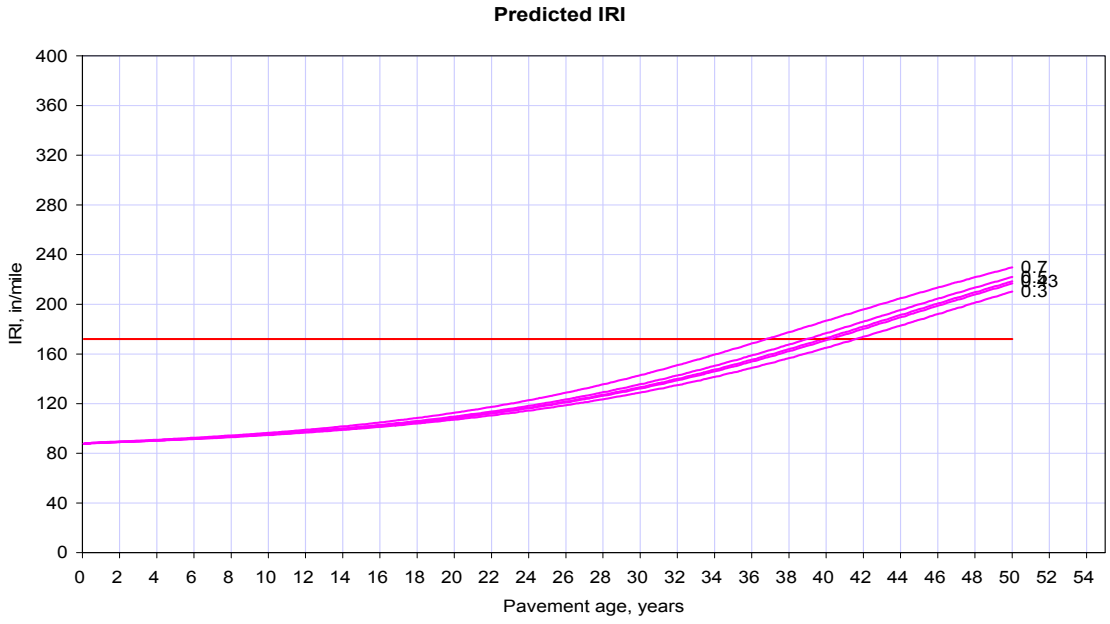
Predicted IRI
IRI, in/mile
Pavement age, years
0 2 4 6 8 10 12 14 16 18 20 22 24 26 28 30 32 34 36 38 40 42 44 46 48 50 52 54
0 40 80 120 160 200 240 280 320 360 400

A5.10 Aggregate Type

Different aggregate types were used in the given range to analyze this parameter. Those types are Limestone, Dolomite, Granite, Quartzite, Rhyolite, Basalt, Cynetite, Gabbro and Chert. Following is the detailed output for all these aggregate types.

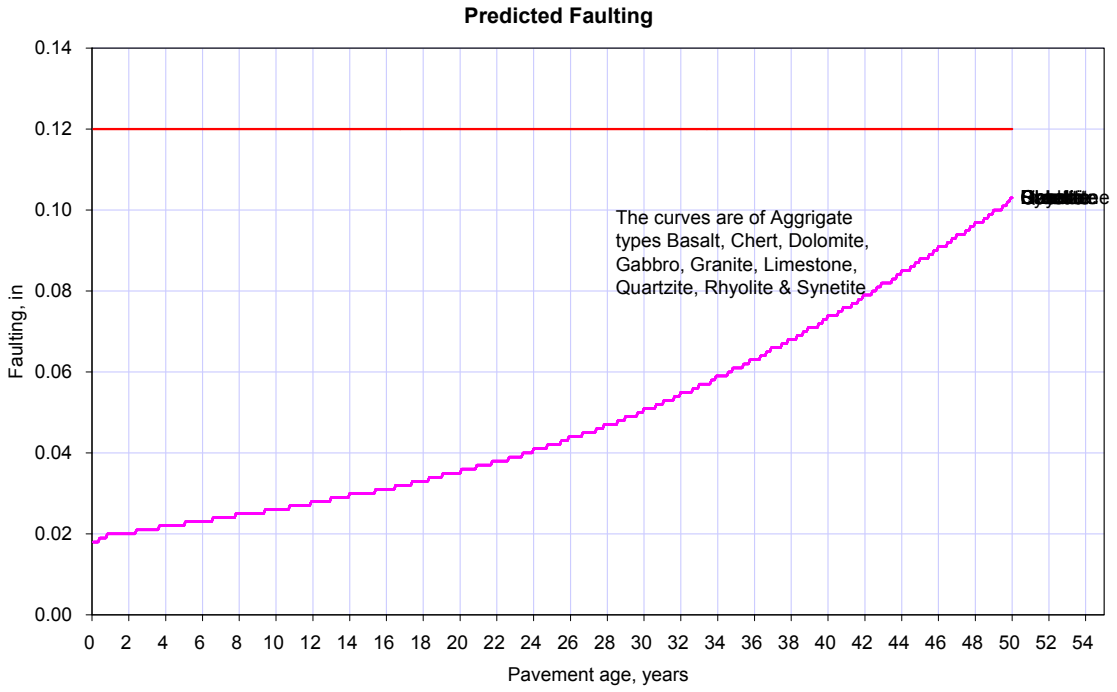

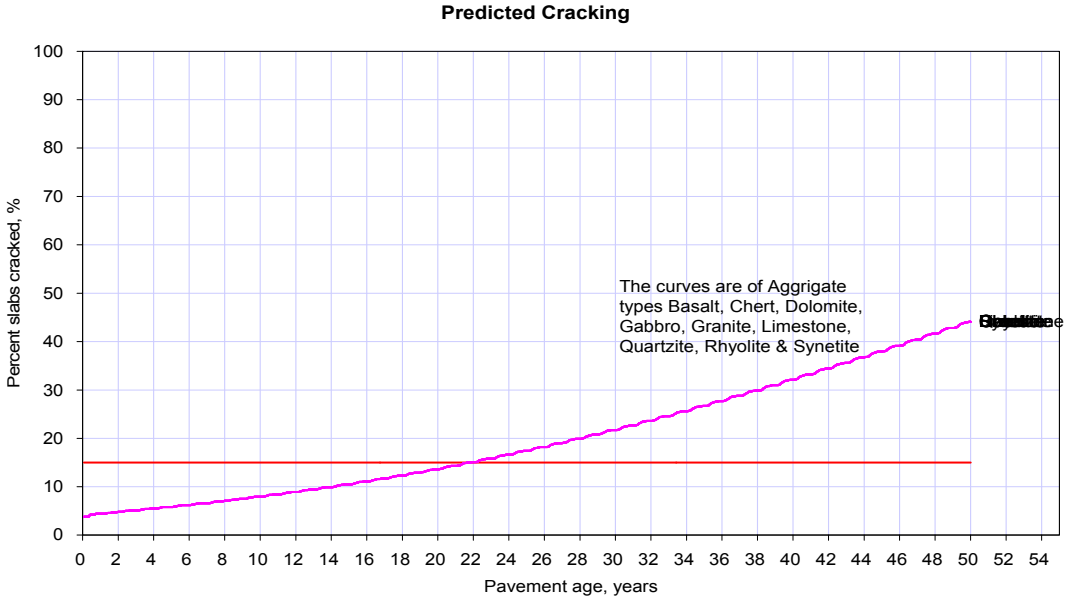

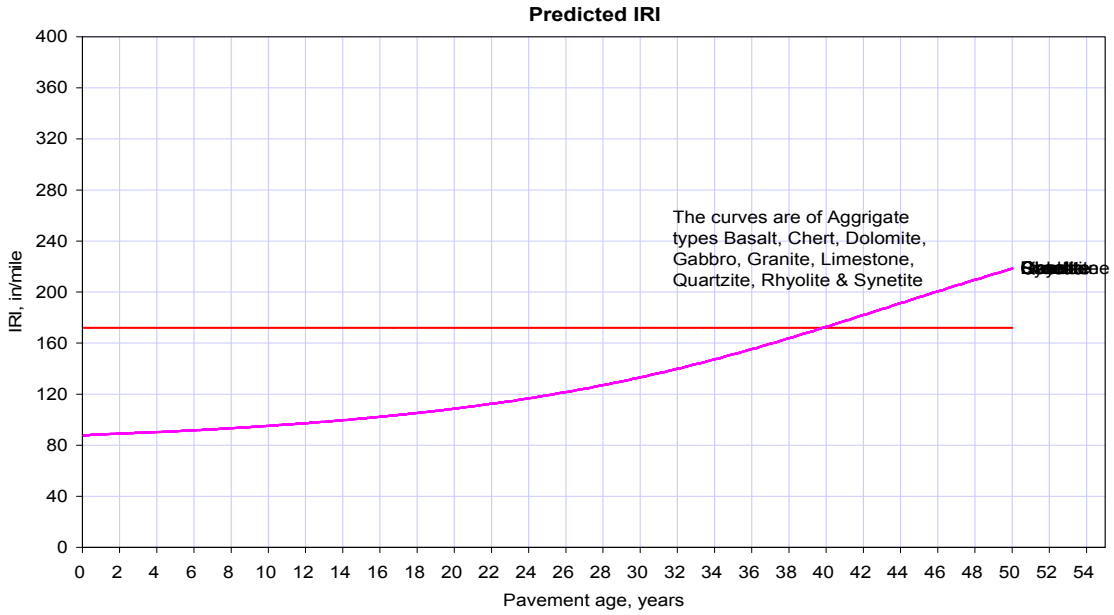
Predicted IRI
IRI, in/mile
Pavement age, years
The curves are of Aggrigate types Basalt, Chert, Dolomite, Gabbro, Granite, Limestone, Quartzite, Rhyolite & Synetite
0
40
80
120
160
200
240
280
320
360
400
0 2 4 6 8 10 12 14 16 18 20 22 24 26 28 30 32 34 36 38 40 42 44 46 48 50 52 54

A5.11 Reversible Shrinkage (% of Ultimate Shrinkage)

This is the percentage of the ultimate shrinkage that is reversible in the concrete up on rewetting. A value of 50 percent is typically used for this parameter.

Different values from the given range were used to analyze this parameter. These values are 30%, 50%, 55% and 80%.

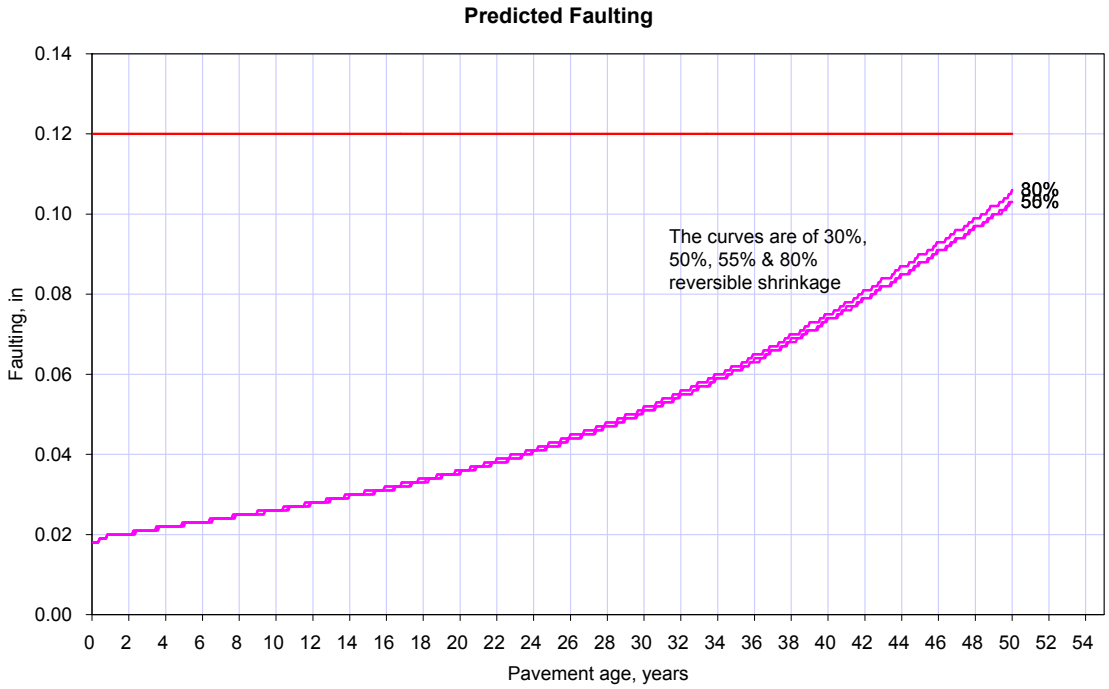

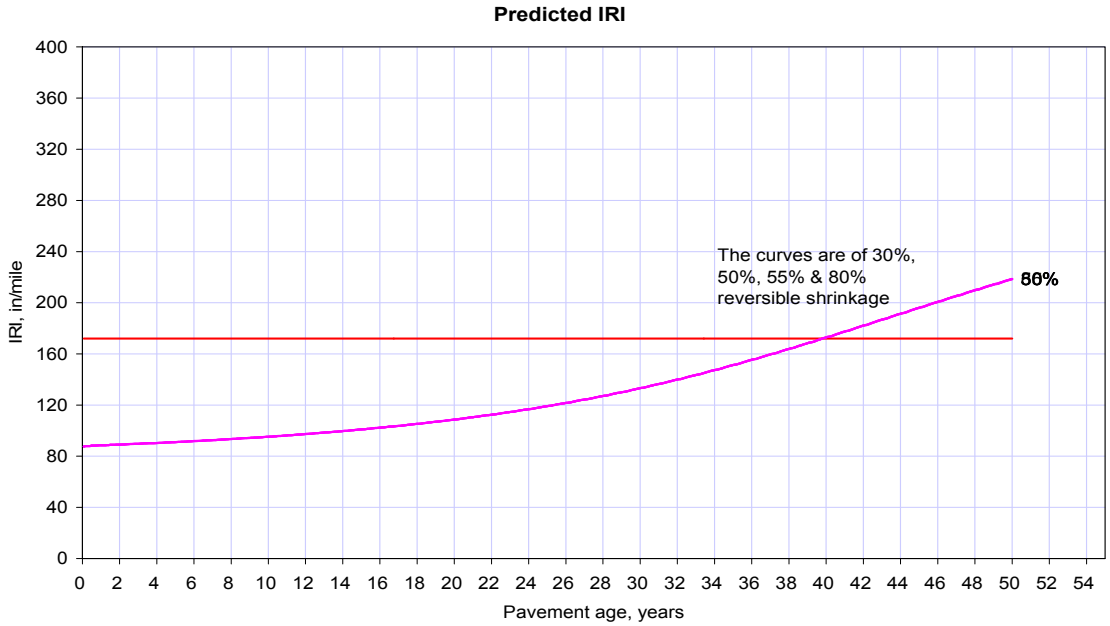
Predicted IRI
IRI, in/mile
400
360
320
280
240
200
160
120
80
40
0
0 2 4 6 8 10 12 14 16 18 20 22 24 26 28 30 32 34 36 38 40 42 44 46 48 50 52 54
Pavement age, years
The curves are of 30%, 50%, 55% & 80% reversible shrinkage
80%

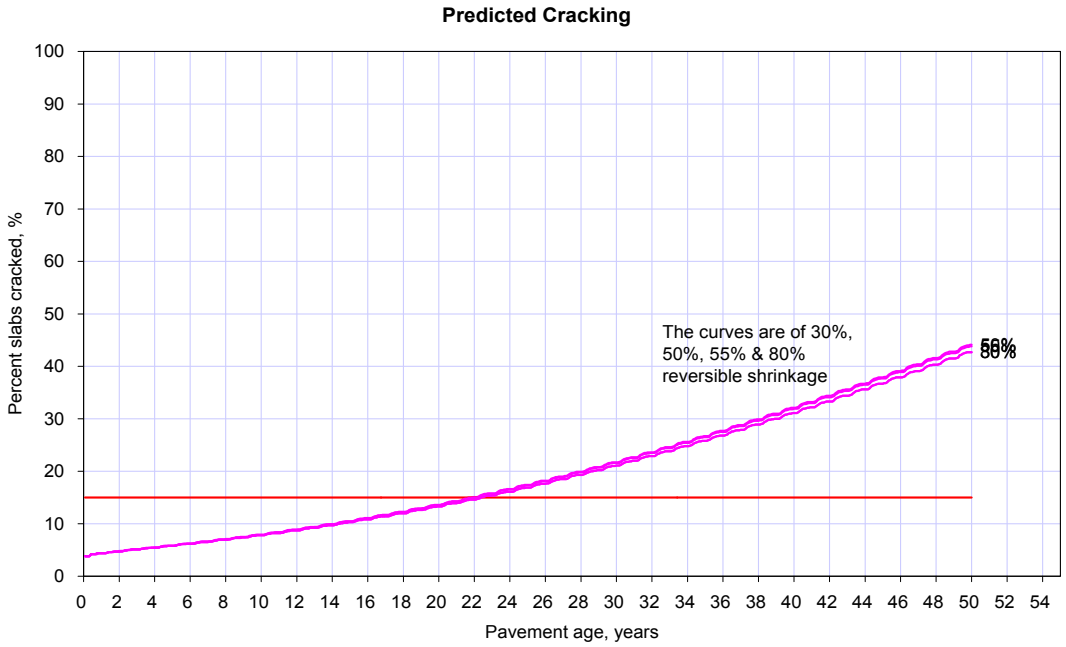
Predicted Cracking
Percent slabs cracked, %
100
90
80
70
60
50
40
30
20
10
0
0 2 4 6 8 10 12 14 16 18 20 22 24 26 28 30 32 34 36 38 40 42 44 46 48 50 52 54
Pavement age, years
The curves are of 30%, 50%, 55% & 80% reversible shrinkage
50%
80%

A5.12 Time to develop 50% of ultimate shrinkage (days)

This input refers to the time taken in days to attain 50 percent of the ultimate shrinkage at the standard RH conditions.

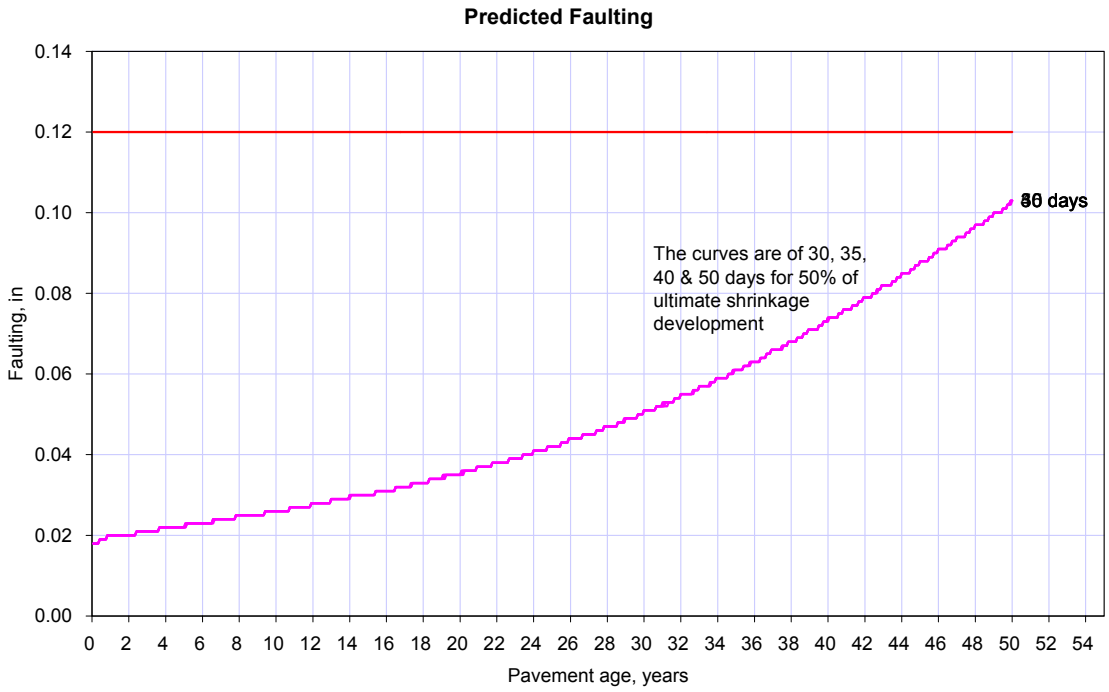

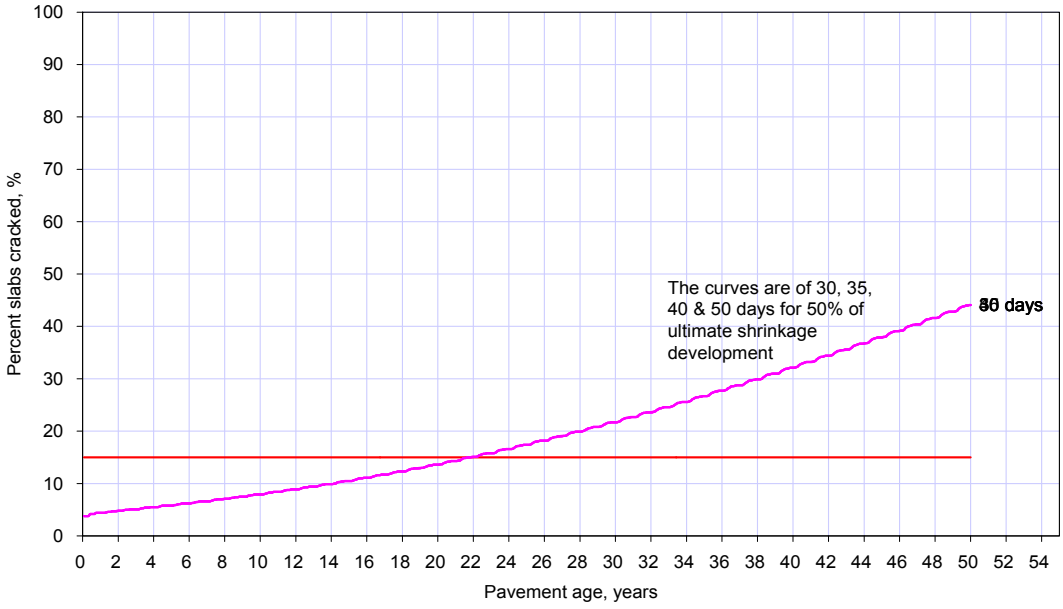

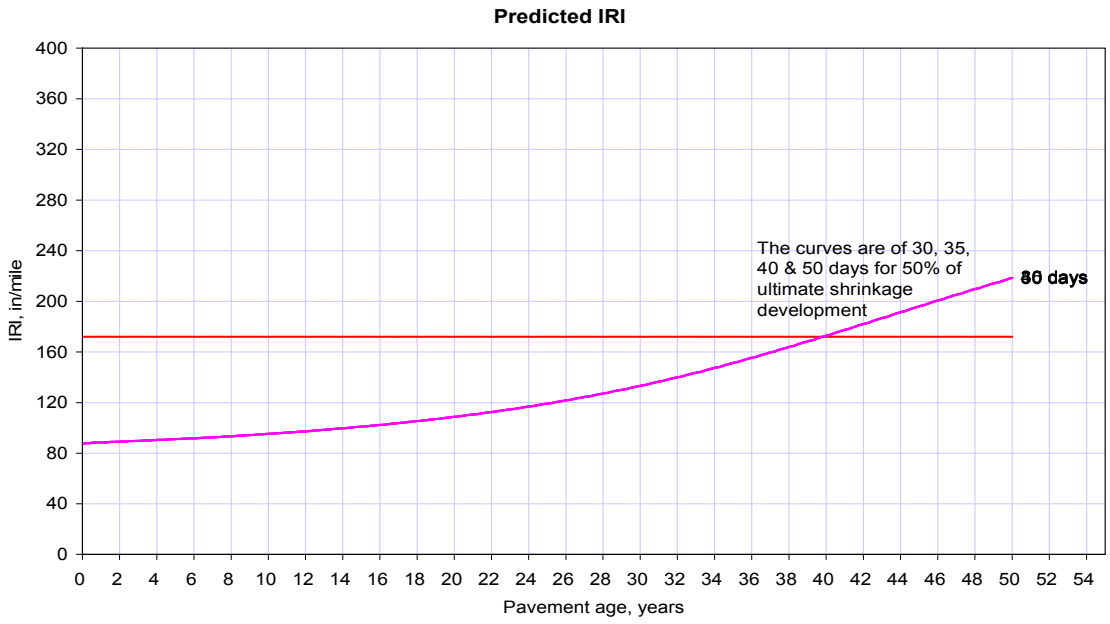
Predicted IRI
IRI, in/mile
400
360
320
280
240
200
160
120
80
40
0
0 2 4 6 8 10 12 14 16 18 20 22 24 26 28 30 32 34 36 38 40 42 44 46 48 50 52 54
Pavement age, years
The curves are of 30, 35, 40 & 50 days for 50% of ultimate shrinkage development
30 days

A5.13 Curing Method

Analyses were done to compare the two curing methods which are Curing compound and wet curing.

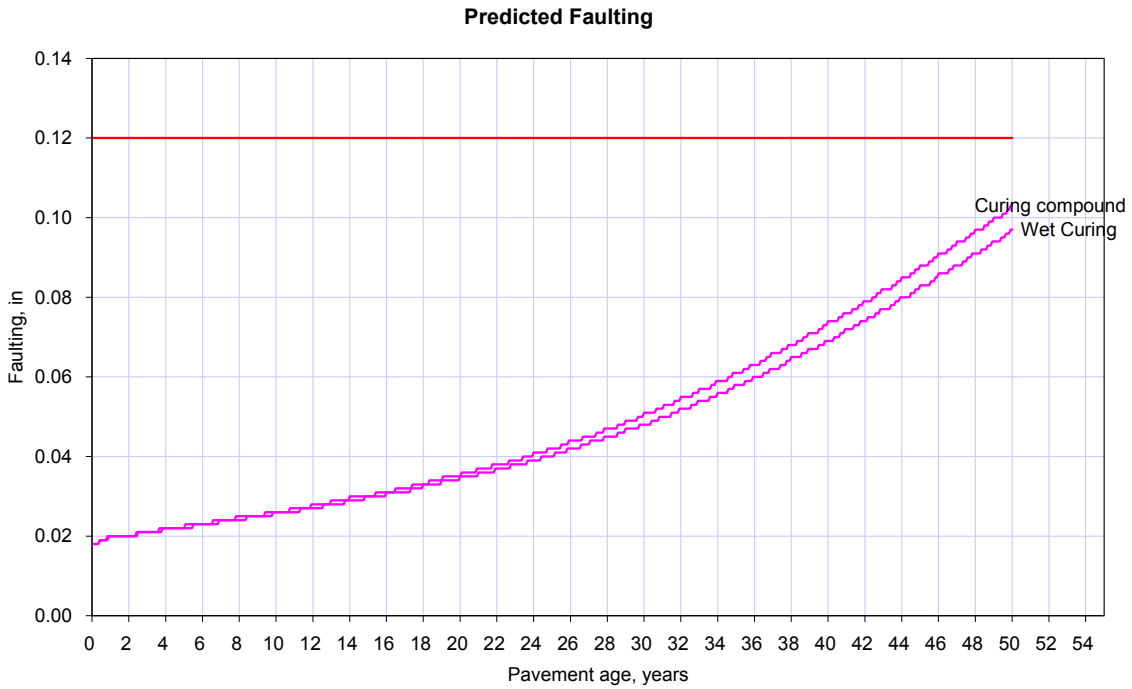

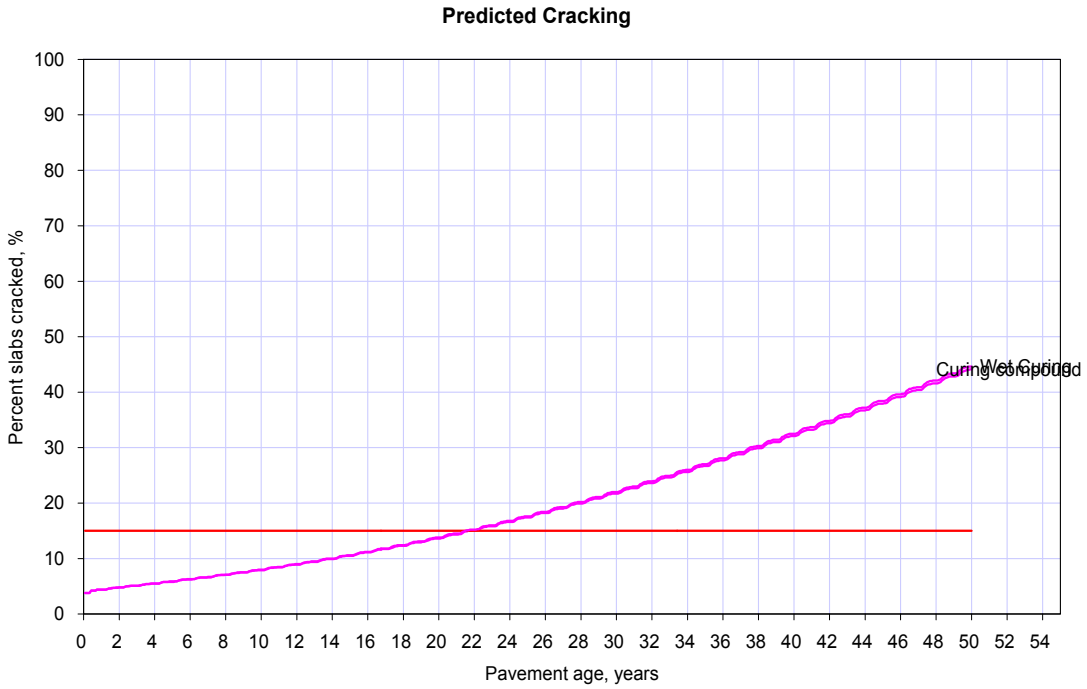
Predicted Cracking
Percent slabs cracked, %
Pavement age, years
Curing compound
Wet Curing

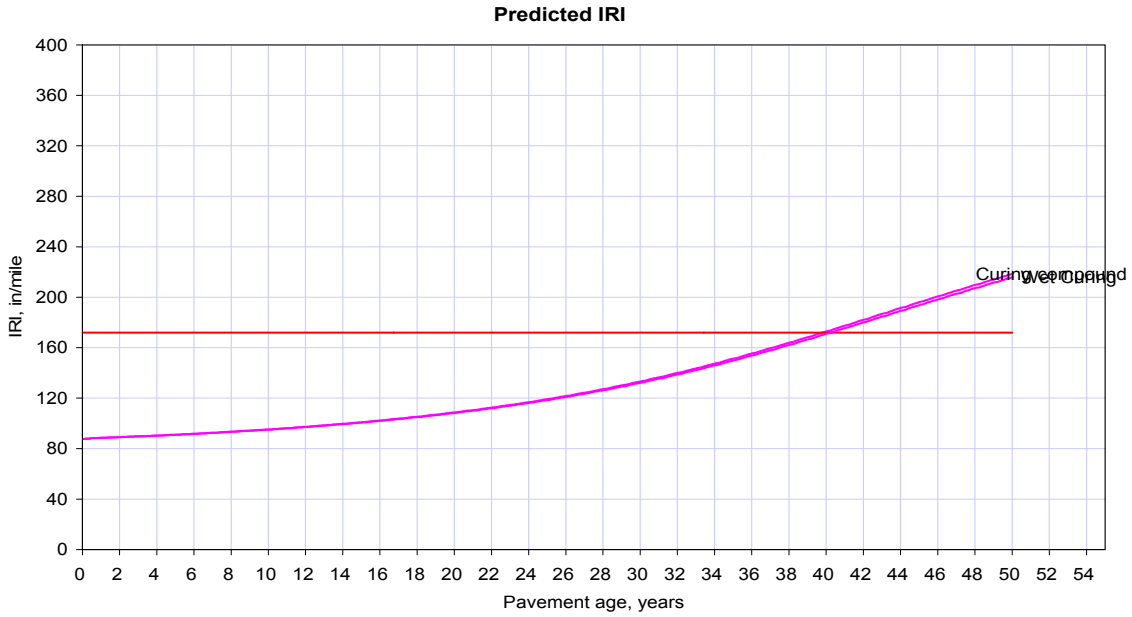
Predicted IRI
IRI, in/mile
Pavement age, years
Curing compound
Wet Curing

A5.14 Modulus of Elasticity

A5.14.1 7 day Modulus of Elasticity (psi)

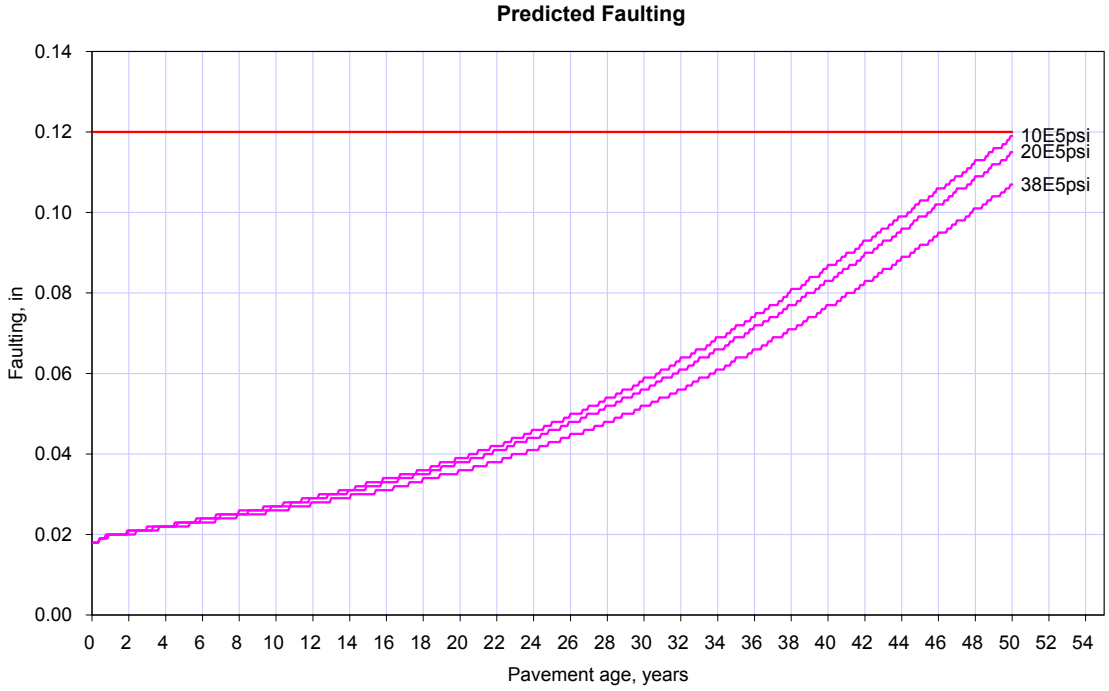

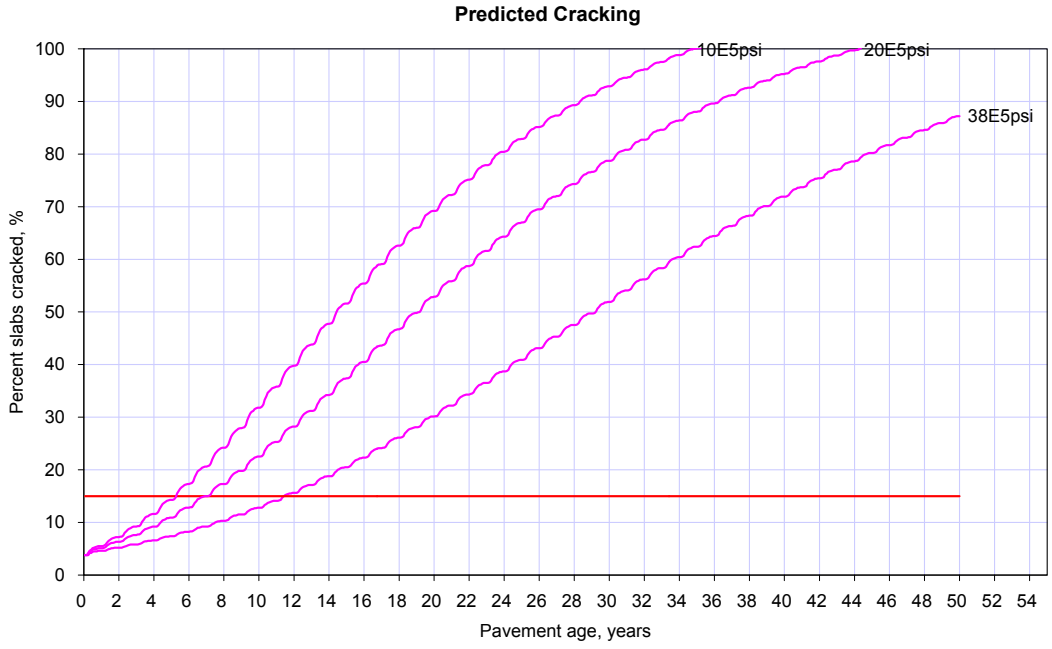

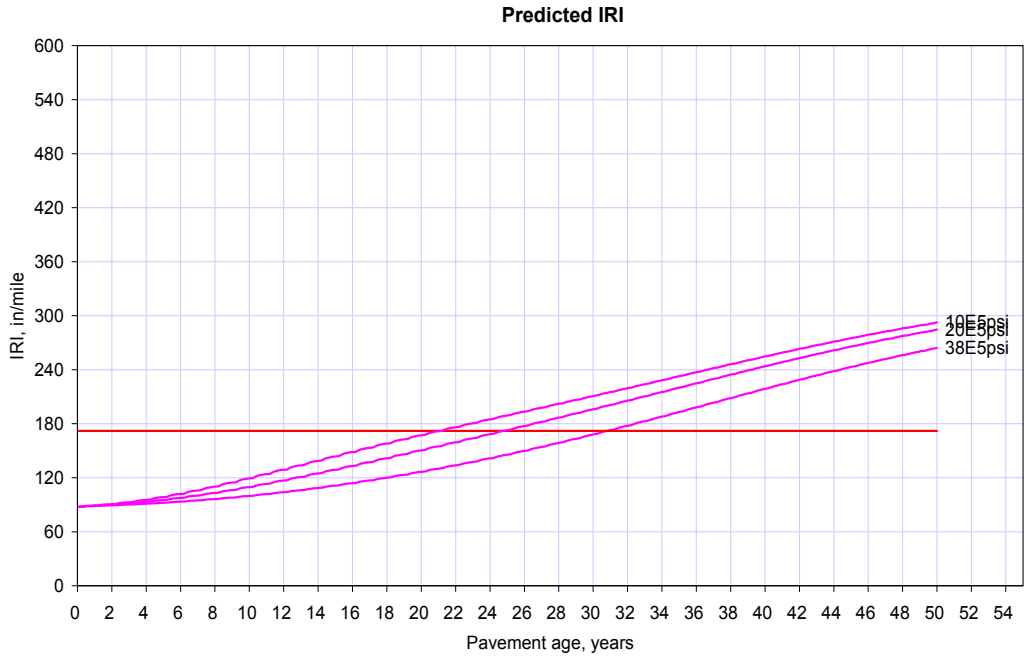

A5.14.2 28 day Modulus of Elasticity (psi)

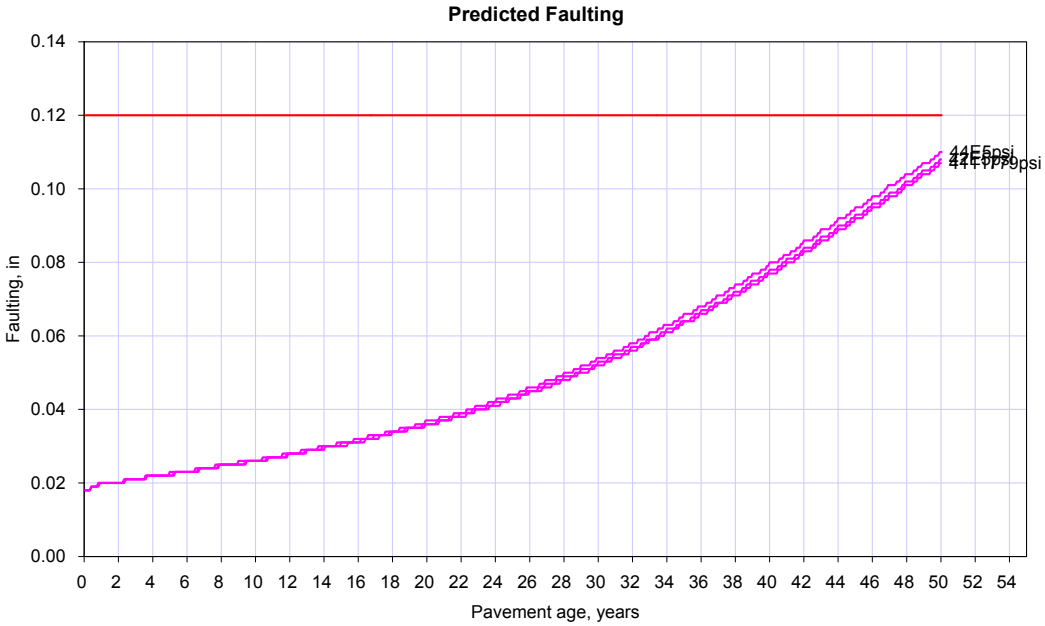

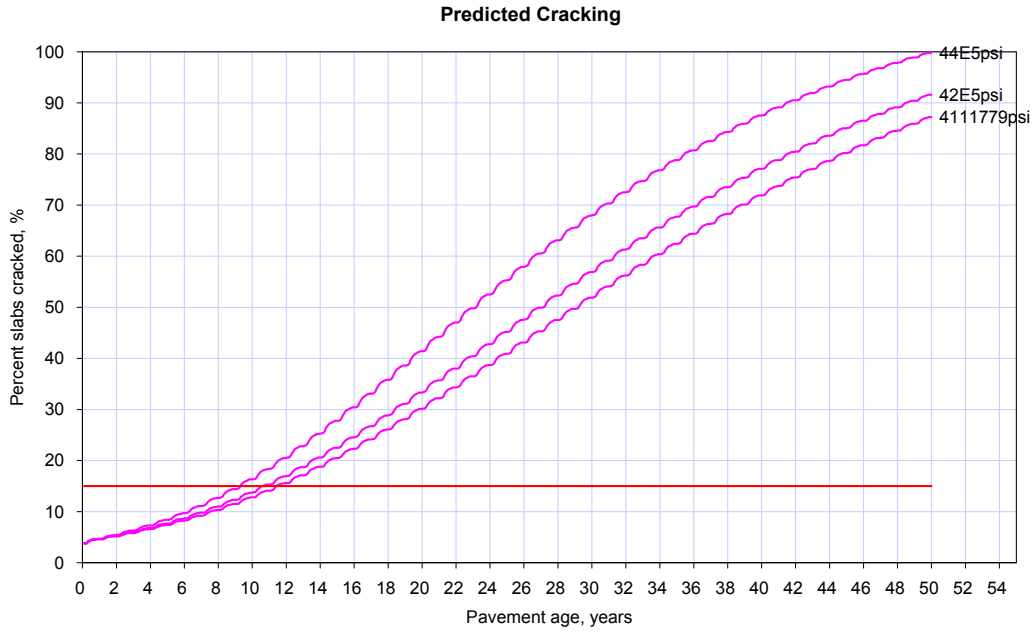
Predicted Cracking
Percent slabs cracked, %
Pavement age, years
44E5psi
42E5psi
4111779psi

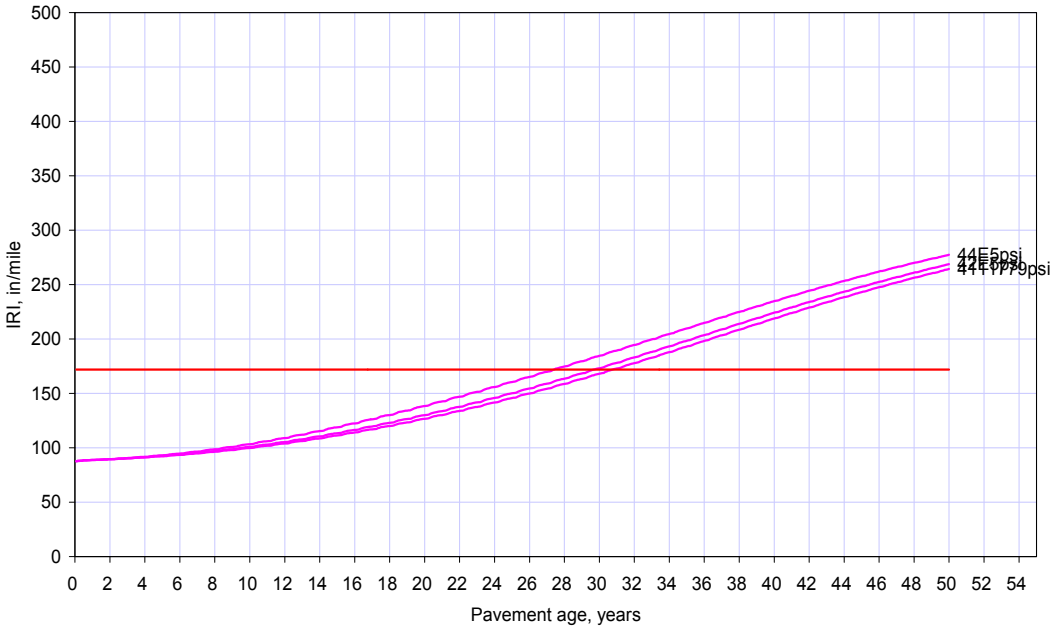
Predicted IRI
IRI, in/mile
Pavement age, years
44E5psi
4111779psi

A5.14.3 Ratio of 20-year to 28-day for Modulus of Elasticity

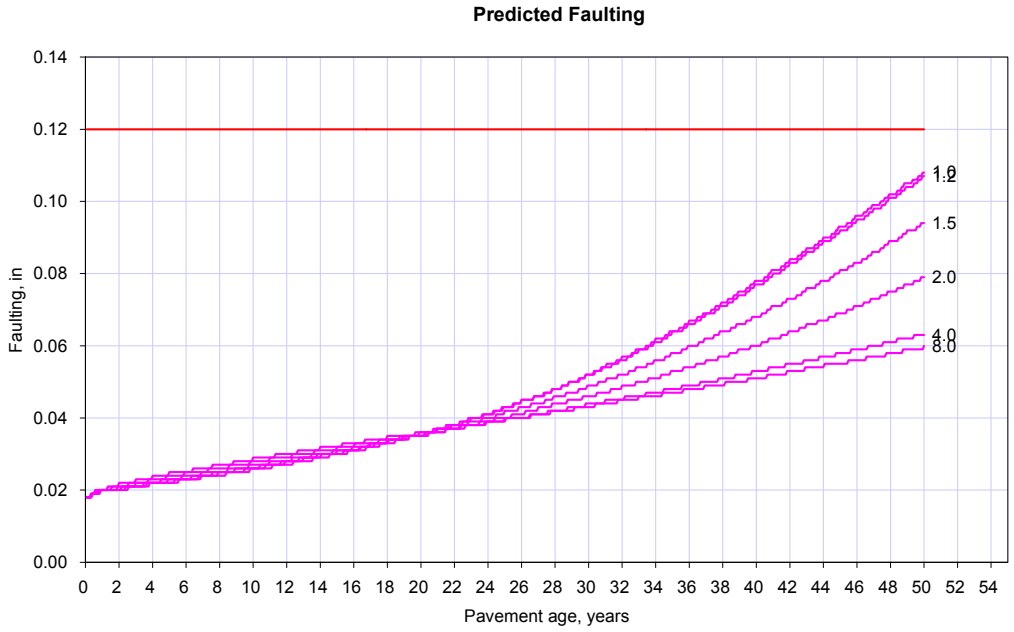

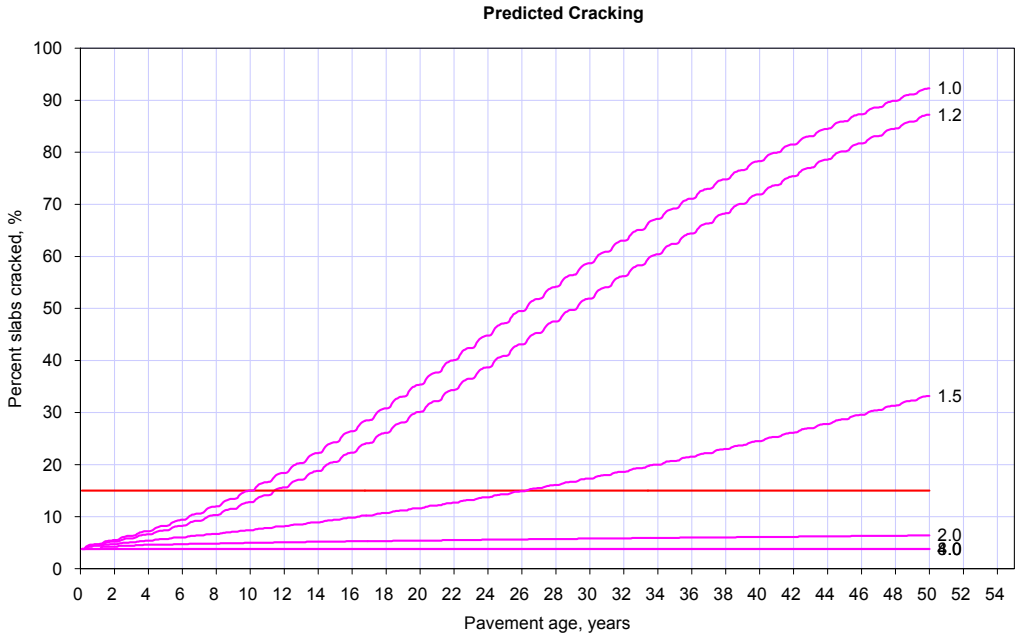

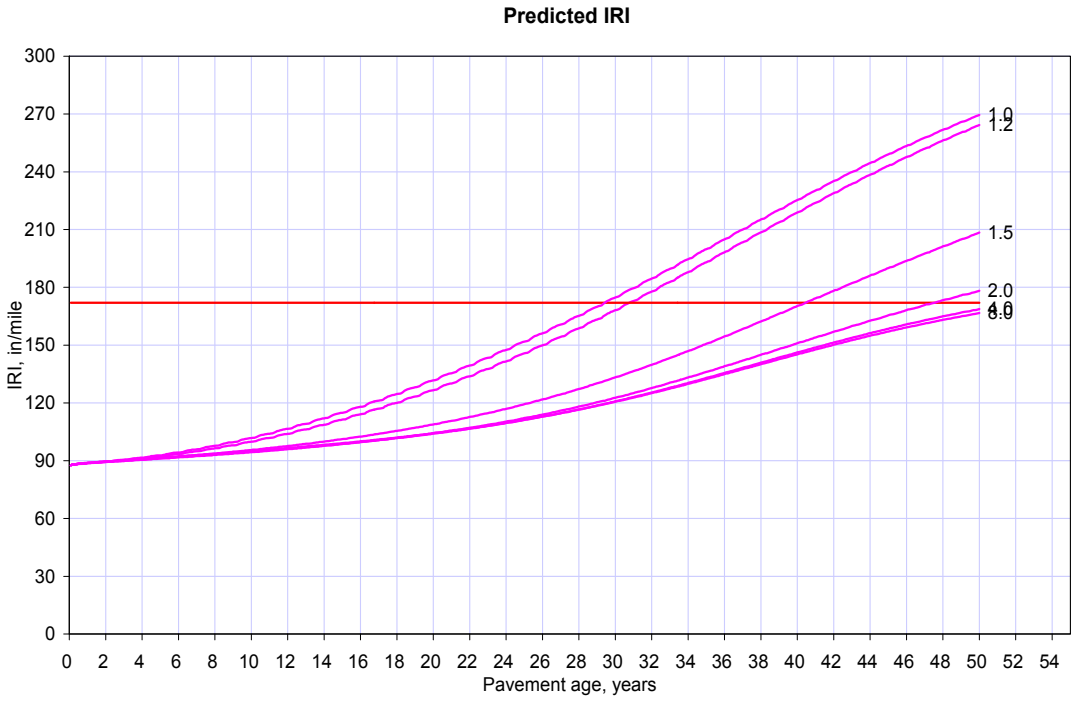
Predicted IRI
IRI, in/mile
Pavement age, years
1.0
1.2
1.5
2.0
4.0
6.0

A5.15 Rupture Modulus

A5.15.1 7 day Rupture Modulus (psi)

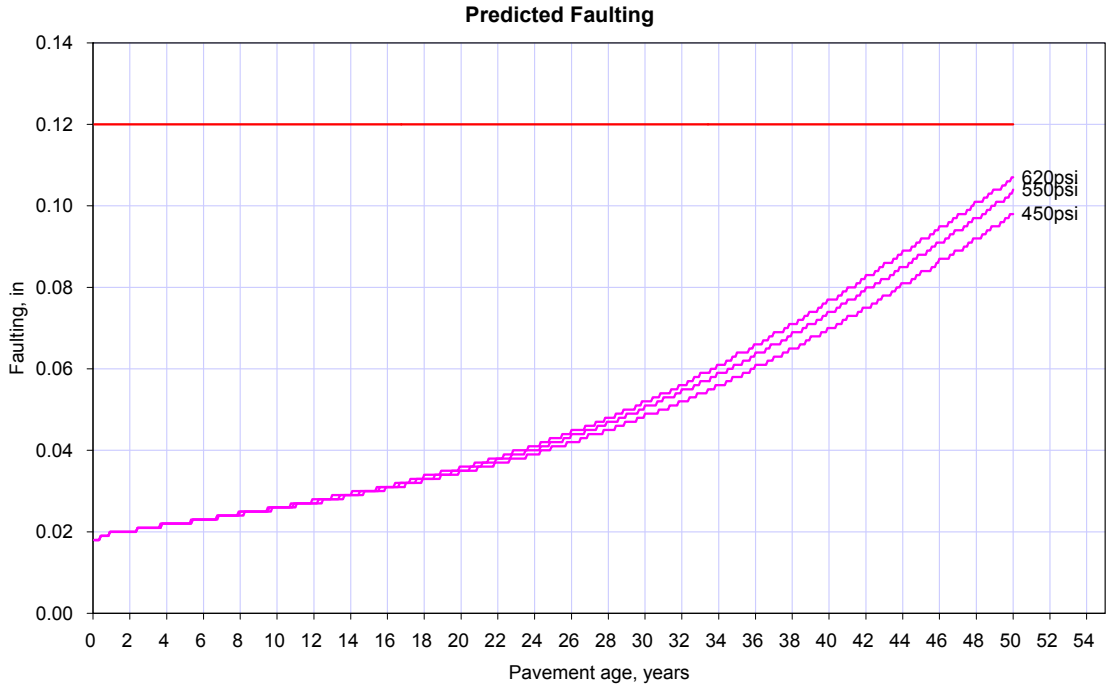

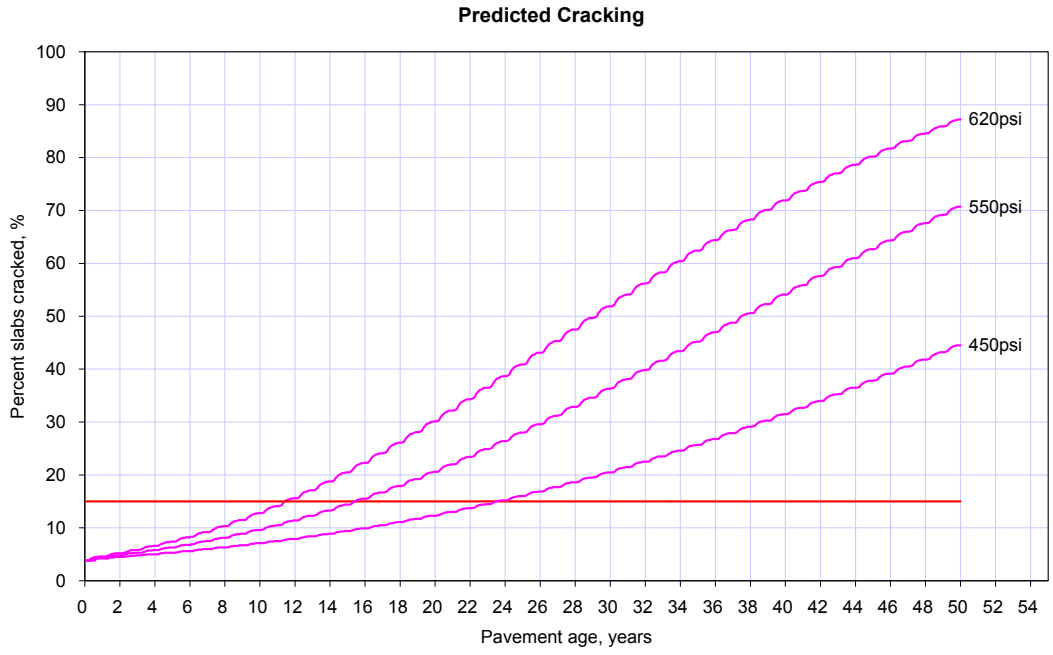

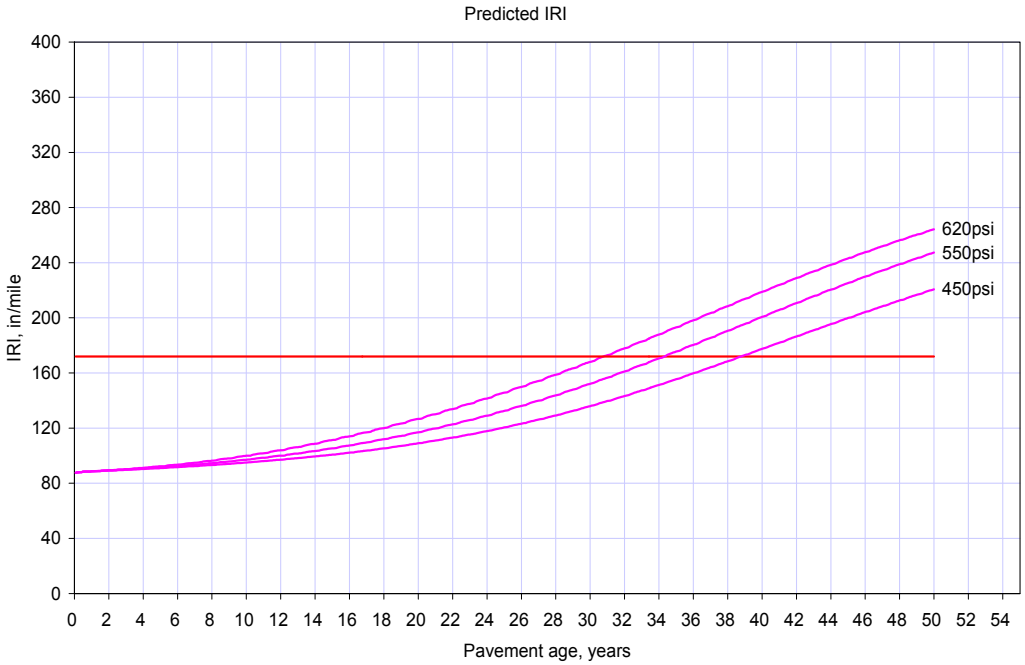

A5.15.2 Ratio of 20-year to 28-day for Rupture Modulus

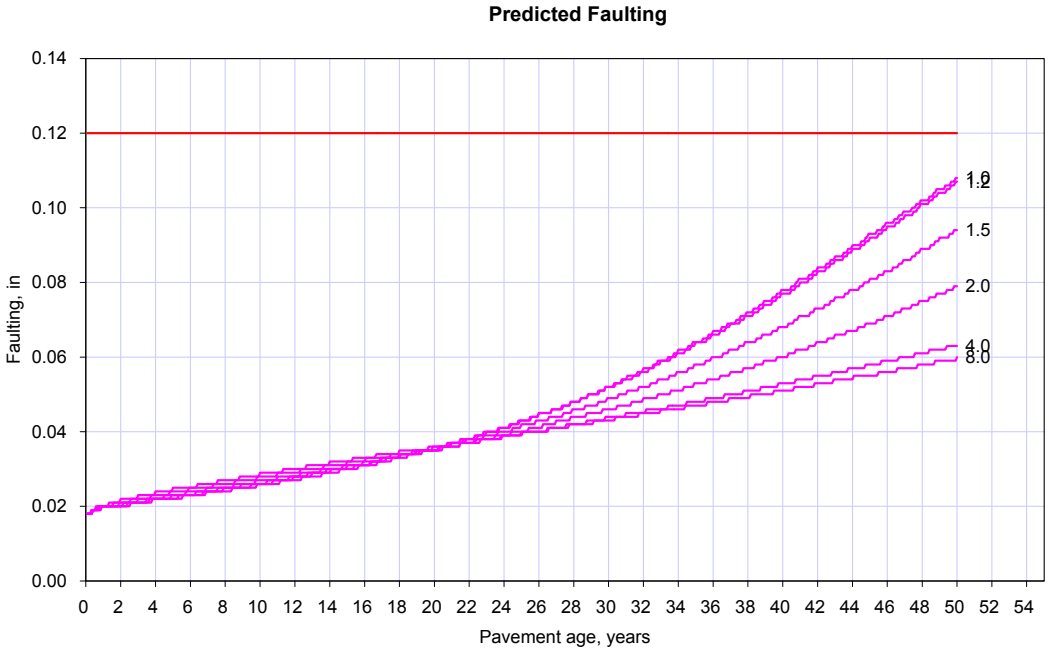

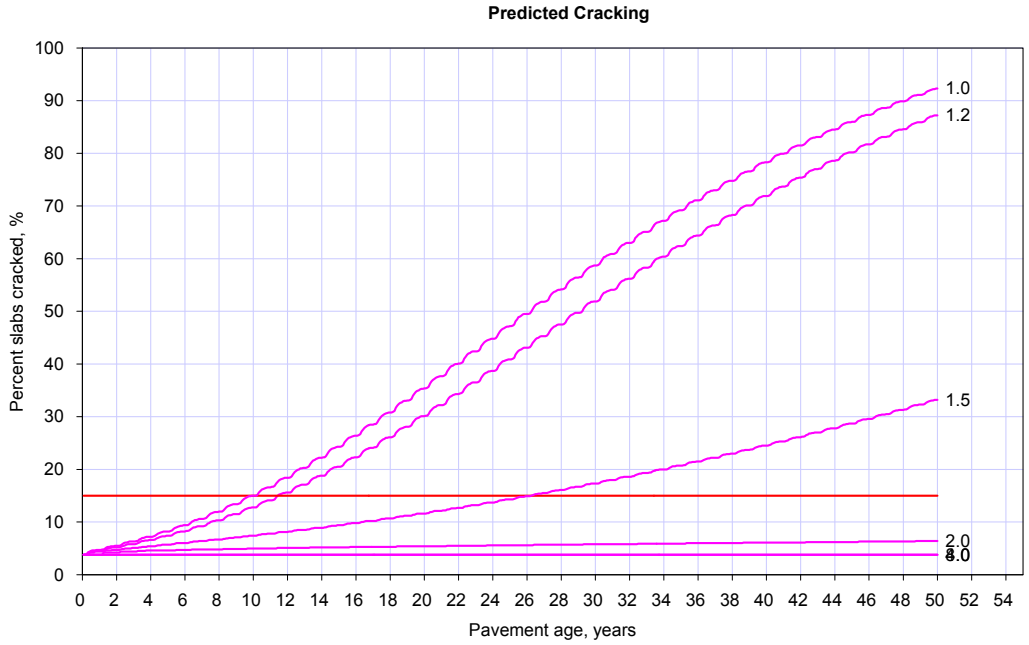
Predicted Cracking
Percent slabs cracked, %
Pavement age, years
1.0
1.2
1.5
2.0
3.0

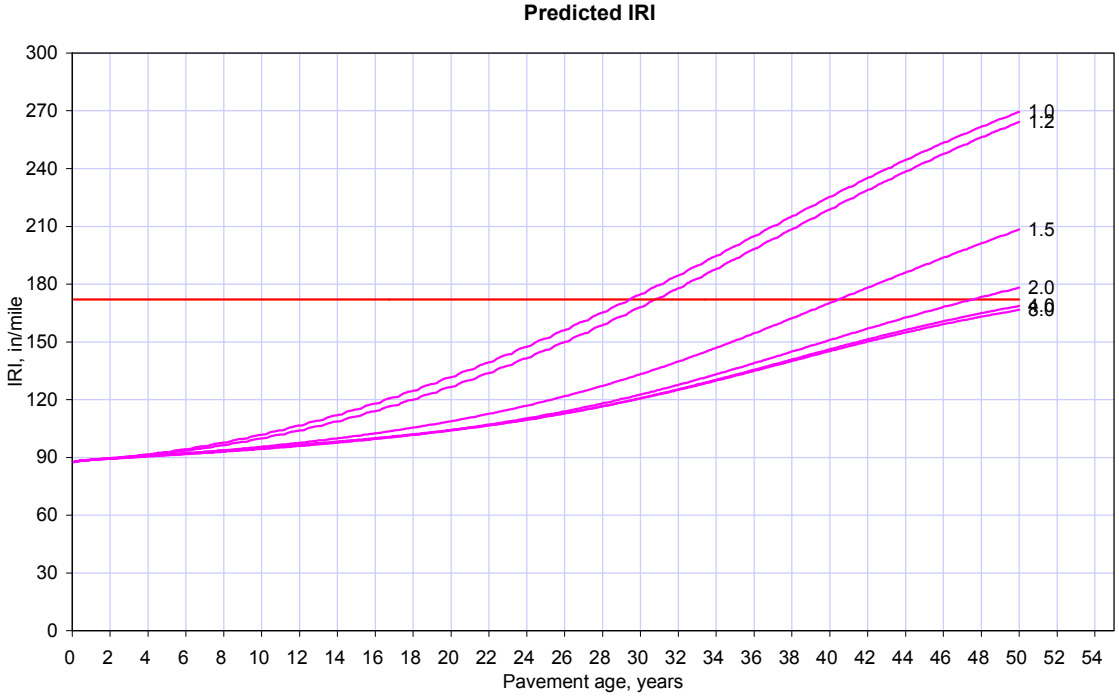
Predicted IRI
IRI, in/mile
Pavement age, years
1.0
1.2
1.5
2.0
3.0

A5.16 Compressive Strength (psi)

A5.16.1 7 day Compressive Strength (psi)

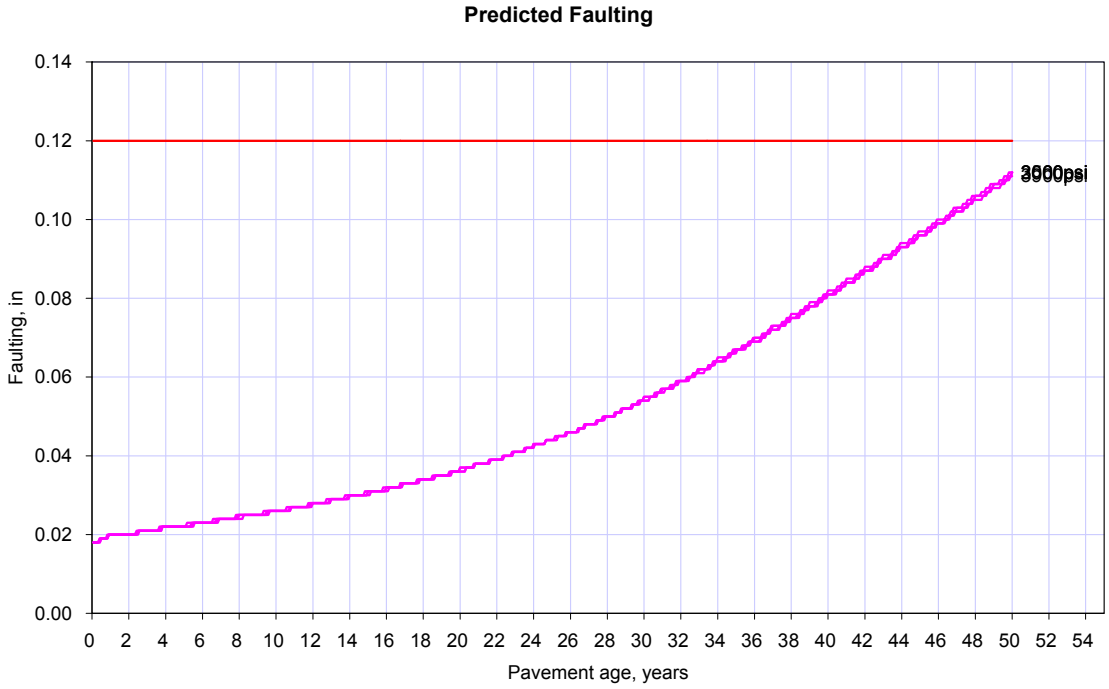

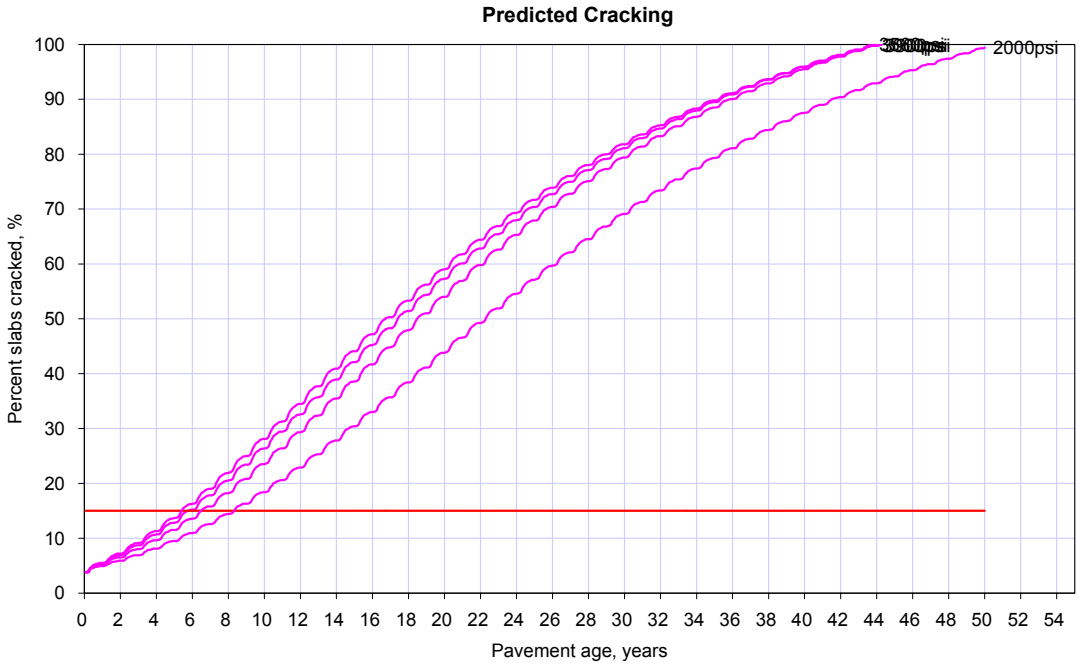

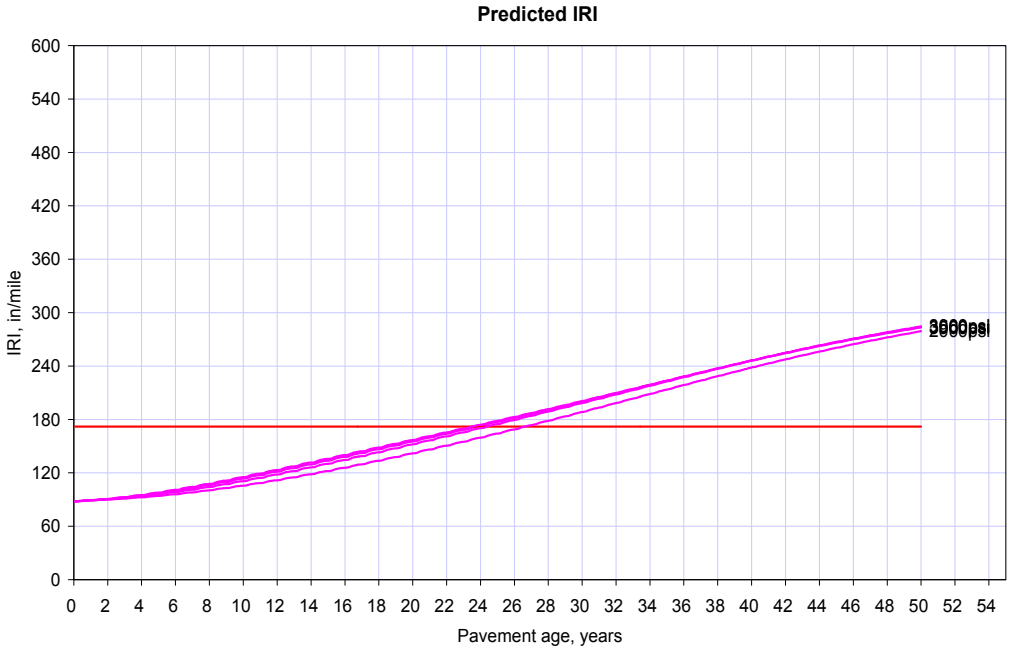

A5.16.2 28 day Compressive Strength (psi)

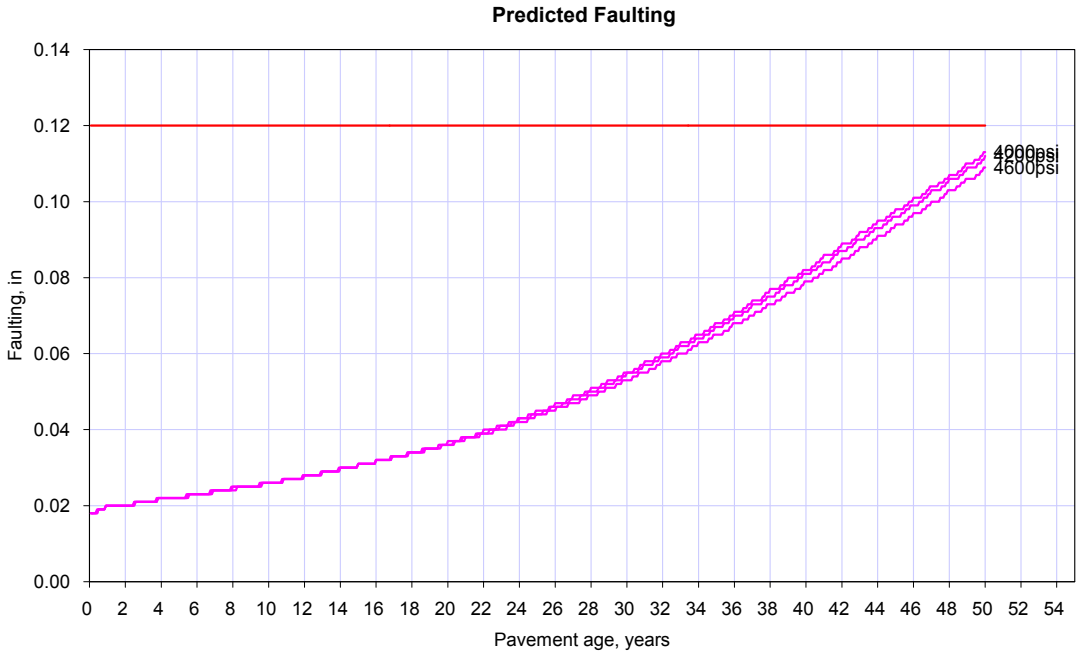

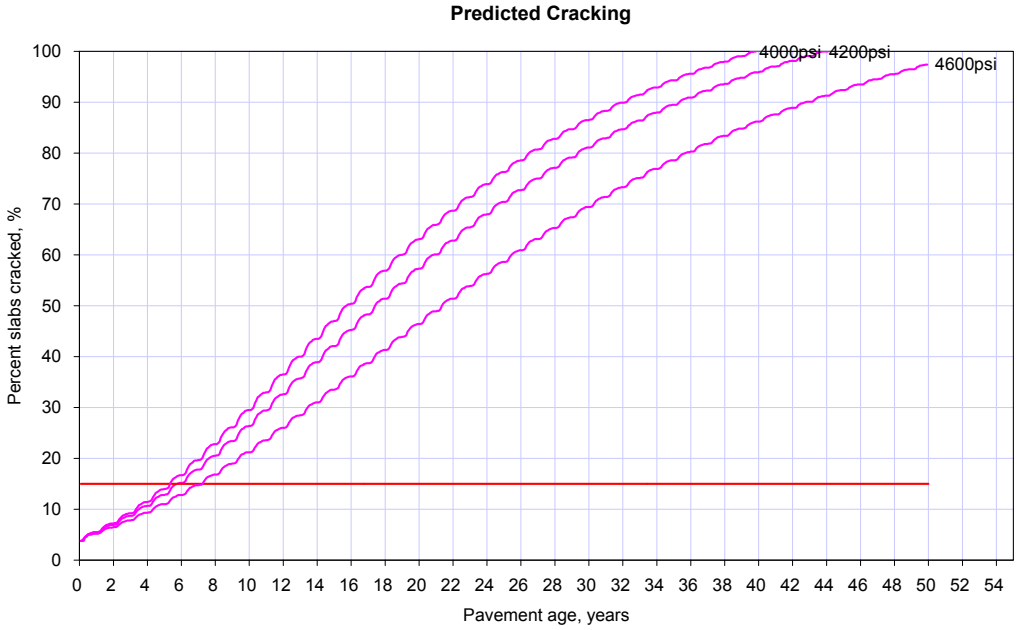
Predicted Cracking
Percent slabs cracked, %
Pavement age, years
4000psi
4200psi
4600psi

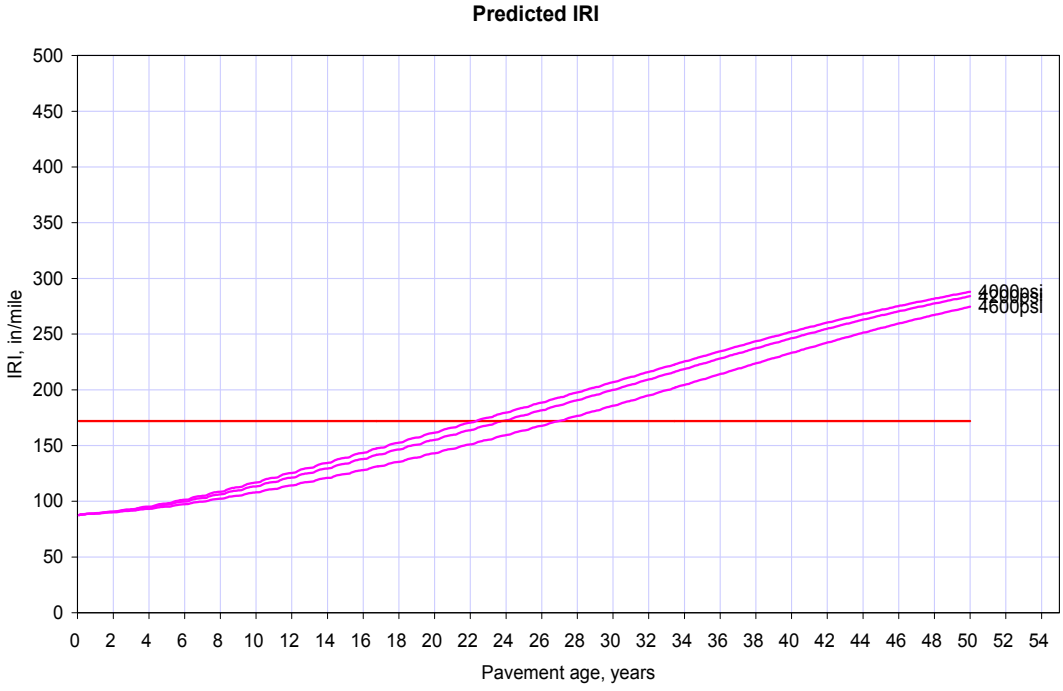
Predicted IRI
IRI, in/mile
Pavement age, years
4000psi
4200psi
4600psi

A5.16.3 Ratio of 20-year to 28-day for Compressive Strength

The expected long-term strength is to be specified as a ratio of the 20-year strength to the 28-day strength. A value of 1.44 is recommended for this ratio of long term to 28-day compressive strength.

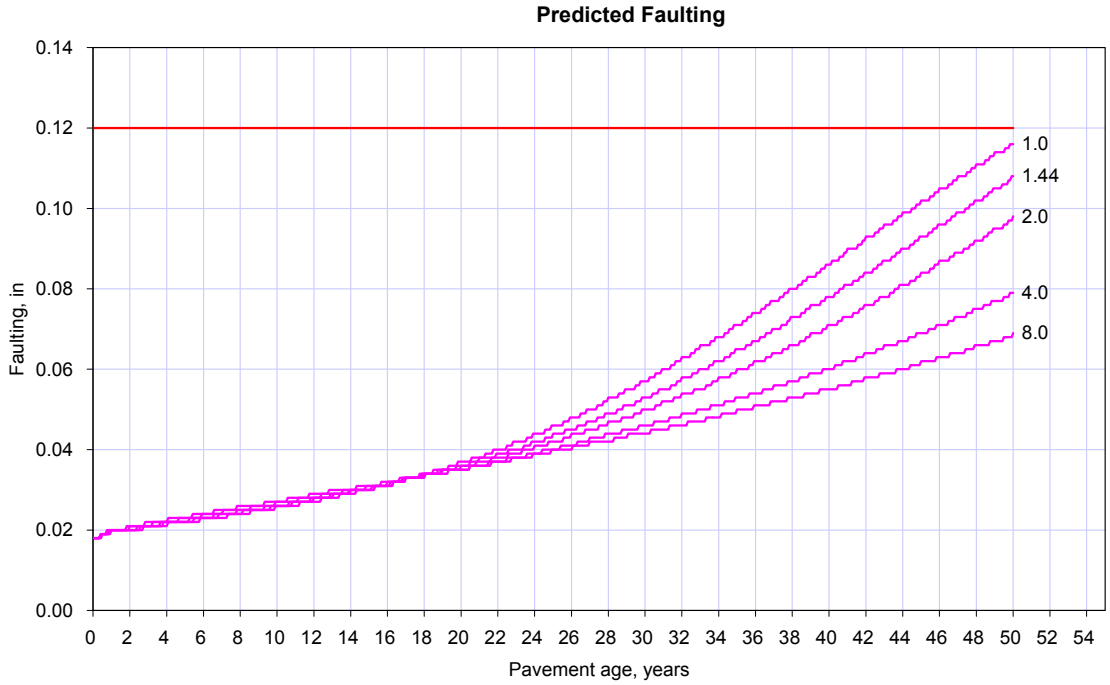

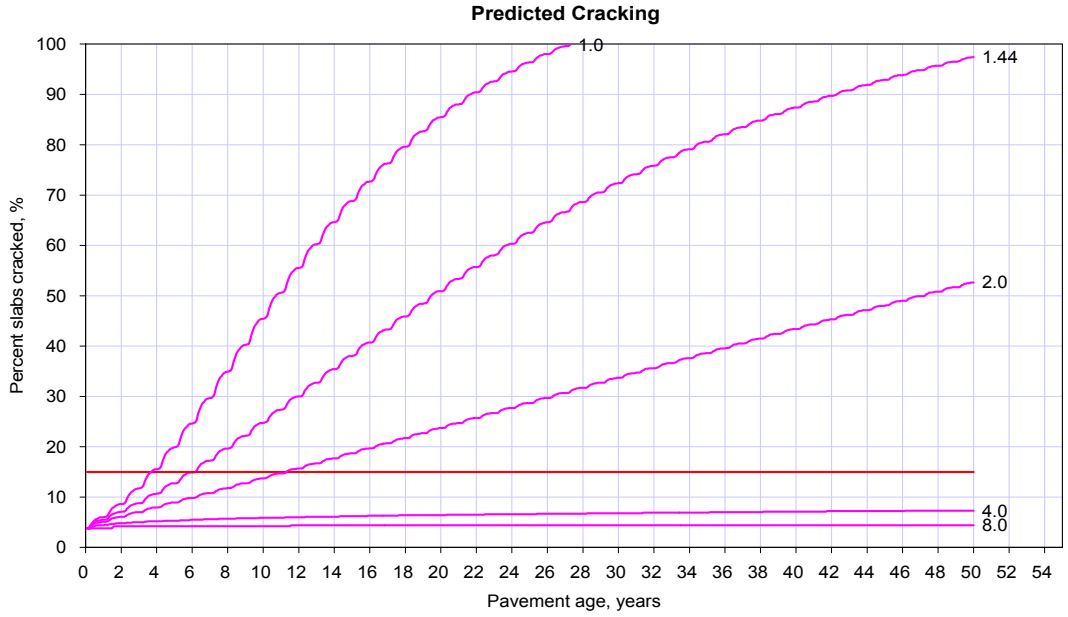

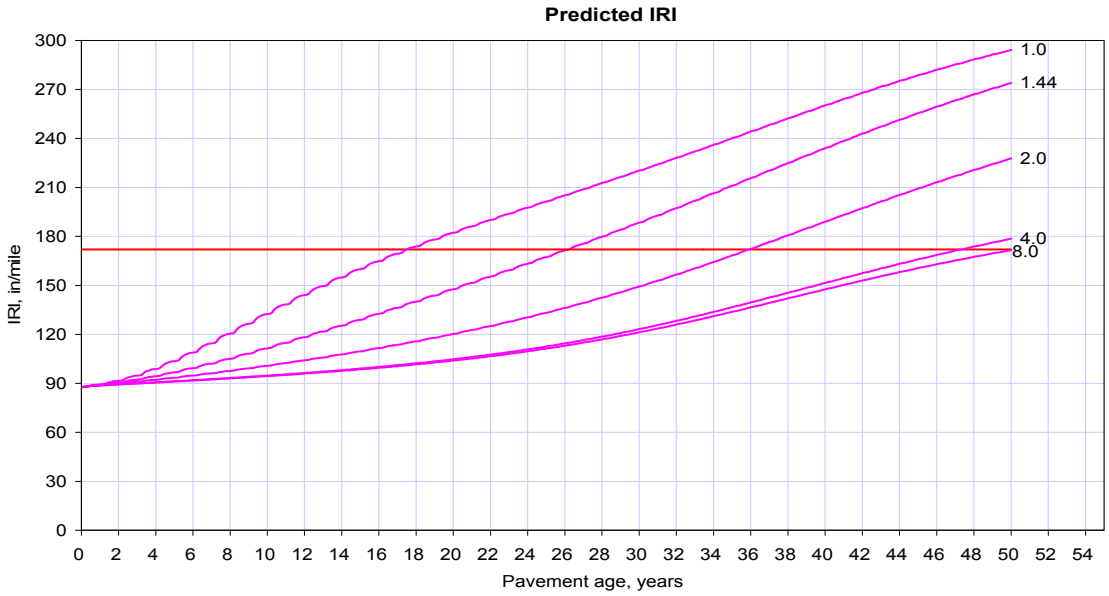

A5.16.4 28-day PCC Compressive Strength (psi)

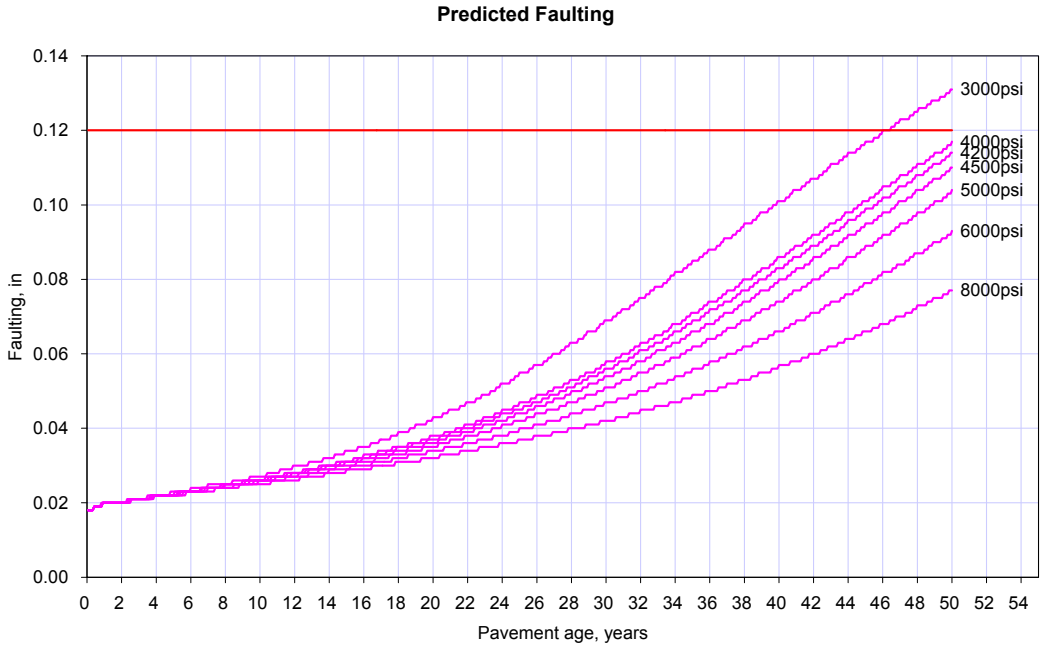

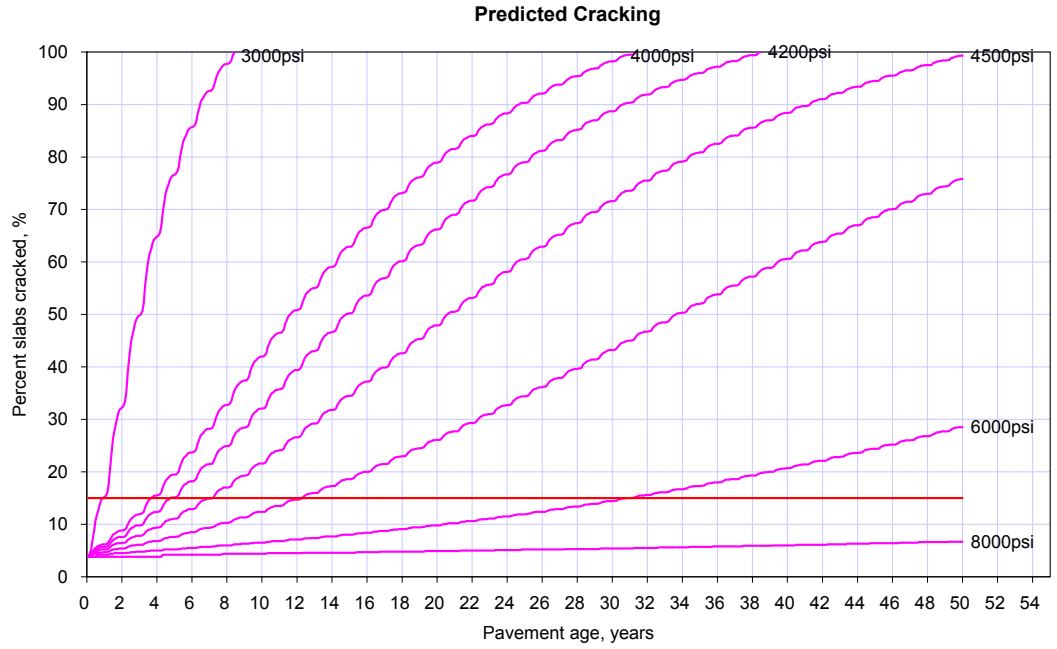
Predicted Cracking
Percent slabs cracked, %
Pavement age, years
3000psi
4000psi
4200psi
4500psi
6000psi
8000psi

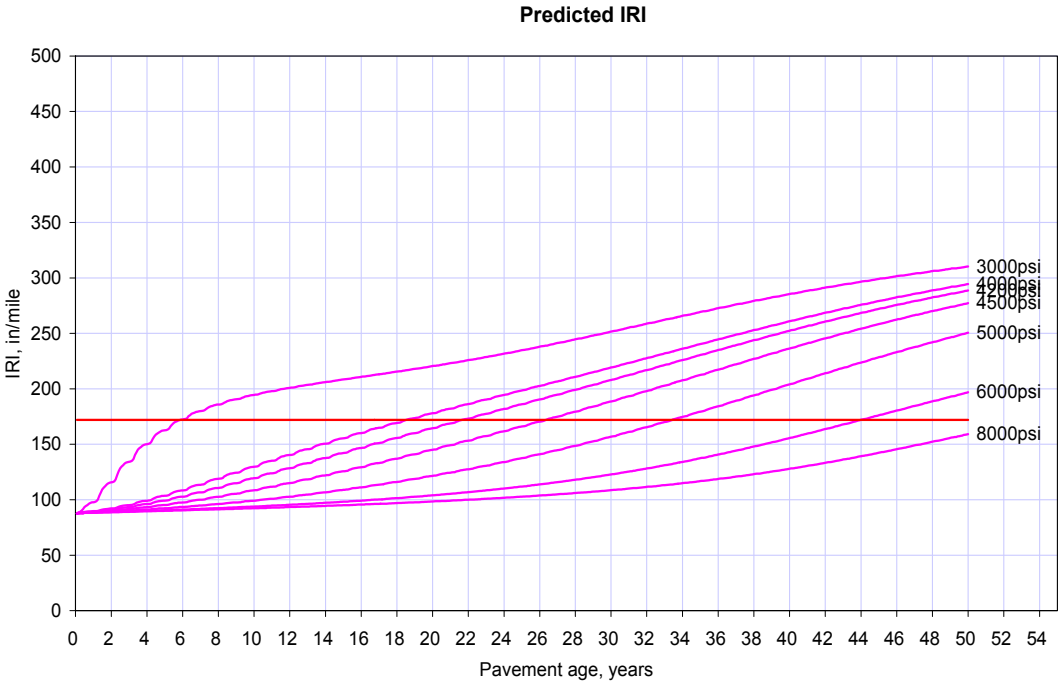
Predicted IRI
IRI, in/mile
Pavement age, years
3000psi
4000psi
4200psi
4500psi
5000psi
6000psi
8000psi

A5.16.5 28-day PCC Modulus of Rupture (psi)

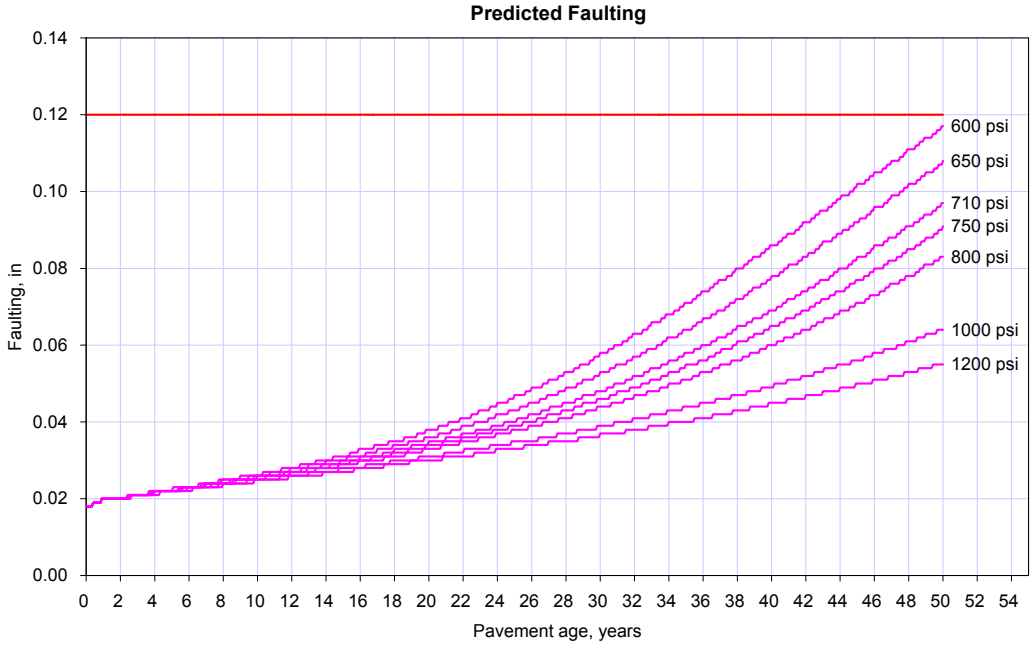

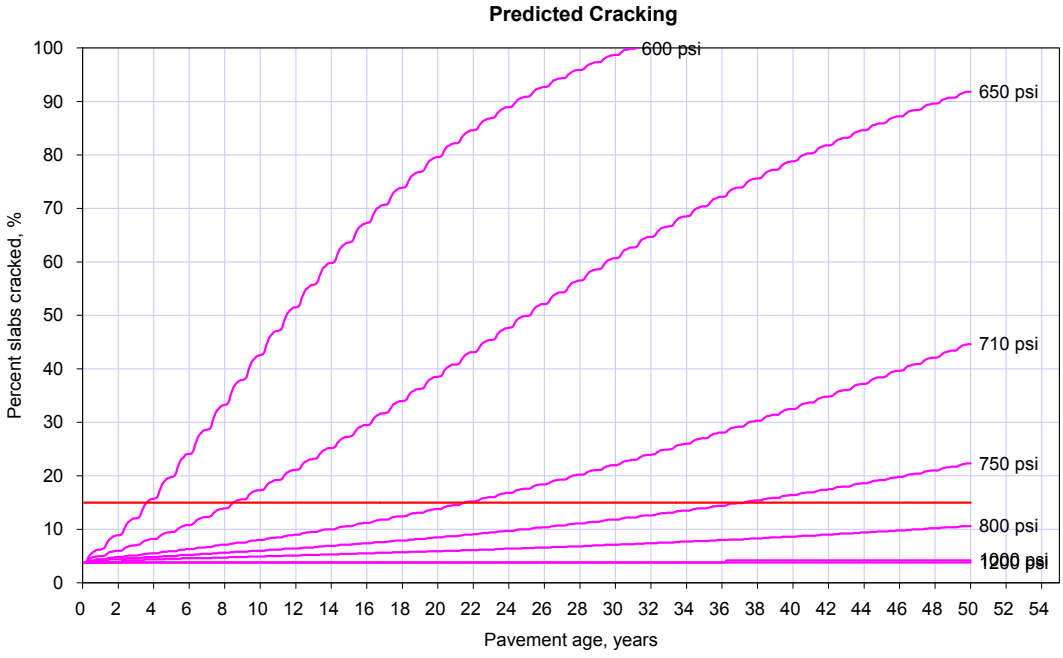

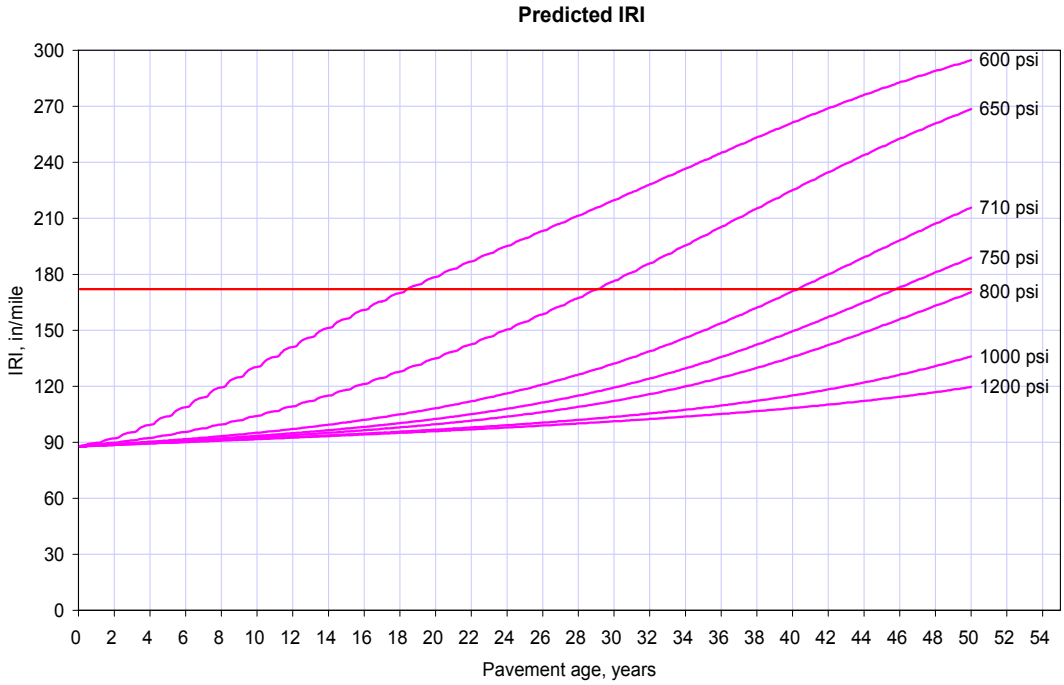
Predicted IRI
IRI, in/mile
Pavement age, years
600 psi
650 psi
710 psi
750 psi
800 psi
1000 psi
1200 psi
0
30
60
90
120
150
180
210
240
270
300
0 2 4 6 8 10 12 14 16 18 20 22 24 26 28 30 32 34 36 38 40 42 44 46 48 50 52 54

A6 Granular Base/Subbase/Subgrade Inputs

A6.1 Material Type

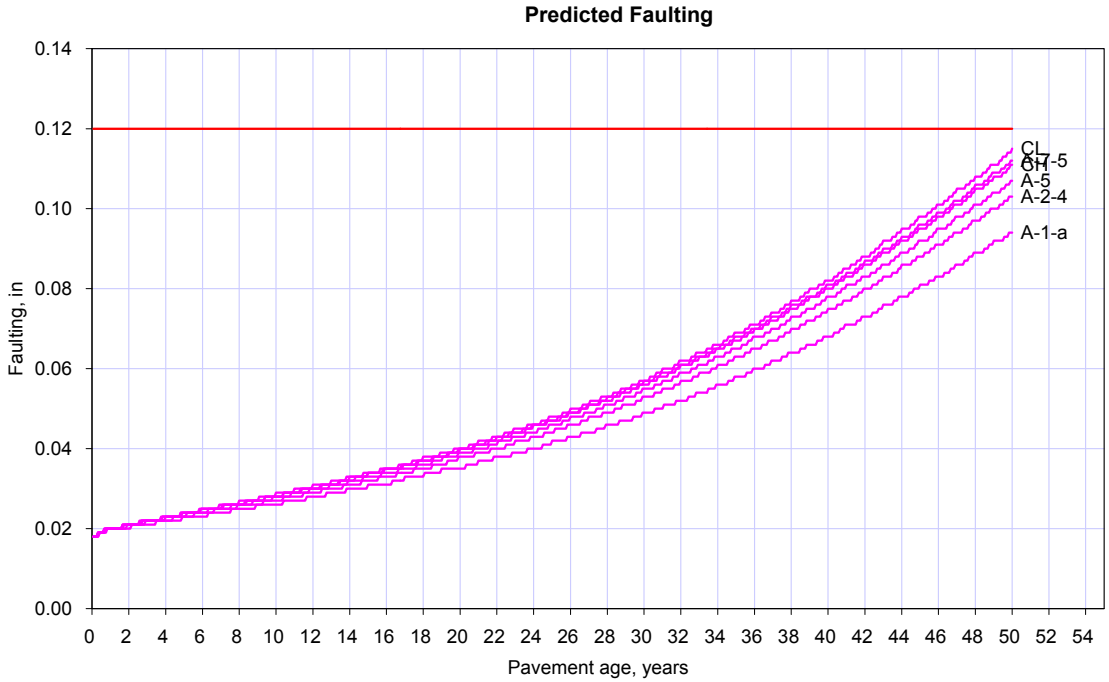

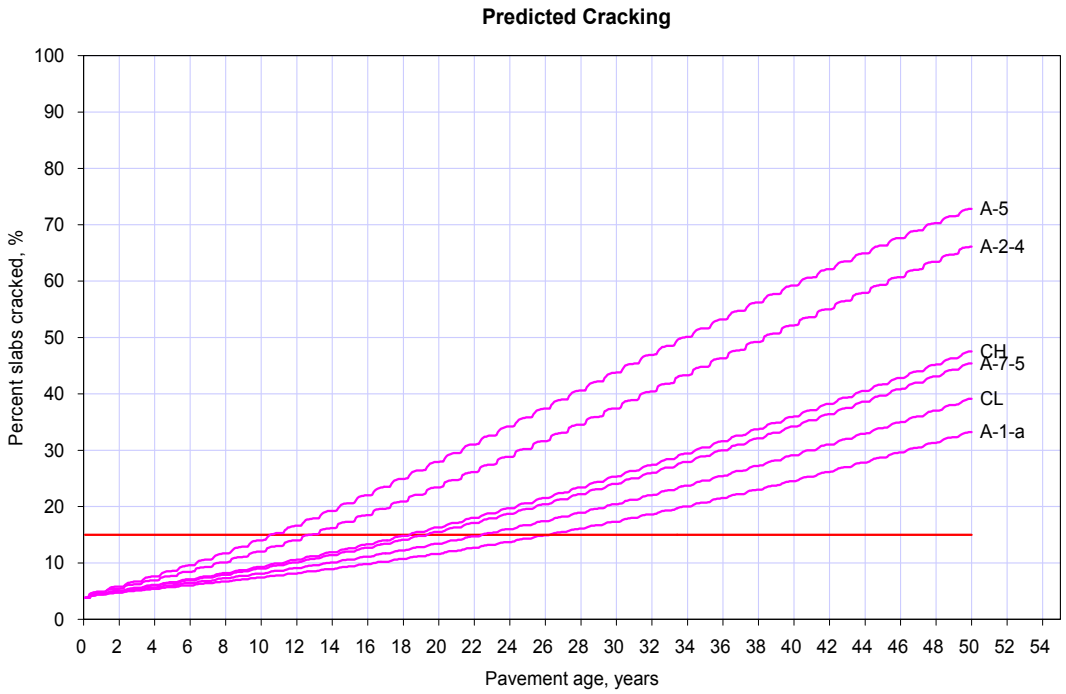
Predicted Cracking
Percent slabs cracked, %
Pavement age, years
A-5
A-2-4
CH
A-7-5
CL
A-1-a

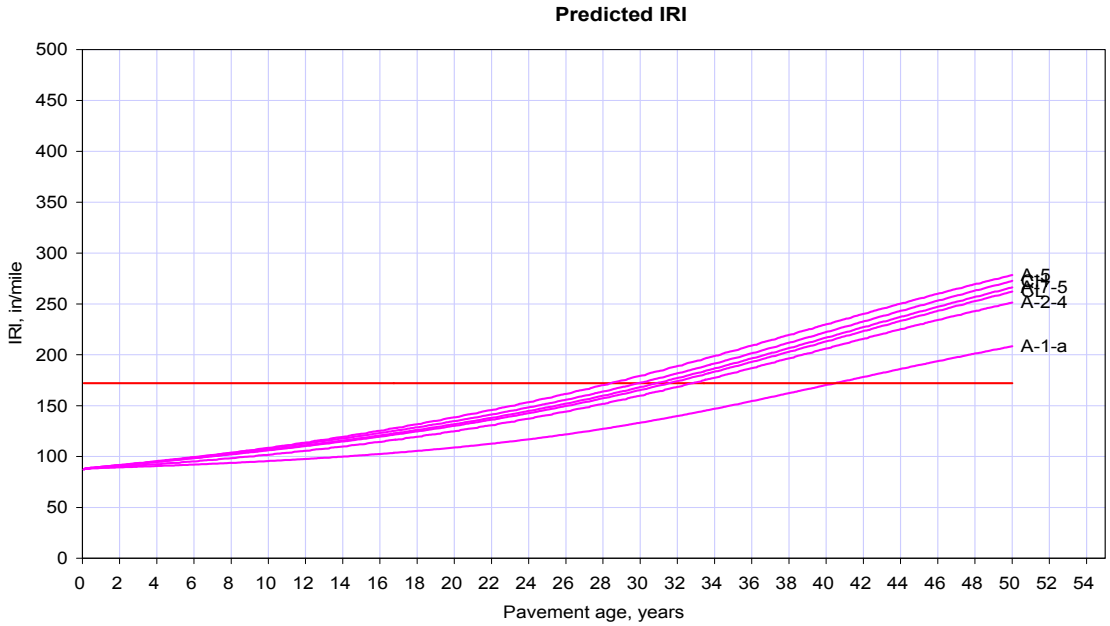
Predicted IRI
IRI, in/mile
Pavement age, years
A-5
A-2-4
A-1-a

A6.2 Material Thickness

This is the thickness of the granular base under the PCC. For analyses the base material thicknesses of 6in to 24in with different increments were used.

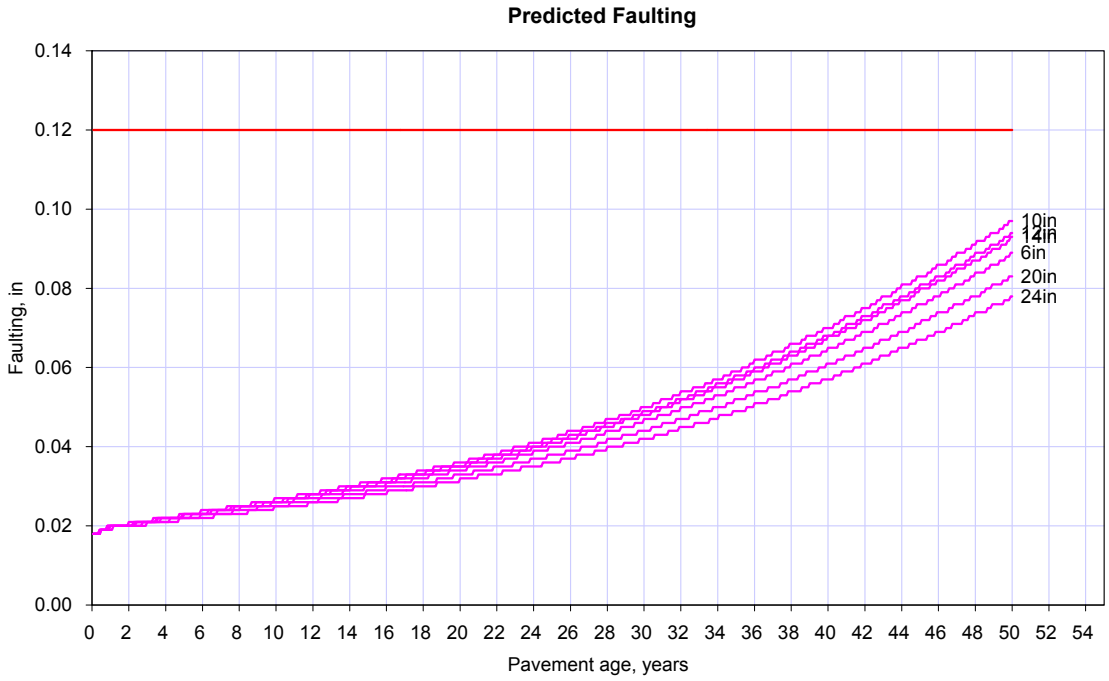

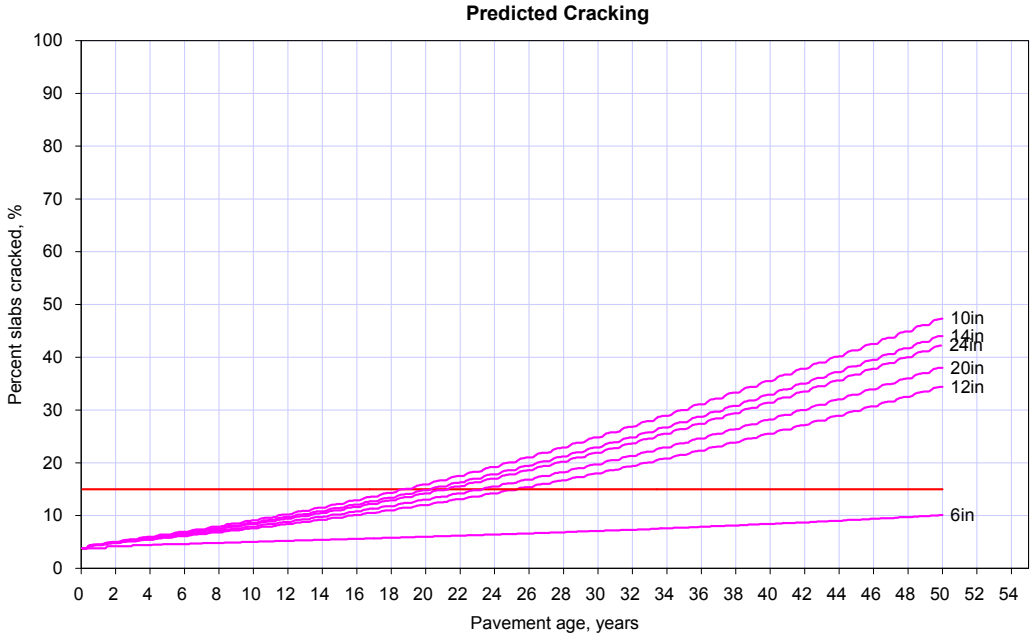

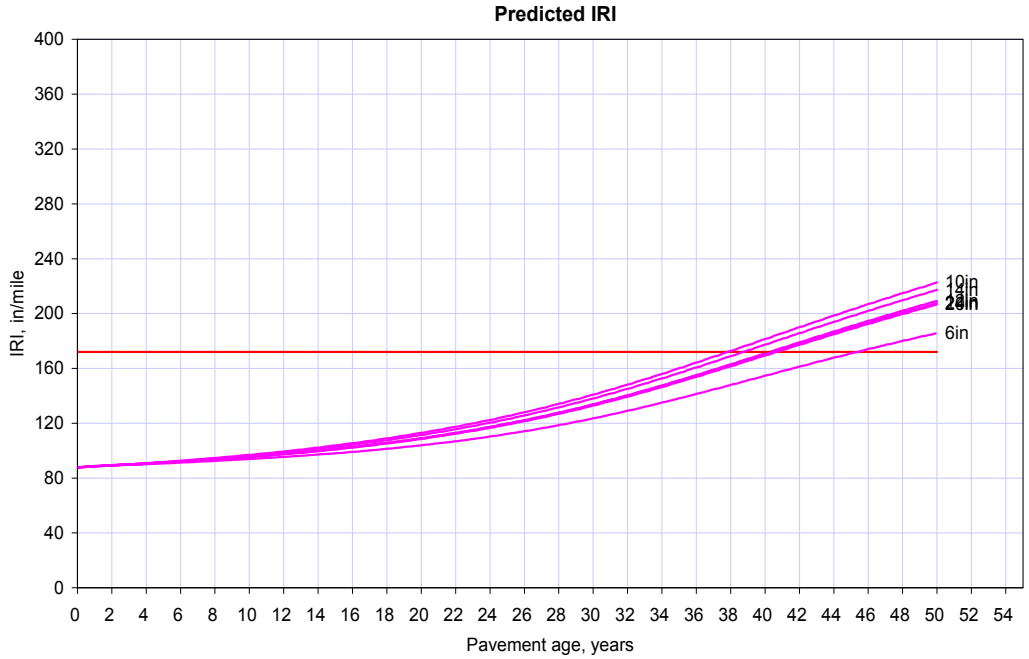

A6.3 Poisson's ratio

This is the poisson's ratio of base, sub-base and/or subgrade. For analyses poisson's ratios of 0.1, 0.2, 0.3, 0.35 & 0.4 were used as shown in the following graphs.

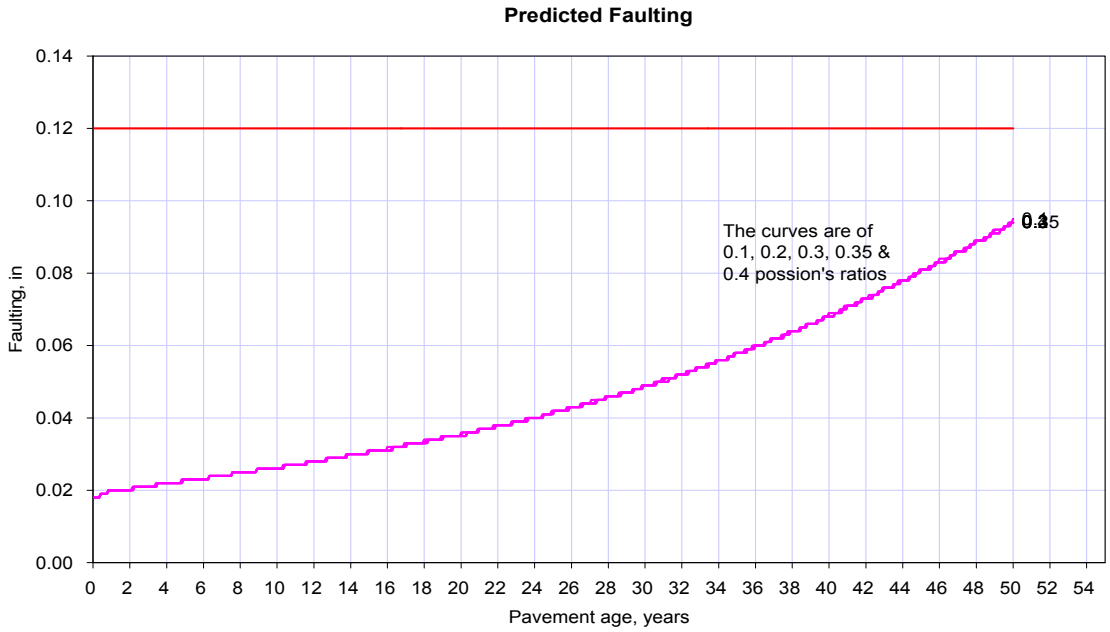

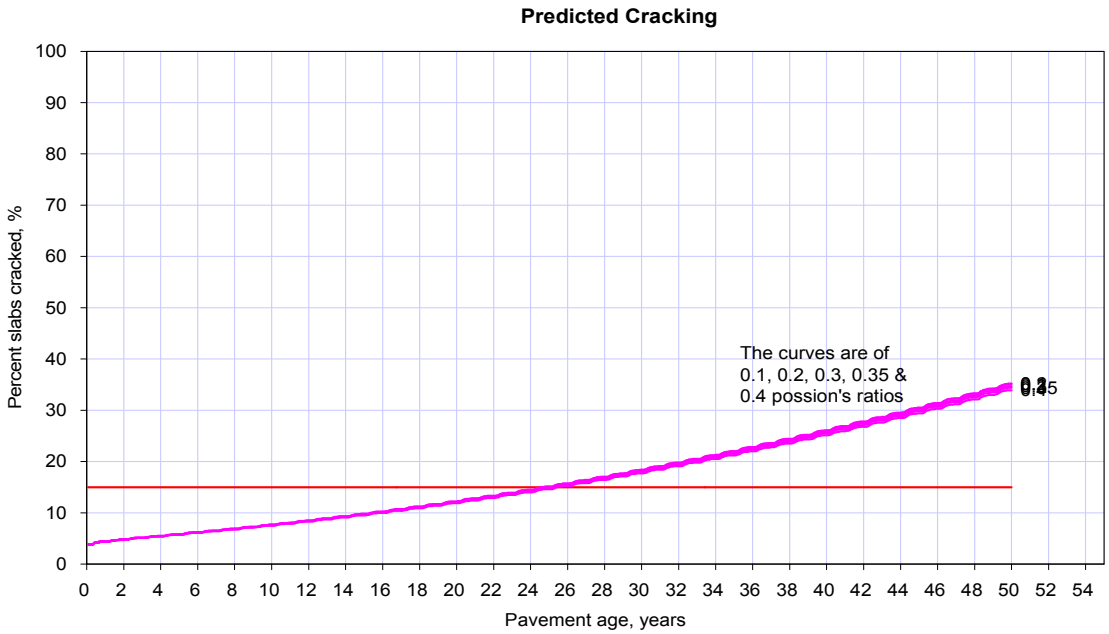
Predicted Cracking
Percent slabs cracked, %
Pavement age, years
The curves are of
0.1, 0.2, 0.3, 0.35 &
0.4 possion's ratios

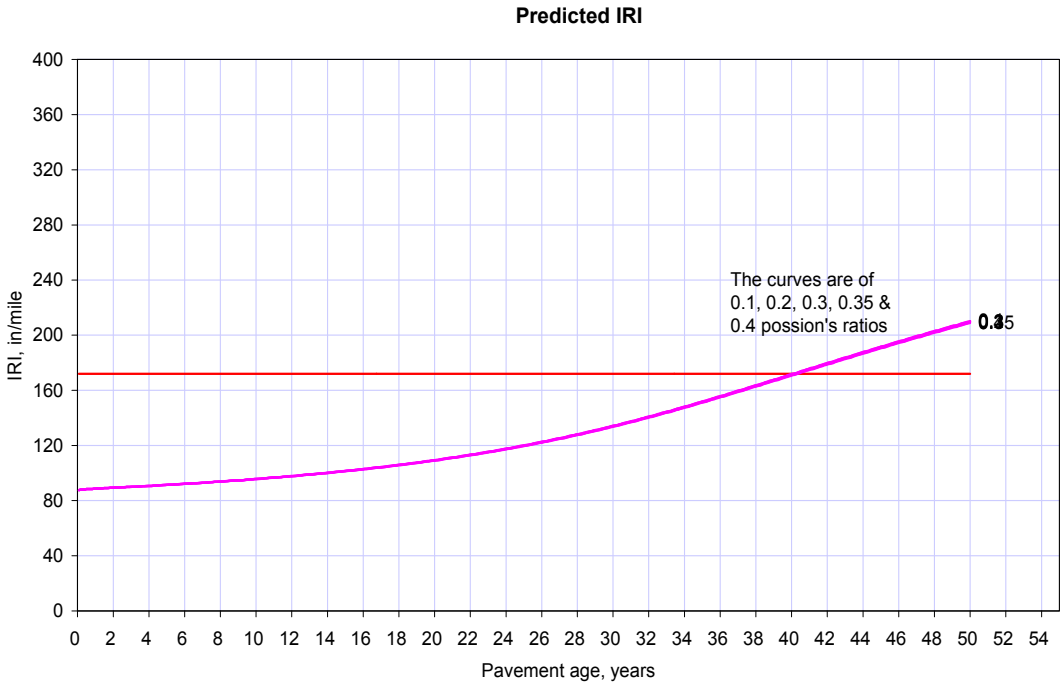
Predicted IRI
IRI, in/mile
Pavement age, years
The curves are of
0.1, 0.2, 0.3, 0.35 &
0.4 possion's ratios

A6.4 Coefficient of lateral pressure (Ko)

Refers to the coefficient of lateral pressure of the base, subbase and/or subgarde. For analyses purposes coefficients of lateral pressure of 0.4, 0.5, 1.0 and 3.0 were used. Following graphs show the detail output.

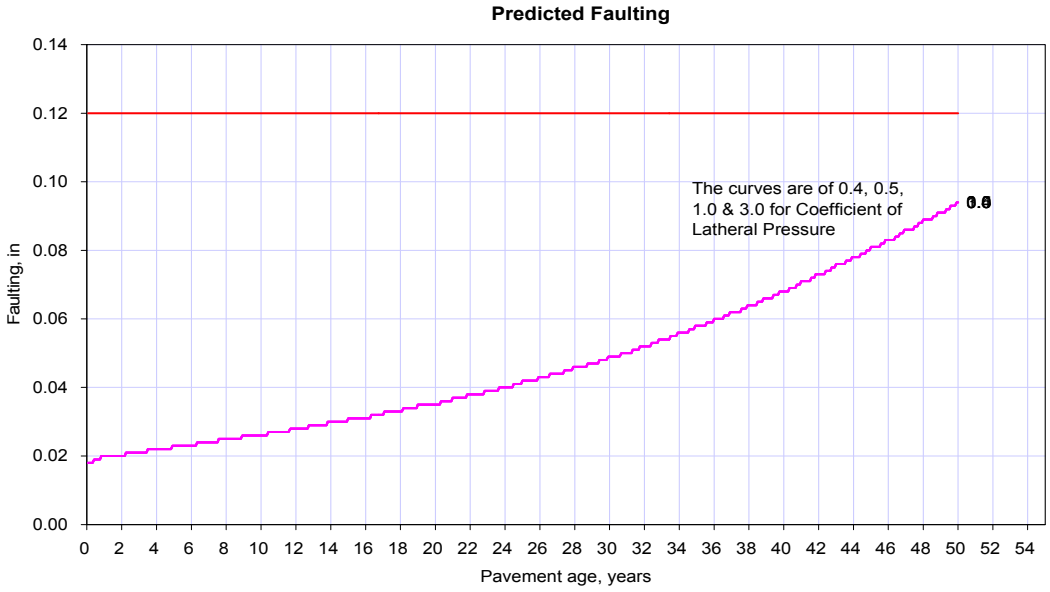

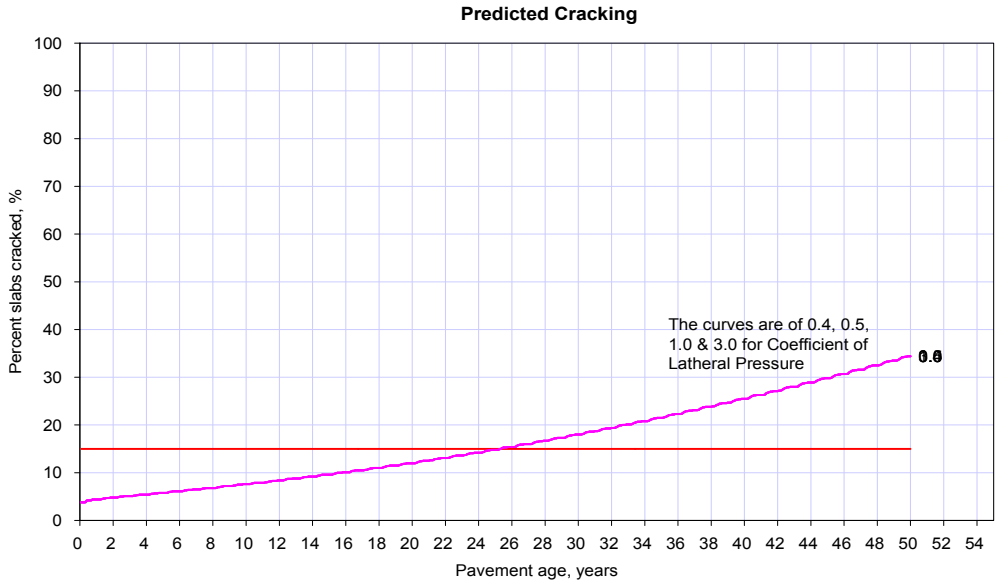

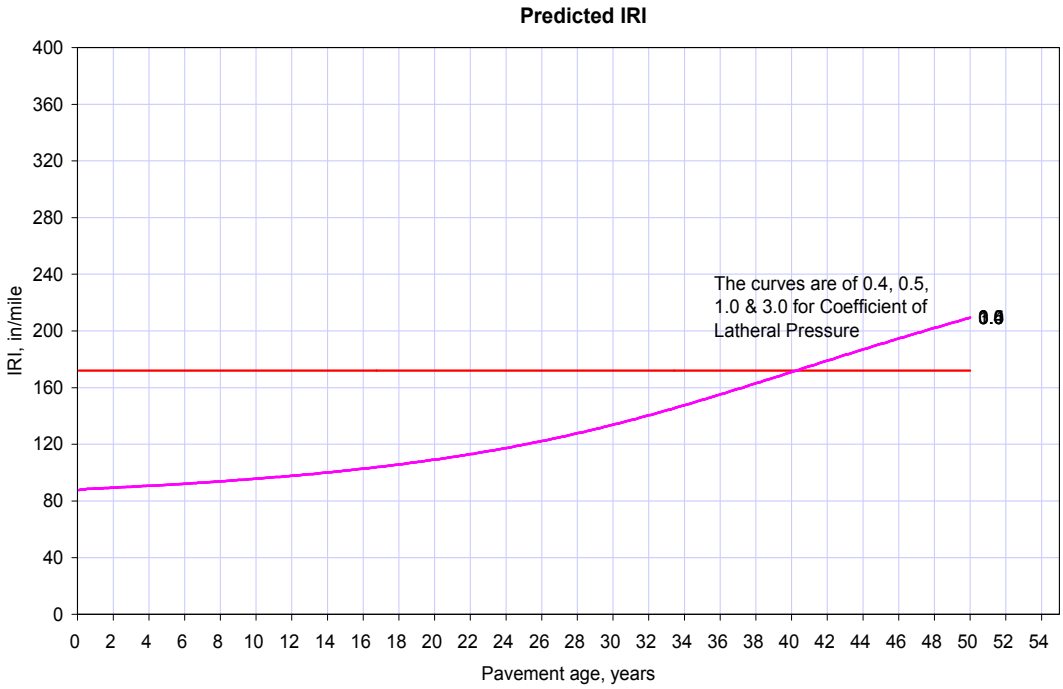
Predicted IRI
IRI, in/mile
400
360
320
280
240
200
160
120
80
40
0
0 2 4 6 8 10 12 14 16 18 20 22 24 26 28 30 32 34 36 38 40 42 44 46 48 50 52 54
Pavement age, years
The curves are of 0.4, 0.5, 1.0 & 3.0 for Coefficient of Latheral Pressure

A6.5 Resilient Modulus

The Design Guide allows the user to use either of the following soil indices to estimate Mr from the aforementioned correlation:

- CBR
- R-value
- Layer coefficient
- Penetration from DCP
- Based up on PI and Gradation (Enter on ICM screen)

A number of resilient modulus values from the given range were used for analyzing this parameter.

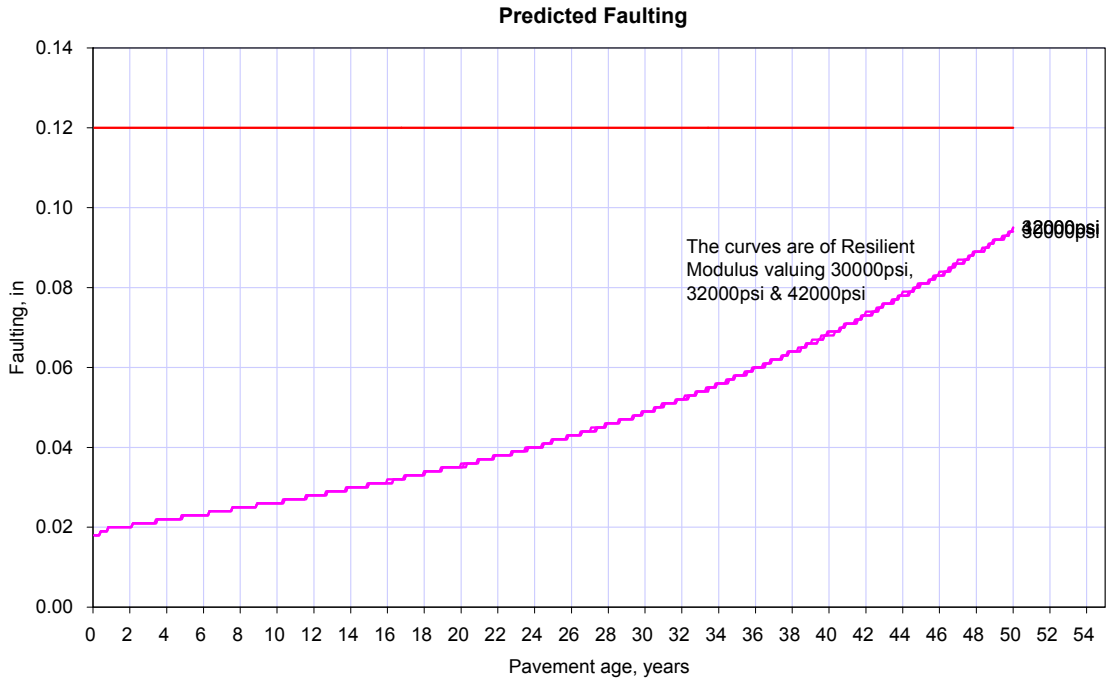

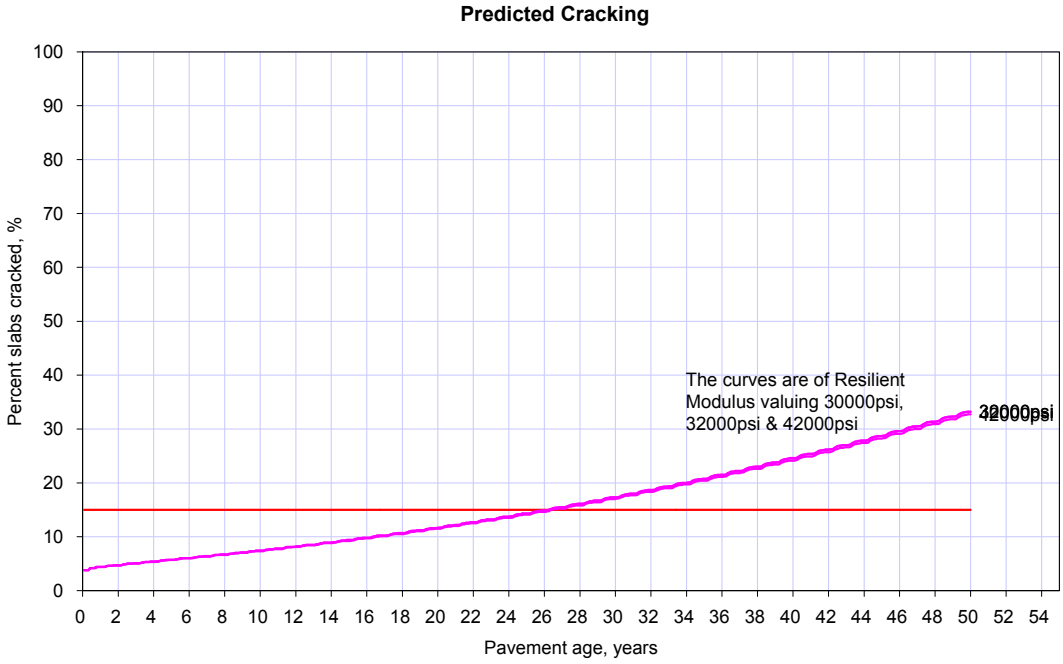
Predicted Cracking
Percent slabs cracked, %
Pavement age, years
The curves are of Resilient Modulus valuing 30000psi, 32000psi & 42000psi
30000psi
32000psi
42000psi

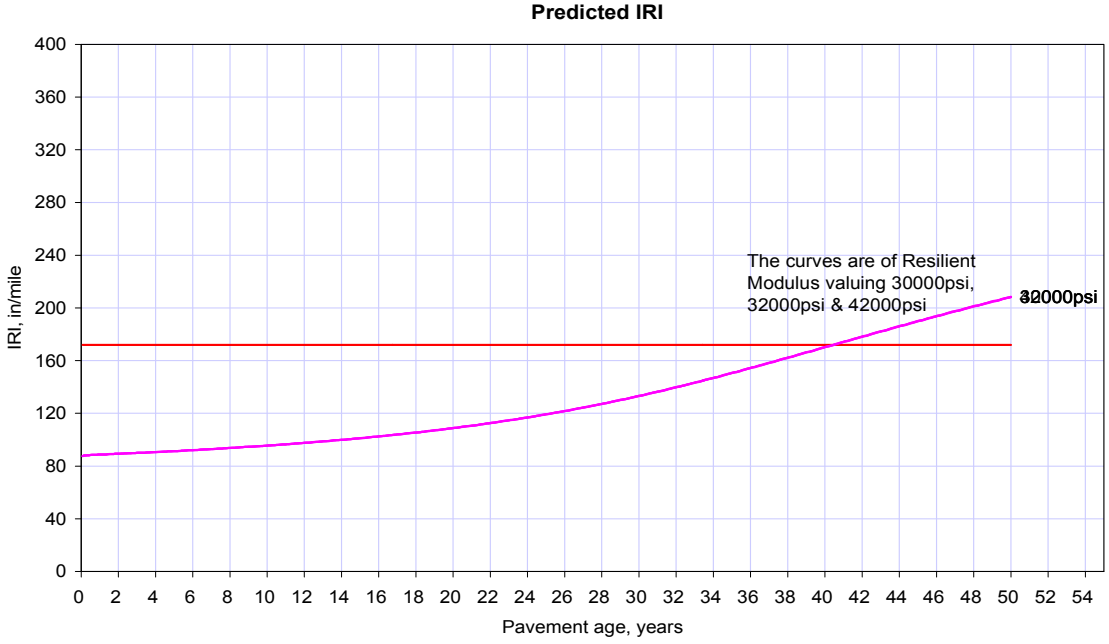
Predicted IRI
IRI, in/mile
Pavement age, years
The curves are of Resilient Modulus valuing 30000psi, 32000psi & 42000psi
30000psi
32000psi
42000psi

A7 Stabilized Base Inputs

A7.1 Material Type

These materials are lean concrete, cement Stabilized, open graded cement Stabilized, soil cement, lime- cement -fly ash, and lime treated materials.

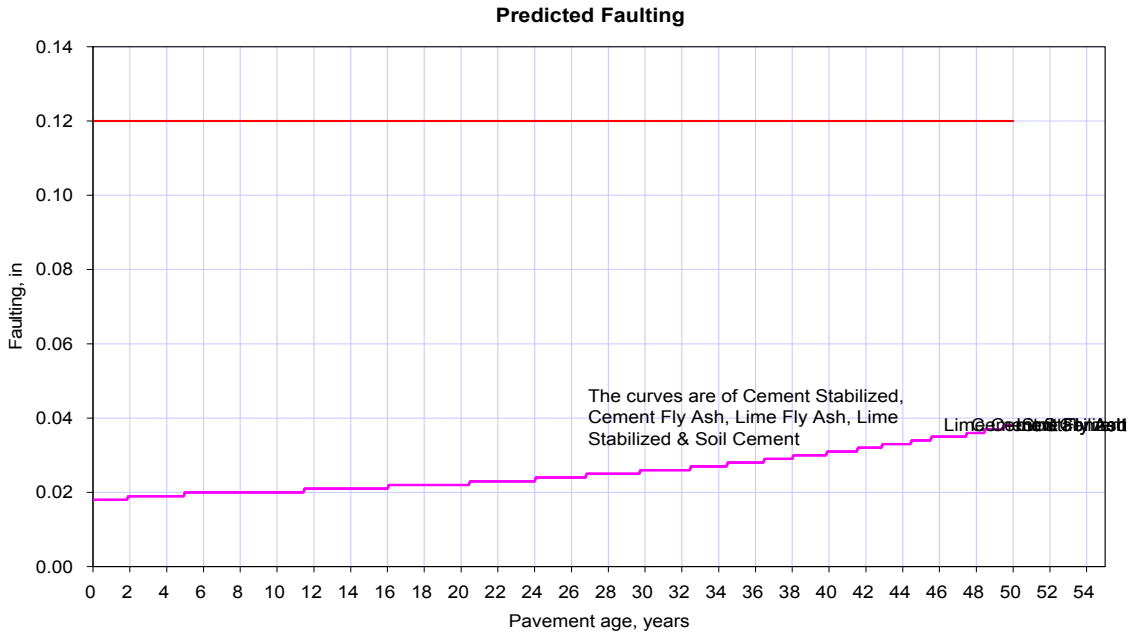

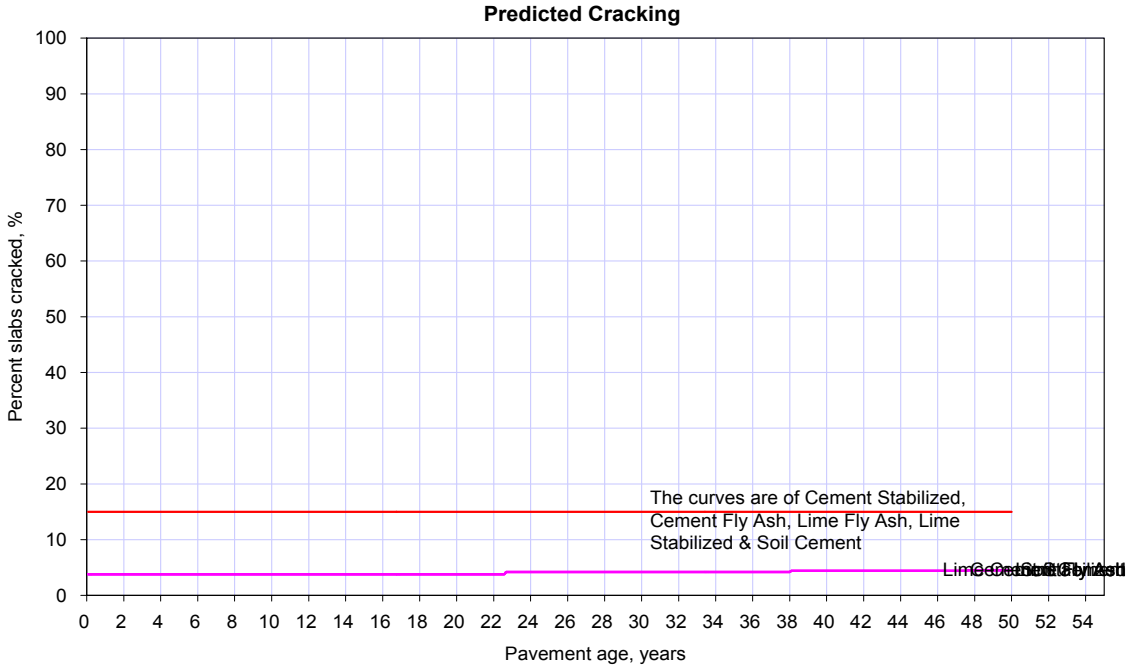
Predicted Cracking
Percent slabs cracked, %
Pavement age, years
The curves are of Cement Stabilized, Cement Fly Ash, Lime Fly Ash, Lime Stabilized & Soil Cement

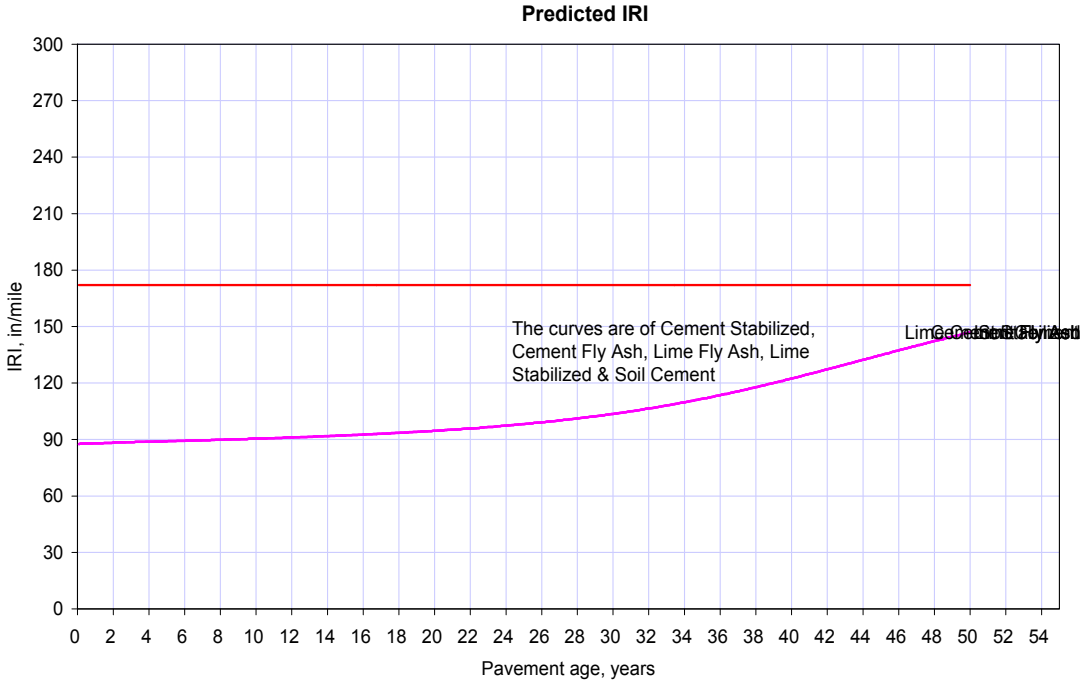
Predicted IRI
IRI, in/mile
Pavement age, years
The curves are of Cement Stabilized, Cement Fly Ash, Lime Fly Ash, Lime Stabilized & Soil Cement

A7.2 Layer thickness (in)

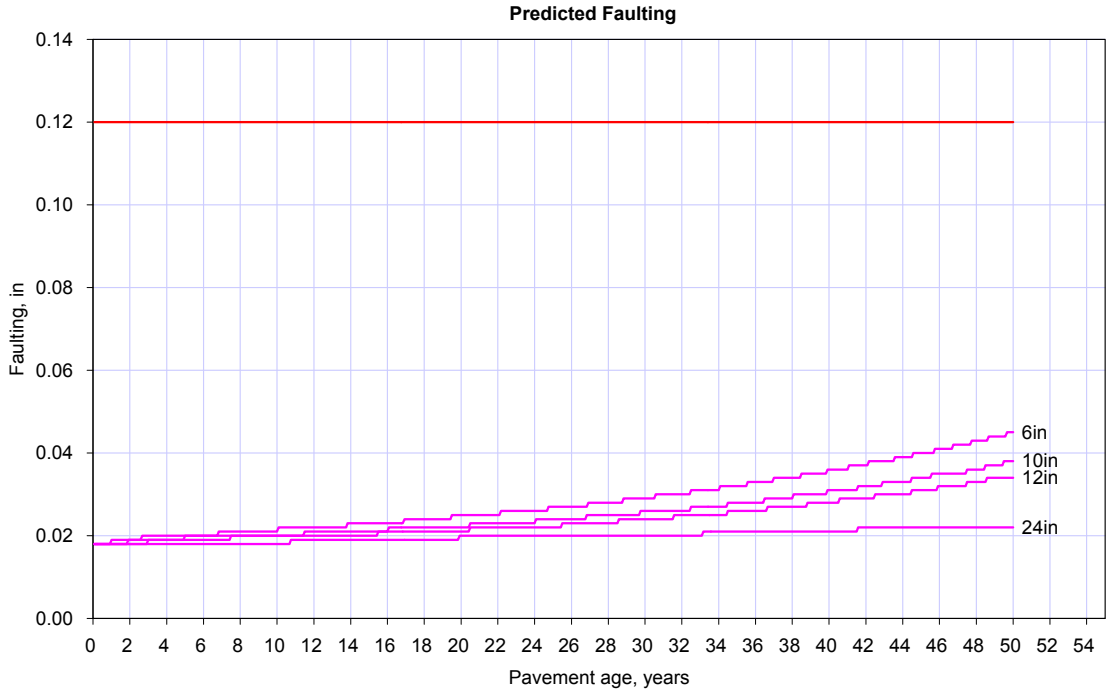

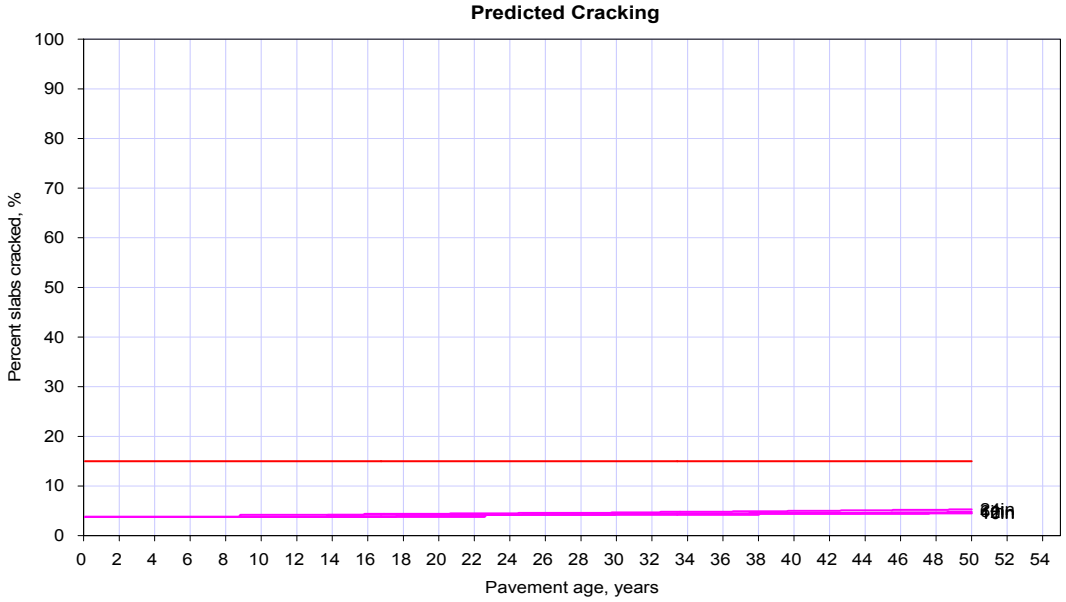

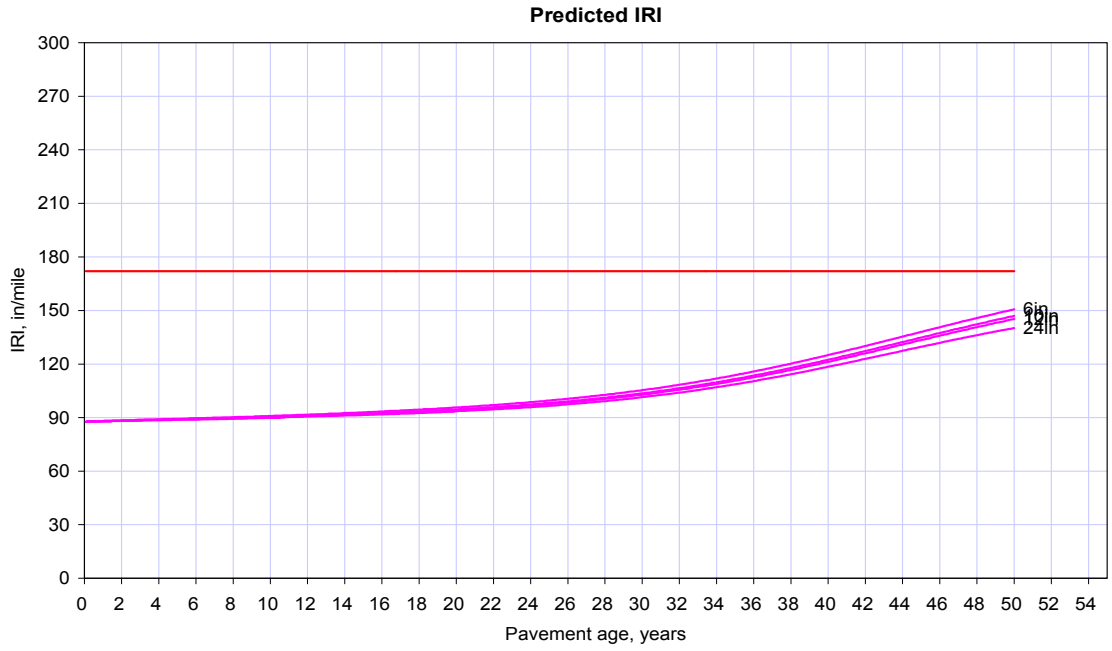

A7.3 Unit Weight (pcf)

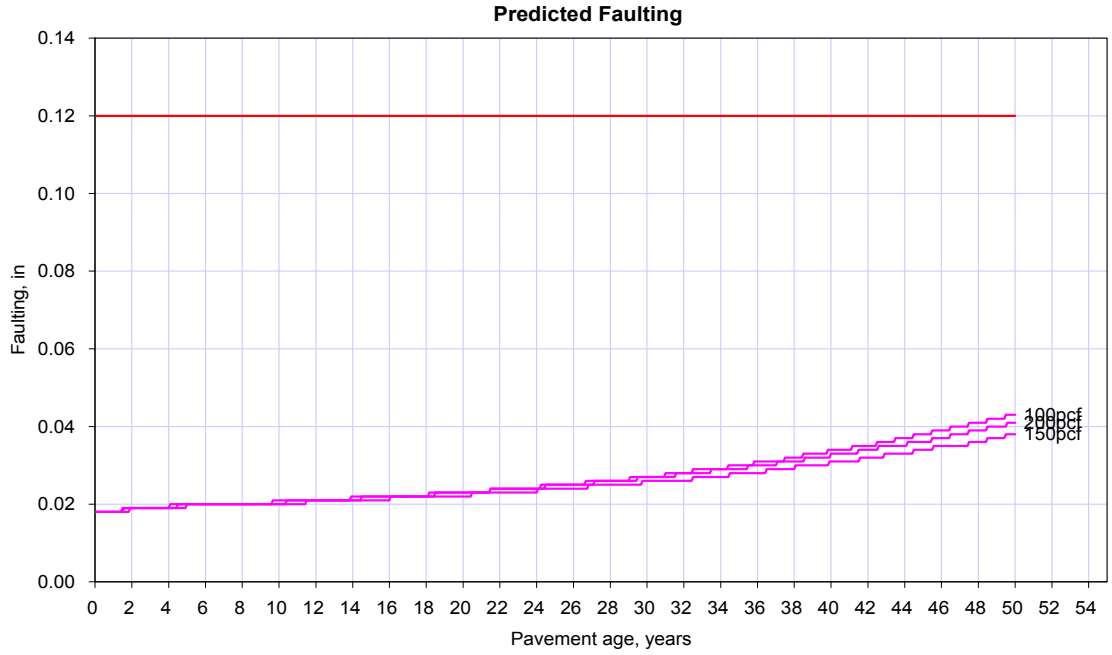

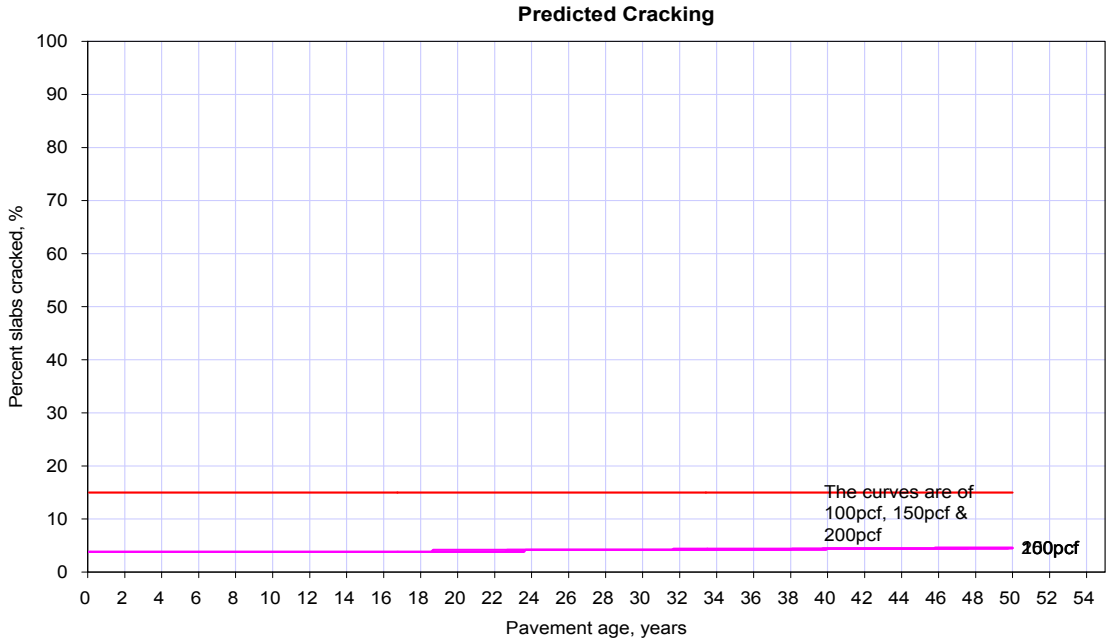
Predicted Cracking
Percent slabs cracked, %
Pavement age, years
The curves are of
100pcf, 150pcf &
200pcf
100
90
80
70
60
50
40
30
20
10
0
0 2 4 6 8 10 12 14 16 18 20 22 24 26 28 30 32 34 36 38 40 42 44 46 48 50 52 54

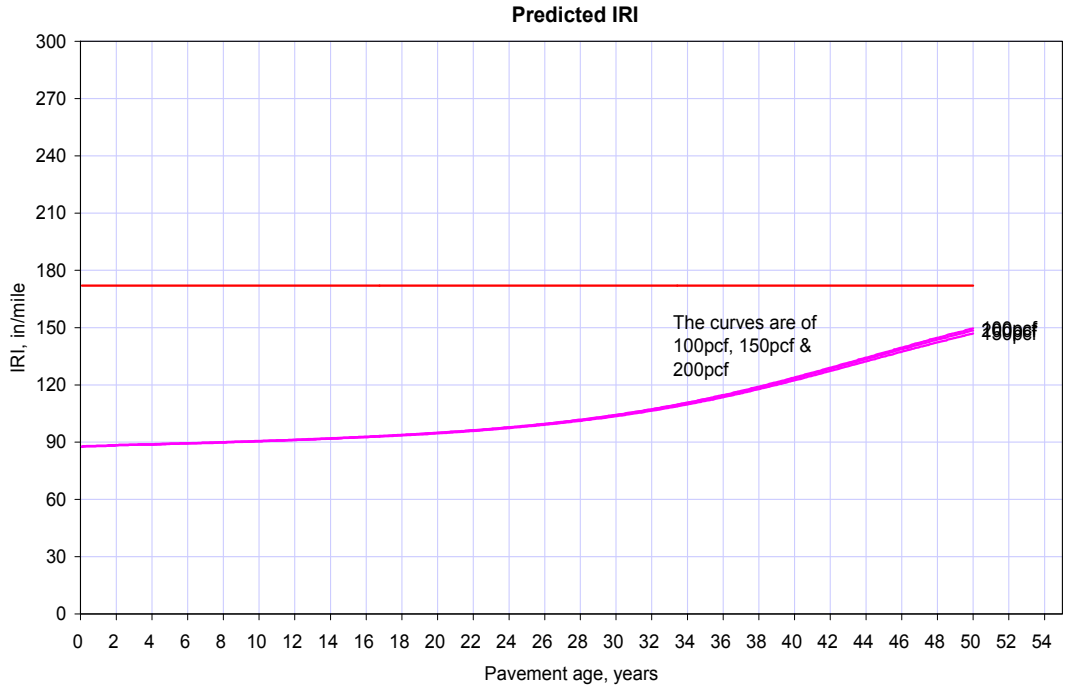
Predicted IRI
IRI, in/mile
Pavement age, years
The curves are of
100pcf, 150pcf &
200pcf
300
270
240
210
180
150
120
90
60
30
0
0 2 4 6 8 10 12 14 16 18 20 22 24 26 28 30 32 34 36 38 40 42 44 46 48 50 52 54

A7.4 Poisson's ratio

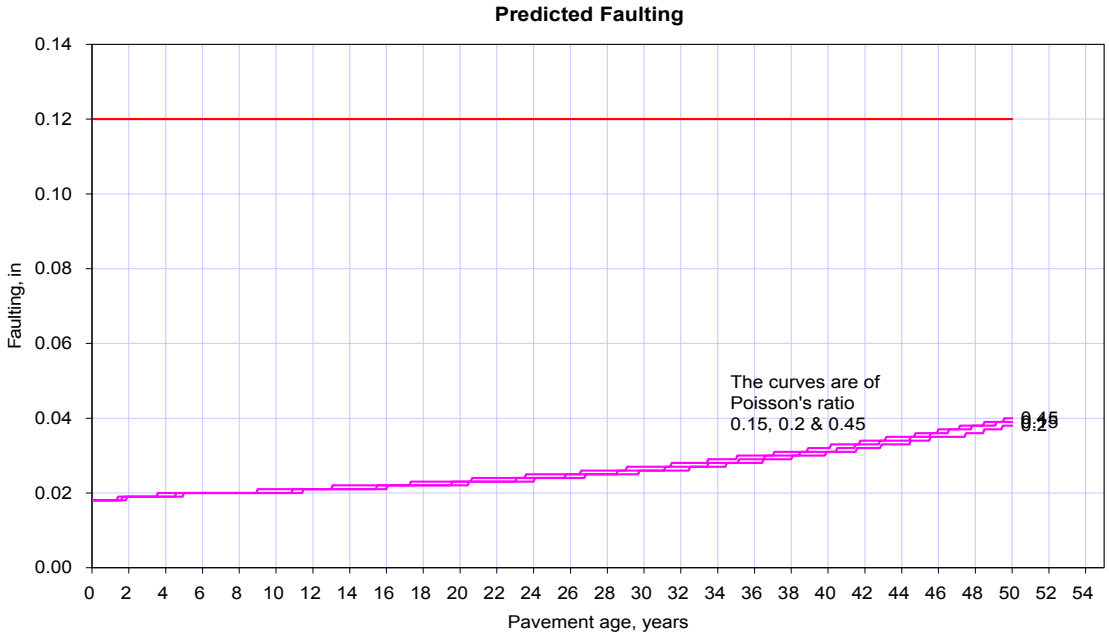

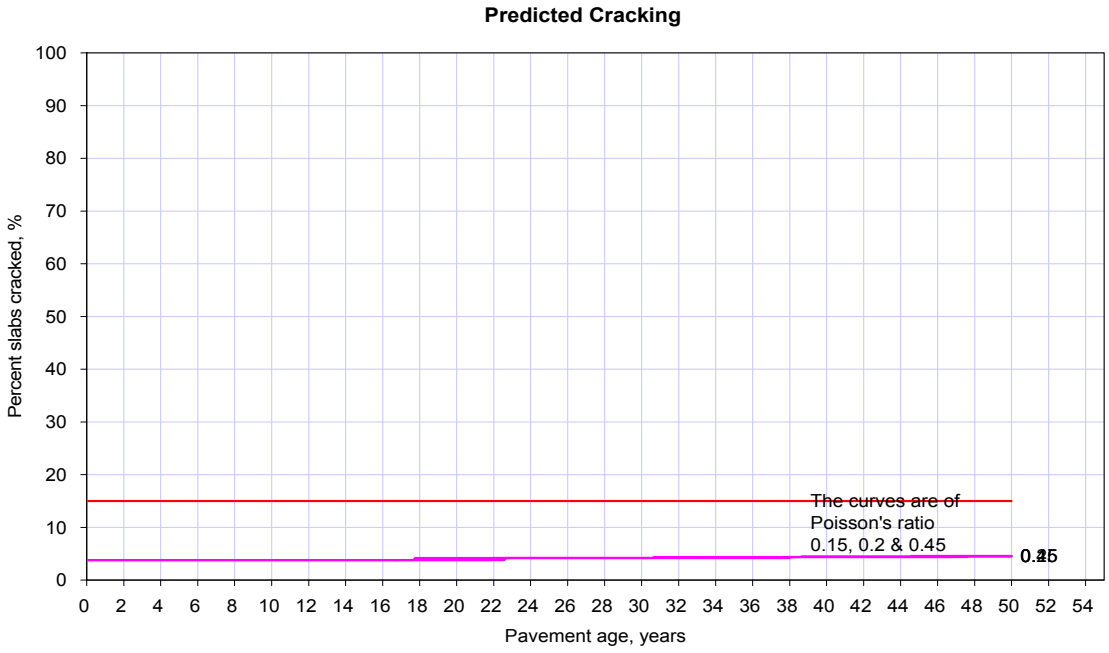

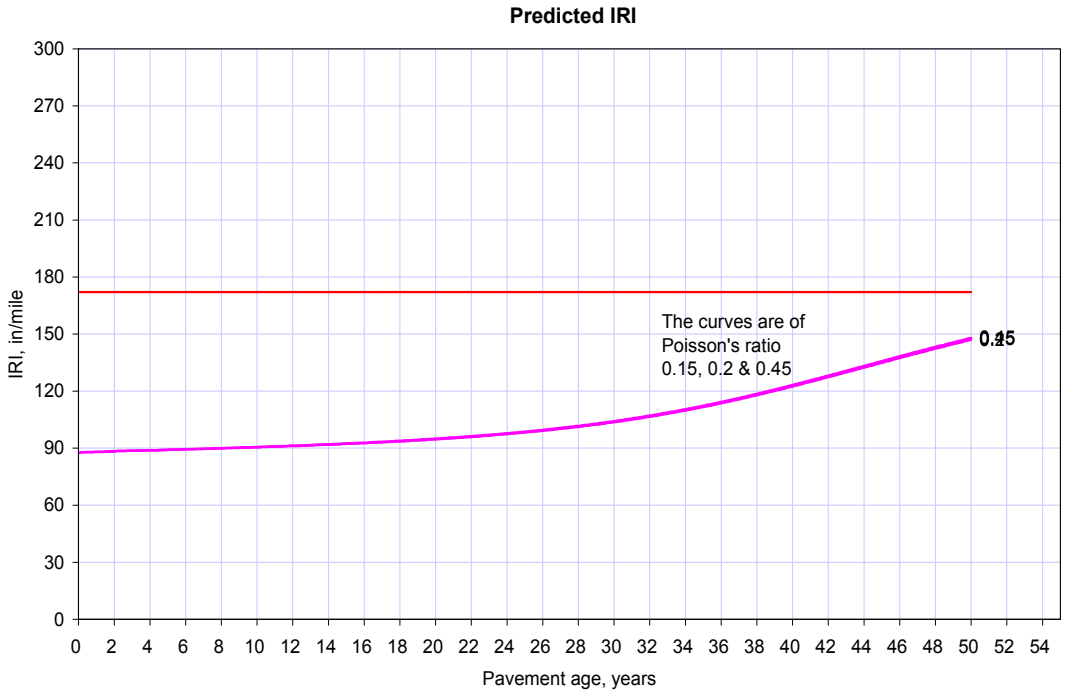

A7.5 Elastic/Resilient Modulus (psi)

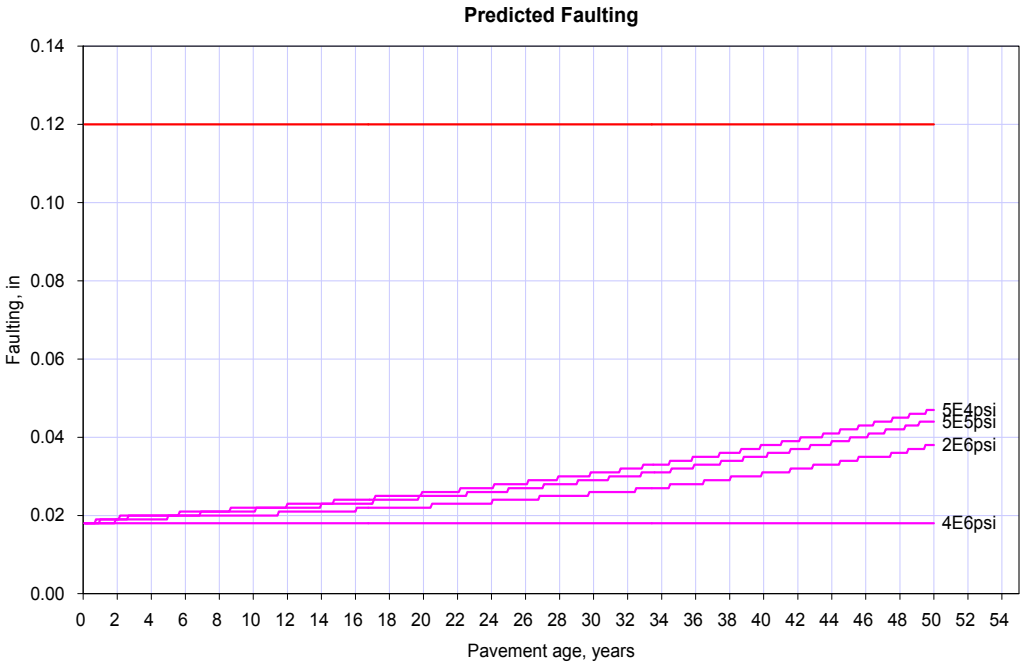

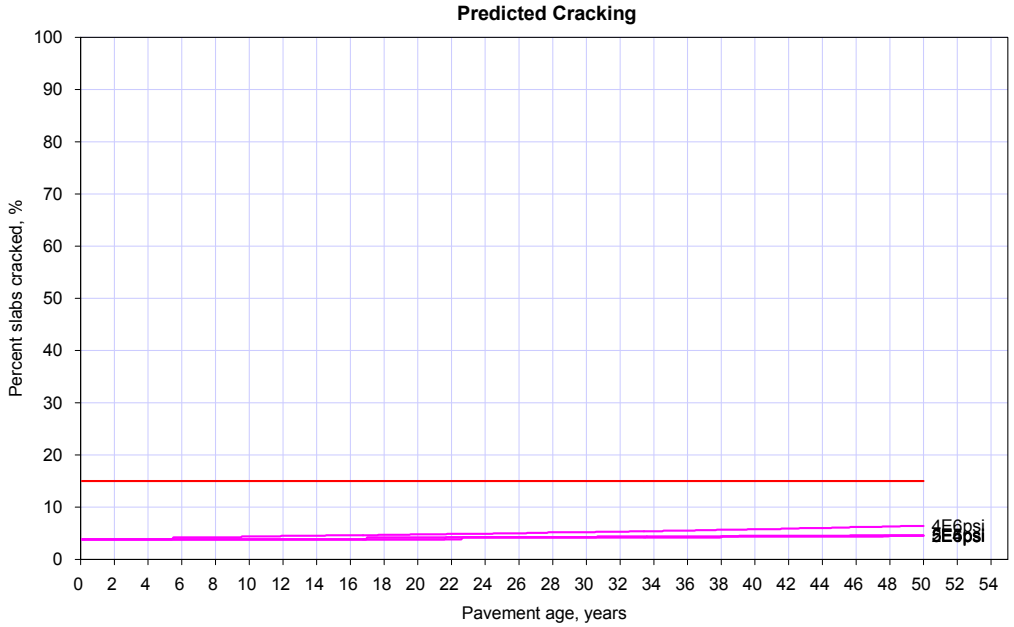
Predicted Cracking
Percent slabs cracked, %
Pavement age, years
4E6psi

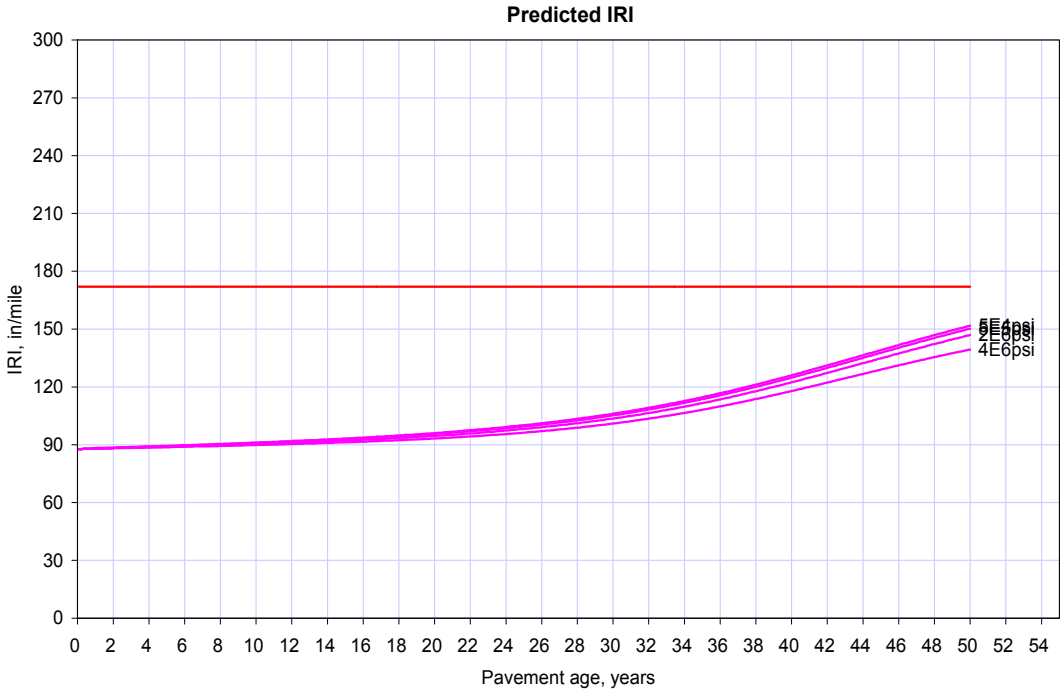
Predicted IRI
IRI, in/mile
Pavement age, years
4E6psi

A7.6 Thermal Conductivity (BTU/hr-ft-F˚)

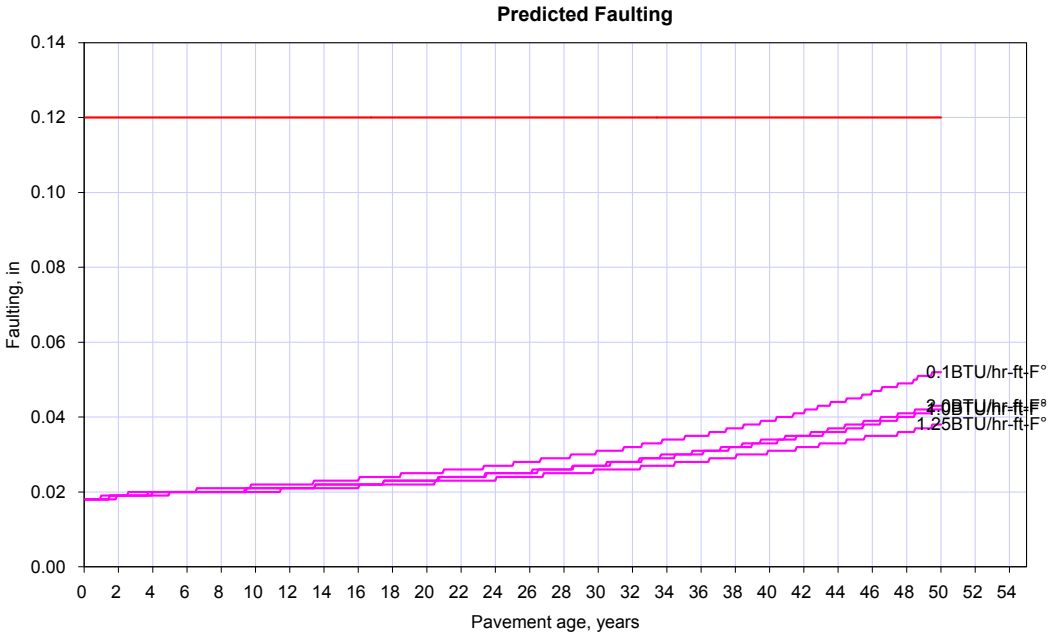

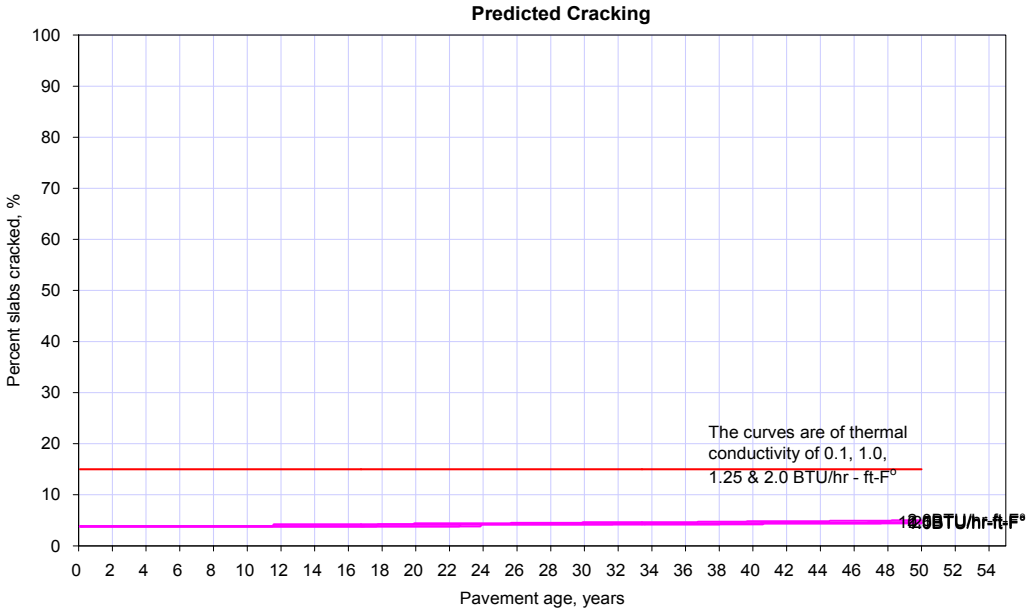

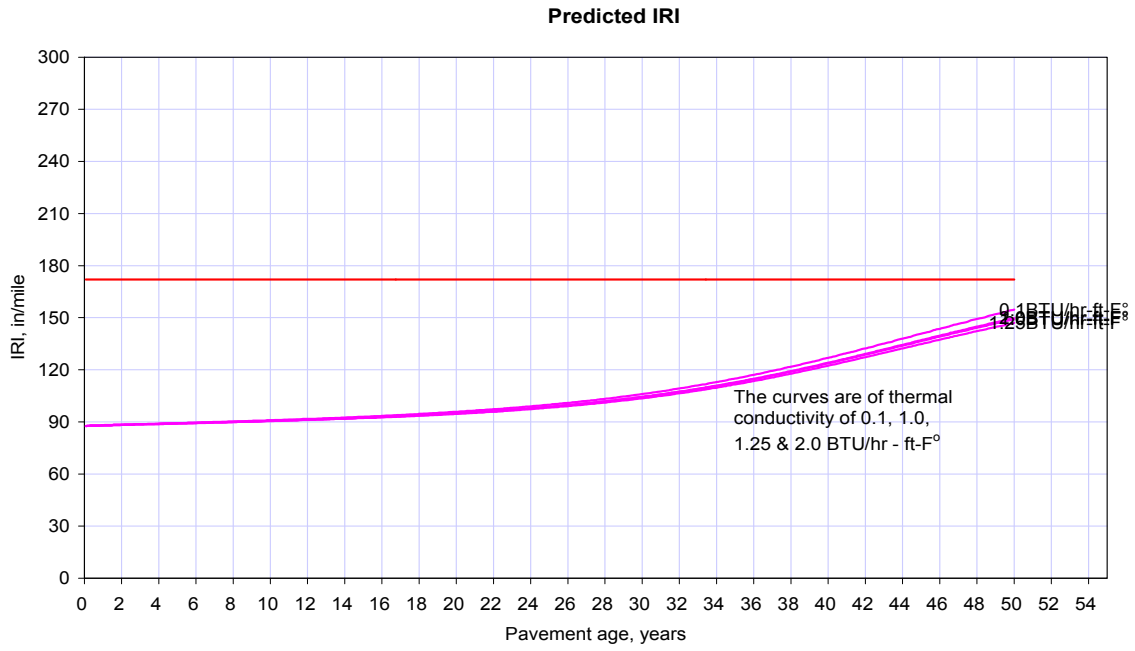

A7.7 Heat Capacity (BTU/lb-F˚)

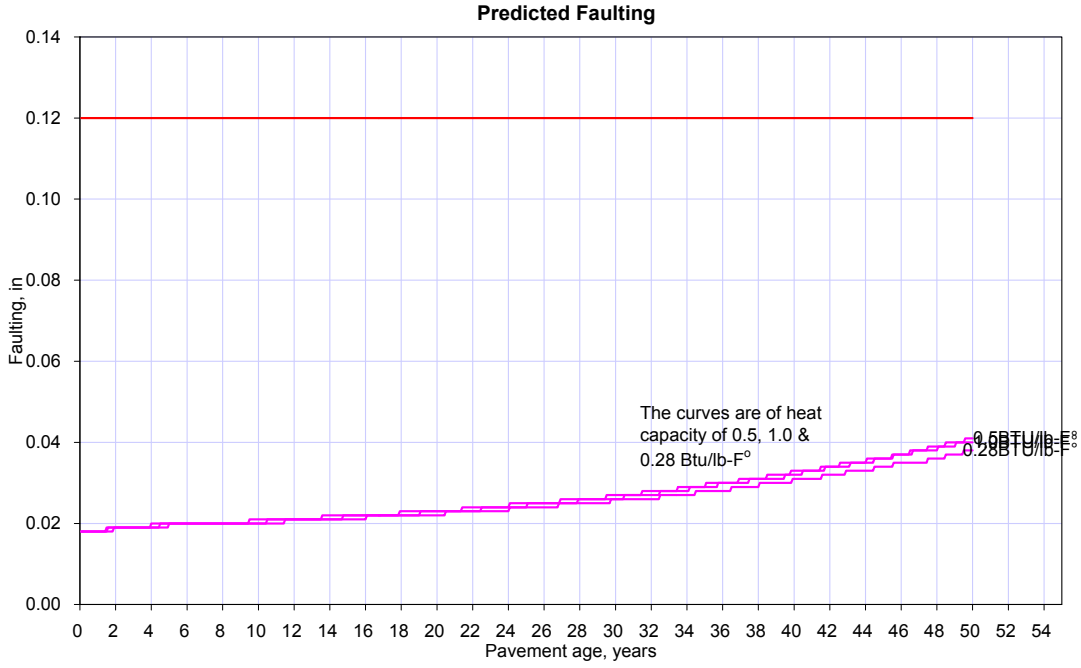

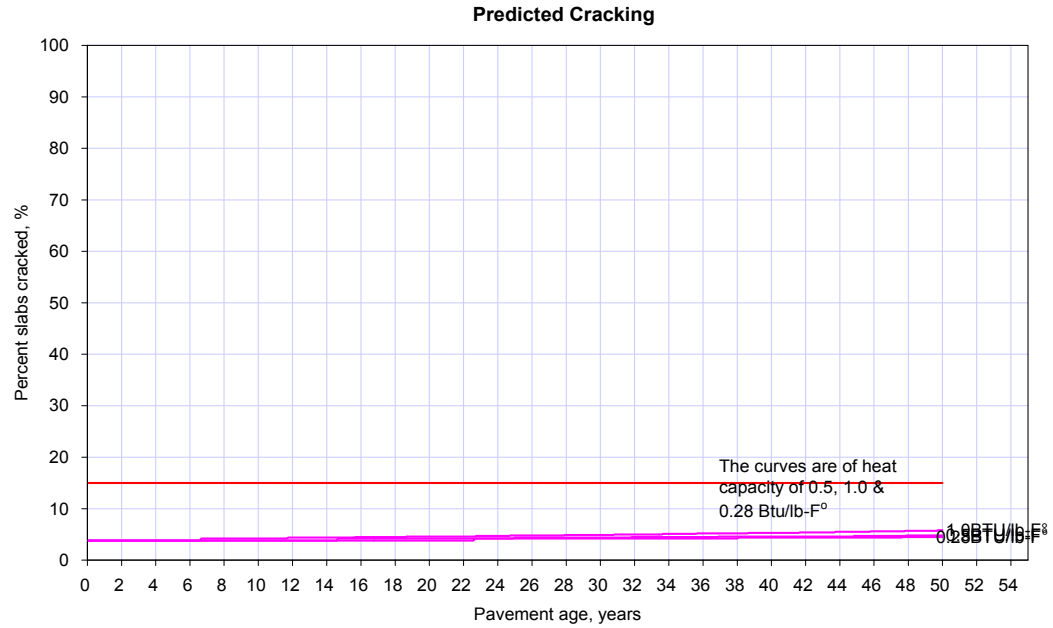
Predicted Cracking
Percent slabs cracked, %
Pavement age, years
The curves are of heat capacity of 0.5, 1.0 & 0.28 Btu/lb-F°

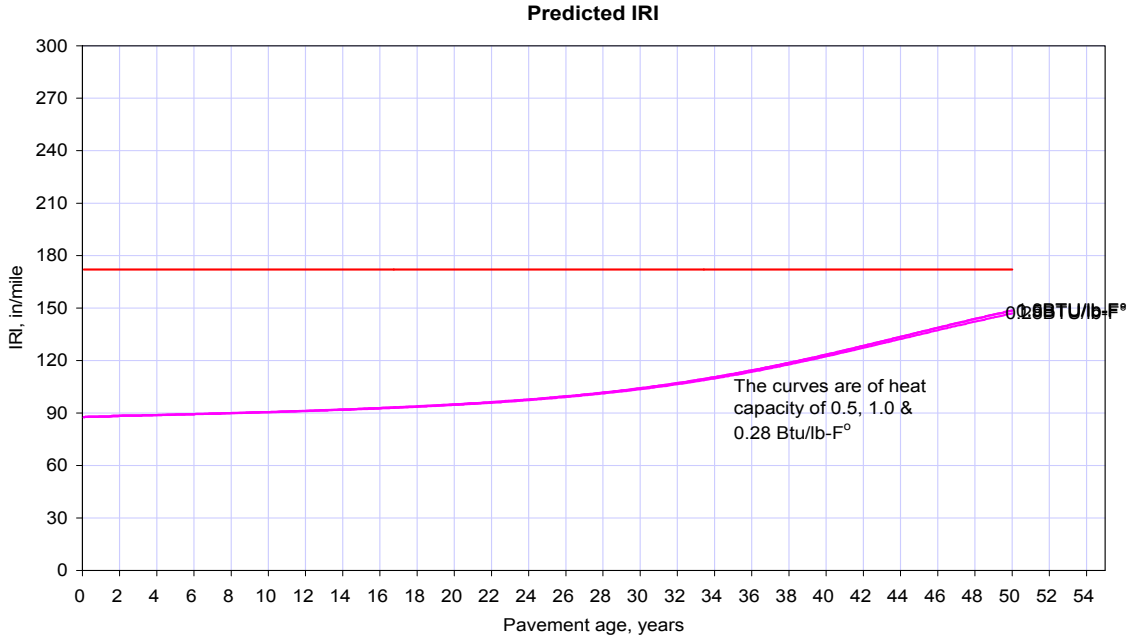
Predicted IRI
IRI, in/mile
Pavement age, years
The curves are of heat capacity of 0.5, 1.0 & 0.28 Btu/lb-F°

A8 Bedrock Inputs

A8.1 Material Type

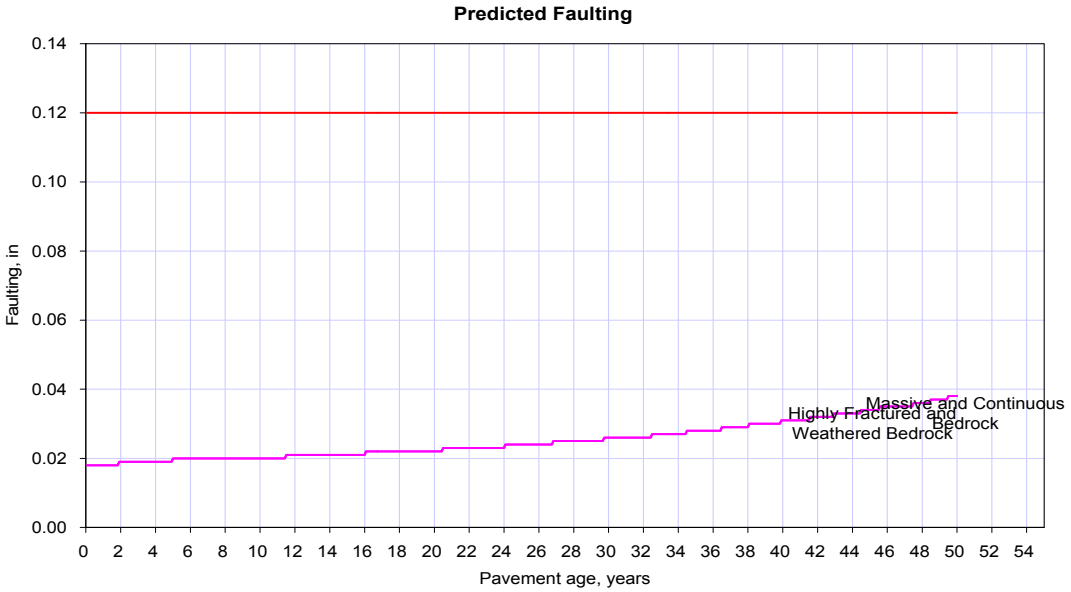

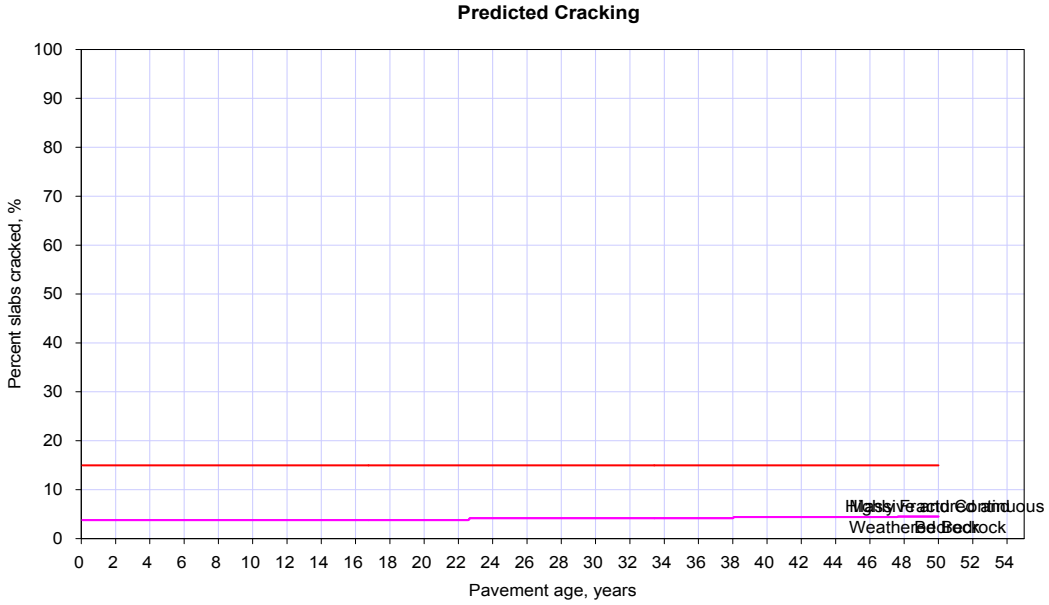

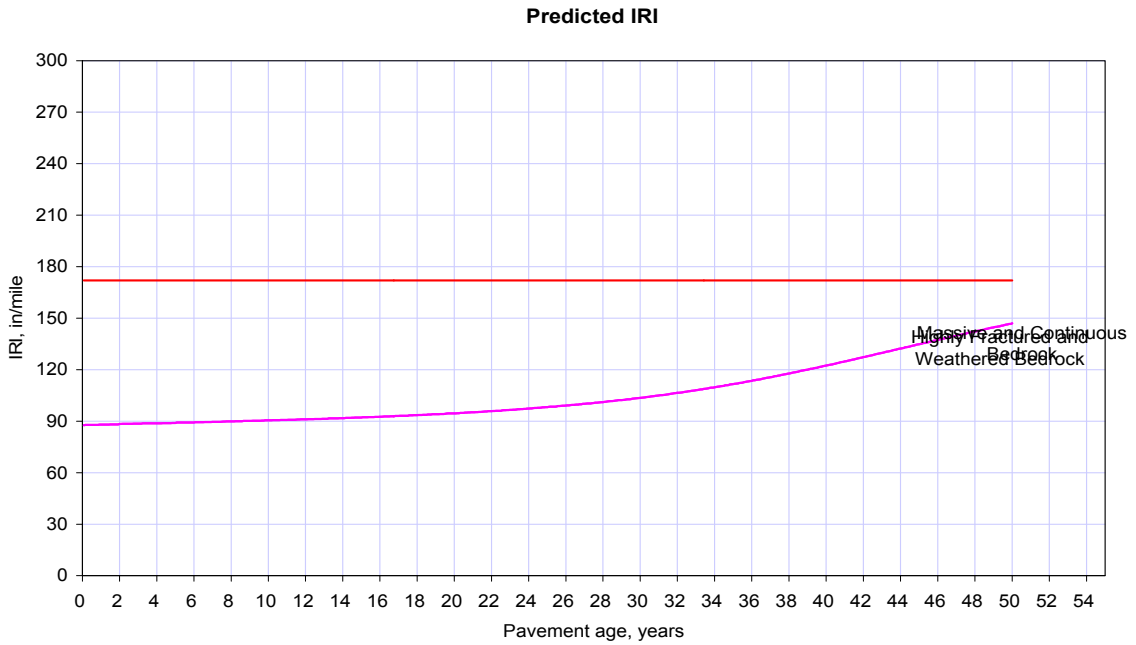

A8.2 Layer Thickness (in)

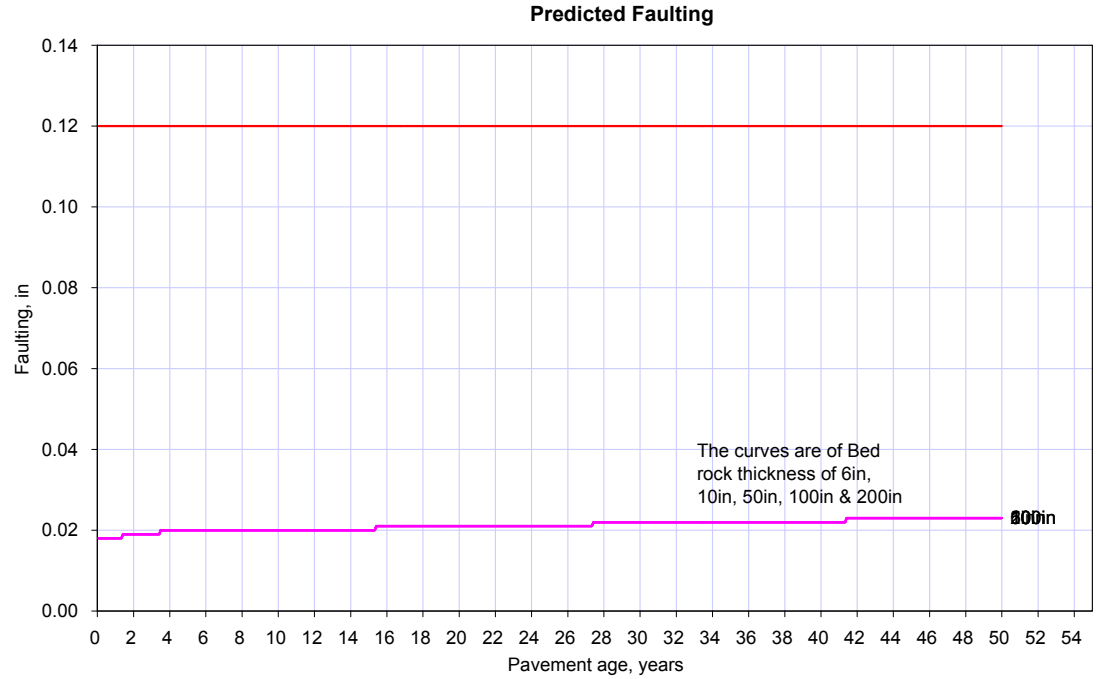

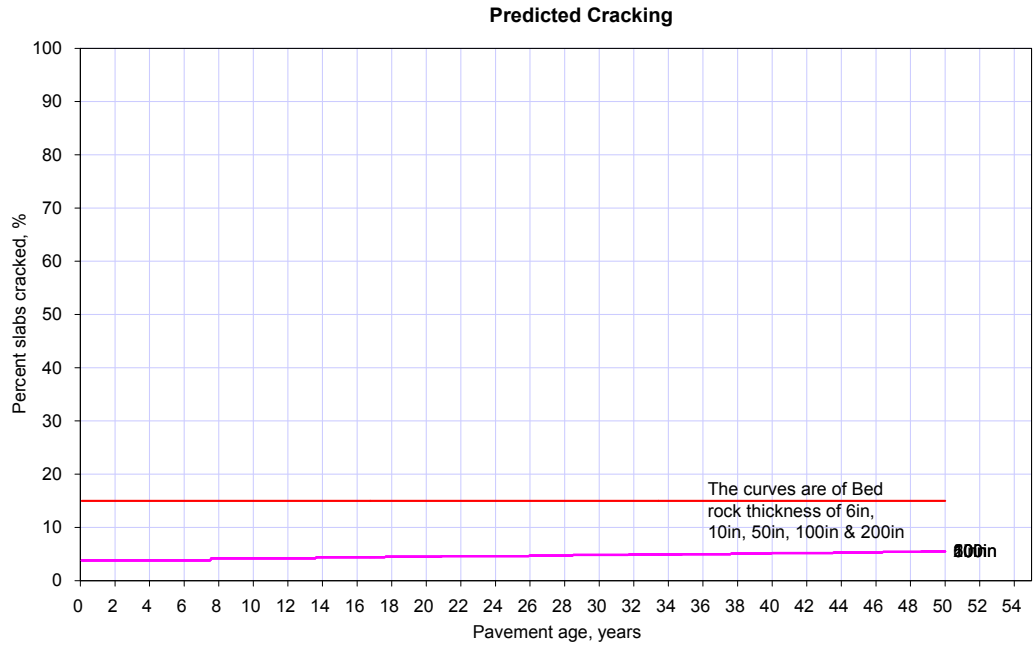
Predicted Cracking
Percent slabs cracked, %
Pavement age, years
The curves are of Bed rock thickness of 6in, 10in, 50in, 100in & 200in

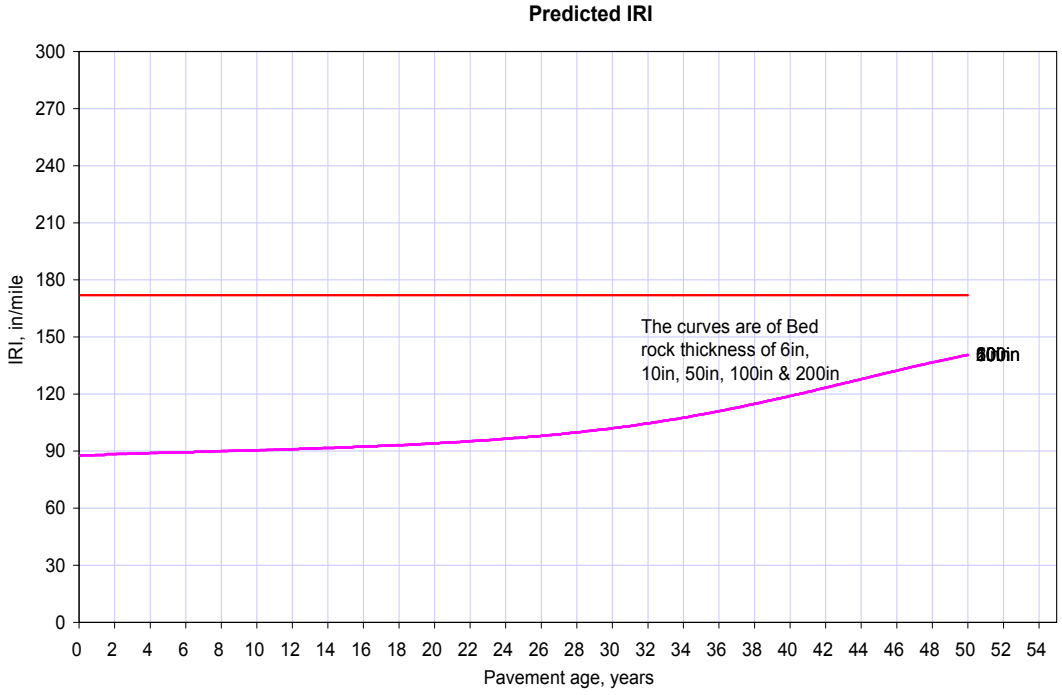
Predicted IRI
IRI, in/mile
Pavement age, years
The curves are of Bed rock thickness of 6in, 10in, 50in, 100in & 200in

A8.3 Unit Weight (pcf)

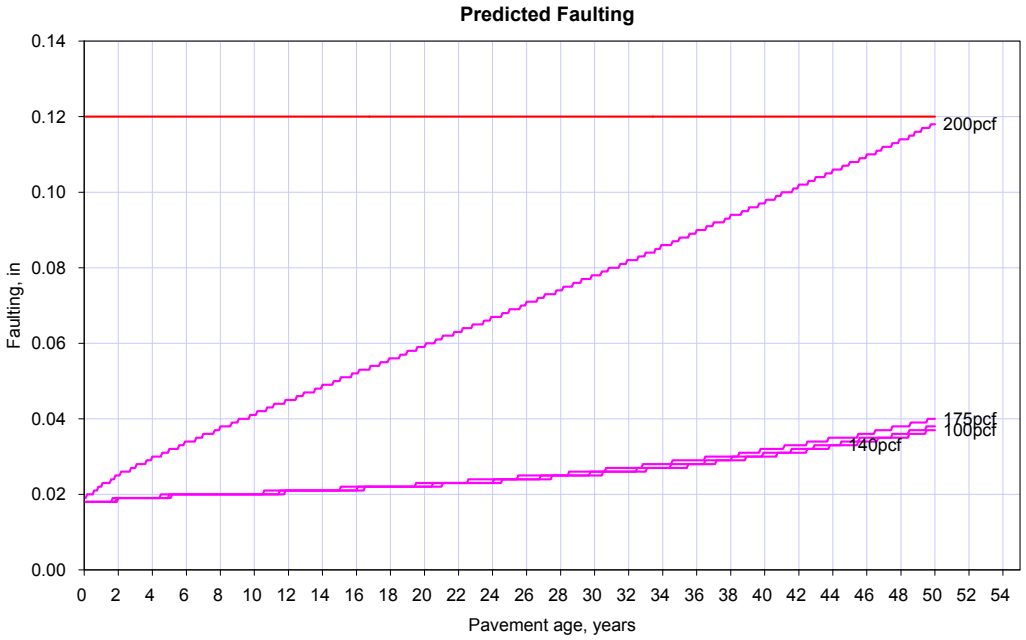

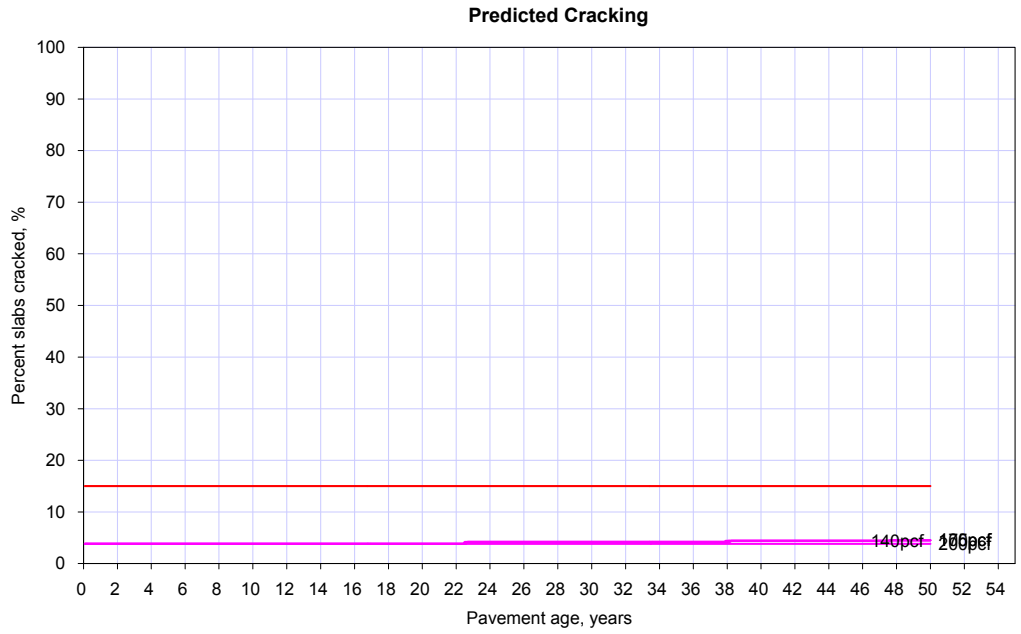

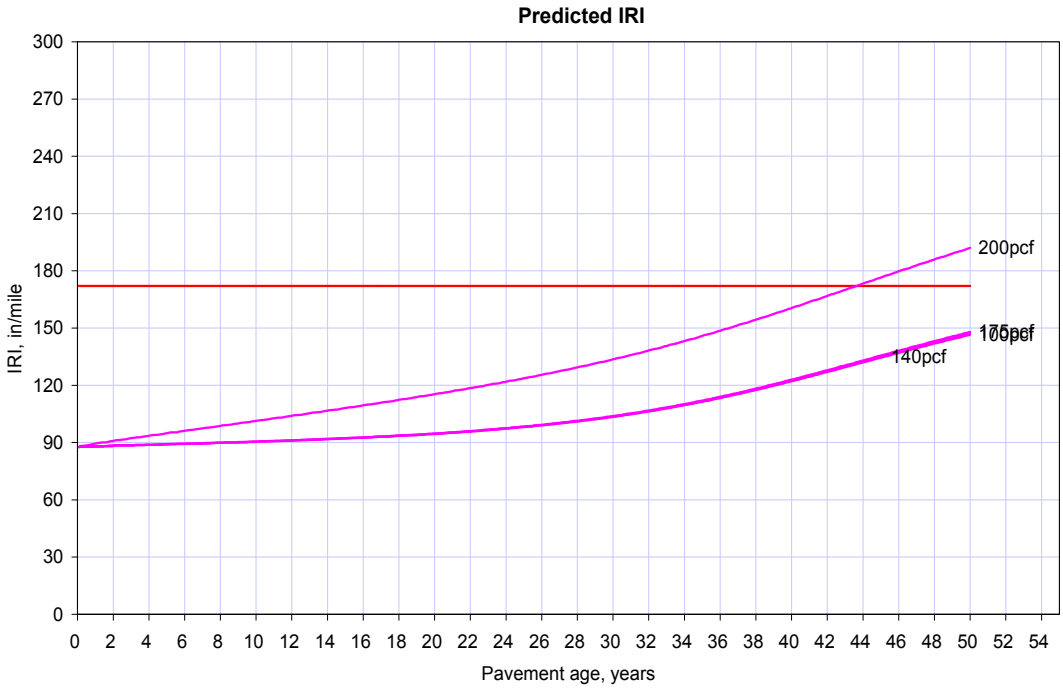

A8.4 Poisson's ratio

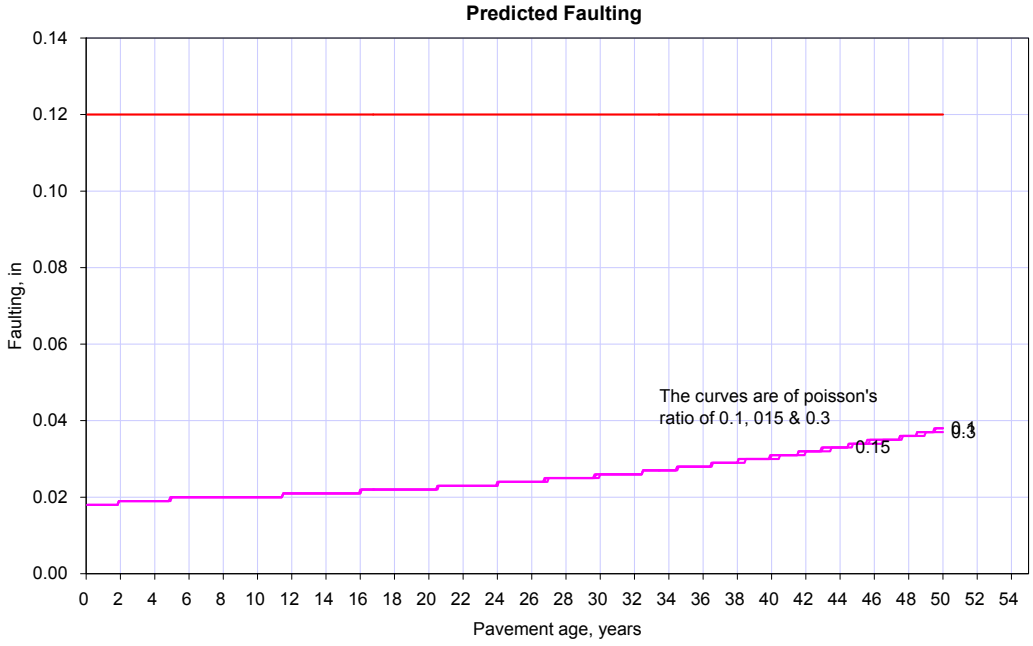

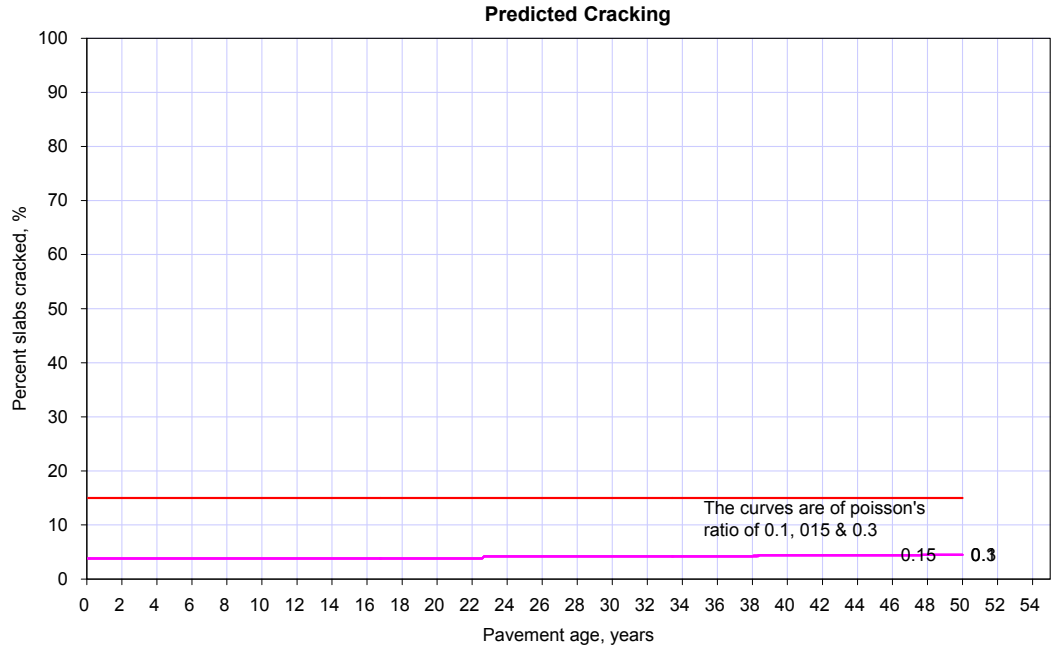
Predicted Cracking
Percent slabs cracked, %
Pavement age, years
The curves are of poisson's ratio of 0.1, 015 & 0.3
0.15
0.3

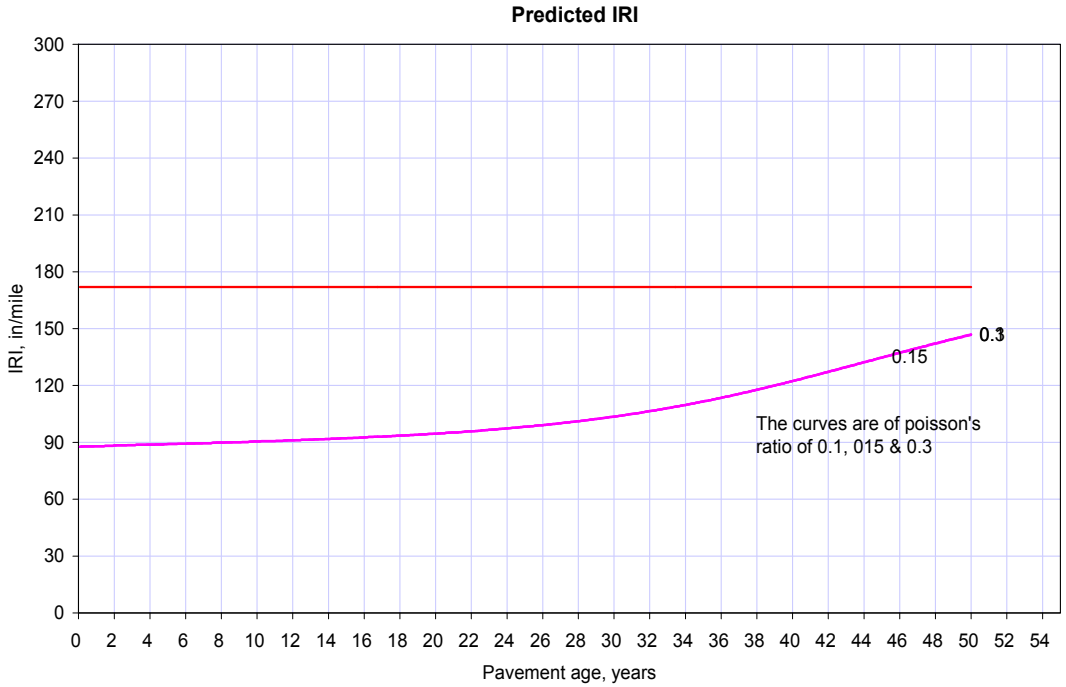
Predicted IRI
IRI, in/mile
Pavement age, years
0.3
0.15
The curves are of poisson's ratio of 0.1, 015 & 0.3

A8.5 Resilient Modulus (psi)

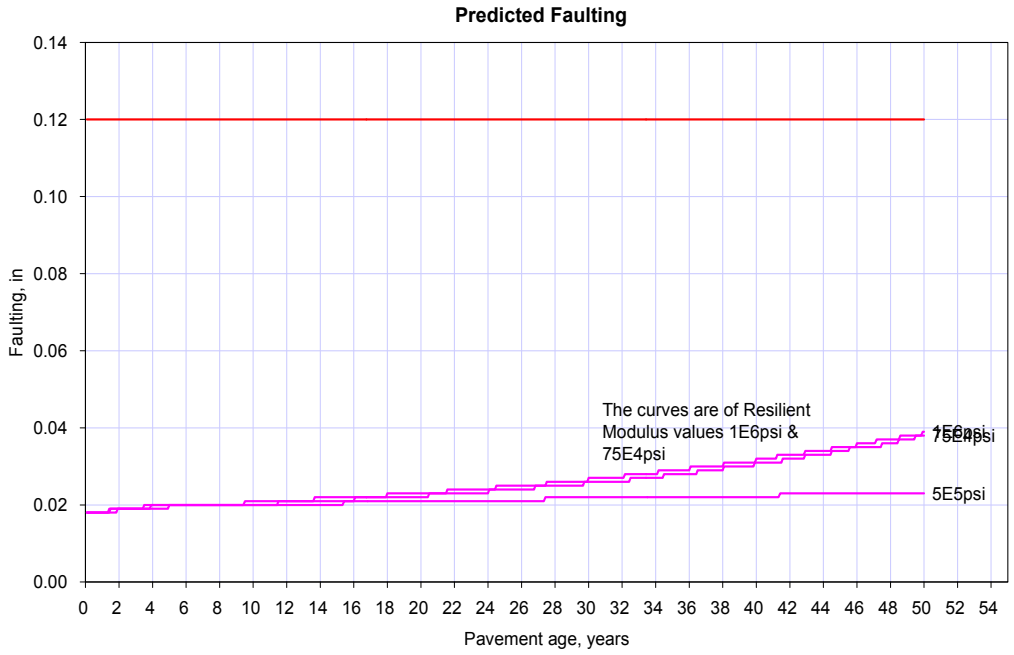

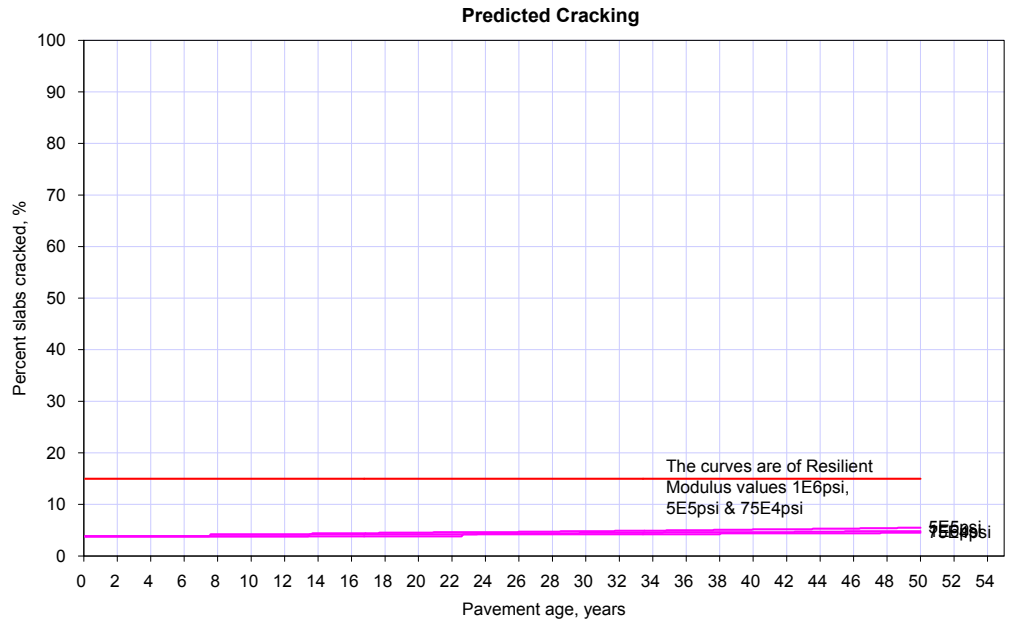

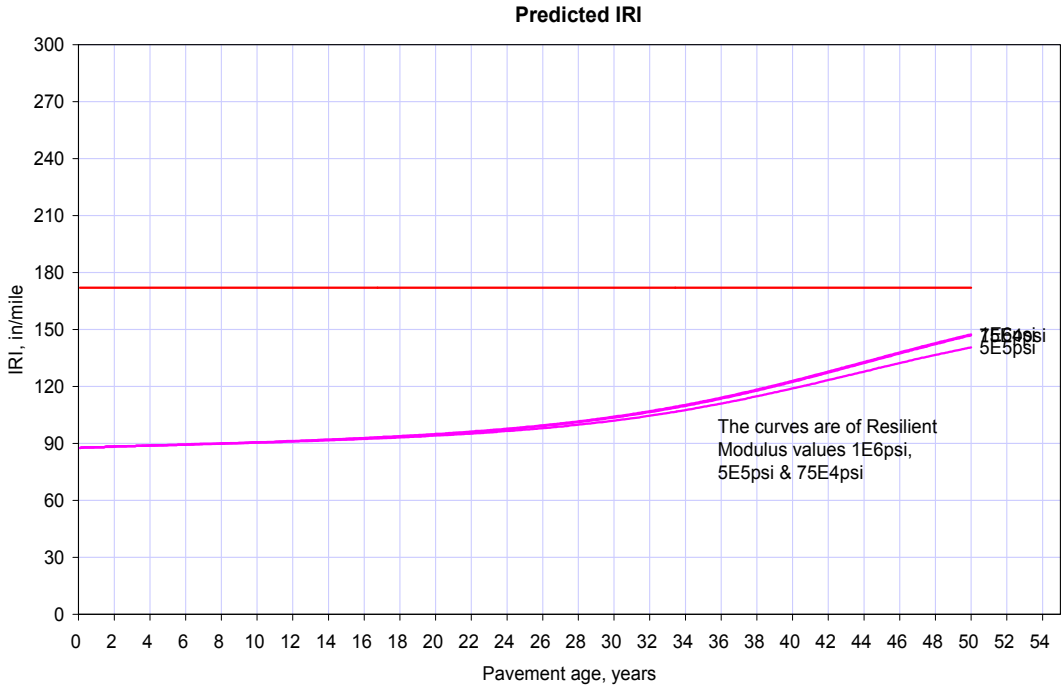
Predicted IRI
IRI, in/mile
300
270
240
210
180
150
120
90
60
30
0
0 2 4 6 8 10 12 14 16 18 20 22 24 26 28 30 32 34 36 38 40 42 44 46 48 50 52 54
Pavement age, years
1E6psi
5E5psi
The curves are of Resilient Modulus values 1E6psi, 5E5psi & 75E4psi